

**Development of Ion-Pair Cooperative Asymmetric Catalyses of Chiral
Tetraaminophosphonium Salts Possessing Organic Anions**

UEKI Yusuke

主論文

**Development of Ion-Pair Cooperative Asymmetric Catalyses of Chiral
Tetraaminophosphonium Salts Possessing Organic Anions**

有機アニオンを備えたキラルテトラアミノホスホニウム塩のイオン対協奏型触媒機能創出

UEKI Yusuke

上木 佑介

Department of Applied Chemistry, Graduate School of Engineering
Nagoya University

2012

Contents

| | | |
|----------------------|--|-----|
| Chapter 1 | Introduction and General Summary | 1 |
| Chapter 2 | Chiral Tetraaminophosphonium Carboxylate-Catalyzed Direct Mannich-Type Reaction | 26 |
| Chapter 3 | Chiral Organic Ion Pair Catalysts Assembled Through a Hydrogen-Bonding Network | 62 |
| Chapter 4 | Controlled Assembly of Chiral Tetraaminophosphonium Aryloxide-Arylhydroxide(s) in Solution | 89 |
| Chapter 5 | Catalytic Asymmetric Conjugate Addition of Acyl Anion Equivalent to Nitroolefins | 109 |
| List of publications | | 130 |
| Acknowledgements | | 131 |

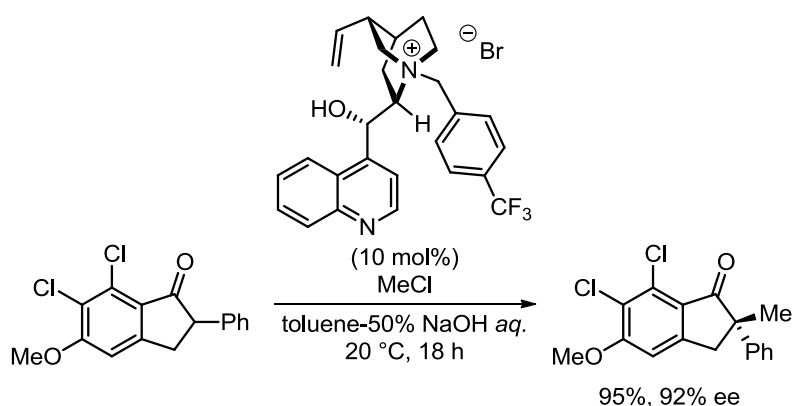
Chapter 1

Introduction and General Summary

Chiral quaternary onium salts have been widely used as a phase-transfer catalyst and have attracted much attention in the industrial and academic communities because of their high performance in controlling a desired transformation under mild conditions. In the catalyses of chiral quaternary onium salts, the structural features of the cations have been regarded as the most important element for achieving high reactivity and selectivity. However, the anionic components of the quaternary onium salts rarely contribute to the overall efficiency and/or stereoselectivity of the target transformation because of multiple ion-exchange processes that occur under phase-transfer conditions. In this context, the author is interested in the possibility of establishing a new cation/anion cooperative catalysis of highly stereoselective bond-forming reactions by using chiral onium salts possessing high recognition ability toward anion moieties via double hydrogen bonding and an appropriate organic anion.

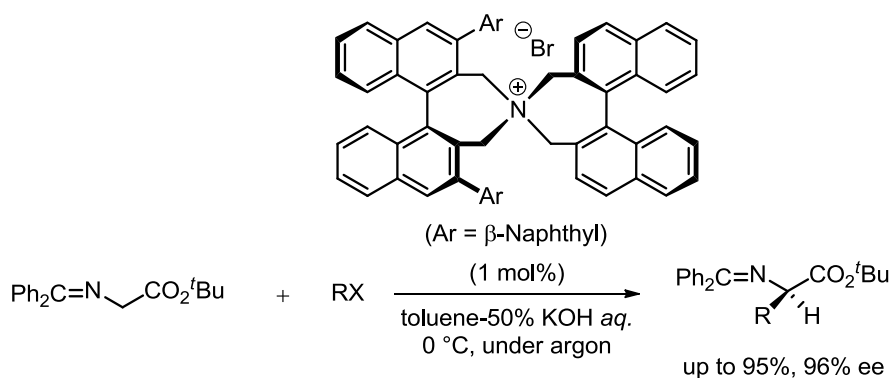
1.1 Chiral Quaternary Onium Salts for Phase-Transfer Catalysis

Quaternary onium salts, represented by quaternary ammonium and phosphonium salts, have been routinely employed in synthetic organic chemistry and have played various important roles as stoichiometric reagents, reactive intermediates, ionic liquids, and catalysts. The use of this class of compounds, particularly chiral nonracemic ones, as catalysts gather significant attention because of their unique properties such as chemical stability, ease of handling, and the ability of directly controlling the reactivity of the anion species.¹ The first example of a successful asymmetric catalysis of a chiral quaternary onium salt was reported in 1984 by the Merck group: a cinchona-alkaloid-derived ammonium salt was used as a phase-transfer catalyst for the enantioselective alkylation of an enolate under biphasic conditions (Scheme 1).²



Scheme 1.

Since then, the main focus in this research field has been the development of chiral quaternary ammonium salts and their catalyst systems for phase-transfer conditions.³ A considerable number of effective and practical catalyst systems has been introduced and applied to a large variety of useful transformations. In 1999, Maruoka reported the development of *N*-spiro C_2 -symmetric chiral quaternary ammonium bromides as a novel chiral phase-transfer catalyst, which were derived from readily available optically pure 1,1'-bi-2-naphthols, and their successful application to highly efficient, catalytic enantioselective alkylation of *tert*-butyl glycinate–benzophenone Schiff base under mild liquid-liquid biphasic conditions (Scheme 2).⁴



Scheme 2.

After this report, asymmetric phase-transfer catalysis based on the use of structurally well-defined chiral, nonracemic catalysts has greatly expanded their use as asymmetric catalysts for the construction of various chiral stereocenters under mild phase-transfer-catalyzed conditions. Thus, the chiral quaternary onium salts have now become a topic of great academic and industrial interest because of its high performance for controlling a desired transformation under mild conditions.³

1.2 General Mechanism of Phase-Transfer Catalysis

These quaternary ammonium salt catalyzed phase-transfer reactions are supported by an interfacial mechanism involving, first, the formation of metal carbanion $[M^+ \cdot C^-]$ at the interface of the organic and aqueous phases, followed by the extraction of the formed carbanion species from the interface into the organic phase by the action of an ammonium ion of a phase-transfer catalyst. After the formation of a new ion pair $[Q^+ \cdot C^-]$ in the organic phase, the initial anion of the quaternary ammonium salt (X^-) is simultaneously liberated into the aqueous phase in the form of $[M^+ \cdot X^-]$. A subsequent stereoselective C–C bond formation with RX would afford the regeneration of the chiral ammonium salt $[Q^+ \cdot X^-]$. Accordingly, in contrast to well recognized importance of the cation structure, the existence of the anion is often neglected because it does not contribute significantly to the overall reaction efficiency and stereoselectivity owing to multiple ion-exchange processes in the catalytic cycle of the biphasic reaction (Figure 1).^{3,5}

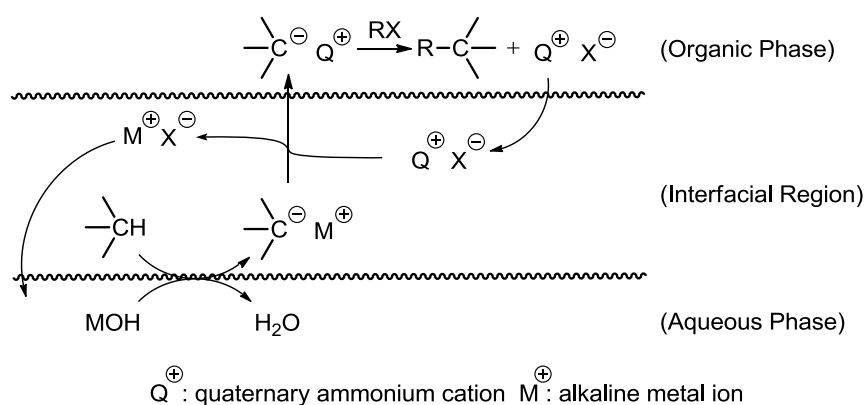
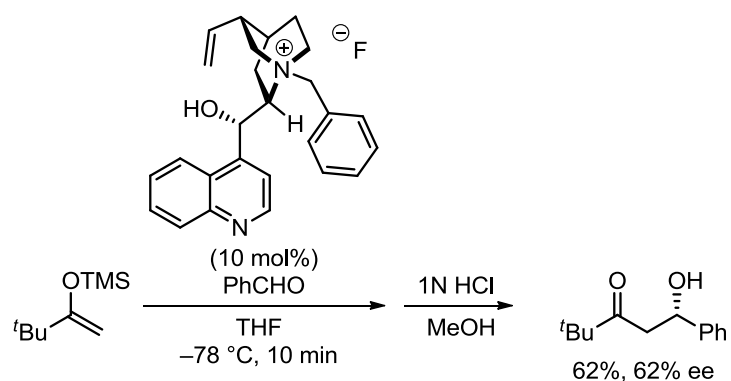


Figure 1. Proposed interfacial mechanism of the phase-transfer catalysis.

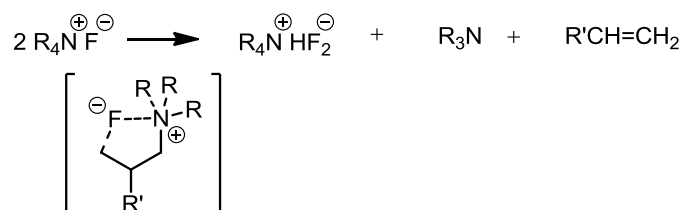
1.3 Chiral Onium Salts Bearing Lewis Basic Anions

Previous examples of chiral onium salts having a functional organic anion are very rare and limited to chiral onium salts bearing Lewis basic anions, e.g., fluoride, hydrogen bifluoride, and phenoxide. In 1993, Shioiri *et al.* reported cinchonium fluoride catalyzed-enantioselective Mukaiyama-type aldol reaction in moderate enantiomeric excess. In this reaction, a fluoride ion served as an efficient Lewis base to activate silyl enol ethers because of the affinity of silicon for fluorine (Scheme 3).^{7a}

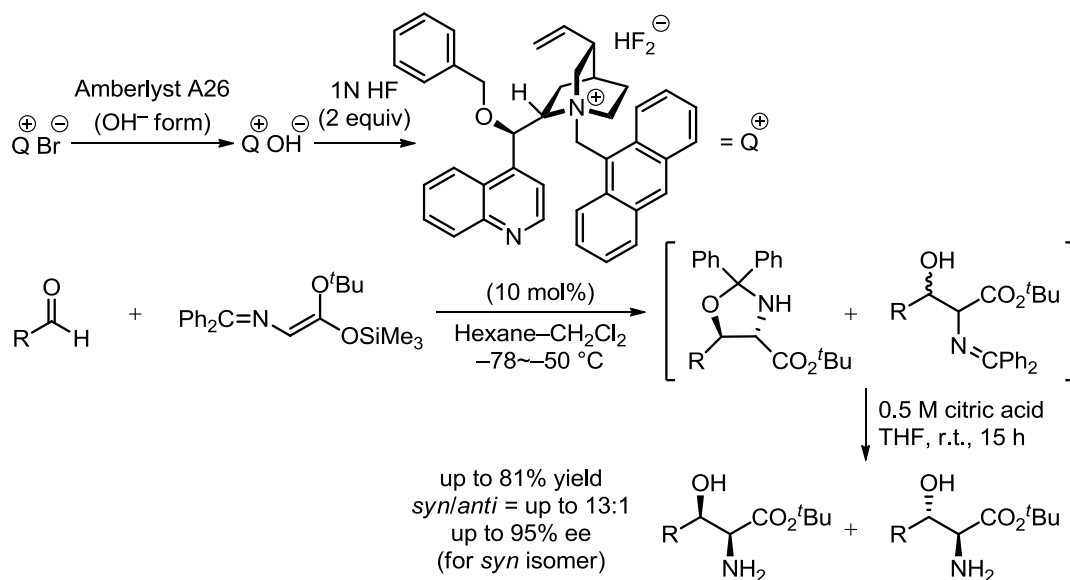


Scheme 3.

The use of anions as a Lewis base has been studied, and some effective catalysts for the Mukaiyama-type aldol reaction have been developed by utilizing the ability to generate nucleophiles from organosilicon compounds. However, because of the strongly basic nature of tetraalkylammonium fluorides, self-destruction of the tetraalkylammonium cation via Hofmann elimination is induced by the fluoride anion under anhydrous conditions to afford tetraalkylammonium bifluoride, trialkylamine, and olefin (Scheme 4). This phenomenon suggests that tetraalkylammonium bifluoride is expected to be more stable and easier to handle than tetraalkylammonium fluoride. Corey and coworkers revealed that the cinchonidine-derived bifluoride could be prepared from the corresponding bromide by neutralization of cinchonidinium hydroxide, which was prepared using Amberlyst A-26 OH⁻ form with 2 equiv. of 1 N HF solution. They also found that the cinchonidine-derived bifluoride exhibits catalytic activity and chiral efficiency for the Mukaiyama-type aldol reaction of ketene silyl acetal with aldehydes. In this reaction, high enantioselectivity for major diastereomers was observed for a wide range of aldehydes (Scheme 5).^{7b}

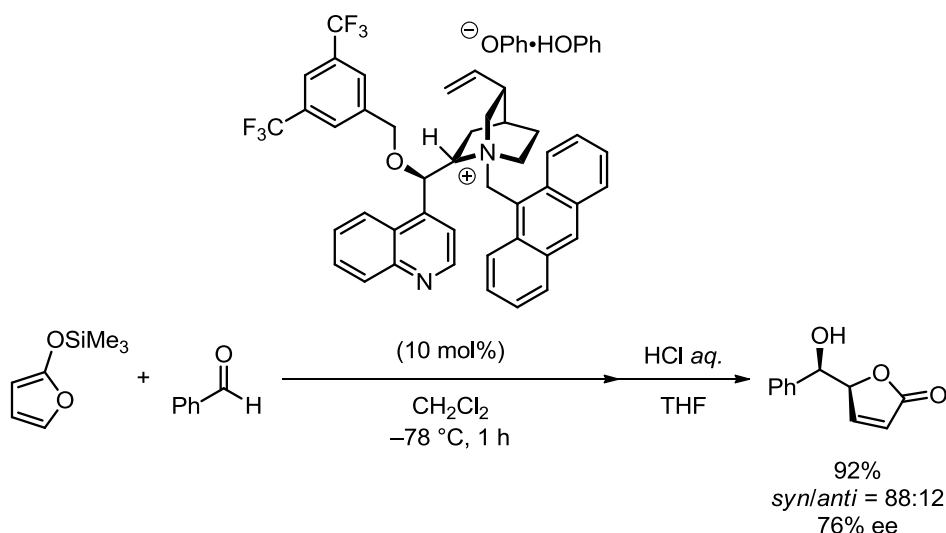


Scheme 4.



Scheme 5.

In the course of the above study, Mukaiyama and coworkers reported the synthesis of chiral ammonium phenoxides which are less hygroscopic salts than their fluoride analogues and the application of them as Lewis base catalysts to highly stereoselective transformations.^{7c} The catalysts can be easily prepared from readily available cinchonine or cinchonidine as the starting materials. When the catalyst has an electron-withdrawing group on C-9 oxygen, an even less hygroscopic quaternary ammonium phenoxide–phenol complex was prepared, which can be compared with the hydrogen bifluoride catalysts (Scheme 5).^{7d}



Scheme 5.

1.4 Plausible Mechanism of the Catalysis: Chiral Onium Salts Catalysts Bearing Lewis Basic Anions

As described above, some chiral onium salts bearing Lewis basic anions have been reported, providing a unique platform for establishing otherwise difficult asymmetric transformations. However, even in this case, the Lewis basic anions act as an activator of the silyl compound to generate the nucleophile at the initial stage of the reaction and it no longer participates in the catalytic cycle (Figure 2).⁶

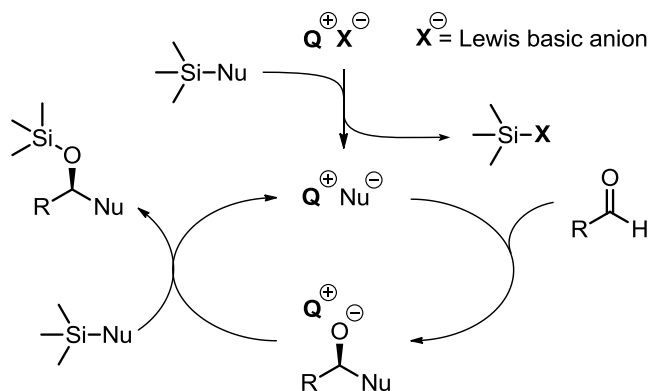


Figure 2. Chiral onium salt catalysts bearing a Lewis basic anion: plausible mechanism of the catalysis.

Thus, the importance of incorporating tunable, functional anions into the original salts remains unexplored. Therefore, the author is interested in the possibility of establishing new cooperative catalysis of chiral onium salts possessing an appropriate organic anion. If such catalysis could be fulfilled, the reaction can be controlled by the structural modification of not only the cation but also the initial anion through its continuous participation in the catalytic cycle.

1.5 Phosphonium Salts Catalysts

While quaternary phosphonium salts are readily accessible and widely applicable stoichiometric reagents in organic synthesis as precursors of ylides, the reagents developed by Georg Wittig for carbonyl olefination, their utilization as a catalyst is very limited.^{8,9} Typically, this is because phosphonium cations are liable to deprotonation at the α - or β -position by bases and decomposition by nucleophilic attack, which is a major obstacle in making them sufficiently stable for use as catalysts (Figure 3).

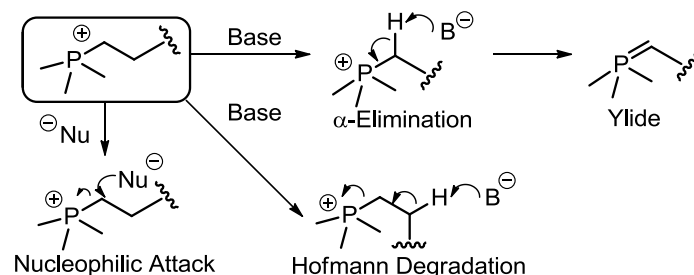
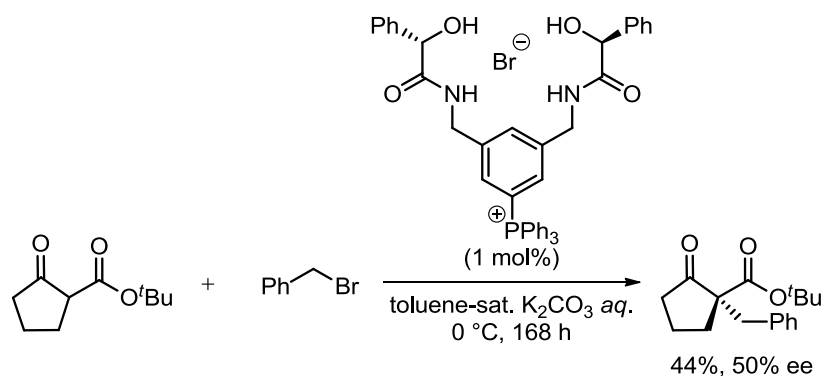


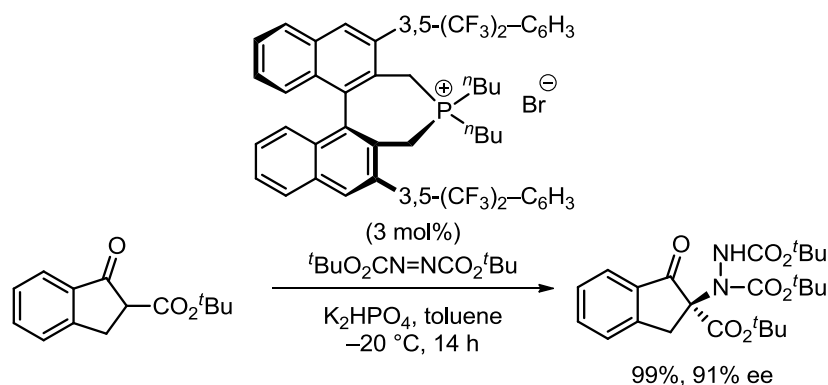
Figure 3. Decomposition modes of phosphonium salts.

A pioneering study in catalytic asymmetric reactions with chiral phosphonium salts was conducted by Manabe's group in 1998. They reported a novel asymmetric phase-transfer alkylation catalyzed by a chiral quaternary phosphonium salt. Although the phosphonium salts accelerated the reaction and showed moderate enantioselectivity, the yields and enantioselectivities needed further improvement.^{9b} Accordingly, the development of phosphonium salts which is effective for the asymmetric reaction is highly desired.



Scheme 6.

Recently, Maruoka and coworkers reported the synthesis of binaphthyl-based quaternary phosphonium salts and demonstrated the catalytic efficiency in the development of the highly enantioselective α -amination of cyclic β -keto esters and β -diketones under phase-transfer conditions. This is the first successful use of a chiral quaternary tetraalkylphosphonium salt as a phase-transfer catalyst in asymmetric synthesis.^{10(a)}



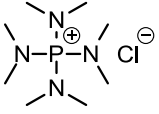
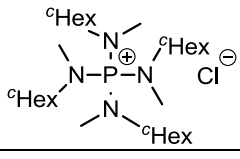
Scheme 7.

Extensive studies have also been conducted on some other chiral phosphonium-catalyzed asymmetric bond-forming reactions. However, these studies were limited by factors such as complete absence of a base or weakly basic conditions required for use of chiral tetraalkylphosphonium salts.¹⁰ This is mainly because of that the tetraalkylphosphonium salts are essentially unstable under basic conditions. Therefore, the author is interested in establishing a new class of chiral phosphonium salts that are widely applicable to the development of hitherto unknown catalytic asymmetric bond-forming processes.

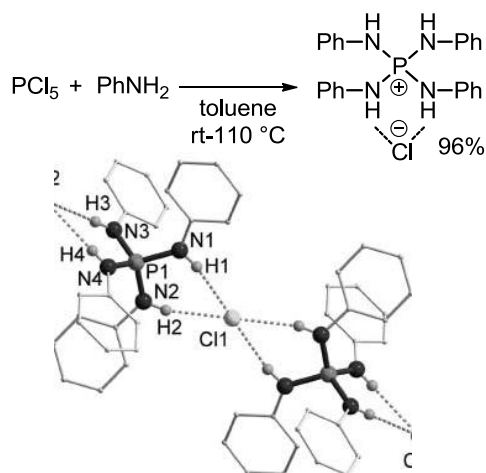
1.6 Tetraaminophosphonium Salts

At the outset of our study, the [5,5]-*P*-spirocyclic tetraaminophosphonium framework was selected as the primary structure of the key onium ion. Tetraaminophosphonium salts exhibit unique properties which are rather different from those of common alkyl-substituted phosphonium salts.¹¹ For example, aminophosphonium salts are highly stable under strongly basic aqueous conditions, under which the corresponding ylides could be generated from tetraalkylphosphonium salts. Furthermore, in contrast to phosphorus acid esters, the amino series is generally not susceptible to the *P*-*N* bond cleavage caused by a nucleophilic anion, such as a halide, and thus, the salts are usually inert even in the presence of excess anions. In fact, a series of peralkylated polyphosphazanium cations exhibits extraordinary high resistance to base under biphasic conditions. Their half-lives under these conditions greatly exceed those of conventional organic cations (Table 1).¹²

Table 1. Half Lives in 50% NaOH / Chlorobenzene.

| Phosphonium salt | $\text{Bu}_4\text{P}^+\text{Cl}^-$ |  |  |
|------------------|------------------------------------|---|--|
| $t_{1/2}$ | 0.08 h / 20 °C | 0.33 h / 100 °C | 67 h / 100 °C |

Moreover, the steric environment around a phosphorus cation can be controlled by introducing the appropriate substituents on nitrogen atoms, and the positive charge on a phosphorus center tends to be delocalized by the participation of four nitrogen atoms, both of which would enhance the tolerance to an attack by external nucleophiles. It should also be noted that the structural diversity of aminophosphonium salts can be easily attained by varying each nitrogen substituent. In addition, tetraaminophosphonium ion, which is prepared by the reaction of PCl_5 with excess aniline, display high performance in the recognition of anions via double hydrogen-bonding interaction (Figure 4).^{11d}

**Figure 4.** The picture of tetraaminophosphonium ion interacting with chloride via double hydrogen-bonding.

With the abovementioned structural property in our mind, our group designed new chiral phosphonium salts.¹³ The details of the molecular design concept and the synthesis of *P*-spiro tetraaminophosphonium salts are described below. Our strategy for molecular design was to introduce a phosphorus-centered [5,5]-*P*-spirocyclic core using the readily accessible chiral 1,2-diamine derived from α -amino acids.¹⁴ One of the advantages of this structural motif is that it is possible to achieve various modifications of the structure by selecting amino acid-derived alkyl substituents and aryl substituents introduced in the process of 1,2-diamine

synthesis. Another advantage is that the *N-H* protons would be rigorously regulated, making it possible to fully appreciate the intrinsic hydrogen-bonding capability for anion recognition (Figure 5).

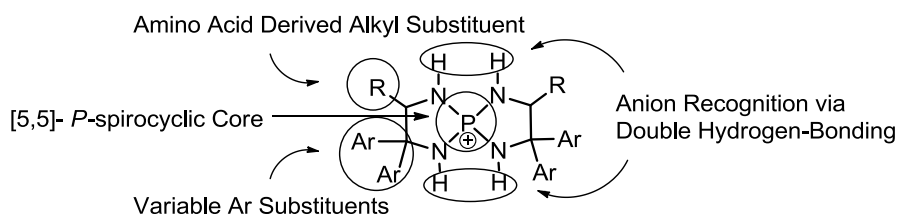
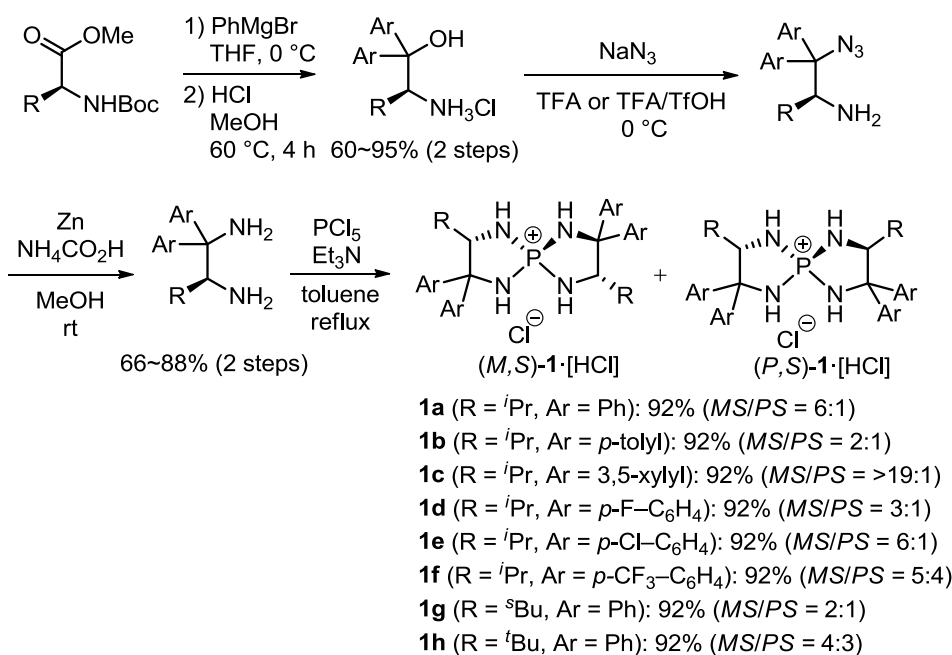


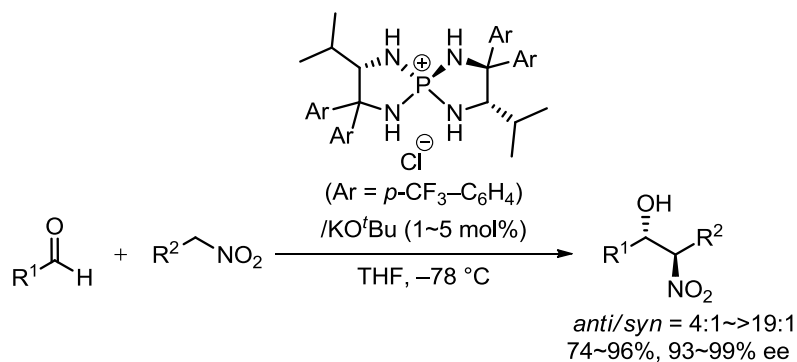
Figure 5. Design concept for *P*-spiro tetraaminophosphonium ions.

First of all, our group established reliable synthetic protocol for the [5,5]-*P*-spirocyclic tetraaminophosphonium salts from *N*-Boc amino acid esters. According to the literature procedure, various geminal aromatic groups were introduced to *N*-Boc amino acid esters, and the crude product was subsequently treated with 1M HCl in methanol at 50 °C.^{14(a)} In the next substitution of the tertiary hydroxyl group of the resulting amino alcohol hydrochloride, the use of trifluoroacetic acid as the solvent is crucial to prepare the corresponding chiral 1,2-diamines with an alkyl-substituted aromatic group after the reduction of the azide moiety. In addition, the author found that using trifluoromethanesulfonic acid (TfOH) as the co-solvent was effective for substrates with aromatic nuclei bearing electron-withdrawing groups. With a wide variety of chiral 1,2-diamines at our disposal, the author undertook the tuning of reaction parameters for assembling into chiral tetraaminophosphonium salts. Eventually, I concluded that the treatment of 1,2-diamines with PCl₅ and triethylamine in toluene at 110 °C resulted in the facile formation of the desired phosphonium salts as a diastereomeric mixture on the phosphorus stereogenic center (spiro chirality; *P* and *M*). These diastereomers can be separated, and essentially pure (*M,S*)-**1** can be obtained through silica-gel column chromatography and recrystallization (Scheme 8).¹⁵



Scheme 8.

In 2007, our group developed that the chiral triaminoiminophosphoranes, generated in situ from the chiral tetraaminophosphonium salts and a strong base such as potassium *tert*-butoxide, could efficiently catalyze the highly *anti*- and enantioselective Henry reaction¹⁶ with a wide range of aldehydes under mild conditions (Scheme 9).^{13a,17}



Scheme 9.

In this reaction, a nitroalkane would be initially deprotonated by a basic chiral triaminoiminophosphorane, which is known as a nucleophilic component of the aza-Wittig reaction as well as a strongly basic reagent.^{18,19} Because the resulting nitronate is a bidentate hydrogen-bonding acceptor, the chiral phosphonium ion and the nitronate could form a structured ion pair. Subsequent stereoselective addition to an aldehyde would afford an ionic product precursor, which could be protonated by either the phosphonium ion or a nitroalkane (Figure 6).¹² Moreover, rapid access to some natural products has been achieved by utilizing

this transformation.^{13e}

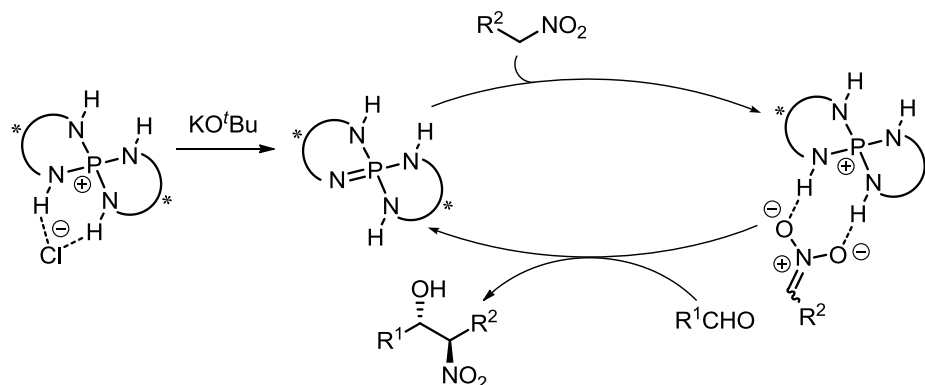
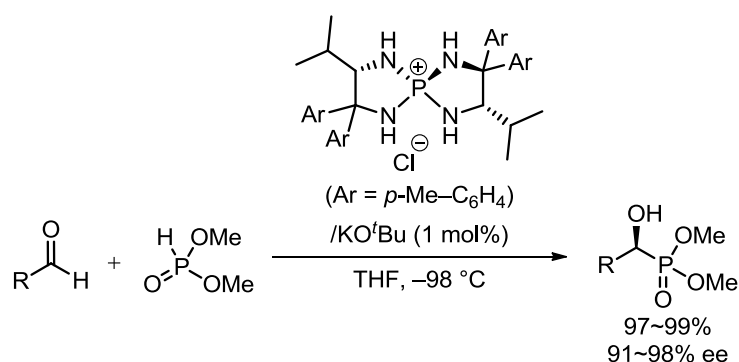


Figure 6. Working hypothesis for the catalytic asymmetric Henry reaction of aldehydes catalyzed by a chiral triaminoiminophosphorane.

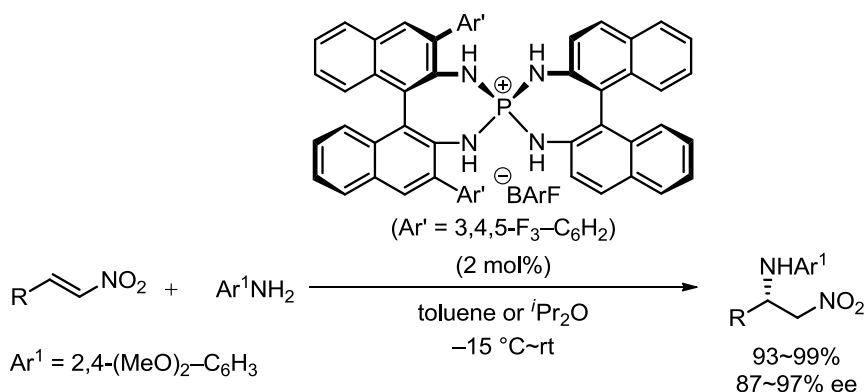
More recently, this remarkably high performance of the intermediary generated chiral tetraaminophosphonium nitronate for discriminating the enantiotopic faces of carbonyl compounds was also applied to the Henry reaction of activated ketones, i.e., pyruvate derivatives in good yields with high stereoselectivities.^{20c} Furthermore, the strong basicity and high anion recognition ability of chiral triaminoiminophosphorane was used in the enantioselective addition of dialkylphosphonate to carbonyl compounds, such as aldehydes and ynones (Scheme 10).^{20b,d}



Scheme 10.

In addition, our group disclosed the fact that aromatic amine derived chiral tetraaminophosphonium salts, featuring sufficient acidity of the *N-H* protons, could function as a Brønsted acid.²¹ To fully realize the potential of the phosphonium salts as a Brønsted acid catalyst, it was important that the chloride anion was exchanged with barfate [(3,5-(CF₃)₂-C₆H₃)₄B⁻(BArF)], which is one of the most weakly coordinating anion.²² This chiral arylaminophosphonium barfate could engage in the activation of electronically neutral

substrates.²³ Their reactivity and selectivity have been clearly demonstrated in the development of the first highly enantioselective conjugate addition of arylamines to nitroolefins (Scheme 11).²⁰



Scheme 11.

1.7 Development of Ion-Pair Cooperative Asymmetric Catalyses of Chiral Tetraaminophosphonium Salts Possessing Functional Organic Anions

Despite fruitful advancement in chiral quaternary onium salts catalyses and the fact that the importance of the cation structure is generally well recognized, the existence of its counter anion is often neglected in these catalyses. This is primarily because the counter anion does not contribute significantly to the overall reaction efficiency and stereoselectivity owing to multiple ion-exchange processes in the catalytic cycle of the biphasic reaction, as described in Section 1.1. In fact, the synthetic importance of incorporating tunable, functional anions into the original salts remains unexplored.^{24,25} The author is interested in the possibility of establishing a new cooperative catalysis of chiral onium salts possessing an appropriate organic anion.²⁶ By such catalysis, the reaction can be controlled not only by the structural modification of the cation but also by that of the initial anion through its continuous participation in the catalytic cycle.

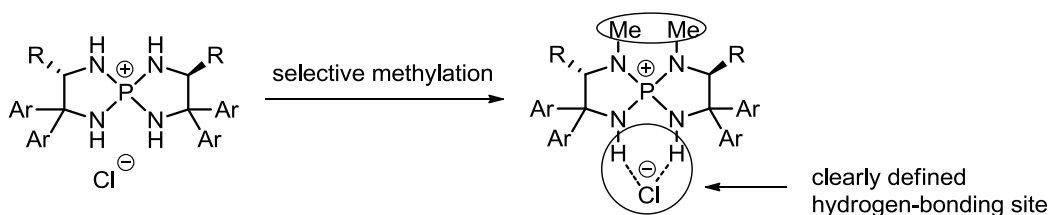
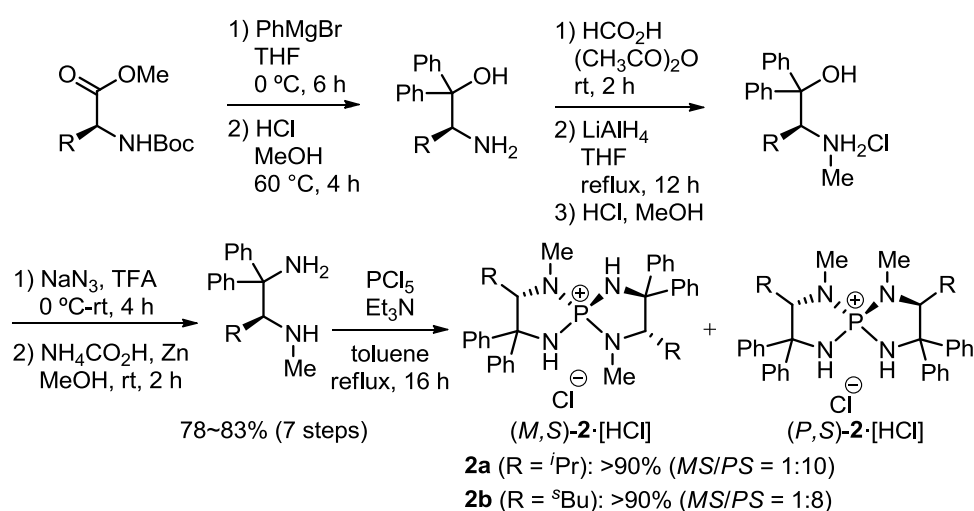


Figure 7. Selective methylation for clearly defined hydrogen-bonding site

The *P*-spirocyclic tetraaminophosphonium framework was selected as a chiral cationic

component in consideration of its synthetic versatility described above.²⁷ As already mentioned, this onium cation has several characteristic features, including the ability of recognizing and controlling anions or nonionic Lewis bases through double hydrogen bonding, which have been described in Section 1.6.^{13,16,17} Here, two of the nitrogen atoms were selectively methylated to define the position for hydrogen-bonding interactions with an enolate anion (Figure 7). The actual synthesis of the requisite chiral tetraaminophosphonium salts was implemented by following the procedure developed by our group except for selective methylation of the corresponding amino alcohols through the formylation of the amino group and subsequent reduction of the formyl moiety.¹⁵



Scheme 12.

In this thesis, the readily accessible basic anions, such as carboxylates and phenoxides, were selected as functional organic anions. The chiral tetraaminophosphonium salts possessing functional organic anions were prepared from the corresponding chloride by the passage of its methanolic solution through an Amberlyst A-26 OH⁻ column and subsequent neutralization with corresponding conjugate acids.²⁸ The expected catalytic cycle is as follows: a basic anion would abstract the active methylene or methine proton of the pro-nucleophile to give a chiral structured ion pair and the corresponding conjugate acid. Subsequent stereoselective nucleophilic addition to the electrophile would afford an ionic product precursor. The rapid protonation of this anion by the conjugate acid could give the product concomitant with regenerating the parent chiral phosphonium salt catalyst. If this is operative, the anion of the catalyst could continuously participate in the catalytic cycle through deprotonation and reprotonation processes (Figure 8).

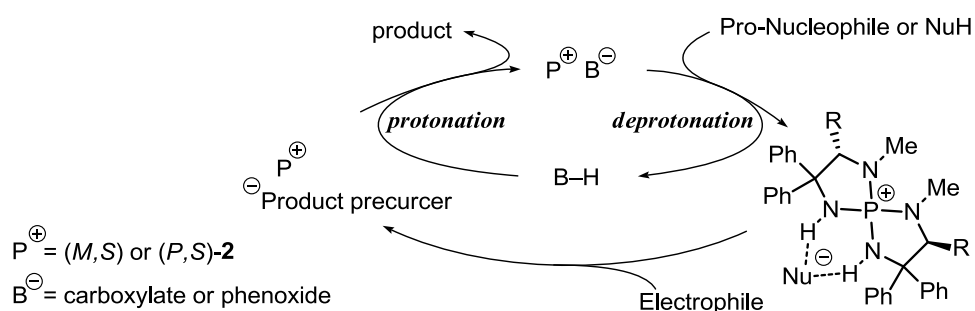
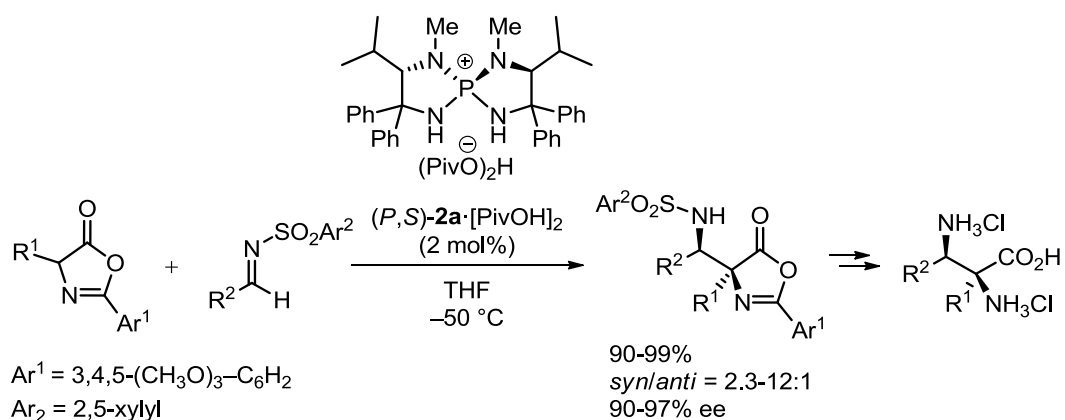


Figure 8. Working hypothesis for the ion-pair catalysis.

The details of the author's investigation for this project are described in the following sections. The ion-pair cooperative catalysis of a chiral *P*-spiro tetraaminophosphonium carboxylate for the Mannich-type reaction of azlactones is described in Chapter 2. Chapter 3 explains the process for the supramolecularly assembled ion pair—chiral tetraaminophosphonium aryloxide–aryl hydroxide(s)—as a chiral molecular catalyst for the enantioselective conjugate additions of acyl anion equivalents. This process involving molecular assembly was analyzed in solution and solid phase by low-temperature ^{31}P NMR and X-ray diffraction analysis. Chapter 4 presents that there are three kinds of molecular assembly whose equilibrium is controllable depending on the stoichiometry of aryl hydroxides to iminophosphorane. In addition, the author also found the polarity dependence of molecular associations of this supramolecular catalyst and realized a highly enantioselective conjugate addition of 2-unsubstituted azlactone to nitroolefins by selectively utilizing a requisite molecular assembly, which is described in Chapter 5.

1.8.1 Chiral Tetraaminophosphonium Carboxylate-Catalyzed Direct Mannich-Type Reaction: Chapter 2

The ion-pair cooperative catalysis of chiral tetraaminophosphonium carboxylate $2\mathbf{a}\cdot[\text{RCO}_2\text{H}]_2$, such as $(P,S)\text{-}2\mathbf{a}\cdot[\text{PivOH}]_2$, was established and its synthetic utility was successfully demonstrated in the highly enantioselective direct Mannich-type reaction²⁹ of azlactones³⁰ with *N*-sulfonyl imines (Scheme 13).



Scheme 13.

The reaction with a wide range of aliphatic imines gave the corresponding Mannich adducts in almost quantitative yields with high stereoselectivities. Moreover, the product can be easily converted to the corresponding α,β -diamino acid dihydrochloride in two steps with no loss in enantiopurity.³¹ Since the carboxylate anion continuously participates in the catalytic cycle, the catalytic performance of $(P,S)\text{-2a}\cdot[\text{RCO}_2\text{H}]_2$ can be controlled not only by the structural modification of the cation $(P,S)\text{-2a}\cdot\text{H}$ but also by that of the initial anion RCO_2^- . Based on single-crystal X-ray diffraction analysis, I believe that the formation of the structured ion pair through double hydrogen bonding is crucial in inducing high levels of selectivity (Figure 9).^{26a}

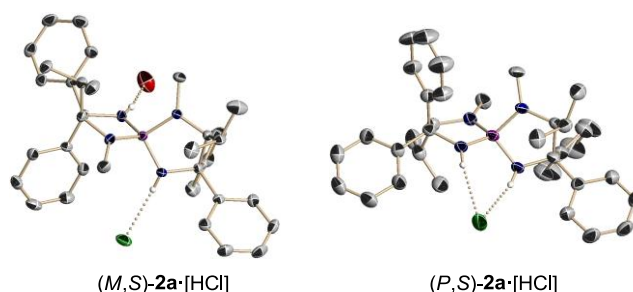


Figure 9. Three dimensional structure of (M,S) - and $(P,S)\text{-2a}\cdot[\text{HCl}]$.

1.8.2 Chiral Organic Ion Pair Catalysts Assembled Through a Hydrogen-Bonding Network: Chapter 3

In the course of the study, the author found that a designer tetraaminophosphonium ion $(P,S)\text{-2a}\cdot\text{H}$, two phenols (**3a**), and a phenoxide can self-assemble into a catalytically relevant supramolecular architecture $(P,S)\text{-2a}\cdot[\mathbf{3a}]_3$ through an intermolecular hydrogen-bonding interaction.³² The solid-state structure of the molecular assembly was unambiguously determined by X-ray diffraction analysis, which revealed a 10-membered antidromic circular

network of hydrogen bonding (Figure 10).³³

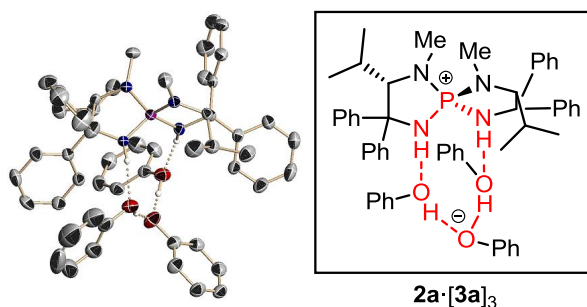
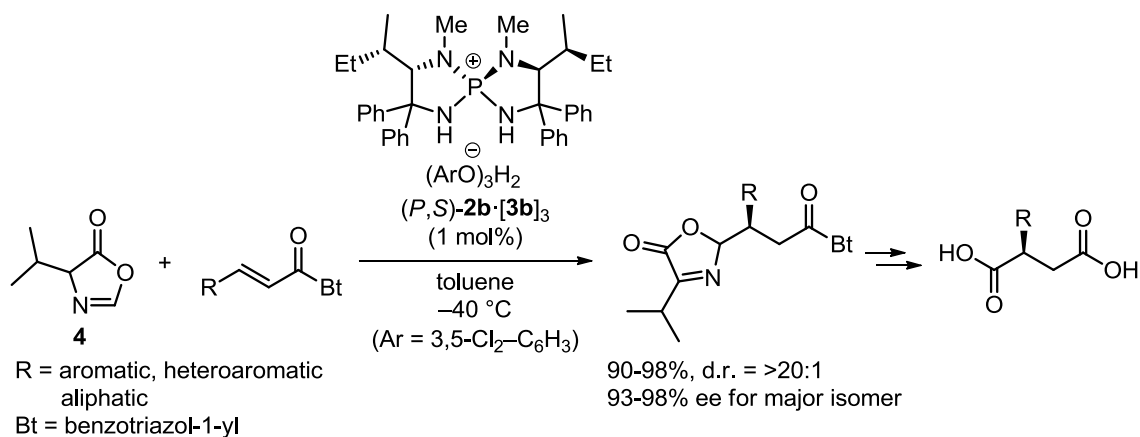


Figure 10.

Furthermore, in solution, the catalyst complex (P,S) -**2b**·**[3b]₃, assembled from L-isoleucine-derived iminophosphorane (P,S) -**2b** and three equivalents of 3,5-dichlorophenol (**3b**), effectively promotes a highly stereoselective conjugate addition of 2-unsubstituted azlactone **4**—an acyl anion equivalent³⁴—to α,β -unsaturated acylbenzotriazoles³⁵ with a broad substrate scope (Scheme 14). The effect of catalyst concentration on the propensity for molecular association in solution was confirmed. As I had assumed, both increased catalyst loading and decreased solvent volume improved enantioselectivity, which also argues the role of requisite molecular assembly. In this system, all structural components of the catalyst assembly, i.e., phosphonium ion, aryloxide, and aryl hydroxide, cooperatively participate in the stereocontrolling event.^{26b,36}**



Scheme 14.

1.8.3 Controlled Assembly of Chiral Tetraaminophosphonium Aryloxide-Arylhydroxide(s) in Solution: Chapter 4

Although the solid-state structure of (P,S) -**2a**·**[3a]₃** was determined by X-ray diffraction

analysis as described above, the actual behavior of this type of supramolecular catalyst in solution remained unclear. The author tackled this important problem using low-temperature ^{31}P NMR, which unexpectedly revealed that (P,S) -**2a** and **3b** selectively assemble into three discrete molecular structures— (P,S) -**2a**·**[3b]**₁, (P,S) -**2a**·**[3b]**₂, and (P,S) -**2a**·**[3b]**₃—in a stepwise manner in solution, depending on the stoichiometry of (P,S) -**2a** and **3b**. These three different assemblies were also isolated as single crystals and their structures were verified by X-ray diffraction analysis (Figure 11). More importantly, this enables a facile and selective generation of a requisite mode of assembly in solution, which could not only amplify the structural diversity of this type of chiral supramolecular catalysts but also constitute a basis for the mechanistic elucidation of their catalyses as demonstrated in actual asymmetric reaction system.^{26d}

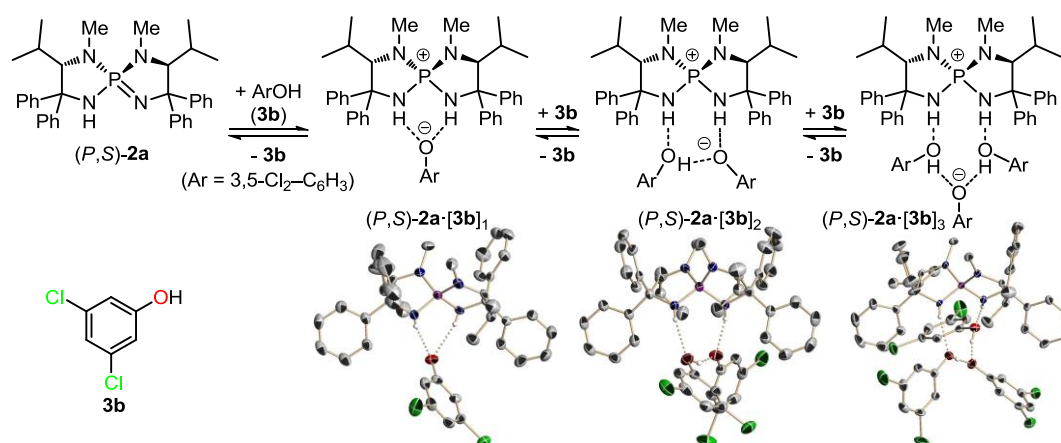
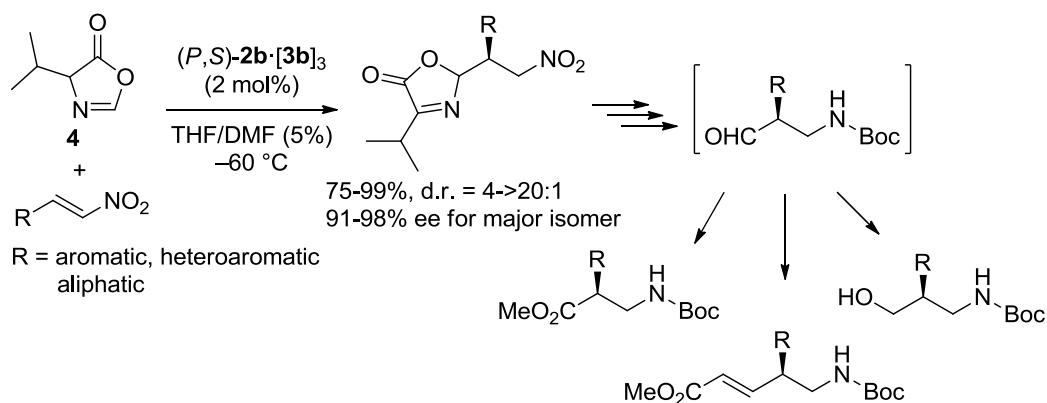


Figure 11.

1.8.4 Catalytic Asymmetric Conjugate Addition of Acyl Anion Equivalent to Nitroolefins: Chapter 5

During the course of our continuous efforts toward further eliciting the potential of our unique supramolecular catalyst system,³⁷ The author was intrigued by the possibility of selectively utilizing a requisite molecular assembly for developing synthetically valuable bond-forming processes and realized a highly enantioselective conjugate addition of 2-unsubstituted azlactone **4** to nitroolefins using (P,S) -**2b**·**[3b]**₃ as a catalyst precursor in a THF/DMF solvent system (Scheme 15).³⁸



Scheme 15.

The success of this transformation relies on two important findings. One is the function of phenolic components of the catalyst as an effective proton donor to the intermediary nitronate **A** (Figure 12).

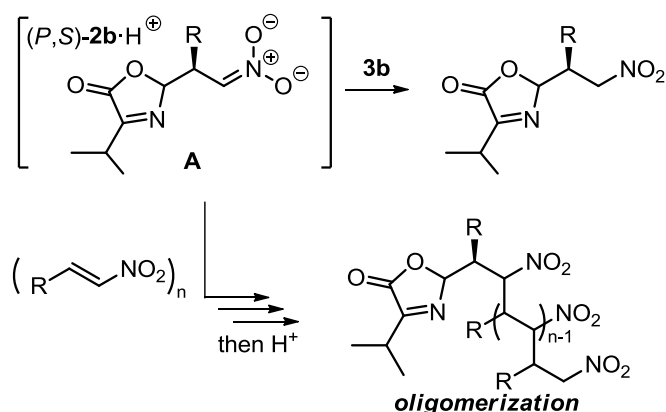


Figure 12. Rapid protonation of the intermediary nitronate and oligomerization pathway.

Thus, addition of more than 6 mol% of **3b** was indispensable for the clean formation of the product by minimizing possible oligomerization. The other is a polarity-dependent mode of the catalyst assembly. When the reaction is performed in toluene, the stereoselectivity was significantly diminished, probably because of the intervention of the molecular assembly of type $(P,S)\text{-}2\mathbf{b}\cdot[\mathbf{3b}]_2\cdot\mathbf{4}$. In contrast, $(P,S)\text{-}2\mathbf{b}\cdot[\mathbf{3b}]_2$ would be predominantly generated from $(P,S)\text{-}2\mathbf{b}\cdot[\mathbf{3b}]_3$ in a polar solvent such as THF and react with **4** to give a more selective intermediate $(P,S)\text{-}2\mathbf{b}\cdot[\mathbf{3b}]_1\cdot\mathbf{4}$ even in the presence of the liberated **3b**, which is necessary as a proton donor for product derivatization (Figure 13). This indicates that the predominant molecular association between $(P,S)\text{-}2\mathbf{b}$ and **3b** in THF is $(P,S)\text{-}2\mathbf{b}\cdot[\mathbf{3b}]_2$ and it is restrained from forming $(P,S)\text{-}2\mathbf{b}\cdot[\mathbf{3b}]_3$ even in the presence of more than two equivalents of **3b**. These phenomena were supported by low temperature ^{31}P NMR analyses of $(P,S)\text{-}2\mathbf{a}\cdot[\mathbf{3b}]_n$ in THF.

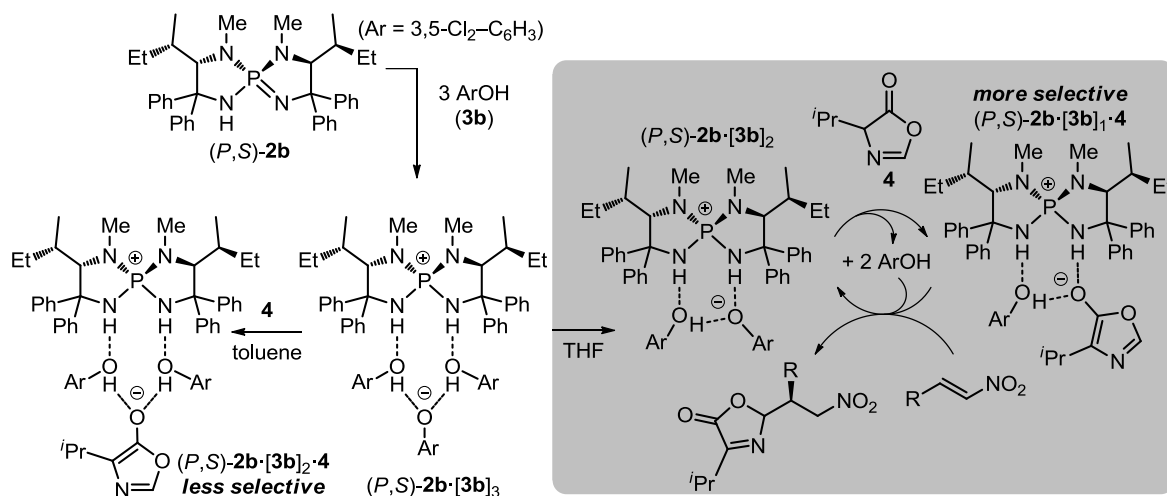


Figure 13. Plausible mode of molecular assembly and reaction mechanism.

The present method was applicable to a wide range of nitroolefins with excellent levels of enantioselectivity. Moreover, the product was easily converted to various optically active amino carbonyl compounds including β^2 -homophenylglycine derivatives, one of the most challenging classes of β^2 -amino acids to be synthesized in a catalytic enantioselective manner (Scheme 15).^{26e,39}

1.9. Conclusion

In these studies, the first ion-pair cooperative catalyses with a unique supramolecular catalyst system have been realized by utilizing the functions of the anion component of the onium salts. This provides a conceptually new approach and an opportunity for the design and evolution of the chiral quaternary onium salt catalysis. Furthermore, the new knowledges, the author have discovered during the course of our efforts toward further eliciting the potential of our unique ion-pair cooperative catalyst system, could represent an important step toward a new direction for the development and applications not only of chiral ion pairs but also of organic molecular catalysis.

References

- (1) (a) *Phase Transfer Catalysis*, 3rd ed.; Dehmlow, E. V.; Dehmlow, S. S., Eds.; Wiley-VCH: Weinheim, Germany, 1993. (b) Starks, C. M.; Liotta, C. L.; Halpern, M. *Phase-Transfer Catalysis*; Chapman & Hall: New York, 1994. (c) *Handbook of Phase-Transfer Catalysis*; Sasson, Y., Neumann, R., Eds.; Blackie Academic & Professional: London, 1997. (d) *Phase-Transfer Catalysis*; Halpern, M. E., Ed.; ACS Symposium Series 659; American Chemical Society: Washington, DC, 1997.
- (2) (a) Dolling, U.-H.; Davis, P.; Grabowski, E. J. J. *J. Am. Chem. Soc.* **1984**, *106*, 446. (b) Hughes, D. L.; Dolling, U.-H.; Ryan, K. M.; Schoenewaldt, E. F.; Grabowski, E. J. J. *J. Org. Chem.* **1987**, *52*, 4745.
- (3) (a) Shioiri, T. In *Handbook of Phase-Transfer Catalysis*; Sasson, Y., Neumann, R., Eds.; Blackie Academic & Professional: London, 1997; Chapter 14. (b) Nelson, A. *Angew. Chem., Int. Ed.* **1999**, *38*, 1583. (c) Shioiri, T.; Arai, S. In *Stimulating Concepts in Chemistry*; Vögtle, F., Stoddart, J. F., Shibasaki, M., Eds.; Wiley-VCH: Weinheim, Germany, 2000; p 123. (d) O'Donnell, M. J. In *Catalytic Asymmetric Syntheses*, 2nd ed.; Ojima, I., Ed.; Wiley-VCH: New York, 2000; Chapter 10. (e) O'Donnell, M. J. *Aldrichim. Acta* **2001**, *34*, 3. (f) Halpern, M. "Phase-Transfer Catalysis" in *Ullmann's Encyclopedia of Industrial Chemistry 2002*, Wiley-VCH, Weinheim. (g) Maruoka, K.; Ooi, T. *Chem. Rev.* **2003**, *103*, 3013. (h) O'Donnell, M. J. *Acc. Chem. Res.* **2004**, *37*, 506. (i) Lygo, B.; Andrews, B. I. *Acc. Chem. Res.* **2004**, *37*, 518. (j) Vachon, J.; Lacour, J. *Chimia* **2006**, *60*, 266. (k) *Asymmetric Phase Transfer Catalysis*; Maruoka, K., Ed.; Wiley-VCH: Weinheim, Germany, 2008. (l) Hashimoto, T.; Maruoka, K. *Chem. Rev.* **2007**, *107*, 5656.
- (4) (a) Ooi, T.; Kameda, M.; Maruoka, K. *J. Am. Chem. Soc.* **1999**, *121*, 6519. (b) Ooi, T.; Kameda, M.; Tannai, H.; Maruoka, K. *Tetrahedron Lett.* **2000**, *41*, 8339. (c) Maruoka, K. *J. Fluorine Chem.* **2001**, *112*, 95. (d) Ooi, T.; Uematsu, Y.; Maruoka, K. *Adv. Synth. Catal.* **2002**, *344*, 288. (e) Ooi, T.; Uematsu, Y.; Maruoka, K. *J. Org. Chem.* **2003**, *68*, 4576. (f) Ooi, T.; Kameda, M.; Maruoka, K. *J. Am. Chem. Soc.* **2003**, *125*, 5139.
- (5) Makosza, M.; Liotta, C. L.; McCoy, S. I. *Phase-Transfer Catalysis Review* **1997**, Issue 2, p.13.
- (6) (a) Ooi, T.; Maruoka, K. *Acc. Chem. Res.* **2004**, *37*, 526. (b) Brière, J.-F.; Oudeyer, S.; Dallab, V.; Levacher, V. *Chem. Soc. Rev.* **2012**, DOI: 10.1039/c1cs15200a.
- (7) (a) Ando, A; Miura, T.; Tatematsu, T.; Shioiri, T. *Tetrahedron Lett.* **1993**, *34*, 1507. (b) Horikawa, M.; Busch-Petersen, J.; Corey, E. J. *Tetrahedron Lett.* **1999**, *40*, 3843. (c) Tozawa, T.; Nagao, H.; Yamane, Y.; Mukaiyama, T. *Chem.-Asian J.* **2007**, *2*, 123-134. (d) Nagao, H.; Kawano, Y.; Mukaiyama, T. *Bull. Chem. Soc. Jpn.* **2007**, *80*, 2406. and

references therein.

- (8) (a) Kosolapoff, G. M. In *Organophosphorus Compounds*, John Wiley & Sons: New York, 1950. (b) *A Guide to Organophosphorus Chemistry*; Quin, L. D., Ed.; John Wiley & Sons: New York, 2000. (c) Wittig, G.; Geissler, G. *Liebigs Ann. Chem.* **1953**, 580, 44. (d) Werner, T. *Adv. Synth. Catal.* **2009**, 351, 1469.
- (9) Phase-transfer catalyst: (a) *Handbook of Phase Transfer Catalysis*, Sasson, Y., Neumann, R., Eds.; Blackie Academic & Professional: London, 1997. (b) Manabe, K. *Tetrahedron* **1998**, 54, 14465. Organic fluoride-ion source: (c) Bohsako, A.; Asakura, C.; Shioiri, T. *Synlett* **1995**, 1033. Lewis acidic promoter: (d) Mukaiyama, T.; Matsui, S.; Kashiwagi, K. *Chem. Lett.* **1989**, 993. (e) Mukaiyama, T.; Kashiwagi, K.; Matsui, S. *Chem. Lett.* **1989**, 1397. (f) McNulty, J. In *Multiphase Homogeneous Catalysis*; Cornils, B., Herrmann, W. A., Horvath, I. T., Leitner, W., Mecking, S., Olivier-Bourbigou, H., Vogt, D., Eds.; Wiley-VCH: New York, 2005; Vol. 2, Chapter 5.2.2.7, p 542-546. (g) Terada, M.; Kouchi, M. *Tetrahedron* **2006**, 62, 401.
- (10) (a) He, R.; Wang, X.; Hashimoto, T.; Maruoka, K. *Angew. Chem., Int. Ed.* **2008**, 47, 9466. (b) He, R.; Ding, C.; Maruoka, K. *Angew. Chem., Int. Ed.* **2009**, 48, 4559. (c) He, R.; Maruoka, K. *Synthesis* **2009**, 2289. (d) Zhu, C.-L.; Zhang, F.-G.; Meng, W.; Nie, J.; Cahard, D.; Ma, J.-A. *Angew. Chem., Int. Ed.* **2011**, 50, 5869.
- (11) Previous studies on (RNH)₄PX-type tetraaminophosphonium salts: (a) Cameron, T. B.; Hanson, H. N.; de la Fuente, G. F.; Huheey, J. E. *Phosphorus, Sulfur, Silicon* **1993**, 78, 37. (b) Schwesinger, R.; Willaredt, J.; Schlemper, H.; Keller, M.; Schmitt, D.; Fritz, H. *Chem. Ber.* **1994**, 127, 2435. (c) Raithby, P. R.; Russell, C. A.; Steiner, A.; Wright, D. S. *Angew. Chem., Int. Ed.* **1997**, 36, 649. (d) Bickely, J. F.; Copesy, M. C.; Jeffry, J. C.; Leedham, A. P.; Russell, C. A.; Stalke, D.; Steiner, A.; Stey, T.; Zacchini, S. *Dalton Trans.* **2004**, 989.
- (12) (a) Schwesinger, R.; Link, R.; Wenzl, P.; Kossek, S.; Keller, M. *Chem. Eur. J.* **2006**, 12, 429. (b) Schwesinger, R.; Link, R.; Wenzl, P.; Kossek, S.; Keller, M. *Chem. Eur. J.* **2006**, 12, 438.
- (13) (a) Uraguchi, D.; Sakaki, S.; Ooi, T. *J. Am. Chem. Soc.* **2007**, 129, 12392. (b) Uraguchi, D.; Ito, T.; Ooi, T. *J. Am. Chem. Soc.* **2009**, 131, 3836. (c) Uraguchi, D.; Ito, T.; Nakamura, S.; Sakaki, S.; Ooi, T. *Chem. Lett.* **2009**, 38, 1052. (d) Uraguchi, D.; Ito, T.; Nakamura, S.; Ooi, T. *Chem. Sci.* **2010**, 1, 488. (e) Uraguchi, D.; Nakamura, S.; Ooi, T. *Angew. Chem., Int. Ed.* **2010**, 49, 7562.
- (14) (a) Wey, S. J.; O'Connor, K. J.; Burrows, C. J. *Tetrahedron Lett.* **1993**, 34, 1905. (b) Ohkuma, T.; Ooka, H.; Hashiguchi, S.; Ikariya, T.; Noyori, R. *J. Am. Chem. Soc.* **1995**, 117, 2675.
- (15) Uraguchi, D.; Sakaki, S.; Ueki, Y.; Ito, T.; Ooi, T. *Heterocycles* **2008**, 76, 1081.

- (16) Recent reviews on the asymmetric Henry reaction: (a) Boruwa, J.; Gogoi, N.; Saikia, P. P.; Barua, N. C. *Tetrahedron: Asymmetry* **2006**, *17*, 3315. (b) Palomo, C.; Oiarbide, M.; Laso, A. *Eur. J. Org. Chem.* **2007**, 2561.
- (17) (a) Nitabaru, T.; Kumagai, N.; Shibasaki, M. *Tetrahedron Lett.* **2008**, *49*, 272. (b) Handa, S.; Nagawa, K.; Sohtome, Y.; Matsunaga, S.; Shibasaki, M. *Angew. Chem., Int. Ed.* **2008**, *47*, 3230. (c) Blay, G.; Domingo, L. R.; Hernández-Olmos, V.; Pedro, J. R. *Chem. Eur. J.* **2008**, *14*, 4725. (d) Sohtome, Y.; Kato, Y.; Handa, S.; Aoyama, N.; Nagawa, K.; Matsunaga, S.; Shibasaki, M. *Org. Lett.* **2008**, *10*, 2231. (e) Ube, H.; Terada, M. *Bioorg. Med. Chem. Lett.* **2009**, *19*, 3895. (f) Nitabaru, T.; Nojiri, A.; Kobayashi, M.; Kumagai, N.; Shibasaki, M. *J. Am. Chem. Soc.* **2009**, *131*, 13860.; for the use of silyl nitronate, see: (g) Ooi, T.; Doda, K.; Maruoka, K. *J. Am. Chem. Soc.* **2003**, *125*, 2054.; for enzymatic approaches, see: (h) Purkarthofer, T.; Gruber, K.; Gruber-Khadjawi, M.; Waich, K.; Skranc, W.; Mink, D.; Griengl, H. *Angew. Chem., Int. Ed.* **2006**, *45*, 3454. (i) Gruber-Khadjawi, M.; Purkarthofer, T.; Skranc, W.; Griengl, H. *Adv. Synth. Catal.* **2007**, *349*, 1445.
- (18) Basicity of iminophosphoranes: (a) Kaljurand, I.; Kütt, A.; Sooväli, L.; Rodima, T.; Mäemets, V.; Leito, I.; Koppel, I. A. *J. Org. Chem.* **2005**, *70*, 1019. (b) Kovačević, B.; Maksić, Z. B. *Chem. Commun.* **2006**, 1524.
- (19) Synthetic application of a phosphazene as a base catalyst: (a) Bensa, D.; Constantieux, T.; Rodriguez, J. *Synthesis* **2004**, 923. (b) Imahori, T.; Hori, C.; Kondo, Y. *Adv. Synth. Catal.* **2004**, *346*, 1090.
- (20) Uraguchi, D.; Nakashima, D.; Ooi, T. *J. Am. Chem. Soc.* **2009**, *131*, 7242.
- (21) For selected recent reviews on Brønsted acid catalysis, see: (a) Doyle, A. G.; Jacobsen, E. N. *Chem. Rev.* **2007**, *107*, 5713. (b) Akiyama, T. *Chem. Rev.* **2007**, *107*, 5744. (c) Yu, X.; Wang, W. *Chem. Asian J.* **2008**, *3*, 516. (d) Terada, M. *Synthesis* **2010**, 1929.
- (22) (a) Nishida, H.; Takada, N.; Yoshimura, M.; Sonods, T.; Kobayashi, H. *Bull. Chem. Soc. Jpn.* **1984**, *57*, 2600. (b) Brookhart, M.; Grant, B.; Volpe, A. F. Jr. *Organometallics*, **1992**, *11*, 3920. (c) Yakelis, N. A.; Bergman, R. G. *Organometallics*, **2005**, *24*, 3579. (d) Annamalai, V. R.; Linton, E. C.; Kozlowski, M. C. *Org. Lett.* **2009**, *11*, 621.
- (23) (a) Schuster, T.; Bauch, M.; Dürner, G.; Göbel, M. W. *Org. Lett.* **2000**, *2*, 179. (b) Schuster, T.; Kurz, M.; Göbel, M. W. *J. Org. Chem.* **2000**, *65*, 1697. (c) Tsogoeva, S. B.; Dürner, G.; Bolte, M.; Göbel, M. W. *Eur. J. Org. Chem.* **2003**, 1661. (d) Huang, J.; Corey, E. *J. Org. Lett.* **2004**, *6*, 5027. (e) Akalay, D.; Dürner, G.; Bats, J. W.; Bolte, M.; Göbel, M. W. *J. Org. Chem.* **2007**, *72*, 5618. (f) Uyeda, C.; Jacobsen, E. N. *J. Am. Chem. Soc.* **2008**, *130*, 9228.
- (24) Examples for chiral counteranion strategy in catalytic asymmetric syntheses: (a) Mayer, S.;

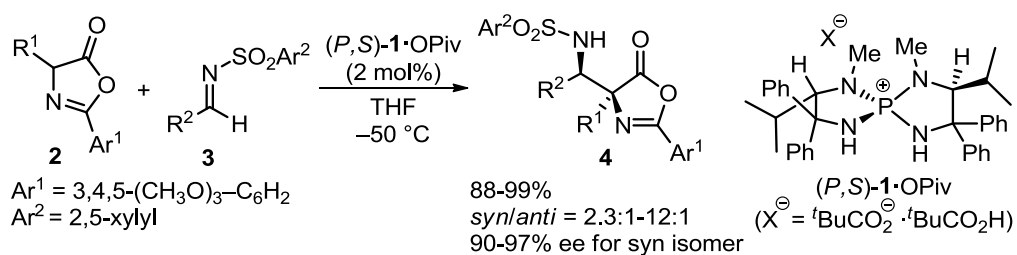
- List, B. *Angew. Chem., Int. Ed.* **2006**, *45*, 4193. (b) Hamilton, G. L.; Kang, E. J.; Mba, M.; Toste, F. D. *Science* **2007**, *317*, 496. (c) Rueping, M.; Antonchick, A. R.; Brinkmann, C. *Angew. Chem., Int. Ed.* **2007**, *46*, 6903. (d) Raheem, I. T.; Thiara, P. S.; Peterson, E. A.; Jacobsen, E. N. *J. Am. Chem. Soc.* **2007**, *129*, 13404. (e) Wang, X.; List, B. *Angew. Chem., Int. Ed.* **2008**, *47*, 1119. There are numbers of important reports on anion effect in the catalysis of chiral amines, which involves protonated ammonium salts; see for example : Mase, N.; Tanaka, F.; Barbas, C. F., III *Angew. Chem., Int. Ed.* **2004**, *43*, 2420.
- (25) (a) Uraguchi, D.; Koshimoto, K.; Ooi, T. *J. Am. Chem. Soc.* **2008**, *130*, 10878. (b) Uraguchi, D.; Koshimoto, K.; Ooi, T. *Chem. Commun.* **2010**, *46*, 300. (c) Uraguchi, D.; Koshimoto, K.; Sanada, C.; Ooi, T. *Tetrahedron: Asymmetry* **2010**, *21*, 1189. (d) Uraguchi, D.; Koshimoto, K.; Miyake, S.; Ooi, T. *Angew. Chem., Int. Ed.* **2010**, *49*, 5567.
- (26) (a) Uraguchi, D.; Ueki, Y.; Ooi, T. *J. Am. Chem. Soc.* **2008**, *130*, 14088. (b) Uraguchi, D.; Ueki, Y.; Ooi, T. *Science* **2009**, *326*, 120. (c) Uraguchi, D.; Ueki, Y.; Ooi, T. *Catalysts and Catalysis*, **2010**, *52*, 509-514. (d) Uraguchi, D.; Ueki, Y.; Ooi, T. *Angew. Chem., Int. Ed.* **2011**, *50*, 3681-3683. (e) Uraguchi, D.; Ueki, Y.; Ooi, T. *Chem. Sci.* **2012**, *3*, DOI: 10.1039/c1sc00678A.
- (27) (a) Uraguchi, D.; Asai, Y.; Ooi, T. *Angew. Chem., Int. Ed.* **2009**, *48*, 733. (b) Uraguchi, D.; Asai, Y.; Seto, Y.; Ooi, T. *Synlett* **2009**, 658.
- (28) Tozawa, T.; Nagao, H.; Yamane, Y.; Mukaiyama, T. *Chem. Asian J.* **2007**, *2*, 123.
- (29) For reviews on organocatalyzed Mannich-type reactions, see: (a) Ting, A.; Schaus, S. E. *Eur. J. Org. Chem.* **2007**, 5797. (b) Verkade, J. M. M.; van Hemert, L. J. C.; Quaedflieg, P. J. L. M.; Rutjes, F. P. J. T. *Chem. Soc. Rev.* **2008**, *37*, 29.
- (30) (a) Fisk, J. S.; Mosey, R. A.; Tepe, J. J. *Chem. Soc. Rev.* **2007**, *36*, 1432. (b) Cabrera, S.; Reyes, E.; Alemán, J.; Milelli, A.; Kobbelgaard, S.; Jørgensen, K. A. *J. Am. Chem. Soc.* **2008**, *130*, 12031.
- (31) Review on α,β -diamino acids: Viso, A.; de la Pradilla, R. F.; García, A.; Flores, A. *Chem. Rev.* **2005**, *105*, 3167.
- (32) (a) *Supramolecular Catalysis*; van Leeuwen, P. W. N. M., Ed.; Wiley-VCH, Weinheim, 2008. (b) *Supramolecular Chemistry*, 2nd ed.; Steed, J. W.; Atwood, J. L., Eds.; Wiley, New York, 2009.
- (33) (a) Saenger, W. *Nature* **1979**, *279*, 343. (b) Mautner, M. *Chem. Rev.* **2005**, *105*, 213. (c) Yamamoto, H.; Futatsugi, K. *Angew. Chem., Int. Ed.* **2005**, *44*, 1924.
- (34) Barco, A.; Benetti, S.; De Risi, C.; Pollini, G. P.; Spalluto, G.; Zanirato, V. *Tetrahedron* **1996**, *52*, 4719.
- (35) Katritzky, A. R.; Zang, Y.; Singh, S. K. *Synthesis* **2003**, 2795.
- (36) Rix, D.; Lacour, J. *Angew. Chem., Int. Ed.* **2010**, *49*, 1918.

- (37) (a) Yoshizawa, M.; Klosterman, J. K.; Fujita, M. *Angew. Chem., Int. Ed.* **2009**, *48*, 3418.
(b) Breit, B.; Seiche, W. *J. Am. Chem. Soc.* **2003**, *125*, 6608. (c) Slagt, V. F.; van Leeuwen, P. W. N. M.; Reek, J. N. H. *Chem. Commun.* **2003**, 2474. For review, see: Meeuwissen, J.; Reek, J. N. H. *Nat. Chem.* **2010**, *2*, 615.
- (38) For review on the asymmetric conjugate addition to nitroolefins, see: Berner, O. M.; Tedeschi L.; Enders, D. *Eur. J. Org. Chem.* **2002**, 1877. 7. Only two examples of the stereoselective conjugate addition of 2,4-disubstituted azlactones to nitroalkenes at 2-position were reported. See: (a) Alemán, J.; Milelli, A.; Cabrera, S.; Reyes E.; Jørgensen, K. A. *Chem. Eur. J.* **2008**, *14*, 10958. (b) Balaguer, A.-N.; Companyó, X.; Calvet, T.; Font-Bardía, M.; Moyano A.; Rios, R. *Eur. J. Org. Chem.* **2009**, 199.
- (39) (a) Seebach, D.; Beck, A. K.; Capone, S.; Deniau, G.; Grošelj, U.; Zass, E. *Synthesis*, **2009**, 1. (b) Weiner, B.; Szymański, W.; Janssen, D. B.; Minnaard, A. J.; Feringa, B. L. *Chem. Soc. Rev.* **2010**, *39*, 1656.

Chapter 2

Chiral Tetraaminophosphonium Carboxylate-Catalyzed Direct Mannich-Type Reaction

Abstract:

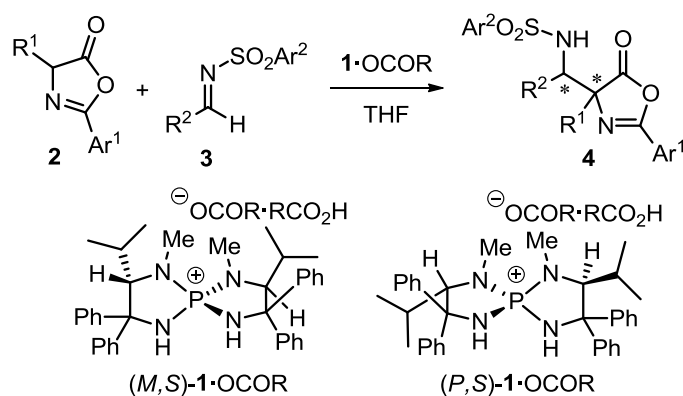


The cooperative asymmetric catalysis of chiral tetraaminophosphonium carboxylate (*P,S*)-**1**·OCOR has been established and its synthetic utility has been successfully demonstrated by the application to the highly enantioselective direct Mannich-type reaction of azlactones with *N*-sulfonyl imines. The present study would stimulate to cultivate the potential of the chiral quaternary onium salt catalysis by the structural modification of organic anion.

1. Introduction

Organic ion pair catalysis, particularly that involves chiral, non-racemic onium salts, occupies a unique place in the recent development of organic molecular catalysis,¹ and its characteristic features have attracted significant attention from industrial and academic communities. In the catalysis of chiral quaternary onium salts, the cation structure is regarded as the most important element for controlling reactivity and selectivity. Accordingly, a catalyst manifold has been created for different types of reactions such as a phase-transfer-catalyzed bond formation by the modification of a cationic moiety.² Although the anion part of the salts is essential for neutralizing the charge, it is hardly associated with the overall efficiency and/or stereoselectivity in the targeted transformation because of the multiple ion-exchange processes. Even in the case of chiral onium salts bearing Lewis basic anions, their roles have been restricted to the activation of silyl nucleophiles for initiating the catalysis.^{3,4} Thus, the inherent etic relevance of incorporating tunable, functional anions to the parent *quaternary* onium salts is yet to be explored.⁵

In this context, the author is interested in the possibility of establishing a novel catalysis of chiral quaternary onium salts possessing an appropriate organic anion, which can be controlled not only by the structural manipulation of the cation but also by that of the initial anion through its continuous participation in the catalytic cycle. Herein, the author report such an asymmetric catalysis of chiral tetraaminophosphonium carboxylate **1**·OCOR and demonstrate its utility in the highly enantioselective direct Mannich-type reaction of azlactones (Scheme 1).



Scheme 1

At the outset of our study, the author sought to employ our recently developed [5,5]-*P*-spirocyclic tetraaminophosphonium framework as a primary structure of the key onium ion and carboxylate as an organic counter anion.⁶ Considering the general basicity of the carboxylate anion,⁷ the author selected the direct and stereoselective Mannich-type reaction⁸ of oxazol-5-(4*H*)-one (**2**), i.e., azlactone,⁹ with sulfonyl imine **3** in order to evaluate the salt

catalysis.¹⁰ The author also recognized that this particular Mannich-type protocol could provide new access to differently protected, optically active α,β -diamino acids with an α -tetrasubstituted carbon stereocenter.^{11,12}

In an illustration of the expected catalytic cycle (Figure 1), a basic carboxylate anion would abstract the active methine proton of azlactone to give the corresponding chiral phosphonium enolate. To achieve high levels of enantiocontrol, enforcing the geometrically identical ion-pairing seemed to be important. This led us to presume that use of partially yet selectively alkylated aminophosphonium cation such as **1** could minimize the mode of the secondary interaction between the phosphonium cation and the enolate anion, thereby rendering the ion pair assembly with a defined hydrogen-bonding network (**A**). Subsequent stereo-selective bond formations with imine would afford phosphonium sulfonamide **B** that could be rapidly protonated by carboxylic acid to regenerate the chiral phosphonium carboxylate.

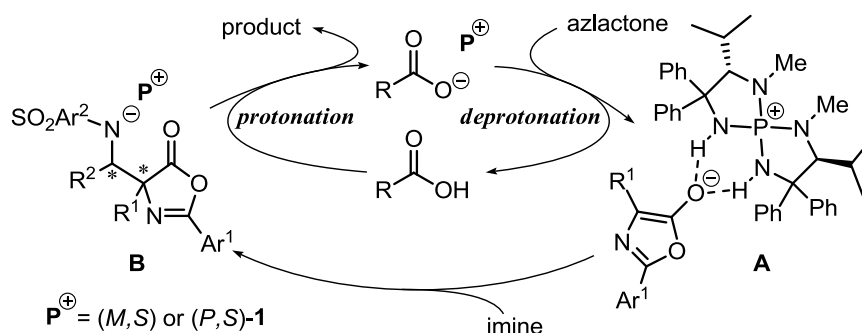


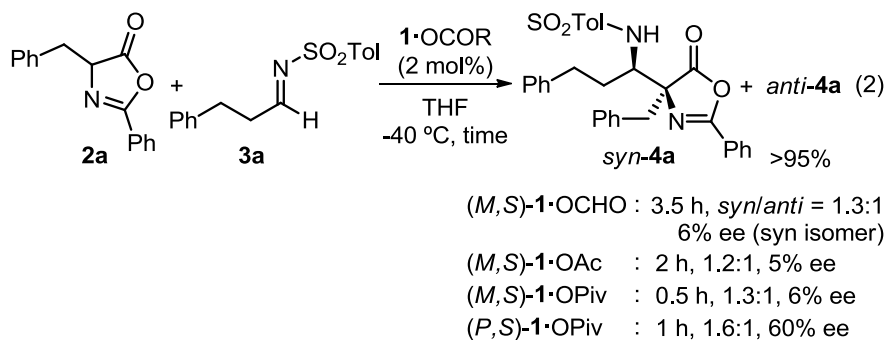
Figure 1. Working hypothesis for the salt catalysis of **1**·OCOR.

2. Result and Discussion

2.1. Effect of Catalyst Components on Reactivity and Selectivity.

Initial experiments to examine this hypothesis were conducted by treating phenylalanine-derived azlactone **2a** with *N*-tosyl imine **3a** in the presence of chiral aminophosphonium formate (*M,S*)-**1**·OCHO (2 mol%), readily prepared from (*M,S*)-**1**·Cl through ion-exchange, in THF at -40 °C (Scheme 2). After 3.5 h of stirring, the desired Mannich adduct **4a** was obtained near quantitatively with *syn/anti* ratio of 1.3:1 (6% ee for the major *syn* isomer). Interestingly, tuning the basicity of the anionic component by changing it to acetate [(*M,S*)-**1**·OAc] and then to pivalate [(*M,S*)-**1**·OPiv] led to a substantial rate enhancement though the stereoselectivities were virtually unaffected.⁷ This observation strongly suggested the intervention of the expected protonation-deprotonation sequence.

Another intriguing observation was that the enantioselectivity was dramatically improved by simply switching the chirality of the phosphorous center of the catalyst, and *syn-4a* was obtained in 60% ee under the influence of (*P,S*)-**1**·OPiv.¹³



Scheme 2.

The origin of this quantum leap of the enantioselectivity could be ascribed to the difference in the hydrogen-bonding manner depending on the *P*-spiro chirality of **1** as revealed by the single crystal X-ray diffraction analyses of (*M,S*)- and (*P,S*)-**1**·Cl (Figure 2). While the two N-H protons of the (*M,S*)-isomer are mutually disposed in opposite directions, and interact with chloride anion and water molecule, respectively, those of the (*P,S*)-isomer are oriented in the same side, capturing the anion simultaneously. The latter, more structured ion-pairing assisted by the double hydrogen-bonding would be crucial for inducing high selectivity.

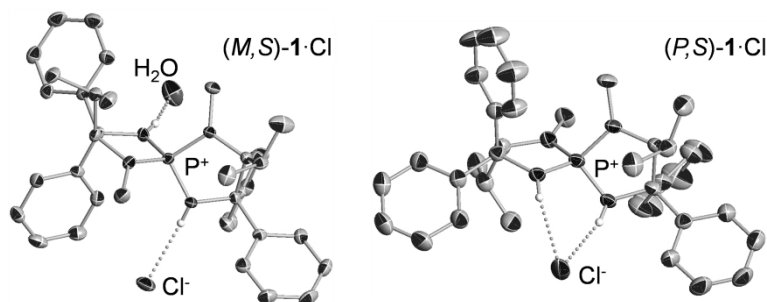


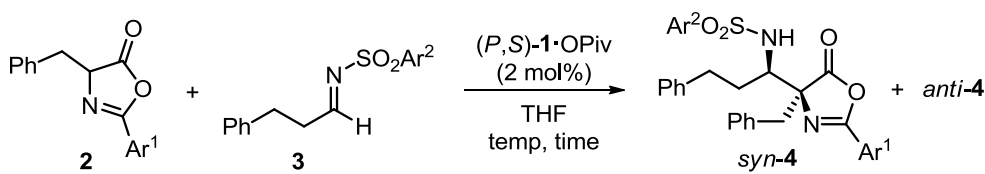
Figure 2. ORTEP diagrams of (*M,S*)- and (*P,S*)-**1**·Cl (all calculated hydrogens and a solvent molecule were omitted for clarity).

2.2. Effect of Protective Group (Ar^1, Ar^2) on Stereoselectivity, and Optimization of Reaction Conditions.

Further optimization was made by examining the effect of the aromatic substituents (Ar^1, Ar^2) in the substrates **2** and **3**. With respect to azlactone **2**, the introduction of more electron-donating, methoxy-substituted phenyl groups enhanced enantioselectivity (entries 1-3

in Table 1). This can be understood by assuming the formation of a tighter ion pair as a consequence of the increased electron density on the oxygen of the enolate of **3**.¹⁴ Moreover, the subsequent screening of the sulfonyl substituent on the imine nitrogen in the reactions with **3** possessing 3,4,5-trimethoxyphenyl moiety revealed its significant impact on the stereoselectivity. A synthetically useful diastereoselectivity and an excellent enantioselectivity were attained when 2,5-xylylsulfonyl imine was employed (entries 3-6). Finally, decreasing the reaction temperature to $-50\text{ }^{\circ}\text{C}$ enabled the highest level of stereochemical control (entry 7).

Table 1. Effect of protective groups (Ar^1 , Ar^2) on stereoselectivity^a.



| entry | Ar^1 (2) | Ar^2 (3) | time (h) | yield ^b (%) | dr ^c (<i>syn/anti</i>) | ee ^d (%) | prod 4 |
|----------------|---|----------------------|-------------|---------------------------|--|------------------------|------------------|
| 1 | 4- $\text{CH}_3\text{O}-\text{C}_6\text{H}_4$ | 4-tolyl | 7 | 97 | 2.2:1 | 64 | 4b |
| 2 | 2- $\text{CH}_3\text{O}-\text{C}_6\text{H}_4$ | | 30 | 89 | 2.2:1 | 65 | 4c |
| 3 | 3,4,5- $(\text{CH}_3\text{O})_3-\text{C}_6\text{H}_2$ | | 5 | 98 | 2.6:1 | 75 | 4d |
| 4 | | mesityl | 9 | 99 | 2.9:1 | 93 | 4e |
| 5 | | 2,4-xylyl | 9 | 97 | 4.5:1 | 96 | 4f |
| 6 | | 2,5-xylyl | 9 | 95 | 6.7:1 | 95 | 4g |
| 7 ^e | | | 20 | 99 | 7.1:1 | 97 | |

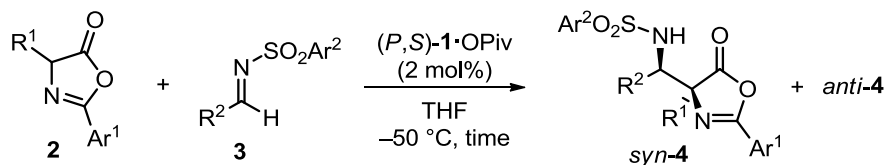
^aUnless otherwise noted, reactions were performed at $-40\text{ }^{\circ}\text{C}$ using (*P,S*)-**1**-OPiv as a catalyst. See Experimental Section for details. ^bIsolated yield. ^cDetermined by ^1H NMR analysis of crude reaction mixture. ^dEnantiomeric excess of *syn* isomer, which was determined by chiral HPLC analysis. Absolute configuration of **4g** was determined to be (*2S,3R*) by X-ray diffraction analysis after hydrolysis of azlactone, and the configurations of the other products were assigned on the analogy. ^eReaction was conducted at $-50\text{ }^{\circ}\text{C}$.

2.3. Substrate Scope and Deprotection of the Adduct.

Experiments were then conducted to probe the scope of the present (*P,S*)-**1**-OPiv-catalyzed, asymmetric direct Mannich-type protocol. The representative results are listed in Table 2. A variety of aliphatic imines having different substitution patterns are well accommodated,¹⁵ and even the reaction with sulfonyl imine derived from acetaldehyde proceeds smoothly in a highly

stereoselective manner (entries 1-7). Not only phenylalanine- but also other α -amino acid-derived azlactones are employable as nucleophilic reacting partners (entries 8 and 9).

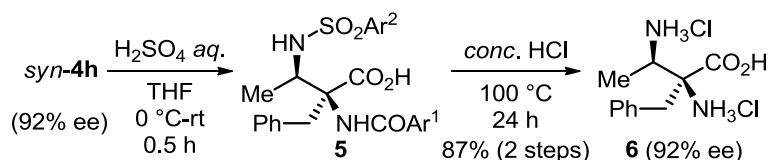
Table 2. Substrate scope of the direct Mannich-type reaction of azlactone^a ($\text{Ar}^1 = 3,4,5\text{-(CH}_3\text{O)}_3\text{-C}_6\text{H}_2$, $\text{Ar}^2 = 2,5\text{-xylyl}$).



| entry | R ¹ (2) | R ² (3) | time (h) | yield ^b (%) | dr ^c (<i>syn/anti</i>) | ee ^d (%) | prod 4 |
|-------|---|--|-------------|---------------------------|--|------------------------|-----------|
| 1 | PhCH ₂ | CH ₃ | 12 | 91 | 4.5:1 | 92 | 4h |
| 2 | | CH ₃ (CH ₂) ₇ | 20 | 92 | 6.6:1 | 96 | 4i |
| 3 | | CH ₂ =CH(CH ₂) ₈ | 21 | 99 | 7.6:1 | 96 | 4j |
| 4 | | PhCH ₂ OCH ₂ | 14 | 98 | 5.3:1 | 95 | 4k |
| 5 | | PhCO ₂ CH ₂ | 24 | 88 | 12:1 | 93 | 4l |
| 6 | | (CH ₃) ₂ CHCH ₂ | 17 | 94 | 4.4:1 | 95 | 4m |
| 7 | | ^c Hex | 37 | 98 | 2.3:1 | 90 | 4n |
| 8 | (CH ₃) ₂ CHCH ₂ | PhCH ₂ CH ₂ | 15 | 99 | 7.8:1 | 96 | 4o |
| 9 | CH ₃ OCH ₂ | | 14 | 97 | 3.1:1 | 90 | 4p |

^aReactions were performed at $-50\text{ }^\circ\text{C}$ with $(P,S)\text{-1-OPiv}$ as a catalyst, see Experimental Section for details. ^{b-d}See footnotes in, Table 1.

The Mannich adduct **4** can easily be converted into the corresponding α,β -diamino acid dihydrochloride **6** in two steps without the loss of enantiopurity. For instance, the treatment of diastereomerically pure *syn*-**4h** (92% ee) with aqueous H₂SO₄ in THF quantitatively afforded the corresponding carboxylic acid. Complete deprotection was then achieved by simple acidic hydrolysis with hydrochloric acid at $100\text{ }^\circ\text{C}$, and subsequent purification through an ion-exchange resin (Amberlite IR120, H⁺ form) gave **6** in 87% yield (92% ee) (Scheme 1).¹⁶



Scheme 1. Deprotection of *syn*-**4h** to α,β -diamino acid dihydrochloride ($\text{Ar}^1 = 3,4,5\text{-(CH}_3\text{O)}_3\text{-C}_6\text{H}_2$, $\text{Ar}^2 = 2,5\text{-xylyl}$)

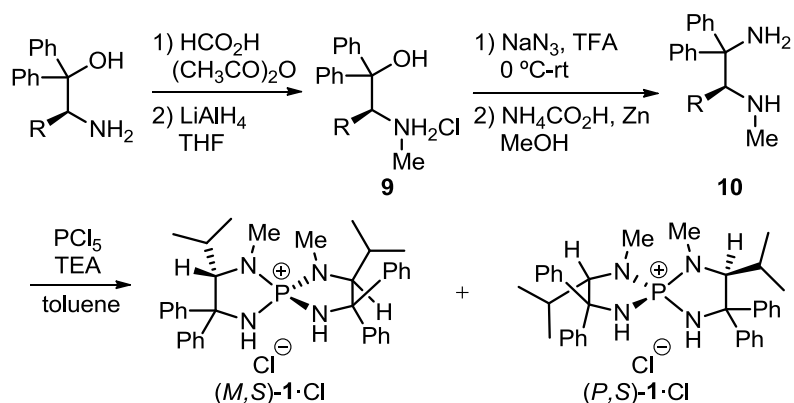
3. Conclusion.

In conclusion, the cooperative asymmetric catalysis of chiral tetraaminophosphonium carboxylate has been presented and its synthetic utility has been successfully demonstrated by the application to the highly enantioselective direct Mannich-type reaction of azlactones with *N*-sulfonyl imines. Further studies based on this concept will be reported in due course.

4. Experimental Section

General Information: Infrared spectra were recorded on a JASCO FT/IR-300E spectrometer. ^1H NMR spectra were recorded on a Varian INOVA-500 (500 MHz) or INOVA-700 (700 MHz) spectrometer. Chemical shifts are reported in ppm from the solvent resonance (D_2O ; 4.79 ppm, CD_3OD ; 3.31 ppm) or tetramethylsilane (0.0 ppm) resonance as the internal standard (CDCl_3). Data are reported as follows: chemical shift, integration, multiplicity (s = singlet, d = doublet, t = triplet, q = quartet, quin = quintet, m = multiplet, br = broad) and coupling constants (Hz). ^{13}C NMR spectra were recorded on a Varian INOVA-500 (126 MHz) or INOVA-700 (175 MHz) spectrometer with complete proton decoupling. Chemical shifts are reported in ppm from the solvent resonance as the internal standard (CDCl_3 ; 77.16 ppm, CD_3OD ; 49.0 ppm, $(\text{CD}_3)_2\text{SO}$; 39.52 ppm). ^{31}P NMR spectra were recorded on a Varian Mercury-300BB (121 MHz) spectrometer with complete proton decoupling. Chemical shifts are reported in ppm from H_3PO_4 (0.0 ppm) resonance as the external standard. Optical rotations were measured on a JASCO DIP-1000 polarimeter. The high resolution mass spectra were conducted at the Research Center for Materials Science, Graduate School of Science, Nagoya University. Analytical thin layer chromatography (TLC) was performed on Merck precoated TLC plates (silica gel 60 GF₂₅₄, 0.25 mm). Flash column chromatography was performed on silica gel 60 (spherical, 40-50 μm ; Kanto Chemical Co., Inc.). Enantiomeric excesses were determined by HPLC analysis using chiral columns (ϕ 4.6 mm x 250 mm, DAICEL CHIRALPAK IA (IA) or CHIRALPAK IC (IC)).

Tetrahydrofuran (THF) were supplied from Kanto Chemical Co., Inc. as “Dehydrated solvent system”. Tetraaminophosphonium salts,¹⁷ azlactones,¹⁸ and imines¹⁹ were prepared by following the literature procedure. Other simple chemicals were purchased and used as such.



Procedure to Prepare Tetraaminophosphonium Salt 1-Cl:

Preparation of *N*-Me Amino Alcohol Hydrochloride 9: The mixture of formic acid (1.3 mL) and acetic anhydride (3.3 mL) was warmed to 60 °C and stirred for 5 h. To the solution was added amino alcohol (2.55 g, 10 mmol) and the reaction mixture was stirred for 0.5 h at room temperature. Resulting solution was diluted with chloroform and the organic phase was washed twice with sat. NaHCO₃ aqueous solution and brine. White solid of almost pure *N*-formyl amino alcohol was obtained by evaporation of all volatile. A THF solution of the *N*-formyl amino alcohol (7 mL) was added to a suspension of LiAlH₄ (0.76 g, 20 mmol) in THF (10 mL) at 0 °C. The reaction mixture was refluxed for 12 h and then cooled to 0 °C. After diluting the mixture with ether, water (0.76 mL), 15% NaOH aq. (0.76 mL), and water (2.2 mL) was sequentially added to the mixture for giving white precipitate. Filtrate was concentrated and the residue was purified by silica gel chromatography (hexane (H)/ethyl acetate (EA) = 2/1) to afford *N*-methyl amino alcohol. Its ammonium salt **9** (2.9 g) was simply prepared by treatment of the amino alcohol with 1N HCl/MeOH following concentration.

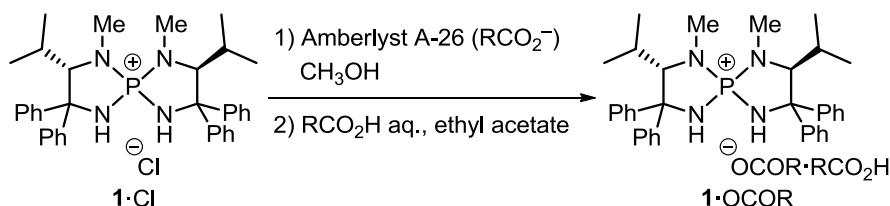
Preparation of *N*-Me Diamine 10: To a solution of NaN₃ (1.63 g, 15 mmol) in TFA (25 mL) was slowly added *N*-Me amino alcohol hydrochloride **9** (1.53 g, 5 mmol) at 0 °C and the reaction mixture was allowed to warm up to room temperature gradually (for ca. 4 h). Resulting slurry was poured onto ice and the aqueous solution thus obtained was neutralized by NaOH pellet. The aqueous phase was extracted with EA and the combined organic phase was washed with brine, dried over Na₂SO₄, and filtered. All volatiles were removed by evaporation to give almost pure amino azide. The crude amino azide was dissolved into MeOH (5 mL) and ammonium formate (0.63 g, 10 mmol) and zinc powder (0.65 g, 10 mmol) was introduced to the solution at room temperature. After being stirred for 2 h, resulting suspension was filtered through a pad of Celite and the filtrate was concentrated. EA was added to the residue and the organic phase was washed with a 4:1 mixture of 1 N NaOH aq. and 2 N EDTA·2Na aq. and then brine. Purification of the crude residue with silica gel column chromatography (H/EA = 1/2) was performed to give diamine **10** (1.1 g) as a colorless viscous oil.

Preparation of Tetraaminophosphonium Salt 1·Cl: To a solution of Et₃N (1 mL, 7.5 mmol) and diamine **10** (0.81 g, 3 mmol) in toluene (7.5 mL) was introduced a solution of PCl₅ (0.31 g, 1.5 mmol) in toluene (7.5 mL) at 110 °C and the reaction mixture was stirred for 18 h under reflux. A chloroform solution of residual solid obtained by concentration of the mixture was washed with 1 N HCl aq. and organic phase was dried over NaSO₄. The crude materials were purified by silica gel chromatography (EA/MeOH = 10/1) to furnish two diastereomers of phosphonium salt as white solid ((*M,S*): 0.20g, 22%; (*P,S*): 0.54g, 60%). Further purification of the salt was usually performed by recrystallization (H/acetone).

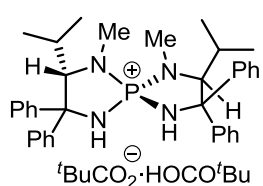
Characterization of Phosphonium Salts:

(*M,S*)-1·Cl: ¹H NMR (500 MHz, CD₃OD) δ 7.52-7.46 (8H, m), 7.41 (2H, t, *J* = 7.0 Hz), 7.27-7.20 (10H, m), 4.09 (2H, dd, *J*_{P-H} = 21.0 Hz, *J*_{H-H} = 7.0 Hz), 3.11 (6H, d, *J*_{P-H} = 9.5 Hz), 1.89 (2H, octet, *J* = 7.0 Hz), 1.07 (6H, d, *J* = 7.0 Hz), 0.55 (6H, d, *J* = 7.0 Hz), N-H protons were not found due to deuterium exchange; ¹³C NMR (126 MHz, CDCl₃) δ 145.7, 139.6 (d, *J*_{P-C} = 11.5 Hz), 129.3, 128.4, 128.1, 127.9, 127.6, 126.5, 72.4 (d, *J*_{P-C} = 12.5 Hz), 70.2 (d, *J*_{P-C} = 9.7 Hz), 35.7 (d, *J*_{P-C} = 5.5 Hz), 30.2, 22.7, 18.7; ³¹P NMR (121 MHz, CDCl₃) δ 35.6; IR (KBr): 3157, 2965, 1446, 1398, 1192, 1064, 1035, 1009, 759, 718 cm⁻¹; HRMS (FAB) Calcd for C₃₆H₄₄N₄P⁺ ([M-Cl]⁺) 563.3304. Found 563.3286; [α]_D²⁷ -324.9° (c = 0.51, CHCl₃).

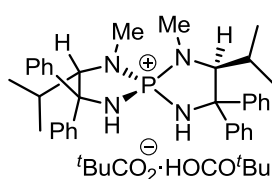
(*P,S*)-1·Cl: ¹H NMR (500 MHz, CDCl₃) δ 7.75 (2H, d, *J* = 16.0 Hz), 7.68 (4H, brs), 7.60 (4H, dd, *J* = 8.0, 1.0 Hz), 7.38 (4H, t, *J* = 8.0 Hz), 7.33 (4H, t, *J* = 8.0 Hz), 7.26 (2H, t, *J* = 8.0 Hz), 7.20 (2H, t, *J* = 8.0 Hz), 3.80 (2H, dd, *J*_{P-H} = 21.5 Hz, *J*_{H-H} = 5.0 Hz), 2.08 (2H, sept-d, *J* = 6.5, 5.0 Hz), 1.81 (6H, d, *J*_{P-H} = 10.0 Hz), 1.05 (6H, d, *J* = 6.5 Hz), 0.56 (6H, d, *J* = 6.5 Hz); ¹³C NMR (125 MHz, CDCl₃) δ 148.0, 139.5 (d, *J*_{P-C} = 11.4 Hz), 128.8, 128.6, 127.7, 127.5, 126.9, 73.4 (d, *J*_{P-C} = 13.3 Hz), 71.0 (d, *J*_{P-C} = 9.6 Hz), 32.3 (d, *J*_{P-C} = 5.9 Hz), 29.6, 23.1, 19.0, one carbon was not found probably due to overlapping; ³¹P NMR (121 MHz, CDCl₃) δ 38.8; IR (KBr): 3059, 2959, 1704, 1447, 1369, 1335, 1192, 1173, 1025, 752 cm⁻¹; HRMS (FAB) Calcd for C₃₆H₄₄N₄P⁺ ([M-Cl]⁺) 563.3304. Found 563.3293; [α]_D²⁶ -271.1 (c = 0.93, CHCl₃).



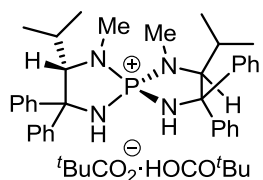
Anion Exchange Procedure to Prepare Chiral Tetraaminophosphonium Carboxylate 1·OCOR: A methanolic solution of chiral tetraaminophosphonium chloride 1·Cl was passed through an ion-exchange resin (amberlyst A-26, RCO₂⁻ form), and the resulting solution was evaporated. The residue was dissolved in ethyl acetate and the solution was washed with 0.5 M aqueous solution of RCOOH twice. The organic layers were washed with water and dried over Na₂SO₄. The organic phase was filtered and concentrated under reduced pressure to give white solids. The residual solids were collected by filtration with the aid of diethyl ether and dried under reduce pressure affording pure 1·OCOR.



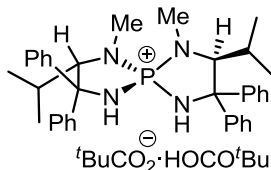
(*M,S*)-1·OCHO: ¹H NMR (700 MHz, CD₃OD) δ 8.48 (2H, s), 7.52-7.46 (8H, m), 7.41 (2H, t, *J* = 7.0 Hz), 7.27-7.19 (10H, m), 4.09 (2H, dd, *J*_{P-H} = 21.0 Hz, *J*_{H-H} = 7.0 Hz), 3.11 (6H, d, *J*_{P-H} = 9.8 Hz), 1.89 (2H, octet, *J* = 7.0 Hz), 1.07 (6H, d, *J* = 7.0 Hz), 0.55 (6H, d, *J* = 7.0 Hz), N-H protons were not found due to deuterium exchange; ¹³C NMR (175 MHz, CD₃OD) δ 169.8, 147.4, 141.5 (d, *J*_{P-C} = 11.4 Hz), 129.9, 129.0, 128.8₁, 128.7₇, 127.9, 73.5 (d, *J*_{P-C} = 12.1 Hz), 71.4 (d, *J*_{P-C} = 10.0 Hz), 35.8 (d, *J*_{P-C} = 6.1 Hz), 31.8, 22.4, 19.7, one carbon was not found probably due to overlapping; ³¹P NMR (121 MHz, CD₃OD) δ 36.6.



(*M,S*)-1·OAc: ¹H NMR (700 MHz, CD₃OD) δ 7.51 (4H, t, *J* = 7.0 Hz), 7.47 (4H, t, *J* = 7.0 Hz), 7.41 (2H, t, *J* = 7.0 Hz), 7.24-7.22 (10H, m), 4.09 (2H, dd, *J*_{P-H} = 21.0 Hz, *J*_{H-H} = 6.3 Hz), 3.12 (6H, d, *J*_{P-H} = 9.8 Hz), 1.94 (6H, s), 1.89 (2H, octet, *J* = 7.0 Hz), 1.07 (6H, d, *J* = 7.0 Hz), 0.55 (6H, d, *J* = 7.0 Hz), N-H protons were not found due to deuterium exchange; ¹³C NMR (175 MHz, CD₃OD) δ 177.6, 147.4, 141.5 (d, *J*_{P-C} = 11.2 Hz), 129.9, 129.0, 128.8₀, 128.7₅, 127.9, 73.5 (d, *J*_{P-C} = 11.4 Hz), 71.4 (d, *J*_{P-C} = 10.0 Hz), 35.8 (d, *J*_{P-C} = 6.0 Hz), 31.8, 22.5, 22.4, 19.7, one carbon was not found probably due to overlapping; ³¹P NMR (121 MHz, CD₃OD) δ 33.6.

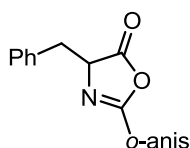


(*M,S*)-1·OPiv: ¹H NMR (700 MHz, CD₃OD) δ 7.50 (4H, t, *J* = 7.0 Hz), 7.47 (4H, t, *J* = 7.0 Hz), 7.41 (2H, t, *J* = 7.0 Hz), 7.27-7.22 (10H, m), 4.10 (2H, dd, *J*_{P-H} = 21.0 Hz, *J*_{H-H} = 6.3 Hz), 3.11 (6H, d, *J*_{P-H} = 9.8 Hz), 1.89 (2H, octet, *J* = 7.0 Hz), 1.17 (18H, s), 1.07 (6H, d, *J* = 7.0 Hz), 0.55 (6H, d, *J* = 7.0 Hz), N-H protons were not found due to deuterium exchange; ¹³C NMR (175 MHz, CD₃OD) δ 184.3, 147.4, 141.5 (d, *J*_{P-C} = 11.9 Hz), 129.9, 129.0, 128.8₀, 128.7₆, 127.9, 73.5 (d, *J*_{P-C} = 12.1 Hz), 71.4 (d, *J*_{P-C} = 10.0 Hz), 39.9, 35.8 (d, *J*_{P-C} = 6.0 Hz), 31.8, 28.1, 22.4, 19.7, one carbon was not found probably due to overlapping; ³¹P NMR (121 MHz, CD₃OD) δ 33.6; IR (KBr): 3060, 2960, 1699, 1481, 1447, 1389, 1190, 1036, 1014, 756 cm⁻¹; HRMS (FAB) Calcd for C₃₆H₄₄N₄P⁺ ([M-tBuCO₂]⁺) 563.3304. Found 563.3306; [α]_D²⁸ -192.0° (c = 0.50, MeOH).

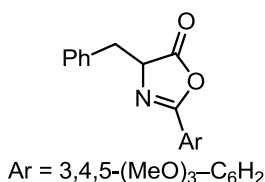


(P,S)-1-OPiv: ^1H NMR (500 MHz, CD_3OD) δ 7.62 (4H, d, $J = 7.5$ Hz), 7.45 (4H, t, $J = 7.5$ Hz), 7.39-7.26 (12H, m), 4.01 (2H, dd, $J_{\text{P-H}} = 20.0$ Hz, $J_{\text{H-H}} = 6.0$ Hz), 1.90 (6H, d, $J_{\text{P-H}} = 10.0$ Hz), 1.91-1.84 (2H, m), 1.17 (18H, s), 0.95 (6H, d, $J = 7.0$ Hz), 0.49 (6H, d, $J = 7.0$ Hz), N-H protons were not found due to deuterium exchange; ^{13}C NMR (175 MHz, CD_3OD) δ 185.7, 148.9, 141.7 (d, $J_{\text{P-C}} = 12.8$ Hz), 130.0, 129.2, 129.0, 128.9, 128.7, 127.9, 72.5 (d, $J_{\text{P-C}} = 10.7$ Hz), 71.7 (d, $J_{\text{P-C}} = 10.0$ Hz), 40.3, 32.8 (d, $J_{\text{P-C}} = 6.1$ Hz), 30.9, 28.5, 22.7, 19.8; ^{31}P NMR (121 MHz, CD_3OD) δ 39.3; IR (KBr): 3060, 2963, 1479, 1447, 1402, 1359, 1193, 1036, 1008, 751 cm^{-1} ; HRMS (FAB) Calcd for $\text{C}_{36}\text{H}_{44}\text{N}_4\text{P}^+$ ($[\text{M}-^t\text{BuCO}_2]^+$) 563.3304. Found 563.3293; $[\alpha]_{\text{D}}^{28} -195.1$ ($c = 0.48$, MeOH).

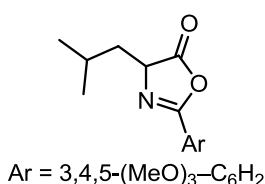
Characterization of Azlactones:



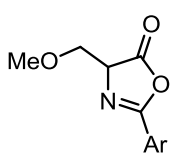
2b: ^1H NMR (500 MHz, CDCl_3) δ 7.60 (1H, dd, $J = 8.0, 1.5$ Hz), 7.47 (1H, dt, $J = 8.0, 1.5$ Hz), 7.30-7.20 (5H, m), 6.99 (1H, d, $J = 8.0$ Hz), 6.98 (1H, t, $J = 8.0$ Hz), 4.71 (1H, t, $J = 6.0$ Hz), 3.91 (3H, s), 3.39 (1H, dd, $J = 14.0, 6.0$ Hz), 3.25 (1H, dd, $J = 14.0, 6.0$ Hz); ^{13}C NMR (126 MHz, CDCl_3) δ 178.0, 160.8, 159.1, 135.3, 133.8, 131.2, 129.9, 128.4, 127.3, 120.6, 115.2, 112.0, 66.6, 56.2, 37.3; IR (liq. film): 2937, 1815, 1648, 1600, 1495, 1465, 1263, 1049, 1021, 751 cm^{-1} ; HRMS (FAB) Calcd for $\text{C}_{17}\text{H}_{16}\text{NO}_3^+$ ($[\text{M}+\text{H}]^+$) 282.1130. Found 282.1135.



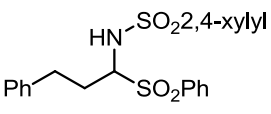
2c: ^1H NMR (500 MHz, CDCl_3) δ 7.30-7.21 (5H, m), 7.15 (2H, s), 4.70 (1H, dd, $J = 6.5, 5.0$ Hz), 3.91 (3H, s), 3.90 (6H, s), 3.36 (1H, dd, $J = 9.0, 5.0$ Hz), 3.20 (1H, dd, $J = 9.0, 6.5$ Hz); ^{13}C NMR (126 MHz, CDCl_3) δ 177.7, 161.5, 153.5, 142.1, 135.4, 129.7, 128.6, 127.4, 120.8, 105.2, 66.8, 61.1, 56.5, 37.5; IR (liq. film): 2938, 1817, 1650, 1586, 1503, 1455, 1416, 1353, 1235, 1127, 913 cm^{-1} ; HRMS (FAB) Calcd for $\text{C}_{19}\text{H}_{20}\text{NO}_5^+$ ($[\text{M}+\text{H}]^+$) 342.1341. Found 342.1342.

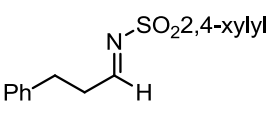


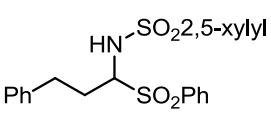
2o: ^1H NMR (500 MHz, CDCl_3) δ 7.24 (2H, s), 4.42 (1H, dd, $J = 8.5, 6.0$ Hz), 3.92₃ (6H, s), 3.91₉ (3H, s), 2.07 (1H, d-octet, $J = 7.5, 6.5$ Hz), 1.84 (1H, ddd, $J = 14.0, 7.5, 6.0$ Hz), 1.70 (1H, ddd, $J = 14.0, 8.5, 6.5$ Hz), 1.04 (3H, d, $J = 6.5$ Hz), 1.01 (3H, d, $J = 6.5$ Hz); ^{13}C NMR (126 MHz, CDCl_3) δ 179.1, 161.2, 153.5, 142.0, 121.1, 105.1, 64.2, 61.1, 56.4, 41.0, 25.2, 22.8, 22.3; IR (liq. film): 2957, 1825, 1650, 1586, 1504, 1416, 1353, 1235, 1128, 913 cm^{-1} ; HRMS (FAB) Calcd for $\text{C}_{16}\text{H}_{22}\text{NO}_5^+$ ($[\text{M}+\text{H}]^+$) 308.1498. Found 308.1508.

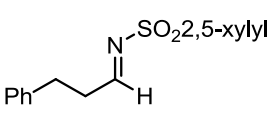

2p: ^1H NMR (500 MHz, CDCl_3) δ 7.27 (2H, s), 4.53 (1H, dd, $J = 4.0, 3.0$ Hz), 3.96 (1H, dd, $J = 10.0, 3.0$ Hz), 3.92₁ (6H, s), 3.91₇ (3H, s), 3.89 (1H, dd, $J = 10.0, 4.0$ Hz), 3.39 (3H, s); ^{13}C NMR (126 MHz, CDCl_3) δ 176.6, 162.6, 153.5, 142.2, 120.8, 105.4, 70.8, 66.9, 61.2, 59.8, 56.5; IR (liq. film): 2940, 1827, 1650, 1585, 1504, 1416, 1353, 1234, 1128, 915 cm^{-1} ; HRMS (FAB) Calcd for $\text{C}_{14}\text{H}_{18}\text{NO}_6^+$ ($[\text{M}+\text{H}]^+$) 296.1134. Found 296.1131.

Characterization of Imines and Their Precursors (α -Amido Sulfones):

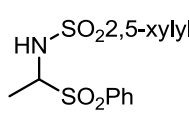

 ^1H NMR (500 MHz, CDCl_3) δ 7.78 (2H, d, $J = 8.0$ Hz), 7.59 (1H, t, $J = 8.0$ Hz), 7.53 (1H, d, $J = 8.0$ Hz), 7.44 (2H, t, $J = 8.0$ Hz), 7.25 (2H, t, $J = 8.0$ Hz), 7.19 (1H, t, $J = 8.0$ Hz), 7.03 (1H, brs), 7.02 (2H, d, $J = 8.0$ Hz), 6.98 (1H, d, $J = 8.0$ Hz), 5.55 (1H, d, $J = 10.0$ Hz), 4.54 (1H, ddd, $J = 10.0, 9.0, 4.0$ Hz), 2.68-2.61 (1H, m), 2.55-2.46 (2H, m), 2.53 (3H, s), 2.35 (3H, s), 2.06-1.98 (1H, m); ^{13}C NMR (126 MHz, CDCl_3) δ 144.0, 139.7, 136.6, 136.0, 135.7, 134.3, 133.4, 129.4, 129.2, 129.0, 128.7, 128.4, 127.0, 126.6, 73.2, 31.3, 30.5, 21.4, 20.6; IR (liq. film): 3271, 3027, 1447, 1334, 1306, 1173, 1147, 1114, 1082, 753 cm^{-1} ; HRMS (FAB) Calcd for $\text{C}_{23}\text{H}_{26}\text{NO}_4\text{S}_2^+$ ($[\text{M}+\text{H}]^+$) 444.1303. Found 444.1321.

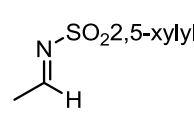

 ^1H NMR (500 MHz, CDCl_3) δ 8.68 (1H, t, $J = 4.0$ Hz), 7.88 (1H, d, $J = 8.0$ Hz), 7.24 (2H, t, $J = 7.5$ Hz), 7.19 (1H, t, $J = 7.5$ Hz), 7.15-7.12 (4H, m), 2.96 (2H, t, $J = 7.5$ Hz), 2.86 (2H, tdd, $J = 7.5, 4.0, 1.0$ Hz), 2.56 (3H, s), 2.39 (3H, s); ^{13}C NMR (126 MHz, CDCl_3) δ 177.4, 144.8, 139.8, 138.9, 133.3, 133.1, 129.8, 128.8, 128.4, 127.1, 126.6, 37.6, 30.7, 21.5, 20.5; IR (liq. film): 2924, 1629, 1453, 1317, 1171, 1158, 1141, 1058, 784, 745 cm^{-1} ; HRMS (FAB) Calcd for $\text{C}_{17}\text{H}_{20}\text{NO}_2\text{S}^+$ ($[\text{M}+\text{H}]^+$) 302.1215. Found 302.1212.

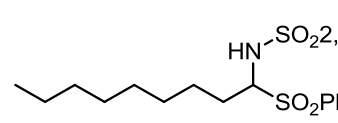

 ^1H NMR (500 MHz, CDCl_3) δ 7.78 (2H, d, $J = 8.0$ Hz), 7.58 (1H, t, $J = 8.0$ Hz), 7.43 (2H, t, $J = 8.0$ Hz), 7.42 (1H, brs), 7.25 (2H, t, $J = 7.5$ Hz), 7.22-7.18 (2H, m), 7.13 (1H, d, $J = 7.5$ Hz), 7.02 (2H, d, $J = 7.5$ Hz), 5.71 (1H, d, $J = 10.0$ Hz), 4.56 (1H, td, $J = 10.0, 4.0$ Hz), 2.69-2.62 (1H, m), 2.57-2.46 (2H, m), 2.54 (3H, s), 2.28 (3H, s), 2.03 (1H, dtd, $J = 19.0, 9.5, 4.0$ Hz); ^{13}C NMR (126 MHz, CDCl_3) δ 139.6, 138.5, 136.4, 136.0, 134.4, 133.9, 133.5, 132.6, 129.4, 129.1, 129.0, 128.7, 128.4, 126.6, 73.2, 31.2, 30.2, 20.9, 20.1; IR (liq. film): 3273, 3027, 1494, 1447, 1335, 1306, 1157, 1081, 894, 752 cm^{-1} ; HRMS (FAB) Calcd for $\text{C}_{23}\text{H}_{26}\text{NO}_4\text{S}_2^+$ ($[\text{M}+\text{H}]^+$) 444.1303. Found 444.1287.

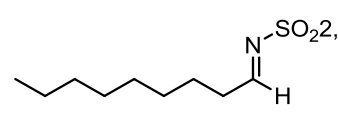

 ^1H NMR (500 MHz, CDCl_3) δ 8.69 (1H, t, $J = 4.0$ Hz), 7.83 (1H, d, $J = 1.5$ Hz), 7.31 (1H, dd, $J = 7.0, 1.5$ Hz), 7.24 (2H, t, $J = 8.0$ Hz), 7.20-7.17 (2H, m), 7.14-7.12 (2H, m), 2.96 (2H, t, $J = 7.5$ Hz), 2.87 (2H, tdd, $J = 7.5, 4.0, 1.0$ Hz).

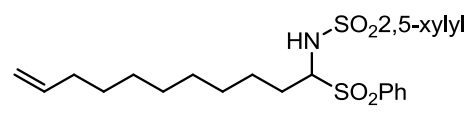
Hz), 2.53 (3H, s), 2.38 (3H, s); ^{13}C NMR (126 MHz, CDCl_3) δ 177.8, 139.7, 136.5, 135.8, 135.5, 134.6, 132.5, 129.9, 128.8, 128.4, 126.6, 37.6, 30.7, 20.9, 20.1; IR (liq. film): 2925, 1629, 1493, 1454, 1315, 1156, 1063, 823, 785, 749 cm^{-1} ; HRMS (FAB) Calcd for $\text{C}_{17}\text{H}_{20}\text{NO}_2\text{S}^+$ ($[\text{M}+\text{H}]^+$) 302.1215. Found 302.1223.


 ^1H NMR (500 MHz, CDCl_3) δ 7.80 (2H, d, $J = 8.0$ Hz), 7.60 (1H, t, $J = 8.0$ Hz), 7.53 (1H, d, $J = 1.5$ Hz), 7.46 (2H, t, $J = 8.0$ Hz), 7.22 (1H, dd, $J = 8.0, 1.5$ Hz), 7.09 (1H, d, $J = 8.0$ Hz), 5.02 (1H, d, $J = 10.5$ Hz), 4.54 (1H, dq, $J = 10.5, 7.0$ Hz), 2.45 (3H, s), 2.32 (3H, s), 1.55 (3H, d, $J = 7.0$ Hz); ^{13}C NMR (126 MHz, CDCl_3) δ 137.5, 136.4, 135.6, 134.4, 134.1, 133.7, 132.8, 129.4₀, 129.3₈, 129.2, 69.4, 20.9, 20.0, 14.8; IR (KBr): 3284, 1448, 1430, 1338, 1309, 1279, 1169, 1126, 1087, 946, 740 cm^{-1} ; HRMS (FAB) Calcd for $\text{C}_{16}\text{H}_{20}\text{NO}_4\text{S}_2^+$ ($[\text{M}+\text{H}]^+$) 354.0834. Found 354.0843.

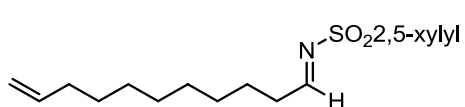

 ^1H NMR (500 MHz, CDCl_3) δ 8.68 (1H, q, $J = 5.0$ Hz), 7.84 (1H, d, $J = 1.0$ Hz), 7.31 (1H, dd, $J = 8.0, 1.0$ Hz), 7.21 (1H, d, $J = 8.0$ Hz), 2.61 (3H, s), 2.38 (3H, s), 2.27 (3H, d, $J = 5.0$ Hz); ^{13}C NMR (126 MHz, CDCl_3) δ 175.4, 136.6, 135.8, 135.5, 134.7, 132.6, 129.9, 22.7, 20.9, 20.2; IR (liq. film): 2925, 1632, 1492, 1423, 1284, 1160, 1064, 886, 758 cm^{-1} ; HRMS (FAB) Calcd for $\text{C}_{10}\text{H}_{14}\text{NO}_2\text{S}^+$ ($[\text{M}+\text{H}]^+$) 212.0745. Found 212.0748.


 ^1H NMR (500 MHz, CDCl_3) δ 7.80 (2H, d, $J = 8.0$ Hz), 7.58 (1H, t, $J = 8.0$ Hz), 7.45 (2H, t, $J = 8.0$ Hz), 7.43 (1H, d, $J = 1.5$ Hz), 7.20 (1H, dd, $J = 7.5, 1.5$ Hz), 7.12 (1H, d, $J = 7.5$ Hz), 5.10 (1H, d, $J = 10.0$ Hz), 4.53 (1H, td, $J = 10.0, 3.5$ Hz), 2.53 (3H, s), 2.28 (3H, s), 2.18 (1H, tdd, $J = 10.0, 7.0, 3.5$ Hz), 1.72 (1H, dtd, $J = 14.5, 10.0, 4.5$ Hz), 1.31-1.06 (12H, m), 0.88 (3H, t, $J = 7.5$ Hz); ^{13}C NMR (126 MHz, CDCl_3) δ 138.6, 136.3, 136.1, 134.3, 133.8, 133.4, 132.6, 129.5, 129.1, 128.9, 73.8, 31.9, 29.3, 29.2₀, 29.1₆, 28.3, 25.0, 22.8, 20.9, 20.2, 14.2; IR (liq. film): 3273, 2925, 2855, 1447, 1336, 1306, 1158, 1132, 1082, 752 cm^{-1} ; HRMS (FAB) Calcd for $\text{C}_{23}\text{H}_{34}\text{NO}_4\text{S}_2^+$ ($[\text{M}+\text{H}]^+$) 452.1929. Found 452.1927.


 ^1H NMR (500 MHz, CDCl_3) δ 8.66 (1H, t, $J = 4.5$ Hz), 7.85 (1H, d, $J = 1.0$ Hz), 7.31 (1H, dd, $J = 7.5, 1.0$ Hz), 7.21 (1H, d, $J = 7.5$ Hz), 2.60 (3H, s), 2.53 (2H, td, $J = 7.5, 4.5$ Hz), 2.38 (3H, s), 1.63 (2H, quin, $J = 7.5$ Hz), 1.36-1.19 (10H, m), 0.87 (3H, t, $J = 7.5$ Hz); ^{13}C NMR (126 MHz, CDCl_3) δ 179.0, 136.5, 135.7₂, 135.6₈, 134.5, 132.5, 129.8, 36.1, 31.8, 29.3, 29.2₀, 29.1₆, 24.8, 22.7, 20.9, 20.2, 14.2; IR (liq. film): 2926, 2855, 1629, 1492, 1457, 1319, 1158, 884, 755, 728 cm^{-1} ; HRMS (FAB) Calcd for $\text{C}_{17}\text{H}_{28}\text{NO}_2\text{S}^+$ ($[\text{M}+\text{H}]^+$) 310.1841. Found 310.1844.

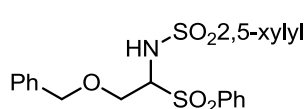

 ^1H NMR (500 MHz, CDCl_3) δ 7.81 (2H, dd, $J = 7.5, 1.0$ Hz), 7.58 (1H, tt, $J = 7.5, 1.0$ Hz), 7.45 (2H, t, $J = 7.5$ Hz), 7.44 (1H, d, $J = 1.5$ Hz), 7.19 (1H, dd, $J = 7.5, 1.5$ Hz), 7.12 (1H,

d, $J = 7.5$ Hz), 5.81 (1H, ddt, $J = 17.0, 10.0, 7.0$ Hz), 5.24 (1H, br), 5.00 (1H, dq, $J = 17.0, 2.0$ Hz), 4.94 (1H, ddt, $J = 10.0, 2.0, 1.0$ Hz), 4.52 (1H, td, $J = 10.5, 3.5$ Hz), 2.52 (3H, s), 2.28 (3H, s), 2.24-2.14 (1H, m), 2.03 (2H, brq, $J = 7.0$ Hz), 1.73 (1H, td, $J = 10.0, 4.5$ Hz), 1.35 (2H, quin, $J = 7.0$ Hz), 1.30-1.02 (10H, m); ^{13}C NMR (126 MHz, CDCl_3) δ 139.3, 138.6, 136.3, 136.1, 134.3, 133.8, 133.4, 132.6, 129.5, 129.1, 128.9, 114.4, 73.8, 33.9, 29.3₃, 29.2₅, 29.2, 29.0₃, 29.0₁, 28.3, 25.0, 20.9, 20.2; IR (liq. film): 2926, 2854, 1629, 1492, 1458, 1320, 1158, 1063, 909, 756 cm^{-1} ; HRMS (FAB) Calcd for $\text{C}_{25}\text{H}_{35}\text{NO}_4\text{S}_2\text{Na}^+$ ($[\text{M}+\text{Na}]^+$) 500.1905. Found 500.1892.



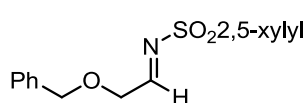
^1H NMR (500 MHz, CDCl_3) δ 8.66 (1H, t, $J = 4.5$ Hz), 7.85 (1H, d, $J = 1.0$ Hz), 7.30 (1H, dd, $J = 7.5, 1.0$ Hz), 7.20 (1H, d, $J = 7.5$ Hz), 5.80 (1H, ddt, $J = 17.0, 10.0, 7.0$ Hz), 4.99

(1H, brd, $J = 17.0$ Hz), 4.93 (1H, brd, $J = 10.0$ Hz), 2.60 (3H, s), 2.53 (2H, td, $J = 7.0, 3.0$ Hz), 2.38 (3H, s), 2.03 (2H, brq, $J = 7.0$ Hz), 1.63 (2H, quin, $J = 7.0$ Hz), 1.40-1.22 (10H, m); ^{13}C NMR (126 MHz, CDCl_3) δ 178.9, 139.1, 136.4, 135.6₄, 135.6₁, 134.5, 132.5, 129.8, 114.3, 36.1, 33.8, 29.3, 29.2, 29.1, 29.0, 28.9, 24.7, 20.9, 20.1; IR (liq. film): 2926, 2854, 1629, 1492, 1456, 1319, 1158, 908, 884, 755 cm^{-1} ; HRMS (FAB) Calcd for $\text{C}_{19}\text{H}_{30}\text{NO}_2\text{S}^+$ ($[\text{M}+\text{H}]^+$) 336.1997. Found 336.2010.



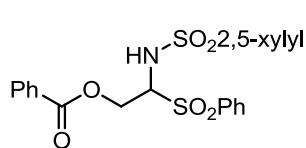
^1H NMR (500 MHz, CDCl_3) δ 7.78 (2H, d, $J = 8.0$ Hz), 7.59 (1H, t, $J = 8.0$ Hz), 7.53 (1H, d, $J = 1.0$ Hz), 7.44 (2H, t, $J = 8.0$ Hz), 7.35-7.28 (3H, m), 7.22-7.19 (3H, m), 7.10 (1H, d, $J = 8.0$ Hz), 5.73 (1H, d, $J = 10.0$ Hz), 4.56

(1H, ddd, $J = 10.0, 4.0, 3.0$ Hz), 4.47 (1H, d, $J = 12.0$ Hz), 4.43 (1H, d, $J = 12.0$ Hz), 4.14 (1H, dd, $J = 11.0, 3.0$ Hz), 3.55 (1H, dd, $J = 11.0, 4.0$ Hz), 2.45 (3H, s), 2.29 (3H, s); ^{13}C NMR (126 MHz, CDCl_3) δ 137.8, 136.7, 136.6, 136.3, 134.3, 134.0₃, 133.9₆, 132.6, 129.5, 129.3, 129.1, 128.6, 128.2, 128.0, 73.9, 72.7, 65.8, 20.9, 20.0; IR (liq. film): 3272, 3029, 2868, 1493, 1447, 1322, 1309, 1159, 1128, 1081, 752 cm^{-1} ; HRMS (FAB) Calcd for $\text{C}_{23}\text{H}_{26}\text{NO}_5\text{S}_2^+$ ($[\text{M}+\text{H}]^+$) 460.1252. Found 460.1242.



^1H NMR (500 MHz, CDCl_3) δ 8.64 (1H, t, $J = 3.0$ Hz), 7.83 (1H, d, $J = 1.5$ Hz), 7.47-7.30 (6H, m), 7.21 (1H, d, $J = 8.0$ Hz), 4.61 (2H, s), 4.38 (2H, d, $J = 3.0$ Hz), 2.60 (3H, s), 2.38 (3H, s); ^{13}C NMR (126 MHz, CDCl_3) δ

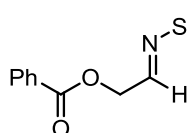
175.7, 136.7, 136.6, 135.9, 135.0, 134.9, 132.6, 130.1, 128.7, 128.4, 128.2, 73.8, 70.5, 20.9, 20.2; IR (liq. film): 3282, 2925, 1492, 1452, 1324, 1160, 1099, 1064, 963, 742 cm^{-1} ; HRMS (FAB) Calcd for $\text{C}_{17}\text{H}_{20}\text{NO}_3\text{S}^+$ ($[\text{M}+\text{H}]^+$) 318.1164. Found 318.1163.



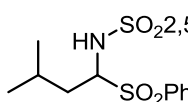
^1H NMR (500 MHz, CDCl_3) δ 7.90 (2H, dd, $J = 8.0, 1.5$ Hz), 7.84 (2H, dd, $J = 8.0, 1.5$ Hz), 7.65 (1H, t, $J = 8.0$ Hz), 7.56 (1H, t, $J = 8.0$ Hz), 7.51 (2H, t, $J = 8.0$ Hz), 7.47 (1H, d, $J = 1.5$ Hz), 7.39 (2H, t, $J = 8.0$ Hz), 6.98 (1H, dd, $J = 7.5, 1.5$ Hz), 6.92 (1H, d, $J = 7.5$ Hz), 5.71 (1H, d, $J = 10.5$ Hz),

4.90 (1H, ddd, $J = 10.5, 6.0, 4.0$ Hz), 4.82 (1H, dd, $J = 12.5, 6.0$ Hz), 4.65 (1H, dd, $J = 12.5, 4.0$ Hz), 2.47

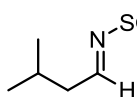
(3H, s), 2.21 (3H, s); ^{13}C NMR (126 MHz, CDCl_3) δ 166.0, 137.8, 136.3, 136.1, 134.8, 133.9, 133.7, 133.5, 132.7, 130.0, 129.6, 129.4, 128.9, 128.7, 128.5, 71.8, 60.7, 20.8, 20.0; IR (liq. film): 3270, 1724, 1448, 1324, 1270, 1159, 1128, 1081, 754, 713 cm^{-1} ; HRMS (FAB) Calcd for $\text{C}_{23}\text{H}_{24}\text{NO}_6\text{S}_2^+$ ($[\text{M}+\text{H}]^+$) 474.1045. Found 474.1065.



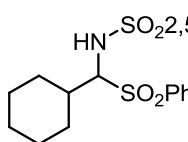
^1H NMR (500 MHz, CDCl_3) δ 8.71 (1H, t, $J = 3.0$ Hz), 8.06 (2H, dd, $J = 8.0, 1.5$ Hz), 7.84 (1H, d, $J = 1.5$ Hz), 7.61 (1H, t, $J = 8.0$ Hz), 7.47 (2H, t, $J = 8.0$ Hz), 7.32 (1H, dd, $J = 8.0, 1.5$ Hz), 7.21 (1H, d, $J = 8.0$ Hz), 5.18 (2H, d, $J = 3.0$ Hz), 2.58 (3H, s), 2.38 (3H, s); ^{13}C NMR (126 MHz, CDCl_3) δ 172.6, 165.9, 136.6, 136.1, 135.0, 134.9, 133.9, 132.7, 130.1, 130.0, 128.9, 128.7, 64.5, 20.9, 20.1; IR (liq. film): 2925, 1727, 1643, 1317, 1271, 1159, 1125, 1063, 759, 708 cm^{-1} ; HRMS (FAB) Calcd for $\text{C}_{17}\text{H}_{18}\text{NO}_4\text{S}^+$ ($[\text{M}+\text{H}]^+$) 332.0957. Found 332.0944.



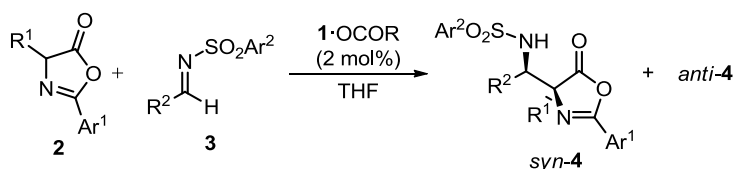
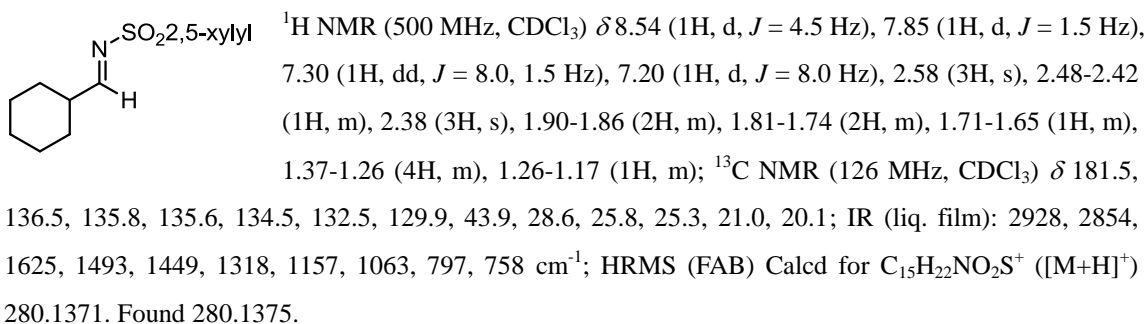
^1H NMR (500 MHz, CDCl_3) δ 7.78 (2H, d, $J = 8.0$ Hz), 7.56 (1H, t, $J = 8.0$ Hz), 7.42_o (2H, t, $J = 8.0$ Hz), 7.42₇ (1H, d, $J = 1.5$ Hz), 7.20 (1H, dd, $J = 7.5, 1.5$ Hz), 7.13 (1H, d, $J = 7.5$ Hz), 5.10 (1H, dd, $J = 14.5, 10.5$ Hz), 4.62 (1H, td, $J = 10.5, 3.0$ Hz), 2.53 (3H, s), 2.28 (3H, s), 1.99 (1H, ddd, $J = 14.5, 10.5, 3.5$ Hz), 1.63 (1H, ddd, $J = 14.5, 10.5, 3.5$ Hz), 1.54-1.49 (1H, m), 0.90 (3H, d, $J = 7.0$ Hz), 0.78 (3H, d, $J = 7.0$ Hz); ^{13}C NMR (126 MHz, CDCl_3) δ 138.7, 136.3, 136.1, 134.3, 133.8, 133.3, 132.5, 129.5, 129.1, 128.9, 72.7, 37.4, 24.2, 23.4, 21.0, 20.9, 20.1; IR (liq. film): 3271, 2960, 1447, 1306, 1158, 1136, 1081, 915, 816, 752 cm^{-1} ; HRMS (FAB) Calcd for $\text{C}_{19}\text{H}_{26}\text{NO}_4\text{S}_2^+$ ($[\text{M}+\text{H}]^+$) 396.1303. Found 396.1302.



^1H NMR (500 MHz, CDCl_3) δ 8.65 (1H, t, $J = 5.0$ Hz), 7.85 (1H, d, $J = 1.5$ Hz), 7.30 (1H, dd, $J = 8.0, 1.5$ Hz), 7.20 (1H, d, $J = 8.0$ Hz), 2.60 (3H, s), 2.41 (2H, dd, $J = 7.0, 5.0$ Hz), 2.38 (3H, s), 2.09 (1H, nonet, $J = 7.0$ Hz), 0.98 (6H, d, $J = 7.0$ Hz); ^{13}C NMR (126 MHz, CDCl_3) δ 178.5, 136.5, 135.7, 135.6, 134.6, 132.5, 129.8, 44.7, 26.0, 22.6, 20.9, 20.1; IR (liq. film): 2959, 1626, 1492, 1465, 1317, 1159, 1064, 886, 755, 735 cm^{-1} ; HRMS (FAB) Calcd for $\text{C}_{13}\text{H}_{20}\text{NO}_2\text{S}^+$ ($[\text{M}+\text{H}]^+$) 254.1215. Found 254.1209.

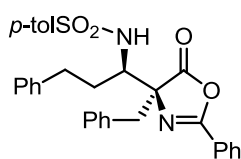


^1H NMR (500 MHz, CDCl_3) δ 7.73 (2H, d, $J = 8.0$ Hz), 7.52 (1H, t, $J = 8.0$ Hz), 7.37 (2H, t, $J = 8.0$ Hz), 7.31 (1H, d, $J = 1.5$ Hz), 7.18 (1H, dd, $J = 7.5, 1.5$ Hz), 7.13 (1H, d, $J = 7.5$ Hz), 5.32 (1H, d, $J = 10.5$ Hz), 4.45 (1H, dd, $J = 10.5, 3.0$ Hz), 2.58 (3H, s), 2.43 (1H, tq, $J = 12.5, 3.5$ Hz), 2.24 (3H, s), 2.10 (1H, brd, $J = 12.5$ Hz), 1.78 (1H, brd, $J = 11.0$ Hz), 1.64 (2H, m), 1.49 (1H, brd, $J = 12.5$ Hz), 1.34-1.24 (2H, m), 1.09 (1H, qd, $J = 12.5, 3.5$ Hz), 1.02 (1H, qt, $J = 13.5, 3.5$ Hz), 0.89 (1H, qd, $J = 12.5, 3.5$ Hz); ^{13}C NMR (126 MHz, CDCl_3) δ 138.9, 137.3, 136.2, 134.0, 133.7, 133.2, 132.5, 129.0₂, 129.0₁, 128.6, 77.6, 37.4, 30.8, 27.3, 26.3, 25.8, 25.7, 20.9, 20.2; IR (liq. film): 3290, 2930, 2855, 1447, 1332, 1304, 1158, 1122, 1081, 753 cm^{-1} ; HRMS (FAB) Calcd for $\text{C}_{21}\text{H}_{28}\text{NO}_4\text{S}_2^+$ ($[\text{M}+\text{H}]^+$) 422.1460. Found 422.1459.

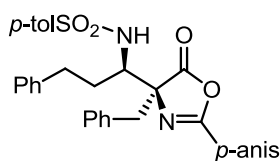


Representative Procedure for Chiral Tetraaminophosphonium Salt **1-OCOR** Catalyzed Asymmetric Direct Mannich Reaction of Azlactones:

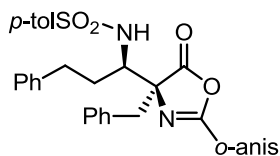
Azlactone **2a** (25.1 mg, 0.1 mmol) and (*M,S*)-**1-OCOR** or (*P,S*)-**1-OCOR** (0.02 equiv, 2.0 μmol) were placed in a dried test tube and dissolved into 0.6 mL of THF under Ar atmosphere. A solution of **3a** (31.6 mg, 0.11 mmol) in THF (0.4 mL) was introduced dropwise slowly at -50 °C and the stirring was continued for 1 h. A solution of trifluoroacetic acid in THF (0.1 M, 40 μL) was then added to the reaction mixture to quench the reaction. All volatiles were removed by evaporation to give crude residue. The diastereomeric ratio was determined by ¹H NMR analysis of it. Subsequent purification by column chromatography on silica gel



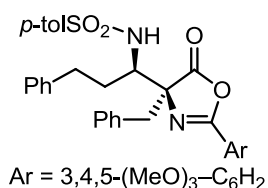
afforded **4a** as a mixture of diastereomers, whose enantiomeric excesses were determined by HPLC analysis. **4a**: IA, hexane (H)/isopropyl alcohol (IPA)/ethyl acetate (EA) = 20:1:2, flow rate = 0.5 mL/min, λ = 260 nm, 30.5 min (major *syn* isomer), 35.2 min (minor *anti* isomer), 37.1 min (major *anti* isomer), 55.6 min (minor *syn* isomer). **syn-4a**: ¹H NMR (500 MHz, CDCl₃) δ 7.80 (2H, d, *J* = 8.5 Hz), 7.72 (2H, d, *J* = 8.5 Hz), 7.50 (1H, t, *J* = 7.5 Hz), 7.38 (2H, t, *J* = 7.5 Hz), 7.29 (2H, d, *J* = 7.5 Hz), 7.21 (2H, t, *J* = 7.5 Hz), 7.09-7.04 (4H, m), 7.04-6.90 (4H, m), 5.09 (1H, d, *J* = 10.0 Hz), 4.14 (1H, td, *J* = 10.0, 4.0 Hz), 3.25 (1H, d, *J* = 13.5 Hz), 3.14 (1H, d, *J* = 13.5 Hz), 2.67 (1H, ddd, *J* = 14.0, 12.0, 5.5 Hz), 2.52 (1H, ddd, *J* = 14.0, 12.0, 5.5 Hz), 2.39 (3H, s), 1.95 (1H, dddd, *J* = 14.0, 11.5, 5.0, 4.0 Hz), 1.67 (1H, dddd, *J* = 14.0, 11.5, 10.0, 5.0 Hz); ¹³C NMR (126 MHz, CDCl₃) δ 178.5, 161.5, 143.8, 141.0, 138.6, 133.6, 133.0, 130.3, 129.8, 128.8, 128.6, 128.4, 128.2, 128.0, 127.4, 127.2, 126.2, 125.1, 77.8, 58.5, 41.3, 34.0, 32.3, 21.7; IR (liq. film): 3280, 3029, 1813, 1654, 1453, 1322, 1159, 1091, 975, 754 cm⁻¹; HRMS (FAB) Calcd for C₃₂H₃₁N₂O₄S ([M+H]⁺) 539.2005. Found 539.1995.



4b: IC, H/EtOH = 10:1, flow rate = 0.5 mL/min, λ = 260 nm, 23.1 min (major *anti* isomer), 27.2 min (minor *anti* isomer), 34.6 min (minor *syn* isomer), 40.0 min (major *syn* isomer). **syn-4b:** ^1H NMR (500 MHz, CDCl_3) δ 7.79 (2H, d, J = 8.5 Hz), 7.67 (2H, d, J = 8.5 Hz), 7.28 (2H, d, J = 8.5 Hz), 7.21 (2H, t, J = 8.5 Hz), 7.09-7.05 (3H, m), 7.04-6.90 (5H, m), 6.86 (2H, d, J = 8.5 Hz), 5.16 (1H, d, J = 10.0 Hz), 4.10 (1H, td, J = 10.0, 4.0 Hz), 3.81 (3H, s), 3.22 (1H, d, J = 13.0 Hz), 3.11 (1H, d, J = 13.0 Hz), 2.66 (1H, ddd, J = 14.0, 12.0, 5.0 Hz), 2.51 (1H, ddd, J = 14.0, 12.0, 5.0 Hz), 2.39 (3H, s), 1.93 (1H, dddd, J = 14.0, 12.0, 5.5, 3.5 Hz), 1.66 (1H, dddd, J = 14.0, 12.0, 10.0, 5.5 Hz); ^{13}C NMR (126 MHz, CDCl_3) δ 178.7, 163.4, 161.1, 143.7, 141.1, 138.6, 133.7, 130.3, 129.9, 129.8, 128.5, 128.4, 128.2, 127.3, 127.1, 126.1, 117.3, 114.3, 77.6, 58.6, 55.6, 41.3, 33.9, 32.3, 21.7; IR (liq. film): 3286, 3028, 1651, 1607, 1513, 1324, 1260, 1159, 1091, 755 cm^{-1} ; HRMS (FAB) Calcd for $\text{C}_{33}\text{H}_{33}\text{N}_2\text{O}_5\text{S}^+$ ($[\text{M}+\text{H}]^+$) 569.2110. Found 569.2123.

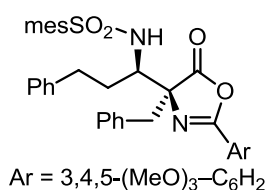


4c: IA, H/IPA = 3:1, flow rate = 0.5 mL/min, λ = 260 nm, 21.2 min (major *anti* isomer), 24.6 min (minor *anti* isomer), 26.8 min (major *syn* isomer), 44.7 min (minor *syn* isomer). **syn-4c:** ^1H NMR (500 MHz, CDCl_3) δ 7.81 (2H, d, J = 8.0 Hz), 7.43 (1H, t, J = 8.0 Hz), 7.29 (2H, d, J = 8.0 Hz), 7.22 (2H, t, J = 8.0 Hz), 7.18-7.12 (5H, m), 7.08 (2H, d, J = 8.0 Hz), 7.03 (2H, d, J = 8.0 Hz), 6.92 (1H, d, J = 8.0 Hz), 6.90 (1H, t, J = 8.0 Hz), 5.23 (1H, d, J = 10.0 Hz), 4.13 (1H, td, J = 10.0, 4.0 Hz), 3.78 (3H, s), 3.25 (1H, d, J = 13.0 Hz), 3.14 (1H, d, J = 13.0 Hz), 2.66 (1H, ddd, J = 14.0, 12.0, 5.0 Hz), 2.53 (1H, ddd, J = 14.0, 12.0, 5.0 Hz), 2.39 (3H, s), 2.01 (1H, dddd, J = 14.0, 12.0, 5.0, 4.0 Hz), 1.68 (1H, dddd, J = 14.0, 12.0, 10.0, 5.0 Hz); ^{13}C NMR (126 MHz, CDCl_3) δ 179.0, 160.6, 158.5, 143.7, 141.3, 138.6, 133.7₄, 133.7₁, 130.5, 130.4, 129.8, 128.5, 128.4, 128.2, 127.4, 127.2, 126.1, 120.5, 115.1, 111.8, 77.5, 58.3, 56.1, 41.0, 34.0, 32.1, 21.7; IR (liq. film): 3287, 3028, 1810, 1651, 1495, 1264, 1160, 1090, 972, 753 cm^{-1} ; HRMS (FAB) Calcd for $\text{C}_{33}\text{H}_{33}\text{N}_2\text{O}_5\text{S}$ ($[\text{M}+\text{H}]^+$) 569.2110. Found 569.2122.

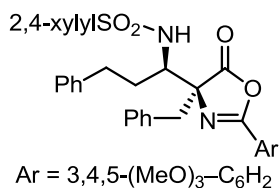


4d: IA, H/ IPA = 3:1, flow rate = 0.5 mL/min, λ = 260 nm, 18.5 min (minor *anti* isomer), 20.1 (major *anti* isomer), 32.4 min (major *syn* isomer), 44.5 min (minor *syn* isomer). **syn-4d:** ^1H NMR (500 MHz, CDCl_3) δ 7.80 (2H, d, J = 8.0 Hz), 7.29 (2H, d, J = 8.0 Hz), 7.22 (2H, t, J = 8.0 Hz), 7.15 (1H, t, J = 8.0 Hz), 7.13-7.09 (4H, m), 7.05-7.01 (3H, m), 6.96 (2H, s), 5.13 (1H, d, J = 10.0 Hz), 4.13 (1H, td, J = 10.0, 4.0 Hz), 3.88 (3H, s), 3.84 (6H, s), 3.24 (1H, d, J = 13.0 Hz), 3.13 (1H, d, J = 13.0 Hz), 2.66 (1H, ddd, J = 13.5, 12.0, 5.0 Hz), 2.51 (1H, ddd, J = 14.0, 12.0, 5.5 Hz), 2.40 (3H, s), 1.94 (1H, dddd, J = 14.0, 12.0, 5.5, 4.0 Hz), 1.67 (1H, dddd, J = 13.5, 12.0, 10.0, 5.0 Hz); ^{13}C NMR (126 MHz, CDCl_3) δ 178.5, 161.2, 153.4, 143.8, 142.3, 141.1, 138.6, 133.6, 130.3, 129.8, 128.6, 128.4, 128.3, 127.5, 127.2, 126.2, 120.0, 105.2, 78.0, 61.0, 58.6, 56.4, 41.3, 34.0, 32.3, 21.7; IR (liq. film): 3268, 2940, 1737, 1503, 1416, 1352, 1237, 1160, 1129, 1091 cm^{-1} ; HRMS (FAB) Calcd for $\text{C}_{35}\text{H}_{37}\text{N}_2\text{O}_7\text{S}^+$ ($[\text{M}+\text{H}]^+$)

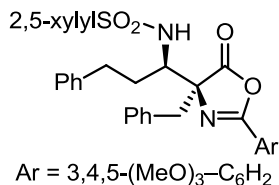
629.2321. Found 629.2300.



4e: IA, H/EtOH/EA = 50:4:1, flow rate = 0.5 mL/min, λ = 260 nm, 22.3 min (minor *syn* isomer), 23.8 min (major *anti* isomer), 25.7 min (major *syn* isomer), 27.7 min (minor *anti* isomer). **syn-4e:** ¹H NMR (500 MHz, CDCl₃) δ 7.24 (2H, t, J = 8.0 Hz), 7.18 (1H, t, J = 8.0 Hz), 7.14-7.08 (4H, m), 7.08-7.04 (2H, m), 7.01-6.97 (1H, m), 6.98 (2H, s), 6.96 (2H, s), 5.20 (1H, d, J = 10.0 Hz), 4.12 (1H, td, J = 10.0, 3.5 Hz), 3.90 (3H, s), 3.87 (6H, s), 3.13 (1H, d, J = 13.0 Hz), 3.06 (1H, d, J = 13.0 Hz), 2.75 (1H, ddd, J = 14.0, 11.5, 5.0 Hz), 2.67 (6H, s), 2.61 (1H, ddd, J = 14.0, 11.5, 5.5 Hz), 2.00 (1H, dddd, J = 14.0, 11.5, 5.5, 3.5 Hz), 1.69 (1H, dddd, J = 14.0, 11.5, 10.0, 5.0 Hz); ¹³C NMR (126 MHz, CDCl₃) δ 178.6, 161.2, 153.4, 142.4, 142.3, 141.1, 138.4, 136.0, 133.6, 132.1, 130.2, 128.6, 128.5, 128.3, 127.5, 126.2, 120.0, 105.2, 77.9, 61.1, 58.8, 56.4, 41.1, 34.2, 32.3, 23.2, 21.1; IR (liq. film): 3260, 2939, 1737, 1503, 1416, 1352, 1237, 1152, 1129, 928 cm⁻¹; HRMS (FAB) Calcd for C₃₇H₄₁N₂O₇S⁺ ([M+H]⁺) 657.2634. Found 657.2626.



4f: IA, H/EtOH = 3:1, flow rate = 0.5 mL/min, λ = 254 nm, 15.0 min (major *anti* isomer), 17.4 min (minor *anti* isomer), 19.4 min (major *syn* isomer), 23.0 min (minor *syn* isomer). **syn-4f:** ¹H NMR (500 MHz, CDCl₃) δ 7.92 (1H, d, J = 8.0 Hz), 7.22 (2H, t, J = 7.5 Hz), 7.20-7.02 (8H, m), 7.00-6.97 (2H, m), 6.97 (2H, s), 5.16 (1H, d, J = 10.0 Hz), 4.05 (1H, td, J = 10.0, 4.0 Hz), 3.89 (3H, s), 3.85 (6H, s), 3.10 (1H, d, J = 13.0 Hz), 3.04 (1H, d, J = 13.0 Hz), 2.73 (1H, ddd, J = 14.0, 11.5, 4.0 Hz), 2.60 (3H, s), 2.58 (1H, ddd, J = 14.0, 11.5, 5.0 Hz), 2.35 (3H, s), 1.99 (1H, dddd, J = 14.0, 11.5, 5.0, 4.0 Hz), 1.70 (1H, dddd, J = 14.0, 11.5, 10.0, 5.0 Hz); ¹³C NMR (126 MHz, CDCl₃) δ 178.5, 161.1, 153.4, 143.8, 142.4, 141.1, 136.6, 136.4, 133.6, 133.3, 130.2, 129.4, 128.6, 128.5, 128.3, 127.5, 127.0, 126.2, 120.0, 105.2, 77.9, 61.1, 58.7, 56.4, 41.1, 34.2, 32.3, 21.5, 20.5; IR (liq. film): 3257, 2938, 1503, 1456, 1416, 1351, 1236, 1129, 927, 915 cm⁻¹; HRMS (FAB) Calcd for C₃₆H₃₉N₂O₇S⁺ ([M+H]⁺) 643.2478. Found 643.2462.



4g: IA, H/EtOH = 10:1, flow rate = 0.5 mL/min, λ = 260 nm, 24.9 min (major *anti* isomer), 28.5 min (minor *anti* isomer), 31.0 min (major *syn* isomer), 36.1 min (minor *syn* isomer). **syn-4a:** ¹H NMR (500 MHz, CDCl₃) δ 7.85 (1H, d, J = 1.5 Hz), 7.26-7.21 (3H, m), 7.20-7.14 (2H, m), 7.10-7.08 (3H, m), 7.07 (2H, d, J = 7.0 Hz), 7.00-6.97 (2H, m), 6.96 (2H, s), 5.23 (1H, d, J = 10.0 Hz), 4.06 (1H, td, J = 10.0, 3.5 Hz), 3.89 (3H, s), 3.84 (6H, s), 3.09 (1H, d, J = 13.0 Hz), 3.02 (1H, d, J = 13.0 Hz), 2.74 (1H, ddd, J = 14.0, 12.0, 5.0 Hz), 2.58 (3H, s), 2.57 (1H, ddd, J = 14.0, 12.0, 5.0 Hz), 2.38 (3H, s), 2.00 (1H, dddd, J = 15.0, 12.0, 5.0, 3.5 Hz), 1.72 (1H, dddd, J = 15.0, 12.0, 10.0, 5.0 Hz); ¹³C NMR (126 MHz, CDCl₃) δ 178.5, 161.1, 153.4, 143.8, 142.4, 141.1, 136.6, 136.4, 133.6, 133.3, 130.2, 129.4, 128.6, 128.5, 128.3, 127.5, 127.0, 126.2, 120.0, 105.2, 77.9, 61.1, 58.7, 56.4,

41.1, 34.2, 32.3, 21.5, 20.5; IR (liq. film): 3257, 2938, 1503, 1455, 1416, 1352, 1236, 1154, 1129, 927 cm^{-1} ; HRMS (FAB) Calcd for $\text{C}_{36}\text{H}_{39}\text{N}_2\text{O}_7\text{S}^+$ ($[\text{M}+\text{H}]^+$) 643.2478. Found 643.2462.

2,5-xylylSO₂-NH

Ar = 3,4,5-(MeO)₃-C₆H₂ **4h**: IC, H/EtOH = 5:1, flow rate = 0.5 mL/min, λ = 260 nm, 18.0 min (major *anti* isomer), 24.2 min (minor *anti* isomer), 27.5 min (major *syn* isomer), 36.0 min (minor *syn* isomer). **syn-4h**: ¹H NMR (500 MHz, CDCl₃) δ 7.86 (1H, d, J = 1.5 Hz), 7.28 (1H, dd, J = 8.0, 1.5 Hz), 7.18 (1H, d, J = 8.0 Hz), 7.13-7.10 (3H, m), 7.05-7.02 (2H, m), 7.01 (2H, s), 4.87 (1H, d, J = 11.0 Hz), 3.90 (3H, s), 3.89-3.85 (1H, m), 3.87 (6H, s), 3.15 (1H, d, J = 13.0 Hz), 3.04 (1H, d, J = 13.0 Hz), 2.53 (3H, s), 2.41 (3H, s), 1.28 (3H, d, J = 11.5 Hz); ¹³C NMR (126 MHz, CDCl₃) δ 178.1, 161.4, 153.4, 142.4, 137.6, 136.3, 134.5, 134.0, 133.7, 132.6, 130.2, 128.3, 128.3, 127.5, 120.0, 105.2, 78.1, 61.1, 56.4, 54.2, 40.5, 21.0, 19.9, 17.6; IR (liq. film): 3241, 1650, 1586, 1504, 1416, 1352, 1156, 1129, 928, 755 cm^{-1} ; HRMS (FAB) Calcd for $\text{C}_{29}\text{H}_{33}\text{N}_2\text{O}_7\text{S}^+$ ($[\text{M}+\text{H}]^+$) 553.2008. Found 553.1995.

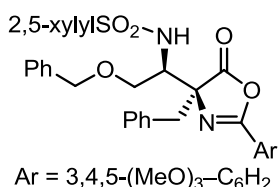
2,5-xylylSO₂-NH

Ar = 3,4,5-(MeO)₃-C₆H₂ **4i**: IA, H/IPA = 10:1, flow rate = 0.5 mL/min, λ = 260 nm, 15.2 min (minor *anti* isomer), 17.9 min (major *anti* isomer), 19.8 min (major *syn* isomer), 27.6 min (minor *syn* isomer). **syn-4i**: ¹H NMR (500 MHz, CDCl₃) δ 7.83 (1H, d, J = 1.0 Hz), 7.23 (1H, dd, J = 7.5, 1.0 Hz), 7.16 (1H, d, J = 7.5 Hz), 7.12-7.09 (3H, m), 7.02-7.00 (2H, m), 6.98 (2H, s), 5.02 (1H, d, J = 10.0 Hz), 3.97 (1H, td, J = 10.0, 4.0 Hz), 3.89 (3H, s), 3.87 (6H, s), 3.17 (1H, d, J = 13.5 Hz), 3.06 (1H, d, J = 13.5 Hz), 2.59 (3H, s), 2.36 (3H, s), 1.60 (1H, dddd, J = 14.0, 10.0, 6.0, 4.0 Hz), 1.34 (1H, dtd, J = 14.0, 10.0, 4.0 Hz), 1.30-1.04 (12H, m), 0.86 (3H, t, J = 7.5 Hz); ¹³C NMR (126 MHz, CDCl₃) δ 178.7, 161.0, 153.4, 142.3, 139.1, 136.3, 133.8, 133.6, 133.5, 132.4, 130.2, 129.6, 128.3, 127.4, 120.1, 105.1, 77.9, 61.1, 58.8, 56.4, 41.2, 32.0, 31.9, 29.4₃, 29.4₁, 29.2, 25.7, 22.8, 21.0, 20.2, 14.2; IR (liq. film): 3264, 2926, 1503, 1463, 1416, 1352, 1156, 1130, 928, 757 cm^{-1} ; HRMS (FAB) Calcd for $\text{C}_{36}\text{H}_{47}\text{N}_2\text{O}_7\text{S}^+$ ($[\text{M}+\text{H}]^+$) 651.3104. Found 651.3110.

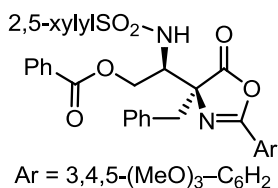
2,5-xylylSO₂-NH

Ar = 3,4,5-(MeO)₃-C₆H₂ **4j**: IA, H/IPA = 15:1, flow rate = 0.5 mL/min, λ = 260 nm, 18.6 min (minor *anti* isomer), 20.6 min (major *anti* isomer), 23.5 min (major *syn* isomer), 33.2 min (minor *syn* isomer). **syn-4j**: ¹H NMR (500 MHz, CDCl₃) δ 7.83 (1H, d, J = 1.5 Hz), 7.23 (1H, dd, J = 7.5, 1.5 Hz), 7.16 (1H, d, J = 7.5 Hz), 7.13-7.08 (3H, m), 7.02-7.00 (2H, m), 6.98 (2H, s), 5.80 (1H, ddt, J = 17.0, 10.0, 7.0 Hz), 5.04 (1H, d, J = 10.0 Hz), 4.99 (1H, dd, J = 17.0, 1.5 Hz), 4.93 (1H, dd, J = 10.0, 1.5 Hz), 3.97 (1H, td, J = 10.0, 3.0 Hz), 3.89 (3H, s), 3.86 (6H, s), 3.16 (1H, d, J = 13.0 Hz), 3.06 (1H, d, J = 13.0 Hz), 2.58 (3H, s), 2.37 (3H, s), 2.02 (2H, q, J = 7.0 Hz), 1.64-1.58 (1H, m), 1.40-1.09 (13H, m); ¹³C NMR (126 MHz, CDCl₃) δ 178.6, 161.0, 153.4, 142.3, 139.2, 139.1, 136.2, 133.8, 133.5, 133.4₄, 132.3₈, 130.2, 129.5, 128.3, 127.4, 120.1, 114.3, 105.1, 77.9, 61.0, 58.8, 56.4, 41.2, 33.9, 31.9, 29.3₉, 29.3₈, 29.2, 29.0, 25.7, 21.0, 20.2, one carbon was not found probably due to overlapping; IR (liq. film): 3259, 2926, 1504, 1462, 1416, 1352, 1156, 1130, 928, 757 cm^{-1} ; HRMS (FAB) Calcd for $\text{C}_{38}\text{H}_{49}\text{N}_2\text{O}_7\text{S}^+$ ($[\text{M}+\text{H}]^+$) 677.3260.

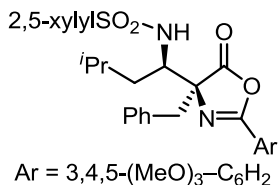
Found 677.3262.



4k: IC, H/EtOH = 3:1, flow rate = 0.5 mL/min, λ = 260 nm, 13.1 min (major *anti* isomer), 14.8 min (minor *anti* isomer), 20.1 min (major *syn* isomer), 24.2 min (minor *syn* isomer). **syn-4k:** ¹H NMR (500 MHz, CDCl₃) δ 7.86 (1H, d, J = 1.0 Hz), 7.26 (1H, dd, J = 8.0, 1.0 Hz), 7.19 (1H, d, J = 8.0 Hz), 7.16-7.12 (4H, m), 7.09 (2H, t, J = 7.5 Hz), 7.06-7.03 (2H, m), 7.00 (2H, d, J = 7.5 Hz), 6.89 (2H, s), 6.04 (1H, d, J = 9.5 Hz), 4.25 (1H, d, J = 12.0 Hz), 4.01 (1H, d, J = 12.0 Hz), 3.99 (1H, td, J = 9.5, 2.0 Hz), 3.90 (3H, s), 3.81 (6H, s), 3.41 (1H, dd, J = 9.5, 2.0 Hz), 3.26 (1H, d, J = 13.5 Hz), 3.14 (1H, dd, J = 9.5, 2.0 Hz), 2.95 (1H, d, J = 13.5 Hz), 2.71 (3H, s), 2.37 (3H, s); ¹³C NMR (126 MHz, CDCl₃) δ 178.2, 161.2, 153.4, 142.1, 138.7, 136.7, 136.3, 134.0, 133.8, 133.4, 132.7, 130.5, 129.6, 128.2₃, 128.2₂, 127.8, 127.5, 127.4, 120.4, 104.9, 73.7, 72.8, 69.2, 61.0, 58.7, 56.3, 41.6, 21.0, 19.8; IR (liq. film): 3367, 2939, 1503, 1456, 1416, 1353, 1160, 1129, 1092, 751 cm⁻¹; HRMS (FAB) Calcd for C₃₆H₃₉N₂O₈S⁺ ([M+H]⁺) 659.2427. Found 659.2397.

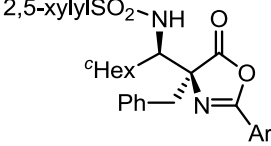


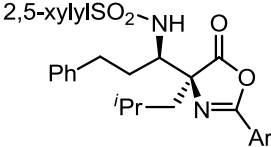
4l: IA, H/EtOH = 5:1, flow rate = 0.5 mL/min, λ = 254 nm, 17.7 min (minor *anti* isomer), 21.1 min (major *anti* isomer), 23.3 min (minor *syn* isomer), 36.3 min (major *syn* isomer). **syn-4l:** ¹H NMR (500 MHz, CDCl₃) δ 7.90 (2H, d, J = 8.0 Hz), 7.87 (1H, d, J = 1.5 Hz), 7.57 (1H, t, J = 8.0 Hz), 7.43 (2H, t, J = 8.0 Hz), 7.25 (1H, dd, J = 8.0, 1.5 Hz), 7.16-7.13 (4H, m), 7.08-7.05 (2H, m), 6.79 (2H, s), 5.97 (1H, d, J = 10.0 Hz), 4.34 (1H, dd, J = 12.0, 2.5 Hz), 4.25 (1H, dt, J = 10.0, 2.5 Hz), 4.15 (1H, dd, J = 12.0, 2.5 Hz), 3.85 (3H, s), 3.71 (6H, s), 3.33 (1H, d, J = 13.5 Hz), 3.09 (1H, d, J = 13.5 Hz), 2.65 (3H, s), 2.38 (3H, s); ¹³C NMR (126 MHz, CDCl₃) δ 178.6, 165.7, 161.5, 153.4, 142.4, 138.1, 136.6, 134.1, 133.8, 133.6, 133.0, 132.9, 130.4, 129.9, 129.7, 129.0, 128.6, 128.4, 127.7, 119.7, 105.0, 73.8, 64.6, 61.0, 57.5, 56.2, 41.4, 21.0, 19.9; IR (liq. film): 3281, 2940, 1649, 1503, 1417, 1352, 1268, 1159, 1129, 756 cm⁻¹; HRMS (FAB) Calcd for C₃₆H₃₇N₂O₉S ([M+H]⁺) 673.2220. Found 673.2225.

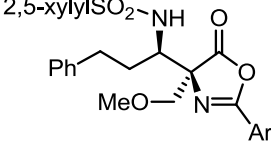


4m: IA, H/EtOH = 10:1, flow rate = 0.5 mL/min, λ = 260 nm, 16.9 min (major *anti* isomer), 19.6 min (minor *anti* isomer), 21.2 min (major *syn* isomer), 28.3 min (minor *syn* isomer). **syn-4m:** ¹H NMR (500 MHz, CDCl₃) δ 7.84 (1H, d, J = 2.0 Hz), 7.23 (1H, dd, J = 7.5, 2.0 Hz), 7.15 (1H, d, J = 7.5 Hz), 7.12-7.07 (3H, m), 7.00-6.94 (2H, m), 6.97 (2H, s), 4.98 (1H, d, J = 10.0 Hz), 4.06 (1H, dt, J = 10.0, 7.0 Hz), 3.90 (3H, s), 3.85 (6H, s), 3.09 (1H, d, J = 13.0 Hz), 3.03 (1H, d, J = 13.0 Hz), 2.55 (3H, s), 2.37 (3H, s), 1.67 (1H, nonet, J = 6.5 Hz), 1.36 (1H, td, J = 9.0, 7.0 Hz), 1.35 (1H, d, J = 9.0, 7.0 Hz), 0.87 (3H, d, J = 6.5 Hz), 0.86 (3H, d, J = 6.5 Hz); ¹³C NMR (126 MHz, CDCl₃) δ 178.6, 161.0, 153.4, 142.2, 139.3, 136.3, 133.8, 133.5, 133.3, 132.3, 130.2, 129.5, 128.3, 127.4, 120.1, 105.1, 78.2, 61.1, 57.3, 56.4, 41.3, 41.1, 24.1, 23.8, 21.3, 21.0, 20.1; IR (liq. film): 3260, 2958,

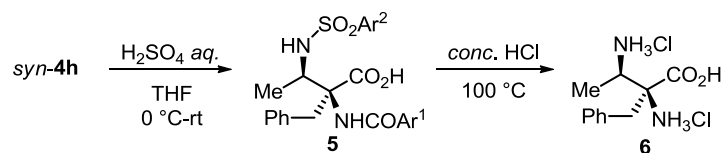
1650, 1586, 1503, 1416, 1352, 1129, 928, 756 cm^{-1} ; HRMS (FAB) Calcd for $\text{C}_{32}\text{H}_{39}\text{N}_2\text{O}_7\text{S}^+$ ($[\text{M}+\text{H}]^+$) 595.2478. Found 595.2472.

**4n:** IA, H/IPA/EtOH = 20:1:1, flow rate = 0.3 mL/min, $\lambda = 260$ nm, 31.7 min (minor *anti* isomer), 34.2 min (major *anti* isomer), 37.1 min (major *syn* isomer), 39.7 min (minor *syn* isomer). **syn-4n:** ^1H NMR (500 MHz, CDCl_3) δ 7.82 (1H, d, $J = 1.5$ Hz), 7.21 (1H, dd, $J = 7.5, 1.5$ Hz), 7.16 (1H, d, $J = 7.5$ Hz), 7.11-7.07 (3H, m), 7.00-6.98 (1H, m), 6.95 (2H, s), 6.94 (1H, d, $J = 7.5$ Hz), 5.22 (1H, d, $J = 10.0$ Hz), 3.97 (1H, dd, $J = 10.0, 2.5$ Hz), 3.90 (3H, s), 3.87 (6H, s), 3.01 (1H, d, $J = 12.5$ Hz), 2.98 (1H, d, $J = 12.5$ Hz), 2.59 (3H, s), 2.36 (3H, s), 1.78-1.62 (3H, m), 1.62-1.52 (2H, m), 1.48 (1H, d, $J = 10.0$ Hz), 1.28-0.75 (5H, m); ^{13}C NMR (126 MHz, CDCl_3) δ 179.1, 160.6, 153.4, 142.3, 139.5, 136.3, 133.4₄, 133.4₀, 133.3, 132.3, 130.3, 129.5, 128.2, 127.4, 120.2, 105.1, 76.6, 63.6, 61.1, 56.5, 42.0, 39.7, 31.6, 27.3, 26.5, 26.3, 26.0, 21.0, 20.2; IR (liq. film): 3394, 2931, 1503, 1416, 1352, 1156, 1129, 929, 755 cm^{-1} ; HRMS (FAB) Calcd for $\text{C}_{34}\text{H}_{41}\text{N}_2\text{O}_7\text{S}^+$ ($[\text{M}+\text{H}]^+$) 621.2634. Found 621.2630.

**4o:** IA, H/IPA/EA = 10:1:1, flow rate = 0.5 mL/min, $\lambda = 260$ nm, 11.5 min (major *anti* isomer), 13.4 min (major *syn* isomer), 16.5 min (minor *syn* isomer), 17.8 min (minor *anti* isomer). **syn-4o:** ^1H NMR (500 MHz, CDCl_3) δ 7.82 (1H, d, $J = 1.0$ Hz), 7.28 (1H, dd, $J = 7.5, 1.0$ Hz), 7.25-7.20 (3H, m), 7.17 (2H, s), 7.17-7.11 (1H, m), 7.07 (2H, d, $J = 7.5$ Hz), 5.08 (1H, d, $J = 10.5$ Hz), 3.92 (3H, s), 3.90 (6H, s), 3.87 (1H, td, $J = 10.5, 3.0$ Hz), 2.79 (1H, ddd, $J = 13.5, 11.5, 5.0$ Hz), 2.63-2.56 (1H, m), 2.60 (3H, s), 2.39 (3H, s), 1.88 (1H, dddd, $J = 13.5, 11.5, 5.5, 3.5$ Hz), 1.60-1.52 (3H, m), 1.34 (1H, nonet, $J = 7.0$ Hz), 0.66 (3H, d, $J = 7.0$ Hz), 0.64 (3H, d, $J = 7.0$ Hz); ^{13}C NMR (126 MHz, CDCl_3) δ 180.0, 160.9, 153.6, 142.5, 141.2, 139.2, 136.3, 133.6, 132.5, 129.6, 128.5₂, 128.5₁, 128.4₅, 126.2, 120.1, 105.3, 75.9, 61.1, 59.7, 56.5, 44.1, 33.7, 32.3, 24.5, 24.0, 23.0, 21.0, 20.2; IR (liq. film): 3262, 2960, 1649, 1503, 1417, 1351, 1155, 1129, 913, 755 cm^{-1} ; HRMS (FAB) Calcd for $\text{C}_{33}\text{H}_{41}\text{N}_2\text{O}_7\text{S}^+$ ($[\text{M}+\text{H}]^+$) 609.2634. Found 609.2623.

**4p:** IC, H/EtOH = 3:1, flow rate = 0.5 mL/min, $\lambda = 260$ nm, 16.0 min (major *anti* isomer), 18.2 min (major *syn* isomer), 19.8 min (minor *anti* isomer), 26.3 min (minor *syn* isomer). **syn-4p:** ^1H NMR (500 MHz, CDCl_3) δ 7.81 (1H, d, $J = 1.5$ Hz), 7.29 (1H, dd, $J = 7.0, 1.5$ Hz), 7.26-7.11 (6H, m), 7.01 (2H, d, $J = 7.0$ Hz), 5.12 (1H, d, $J = 10.0$ Hz), 3.95 (1H, td, $J = 10.0, 3.5$ Hz), 3.91₂ (6H, s), 3.90₉ (3H, s), 3.60 (1H, d, $J = 9.0$ Hz), 3.51 (1H, d, $J = 9.0$ Hz), 3.14 (3H, s), 2.63 (1H, ddd, $J = 14.0, 11.5, 5.5$ Hz), 2.60 (3H, s), 2.44 (1H, ddd, $J = 14.0, 11.5, 5.5$ Hz), 2.39 (3H, s), 1.82 (1H, dddd, $J = 14.0, 11.5, 5.5, 3.5$ Hz), 1.59 (1H, m); ^{13}C NMR (126 MHz, CDCl_3) δ 177.9, 162.2, 153.5, 142.5,

140.9, 138.7, 136.4, 133.7, 133.7, 132.5, 129.7, 128.5, 128.4, 126.2, 120.2, 105.5, 77.1, 73.8, 61.1, 59.6, 56.4, 55.6, 33.7, 31.9, 21.0, 20.2; IR (liq. film): 3264, 2938, 1586, 1503, 1459, 1417, 1352, 1156, 1128, 754 cm^{-1} ; HRMS (FAB) Calcd for $\text{C}_{31}\text{H}_{37}\text{N}_2\text{O}_8\text{S}$ ($[\text{M}+\text{H}]^+$) 597.2271. Found 598.2289.

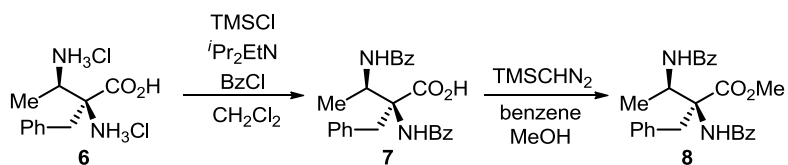


Deprotection of *syn*-4h to α,β -Diamino Acid Dihydrochloride 6 ($\text{Ar}^1 = 3,4,5\text{-(MeO)}_3\text{-C}_6\text{H}_2$, $\text{Ar}^2 = 2,5\text{-xylyl}$):

Hydrolysis of *syn*-4h to the Corresponding Carboxylic Acid 5: A solution of diastereomerically pure *syn*-4h (70.5 mg, 0.128 mmol, 92% ee) in THF (0.5 mL) was added 0.5 mL of 25 wt% H_2SO_4 aqueous solution dropwise at 0 °C. The reaction mixture was vigorously stirred for 30 min and diluted with H_2O . The resulting organic phase was extracted with EA three times. The combined organic extracts were dried over Na_2SO_4 and filtered. After concentration, the residue was purified by column chromatography (H/EA = 1:2 as eluent) to give **5** in quantitative yield. **5**: ^1H NMR (700 MHz, CDCl_3) δ 8.17 (1H, brs), 7.88 (1H, s), 7.24 (1H, d, $J = 7.7$ Hz), 7.24-7.18 (2H, m), 7.18-7.06 (3H, m), 7.16 (1H, d, $J = 7.7$ Hz), 6.87 (2H, s), 5.62 (1H, brs), 4.51 (1H, brs), 3.87 (3H, s), 3.81 (6H, s), 3.78 (1H, q, $J = 7.0$ Hz), 3.62 (1H, d, $J = 14.0$ Hz), 3.46 (1H, d, $J = 14.0$ Hz), 2.59 (3H, s), 2.37 (3H, s), 1.07 (3H, d, $J = 7.0$ Hz); ^{13}C NMR (175 MHz, CDCl_3) δ 173.7, 167.6, 153.3, 141.3, 138.0, 136.5, 136.0, 133.8, 133.6, 132.6, 130.0, 129.5, 128.8, 127.4, 104.52, 77.4, 68.1, 61.0, 56.3, 52.4, 37.0, 21.0, 20.0, 17.1; IR (liq. film): 3385, 2939, 1584, 1495, 1415, 1335, 1237, 1156, 1129, 757 cm^{-1} ; HRMS (FAB) Calcd for $\text{C}_{29}\text{H}_{35}\text{N}_2\text{O}_8\text{S}$ ($[\text{M}+\text{H}]^+$) 571.2114. Found 571.2101.

Preparation of 6 by Complete Deprotection of 5: A suspension of **5** (55.4 mg, 0.097 mmol) in *conc.* HCl was stirred at 100 °C for 24 h. The resulting mixture was concentrated in vacuo with mild heating (40 °C) to give crude residue. It was diluted with 2 mL of water and washed with EA and the aqueous layer was concentrated. Analytically pure **6** was obtained by purification through Amberlite IR 120 resin (H^+ form) in 87 % yield. **6**: ^1H NMR (500 MHz, D_2O) δ 7.45-7.39 (3H, m), 7.28-7.25 (2H, m), 3.82 (1H, q, $J = 7.0$ Hz), 3.56 (1H, d, $J = 14.0$ Hz), 3.06 (1H, d, $J = 14.0$ Hz), 1.45 (3H, d, $J = 7.0$ Hz), N-H and O-H protons were not found due to deuterium exchange; ^{13}C NMR (175 MHz, $(\text{CD}_3)_2\text{SO}$) δ 168.9, 132.6, 130.6, 128.6, 127.7, 64.5, 49.8, 38.4, 14.1; IR (KBr): 3379, 2947, 1737, 1617, 1498, 1457, 1403, 1241, 745, 704 cm^{-1} ; HRMS (FAB) Calcd for $\text{C}_{11}\text{H}_{17}\text{N}_2\text{O}_2$ ($[\text{M}+\text{H}]^+$) 209.1290. Found 209.1288.

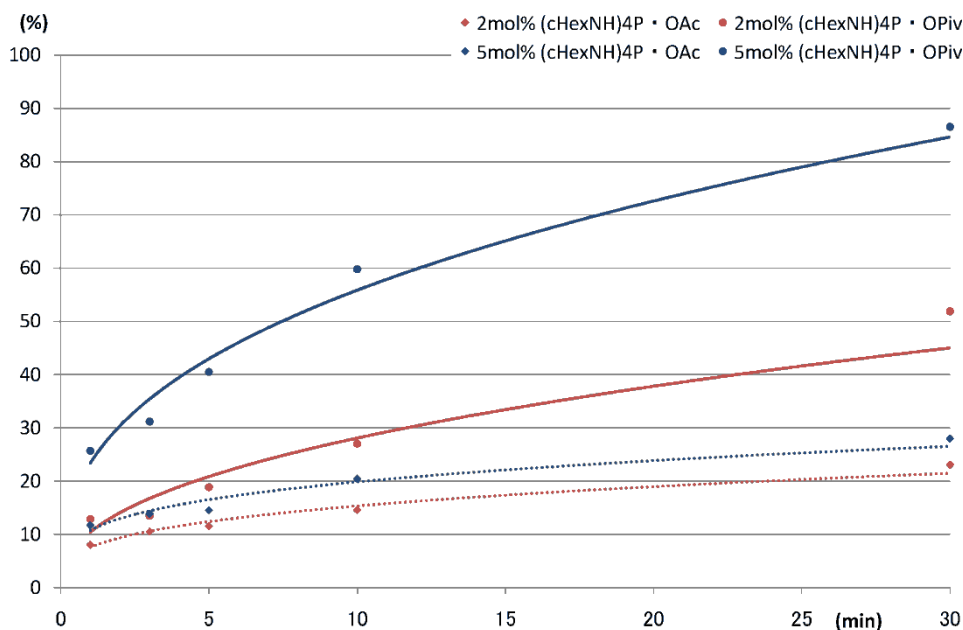
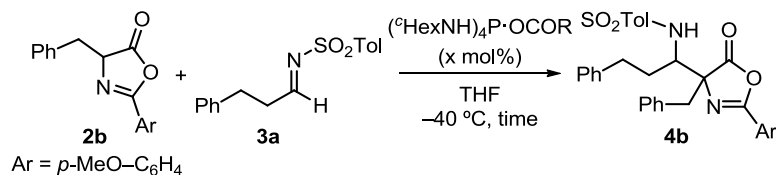
Conservation of Enantiomeric Purity: The enantiomeric purity of **6** was determined by HPLC analysis after protecting all functionalities according to literature procedure.²⁰



Benzoylation of 6: To a suspension of **6** (23.6 mg, 0.084 mmol) in CH_2Cl_2 was added chlorotrimethylsilane (54 μL , 0.42 mmol) at room temperature (rt). The mixture was refluxed for 1 h and then cooled to rt. After the addition of *N,N*-diisopropylethylamine (116 μL , 0.67 mmol), the mixture was again heated to reflux for 1.5 h and then cooled to 0 °C. Benzoyl chloride (24 μL , 0.21 mmol) was then added. The reaction mixture was allowed to warm to rt and stirred for 6 h. The resulting solution was poured onto ice and the aqueous phase was extracted with EA twice. The combined organic extracts were dried over Na_2SO_4 , filtered, and evaporated to afford crude residue (If partial formation of the corresponding azlactone is detected on TLC or ^1H NMR analysis of the crude mixture at this stage, the treatment of the residue with aqueous H_2SO_4 in THF is required.). Purification by column chromatography on silica gel (H/EA = 1:2 as eluent) gave **7** in 88% yield.

Preparation of 8: To a solution of **7** (30.8 mg, 0.074 mmol) in benzene/MeOH (v/v = 7:3, 1.0 mL) was added a solution of trimethylsilyldiazomethane in ether (2 M, 56 μL). The reaction mixture was stirred for 5 min. After being concentrated, the resulting residue was purified by column chromatography (H/EA = 5:1 as eluent) to afford **8** in 94% yield. The enantiomeric purity of **8** was determined to be 92% ee by chiral stationary phase HPLC analysis. **8:** IC, H/EtOH = 10:1, flow rate = 0.5 mL/min, $\lambda = 260$ nm, 45.6 min (major isomer), 64.3 min (minor isomer) ^1H NMR (500 MHz, CDCl_3) δ 8.06 (1H, br), 7.74 (2H, d, $J = 7.5$ Hz), 7.63 (2H, dd, $J = 7.5$ Hz), 7.51 (1H, tt, $J = 7.5, 1.5$ Hz), 7.49 (1H, tt, $J = 7.5, 1.5$ Hz), 7.42 (2H, t, $J = 7.5$ Hz), 7.41 (2H, t, $J = 7.5$ Hz), 7.33-7.26 (3H, m), 7.16 (2H, dd, $J = 7.5, 1.5$ Hz), 6.91 (1H, brs), 5.17 (1H, dq, $J = 9.5, 7.0$ Hz), 3.77 (3H, s), 3.68 (1H, d, $J = 14.0$ Hz), 3.44 (1H, d, $J = 14.0$ Hz), 1.36 (3H, d, $J = 7.0$ Hz).

Counter Anion Dependent Reaction Profile for (⁶HexNH)₄P·OCOR-Catalyzed Direct Mannich Reaction:



Procedure: A solution of azlactone **2b** (28.1 mg, 0.1 mmol) and (⁶HexNH)₄P·OCOR (x mol%) in 0.8 mL of THF was cooled to -78 °C under Ar. To the resulting suspension was added a solution of imine **3a** in THF (0.55 M, 0.2 mL) dropwise. The reaction was considered to start when the mixture was warmed to -40 °C. After stirring for the indicated time, 0.1 M of trifluoroacetic acid in THF (40 μL) was introduced to quench the reaction. The resulting mixture was concentrated and the residue was directly subjected to ¹H NMR analysis to determine the conversion (mesitylene was used for internal standard.).

Crystallographic Structure Determination:

Recrystallization of (M,S)-1·Cl: Tetraaminophosphonium salt (M,S)-1·Cl was recrystallized from hexane/acetone solvent system at room temperature.

The single crystal thus obtained was mounted on CryoLoop. Data of X-ray diffraction were collected at 153 K on a Bruker SMART APEX CCD diffractometer with graphite-monochromated Mo K α radiation ($\lambda = 0.71073 \text{ \AA}$). An absorption correction was made using SADABS. The structure was solved by direct methods and Fourier syntheses, and refined by full-matrix least squares on F^2 by using SHELXTL²¹. All non-hydrogen atoms were refined with anisotropic displacement parameters. Hydrogen atoms bonded to nitrogen atoms were located from a difference synthesis and their coordinates and isotropic thermal parameters refined. The other hydrogen atoms except that bonded to water were placed in calculated positions. The crystallographic data were summarized in the following table.

Table S1. Crystal data and structure refinement for (M,S)-1·Cl·H₂O.

| | | |
|--|--|--|
| Empirical formula | C ₃₆ H ₄₆ Cl N ₄ O P | |
| Formula weight | 617.19 | |
| Temperature | 153(2) K | |
| Wavelength | 0.71073 \AA | |
| Crystal system | Orthorhombic | |
| Space group | P2(1)2(1)2(1) | |
| Unit cell dimensions | a = 13.813(4) \AA b = 15.029(5) \AA c = 15.943(5) \AA | $\alpha = 90^\circ$ $\beta = 90^\circ$ $\gamma = 90^\circ$ |
| Volume | 3309.8(18) \AA^3 | |
| Z | 4 | |
| Density (calculated) | 1.239 Mg/m ³ | |
| Absorption coefficient | 0.198 mm ⁻¹ | |
| F(000) | 1320 | |
| Crystal size | 0.60 x 0.30 x 0.10 mm ³ | |
| Theta range for data collection | 1.86 to 28.30 $^\circ$. | |
| Index ranges | -12 \leq h \leq 18, -17 \leq k \leq 20, -21 \leq l \leq 21 | |
| Reflections collected | 19873 | |
| Independent reflections | 8148 [R(int) = 0.0526] | |
| Completeness to theta = 28.30 $^\circ$ | 99.5 % | |
| Absorption correction | Empirical | |
| Max. and min. transmission | 0.9804 and 0.8902 | |
| Refinement method | Full-matrix least-squares on F^2 | |
| Data / restraints / parameters | 8148 / 0 / 403 | |
| Goodness-of-fit on F^2 | 1.078 | |
| Final R indices [I $>$ 2 σ (I)] | R ₁ = 0.0615, wR ₂ = 0.1293 | |
| R indices (all data) | R ₁ = 0.0772, wR ₂ = 0.1370 | |
| Absolute structure parameter | -0.02(7) | |
| Largest diff. peak and hole | 0.620 and -0.255 e. \AA^{-3} | |

Hydrogen bonds (*M,S*)-1·Cl·H₂O [\AA and $^\circ$].

| D-H...A | d(D-H) | d(H...A) | d(D...A) | \angle (DHA) |
|----------------------|---------|----------|----------|----------------|
| N(4)-H(38)...O(1) | 0.81(4) | 2.15(4) | 2.938(4) | 166(4) |
| N(2)-H(37)...Cl(1)#1 | 0.81(4) | 2.32(4) | 3.118(2) | 168(4) |

Symmetry transformations used to generate equivalent atoms: #1 $-x+1/2, -y+1, z-1/2$

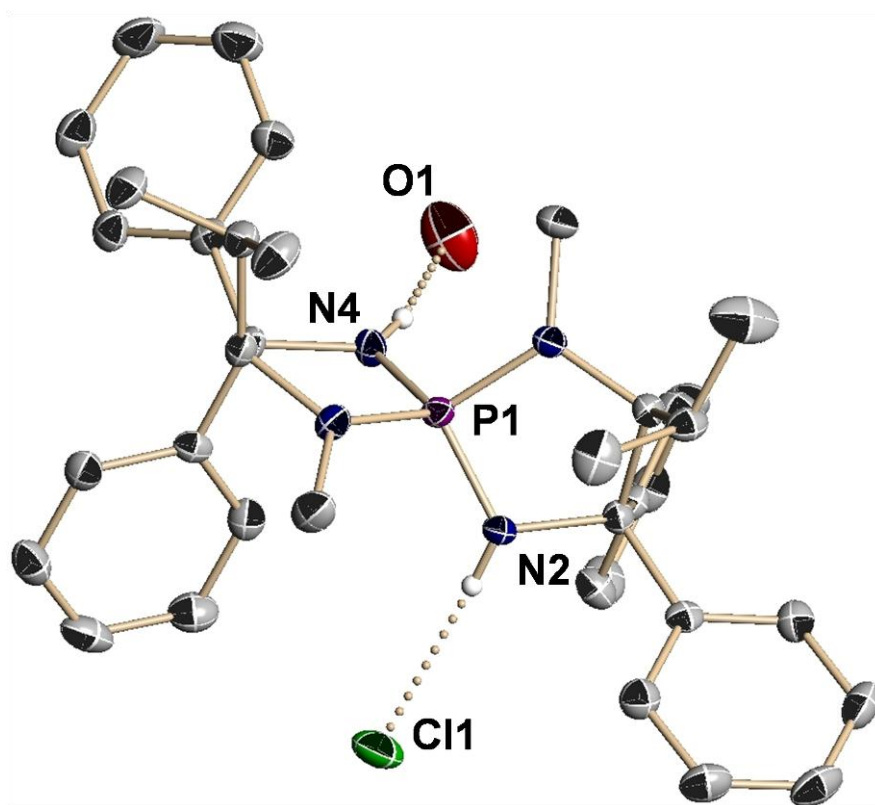


Figure S1. Molecular structure of tetraaminophosphonium salt (*M,S*)-**1**·Cl·H₂O. All calculated hydrogen atoms are omitted for clarity. Purple = phosphorus, blue = nitrogen, green = chlorine, red = oxygen, black = carbon.

Recrystallization of (P,S)-1·Cl: Tetraaminophosphonium salt (P,S)-1·Cl was recrystallized from hexane/EtOH solvent system at room temperature.

The single crystal thus obtained was mounted on CryoLoop. Data of X-ray diffraction were collected at 127 K on a Bruker SMART APEX CCD diffractometer with graphite-monochromated Mo K α radiation ($\lambda = 0.71073 \text{ \AA}$). An absorption correction was made using SADABS. The structure was solved by direct methods and Fourier syntheses, and refined by full-matrix least squares on F^2 by using SHELXTL. All non-hydrogen atoms except solvent molecules and disordered parts were refined with anisotropic displacement parameters. Hydrogen atoms bonded to nitrogen atoms were located from a difference synthesis and their coordinates and isotropic thermal parameters refined. The other hydrogen atoms except that bonded to solvent molecules and disordered parts were placed in calculated positions. Each disorder was modeled over two positions and refined. The crystallographic data were summarized in the following table.

Table S2. Crystal data and structure refinement for (P,S)-1·Cl·EtOH.

| | | |
|--|--|--|
| Empirical formula | C ₃₈ H ₄₉ Cl N ₄ O P | |
| Formula weight | 644.23 | |
| Temperature | 153(2) K | |
| Wavelength | 0.71073 \AA | |
| Crystal system | Orthorhombic | |
| Space group | P2(1)2(1)2(1) | |
| Unit cell dimensions | a = 12.212(3) \AA b = 15.543(3) \AA c = 19.012(4) \AA | $\alpha = 90^\circ$ $\beta = 90^\circ$ $\gamma = 90^\circ$ |
| Volume | 3608.6(13) \AA^3 | |
| Z | 4 | |
| Density (calculated) | 1.186 Mg/m ³ | |
| Absorption coefficient | 0.185 mm ⁻¹ | |
| F(000) | 1380 | |
| Crystal size | 0.50 x 0.30 x 0.10 mm ³ | |
| Theta range for data collection | 1.69 to 28.35 $^\circ$. | |
| Index ranges | -16<=h<=15, -20<=k<=19, -23<=l<=25 | |
| Reflections collected | 27536 | |
| Independent reflections | 8984 [R(int) = 0.0896] | |
| Completeness to theta = 28.35 $^\circ$ | 99.7 % | |
| Absorption correction | Empirical | |
| Max. and min. transmission | 0.9818 and 0.9133 | |
| Refinement method | Full-matrix least-squares on F^2 | |
| Data / restraints / parameters | 8984 / 0 / 410 | |
| Goodness-of-fit on F^2 | 1.058 | |
| Final R indices [I>2 σ (I)] | R ₁ = 0.0822, wR ₂ = 0.1771 | |
| R indices (all data) | R ₁ = 0.1062, wR ₂ = 0.1912 | |
| Absolute structure parameter | 0.09(10) | |
| Largest diff. peak and hole | 0.768 and -0.399 e. \AA^{-3} | |

Hydrogen bonds for (*P,S*)-**1**·Cl [\AA and $^\circ$].

| D-H...A | d(D-H) | d(H...A) | d(D...A) | \angle (DHA) |
|----------------------|---------|----------|----------|----------------|
| N(4)-H(41)...Cl(1)#1 | 0.80(5) | 2.46(6) | 3.244(3) | 166(5) |
| N(2)-H(40)...Cl(1)#1 | 0.68(4) | 2.57(4) | 3.238(4) | 167(5) |

Symmetry transformations used to generate equivalent atoms: #1 x,y-1,z

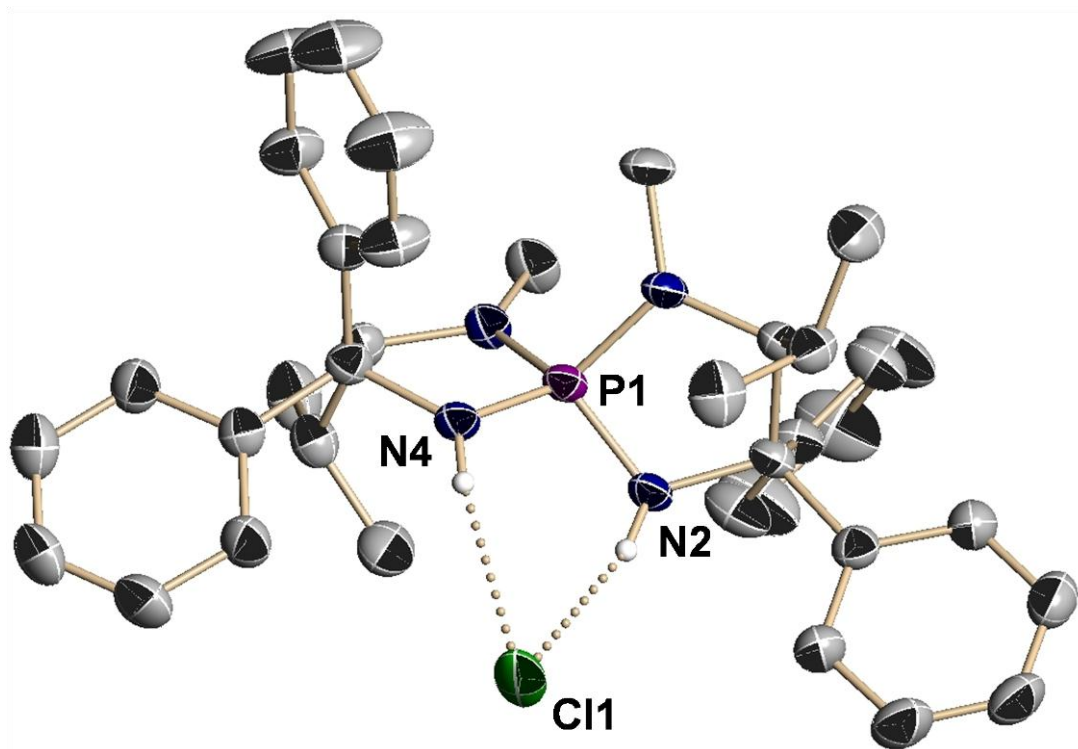


Figure S2. Molecular structure of tetraaminophosphonium salt (*P,S*)-1-Cl. All calculated hydrogen atoms and the solvent molecule (EtOH) are omitted for clarity. Purple = phosphorus, blue = nitrogen, green = chlorine, black = carbon.

Recrystallization of 4g-Derived Diamino Acid: The title compound was recrystallized from hexane/ethyl acetate solvent system at room temperature.

The single crystal thus obtained was mounted on CryoLoop. Data of X-ray diffraction were collected at 153 K on a Bruker SMART APEX CCD diffractometer with graphite-monochromated Mo K α radiation ($\lambda = 0.71073 \text{ \AA}$). An absorption correction was made using SADABS. The structure was solved by direct methods and Fourier syntheses, and refined by full-matrix least squares on F^2 by using SHELXTL. All non-hydrogen atoms were refined with anisotropic displacement parameters. Hydrogen atoms bonded to nitrogen atoms were located from a difference synthesis and their coordinates and isotropic thermal parameters refined. The other hydrogen atoms were placed in calculated positions. The crystallographic data were summarized in the following table.

Table S3. Crystal data and structure refinement for **4g** derived diamino acid with ethyl acetate

| | | |
|--|---|---|
| Empirical formula | C40 H48 N2 O10 S | |
| Formula weight | 748.86 | |
| Temperature | 153(2) K | |
| Wavelength | 0.71073 \AA | |
| Crystal system | Monoclinic | |
| Space group | P2(1) | |
| Unit cell dimensions | a = 11.360(3) \AA b = 50.827(12) \AA c = 13.745(3) \AA | $\alpha = 90^\circ$. $\beta = 90.208(5)^\circ$. $\gamma = 90^\circ$. |
| Volume | 7936(3) \AA^3 | |
| Z | 8 | |
| Density (calculated) | 1.254 Mg/m^3 | |
| Absorption coefficient | 0.140 mm^{-1} | |
| F(000) | 3184 | |
| Crystal size | 0.80 x 0.50 x 0.10 mm^3 | |
| Theta range for data collection | 0.80 to 28.48 $^\circ$. | |
| Index ranges | -14 \leq h \leq 15, -65 \leq k \leq 68, -17 \leq l \leq 18 | |
| Reflections collected | 60804 | |
| Independent reflections | 34870 [R(int) = 0.0414] | |
| Completeness to theta = 28.48 $^\circ$ | 98.7 % | |
| Absorption correction | Empirical | |
| Max. and min. transmission | 0.9862 and 0.8964 | |
| Refinement method | Full-matrix least-squares on F^2 | |
| Data / restraints / parameters | 34870 / 1 / 1963 | |
| Goodness-of-fit on F^2 | 1.021 | |
| Final R indices [I $>$ 2 σ (I)] | R1 = 0.0653, wR2 = 0.1618 | |
| R indices (all data) | R1 = 0.0884, wR2 = 0.1789 | |
| Absolute structure parameter | 0.12(5) | |
| Largest diff. peak and hole | 1.275 and -0.467 e.\AA^{-3} | |

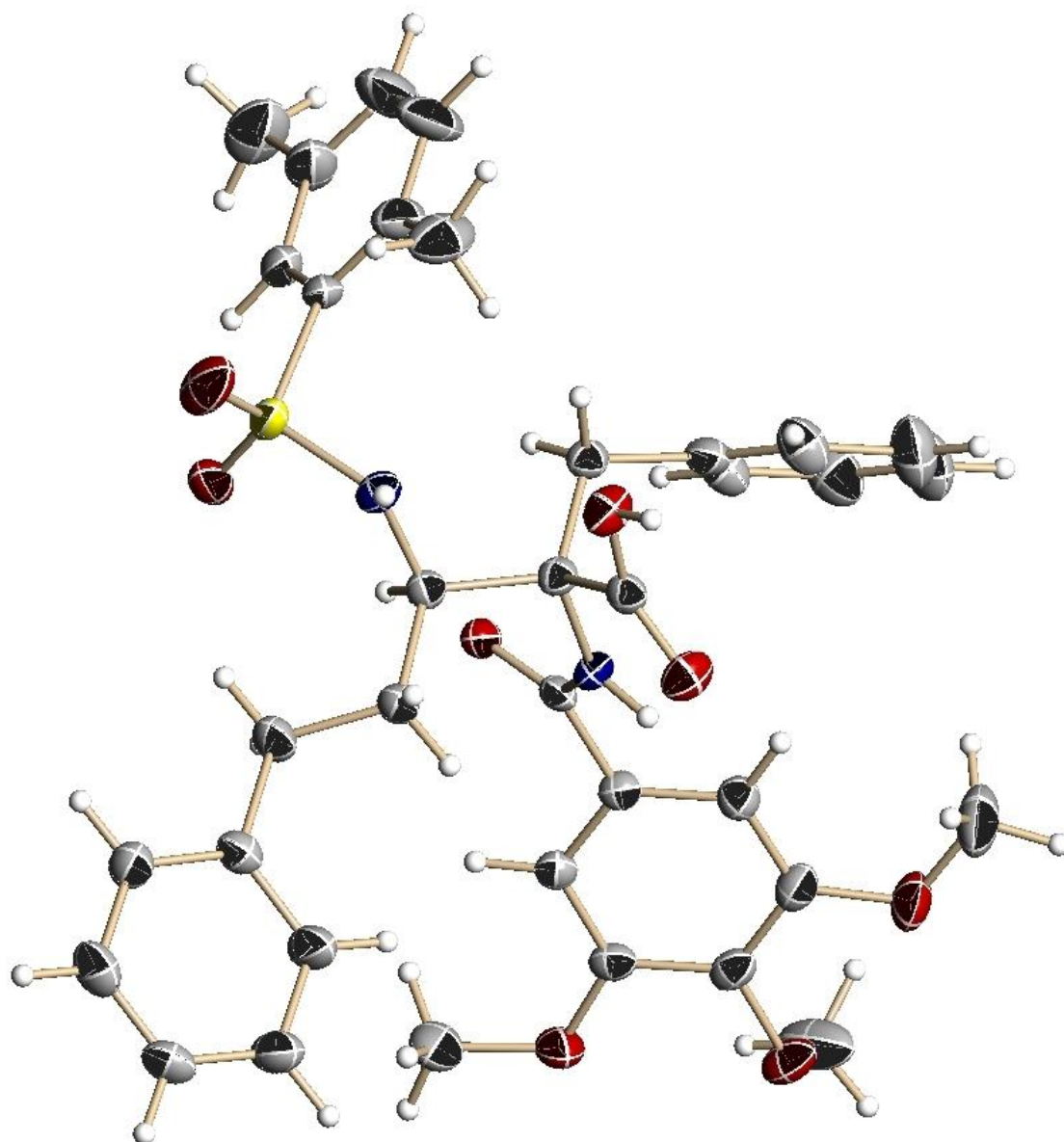


Figure S3. Crystal structure of **4g**-derived diamino acid. Red = oxygen, blue = nitrogen, yellow = sulfur, black = carbon. Although the unit cell contained four molecules of the diamino acid and ethyl acetate, only one molecule was picked up to show its 3D structure for clarity.

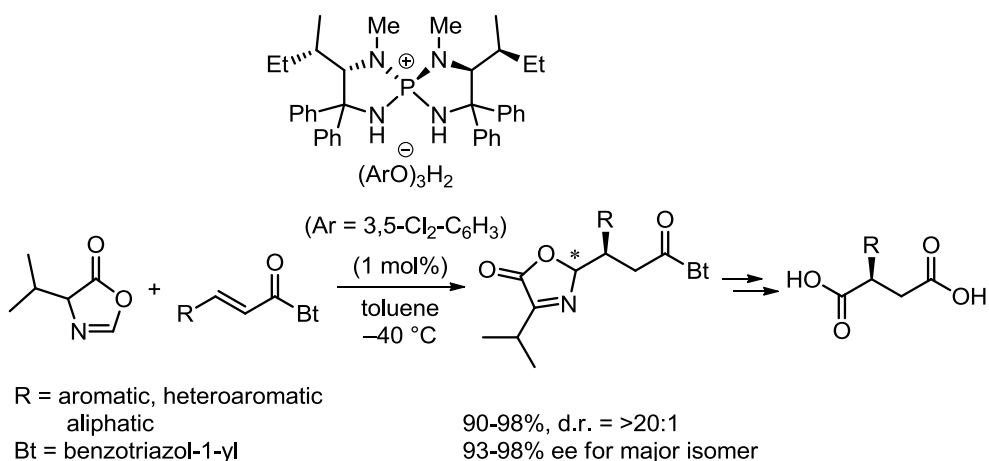
References and Notes

- (1) For reviews on organocatalysis, see: (a) Dalko, P. I.; Moisan, L. *Angew. Chem., Int. Ed.* **2004**, *43*, 5138. (b) Pellissier, H. *Tetrahedron* **2007**, *63*, 9267. (c) Dondoni, A.; Massi, A. *Angew. Chem., Int. Ed.* **2008**, *47*, 4638.
- (2) *Asymmetric Phase Transfer Catalysis*; Maruoka, K., Ed.; Wiley-VCH: Weinheim, Germany, 2008.
- (3) Nagao, H.; Kawano, Y.; Mukaiyama, T. *Bull. Chem. Soc. Jpn.* **2007**, *80*, 2406 and references therein.
- (4) Ooi, T.; Maruoka, K. *Acc. Chem. Res.* **2004**, *37*, 526.
- (5) Examples for chiral counter anion strategy in catalytic asymmetric syntheses: (a) Mayer, S.; List, B. *Angew. Chem., Int. Ed.* **2006**, *45*, 4193. (b) Hamilton, G. L.; Kang, E. J.; Mba, M.; Toste, F. D. *Science*, **2007**, *317*, 496. (c) Rueping, M.; Antonchick, A. R.; Brinkmann, C. *Angew. Chem., Int. Ed.* **2007**, *46*, 6903. (d) Raheem, I. T.; Thiara, P. S.; Peterson, E. A.; Jacobsen, E. N. *J. Am. Chem. Soc.* **2007**, *129*, 13404. (e) Wang, X.; List, B. *Angew. Chem., Int. Ed.* **2008**, *47*, 1119. There are numbers of important reports on anion effect in the catalysis of chiral amines, which involves *protonated* ammonium salts, see for example: Mase, N.; Tanaka, F.; Barbas III, C. F. *Angew. Chem., Int. Ed.* **2004**, *43*, 2420.
- (6) Uraguchi, D.; Sakaki, S.; Ooi, T. *J. Am. Chem. Soc.* **2007**, *129*, 12392.
- (7) pK_a values of selected carboxylic acids in water: formic acid; 3.75, benzoic acid; 4.19, acetic acid; 4.76, pivalic acid; 5.03.
- (8) For reviews on organocatalyzed Mannich-type reactions, see: (a) Ting, A.; Schaus, S. E. *Eur. J. Org. Chem.* **2007**, 5797. (b) Verkade, J. M. M.; van Hemert, L. J. C.; Quaedflieg, P. J. L. M.; Rutjes, F. P. J. T. *Chem. Soc. Rev.* **2008**, *37*, 29.
- (9) (a) Fisk, J. S.; Mosey, R. A.; Tepe, J. J. *Chem. Soc. Rev.* **2007**, *36*, 1432. (b) Cabrera, S.; Reyes, E.; Alemán, J.; Milelli, A.; Kobbelgaard, S.; Jørgensen, K. A. *J. Am. Chem. Soc.* **2008**, *130*, 12031.
- (10) Dalla Croce, P.; Ferraccioli, R.; La Rosa, C. *J. Chem. Soc., Perkin Trans. 1* **1994**, 2499.
- (11) Review on α,β -diamino acids: Viso, A.; de la Pradilla, R. F.; García, A.; Flores, A. *Chem. Rev.* **2005**, *105*, 3167.
- (12) Catalytic asymmetric synthesis of α -substituted α,β -diamino acids: (a) Knudsen, K. R.; Jørgensen, K. A. *Org. Biomol. Chem.* **2005**, *3*, 1362. (b) Chen, Z.; Morimoto, H.; Matsunaga, S.; Shibasaki, M. *J. Am. Chem. Soc.* **2008**, *130*, 2170. (c) Singh, A.; Johnston, J. N. *J. Am. Chem. Soc.* **2008**, *130*, 5866. (d) Uraguchi, D.; Koshimoto, K.; Ooi, T. *J. Am. Chem. Soc.* **2008**, *130*, 10878.

- (13) Tetraaminophosphonium carboxylates without *N*-methyl groups were not suitable for the present transformation in terms of the stereoselectivity.
- (14) Similar observation was reported in the chiral quaternary ammonium salt-catalyzed asymmetric phase-transfer alkylation: Corey, E. J.; Bo, Y.; Busch-Petersen, J. *J. Am. Chem. Soc.* **1998**, *120*, 13000.
- (15) This protocol is not effective for aromatic imines ($R^1 = \text{PhCH}_2$, $R^2 = \text{Ph}$ in Table 2; 41 h, 98%, dr = 1.1:1, 15% ee for major isomer).
- (16) The conservation of enantiomeric purity was confirmed by HPLC analysis after derivatization to the corresponding fully protected α,β -diamino acid ester. See Supporting Information for details.
- (17) Uragchi, D.; Sakaki, S.; Ooi, T. *J. Am. Chem. Soc.* **2007**, *129*, 12393.
- (18) Tokunaga, M.; Kiyosu, J.; Obora, Y. Tsuji, Y. *J. Am. Chem. Soc.* **2006**, *128*, 4481.
- (19) Wang, Y.-Q.; Song, J.; Hong, R.; Li, H.; Deng, L. *J. Am. Chem. Soc.* **2006**, *128*, 8156.
- (20) Obrecht, D.; Karajiannis, H.; Lehmann, C.; Schönholzer, P.; Spielgler, C.; Müller, K. *Helv. Chim. Acta* **1995**, *78*, 703.
- (21) G. M. Sheldrick, SHELXTL 5.1, Bruker AXS Inc., Madison, Wisconsin, 1997.

Chapter 3

Chiral Organic Ion Pair Catalysts Assembled Through a Hydrogen-Bonding Network



Abstract: Research to develop structurally discrete, chiral supramolecular catalysts for asymmetric organic transformations has met with limited success. Here I report that a chiral tetraaminophosphonium cation, two phenols and a phenoxide anion appear to self-assemble into a catalytically active supramolecular architecture through intermolecular hydrogen-bonding. The structure of the resulting molecular assembly was determined in the solid state by X-ray diffraction analysis. Furthermore, in solution the complex promotes a highly stereoselective conjugate addition of acyl anion equivalents to α,β -unsaturated ester surrogates with broad substrate scope. Importantly, all structural components of the catalyst cooperatively participate in the stereocontrolling event.

1. Introduction

Nature harnesses weak interactions, particularly hydrogen bonds, to construct biologically active supramolecular architectures, as demonstrated by the three-dimensional structures of enzymes and nucleic acids. Inspired by these biological systems, research for the development and application of supramolecular catalysts assembled through noncovalent interactions has attracted interest in the fields of both selective chemical synthesis and molecular recognition.¹ Despite important advances in elaboration of self-assembled molecular receptors and catalyst systems, however, rational design of chiral supramolecular catalysts for stereoselective bond-forming reactions by the utilization of discrete molecular associations remains as a great challenge.¹⁻⁵

Described here are systems in which chiral and achiral small molecules spontaneously assemble through a well-defined array of intermolecular hydrogen bonds to produce structured chiral organic ion pairs. The distinctive feature of the supramolecular ion pair assembly as a chiral molecular catalyst is that its stereocontrolling ability can be fine-tuned by structural modification of both chiral and achiral components. The author thereby developed a catalyst for highly enantioselective conjugate addition of acyl anion equivalents to α,β -unsaturated ester surrogates.

2. Result and Discussion.

2.1. Isolation and Determination of The Solid State Structure of $1a \cdot (\text{PhO})_3\text{H}_2$.

I initially prepared chiral tetraaminophosphonium phenoxides as part of our broader exploration of chiral organic ion pairs for cooperative asymmetric catalysis.⁶ The requisite cation framework **1a** (Figure 1) was readily synthesized from the parent α -amino acid, L-valine, as its chloride salt.⁷

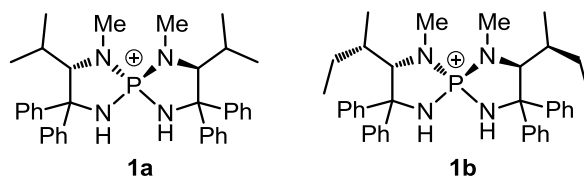


Figure 1. Structures of chiral tetraaminophosphonium cations.

Then, the anion was exchanged with hydroxide, and subsequent neutralization with phenol⁸ yielded $1a \cdot (\text{PhO})_3\text{H}_2$. The solid state structure of $1a \cdot (\text{PhO})_3\text{H}_2$ was unambiguously determined by single crystal X-ray diffraction analysis (Figure 2). Surprisingly, the analysis revealed a

unique molecular assembly, in which an aminophosphonium cation, two phenols and a phenoxide anion were beautifully aligned through a ten-membered cyclic network of intermolecular hydrogen-bonding interactions. Note that the hydrogen-bonding donor capability of the phenols seems to be enhanced by an additional hydrogen bond from the N-H protons of the phosphonium cation, thus facilitating construction of an antidromic circular network.⁹⁻¹¹ Another salient feature of the assembly was that the stereochemical information of the chiral cation moiety was effectively relayed by the two phenol molecules, extending the chiral environment around the remotely located phenoxide anion.

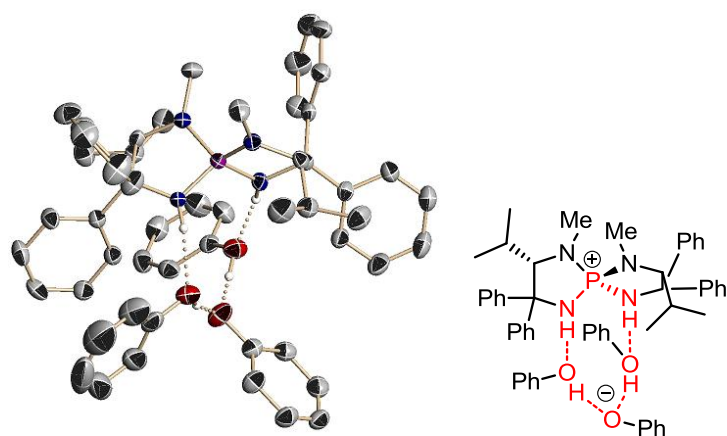


Figure 2. Oak Ridge thermal ellipsoid plot diagram of **1a**·(PhO)₃H₂. All calculated hydrogens were omitted for clarity.

2.2 Effect of Each Component of The Catalyst Assembly for The Conjugate Addition of Acyl Anion Equivalents to α,β -unsaturated Ester Surrogates.

Based on these serendipitous observations, The author explored use of **1**·(ArO)₃H₂ as a chiral molecular catalyst for synthetically valuable stereoselective transformations. For this purpose, I chose 2-unsubstituted oxazol-5(4*H*)-one, namely azlactone, **2** (Figure 3 and Table 1) as a pro-C1-nucleophile¹² with the expectation that the enolate **2'** generated through deprotonation by **1**·(ArO)₃H₂ would behave as a suitable phenoxide anion equivalent; as such it would be captured into a similar hydrogen-bonding network without negatively affecting the preorganization (Figure 3, **1a**·(PhO)₂H₂·**2'**). If this held true, the structures of not only the chiral aminophosphonium cations but also the achiral phenols would affect the stereo-determining step of the addition reaction of the enolate **2'**. To verify this hypothetical synergistic effect of the structural components of the supramolecularly assembled ion-pair catalyst, the author examined the conjugate addition of **2** to α,β -unsaturated acylbenzotriazole

3,¹³ a reactive and readily derivatizable Michael acceptor, under the influence of **1**·(ArO)₃H₂.

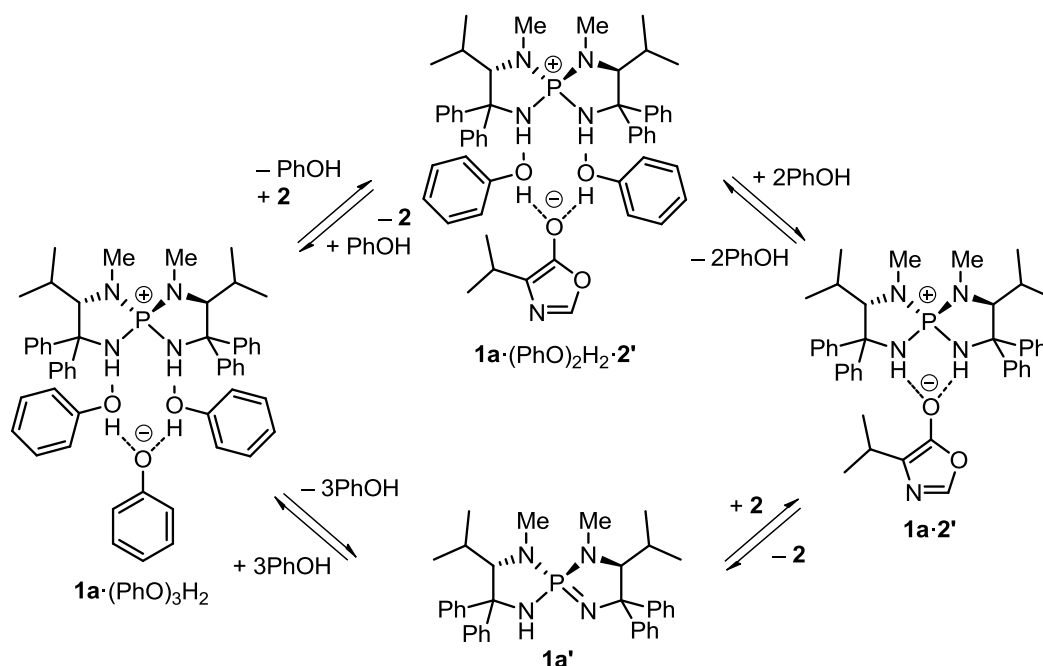


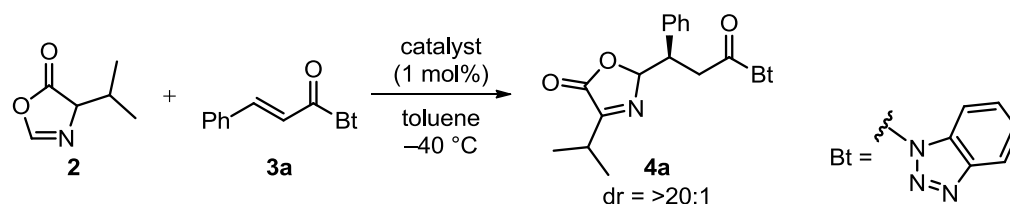
Figure 3. Plausible modes of assembly in catalyst and enolate.

The initial attempt entailed stirring a mixture of **2**, **3a** and **1a**·(PhO)₃H₂ in toluene at -40 °C, giving rise to essentially diastereomerically pure adduct **4a** in a quantitative yield with 60% ee (ee = enantiomeric excess) (Table 1, entry 1). In contrast, use of the independently prepared conjugate base of **1a** (triaminoiminophosphorane **1a'**, Figure 3)¹⁴ as a catalyst led to the formation of **4a** with 34% ee (entry 2). These results clearly indicate the importance of the phenolic component of **1a**·(PhO)₃H₂ in enhancing enantioselectivity. Whereas the reaction with **1a'** proceeds through the generation of chiral aminophosphonium enolate **1a**·**2'**, the expected, highly organized **1a**·(PhO)₂H₂·**2'** complex could be involved in the **1a**·(PhO)₃H₂-catalyzed system, and the two phenols may play a key role in creating an attractive chiral environment around the azlactone enolate **2'**.

Interestingly, treatment of iminophosphorane **1a'** with phenol (3 equiv), followed by the sequential addition of **3a** and **2**, resulted in the formation of **4a** in 98% yield with 62% ee after 10 h of stirring (entry 3). The reactivity and selectivity were scarcely affected by the order of the addition of phenol and azlactone **2** (entry 4). These results suggest that the preorganization of the catalyst is not a prerequisite for the generation of **1a**·(PhO)₂H₂·**2'**, which could be self-assembled from **1a'**, phenols, and **2** by way of either **1a**·(PhO)₃H₂ or **1a**·**2'**. These intriguing observations implied that the selectivity could be tunable through structural modification of the achiral phenolic component. Indeed, although the selectivity decreased when phenols of **1a**·(PhO)₃H₂ were replaced by 4-methylphenol, a series of chloro-substituted

phenols, particularly 3,5-dichlorophenol, induced substantial increases in enantioselectivity (entries 5-9).¹⁵ Furthermore, the author confirmed the effect of the catalyst concentration on the propensity for molecular association in solution. As the author had assumed, both increased catalyst loading and decreased solvent volume improved enantioselectivity (entries 10-12 and 13), which also argues for the role of a requisite molecular assembly.¹⁶ Structural modification of the chiral cationic moiety by using L-isoleucine-derived **1b** (see Figure 1) also appeared to be crucial for achieving the highest selectivity (entry 14). Consequently, all the structural components of the self-assembled catalyst cooperatively participate in realizing the rigorous stereocontrol.

Table 1. Effect of each component of the catalyst assembly.



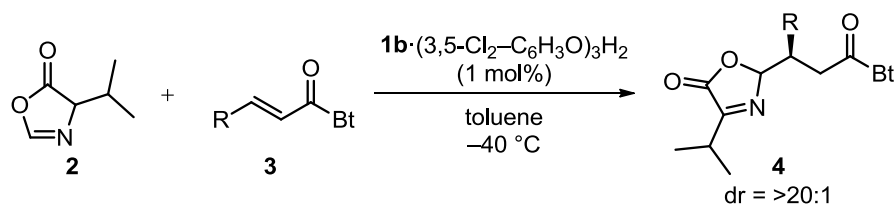
| entry | catalyst (1 ·(ArO) ₃ H ₂) | conc (mM) | time (h) | yield (%) | ee (%) |
|-----------------|---|-----------|----------|-----------|--------|
| 1 | 1a ·(PhO) ₃ H ₂ | 1 | 6 | 99 | 60 |
| 2 | 1a' | 1 | 2 | 99 | 34 |
| 3 | 1a' + 3PhOH | 1 | 10 | 98 | 62 |
| 4 | 1a·2' + 3PhOH | 1 | 16 | 87 | 61 |
| 5 | 1a ·(4-Me-C ₆ H ₄ O) ₃ H ₂ | 1 | 4 | 96 | 58 |
| 6 | 1a ·(4-Cl-C ₆ H ₄ O) ₃ H ₂ | 1 | 10 | 97 | 75 |
| 7 | 1a ·(2-Cl-C ₆ H ₄ O) ₃ H ₂ | 1 | 12 | 94 | 63 |
| 8 | 1a ·(3-Cl-C ₆ H ₄ O) ₃ H ₂ | 1 | 6 | 93 | 70 |
| 9 | 1a ·(3,5-Cl ₂ -C ₆ H ₃ O) ₃ H ₂ | 1 | 16 | 92 | 80 |
| 10 [*] | 1a ·(3,5-Cl ₂ -C ₆ H ₃ O) ₃ H ₂ | 2 | 24 | 99 | 85 |
| 11 [†] | 1a ·(3,5-Cl ₂ -C ₆ H ₃ O) ₃ H ₂ | 5 | 18 | 98 | 89 |
| 12 [‡] | 1a ·(3,5-Cl ₂ -C ₆ H ₃ O) ₃ H ₂ | 10 | 20 | 94 | 89 |
| 13 [§] | 1a ·(3,5-Cl ₂ -C ₆ H ₃ O) ₃ H ₂ | 10 | 4 | 99 | 87 |
| 14 [§] | 1b ·(3,5-Cl ₂ -C ₆ H ₃ O) ₃ H ₂ | 10 | 4 | 95 | 95 |

Unless otherwise noted, the reactions were performed with 0.22 mmol of **2** and 0.2 mmol of **3a** in the presence of **1**·(ArO)₃H₂ (1 mol%) in 2.0 mL of toluene at -40 °C under argon atmosphere. The catalyst concentrations are indicated. The isolated yields are reported. All diastereomeric ratios (dr) and enantiomeric excesses (ee) were determined by ¹H NMR (500 MHz) analysis of crude aliquots and chiral stationary phase HPLC, respectively. The relative stereochemistry was not determined. ^{*}2 mol% of catalyst was used. [†]5 mol% of catalyst was used. [‡]10 mol% of catalyst was used. [§]0.2 mL of toluene was used as solvent.

2.3. Substrate Scope and Derivatization of **4h** to Methylsuccinic Acid **6**.

With the optimal catalyst structure and reaction conditions in hand, the author conducted further experiments to probe the scope of α,β -unsaturated acylbenzotriazole **3**, and the representative results are summarized in Table 2. Generally, use of 1 mol% of **1b**·(3,5-Cl₂-C₆H₃O)₃H₂ and 1.1 equivalents of **2** was sufficient for a smooth reaction, giving **4** in high yield with excellent enantioselectivity. With aryl-substituted **3**, this method tolerated the incorporation of both electron-withdrawing and electron-donating substituents at an arbitrary position on the aromatic scaffold (entries 1-4). In addition, fused- and heteroaromatic β -substituents had no influence on the stereochemical outcome (entries 5 and 6). A range of primary and secondary alkyl groups were also nicely accommodated (entries 7-10).

Table 2. Scope of α,β -Unsaturated Acylbenzotriazole **3**.

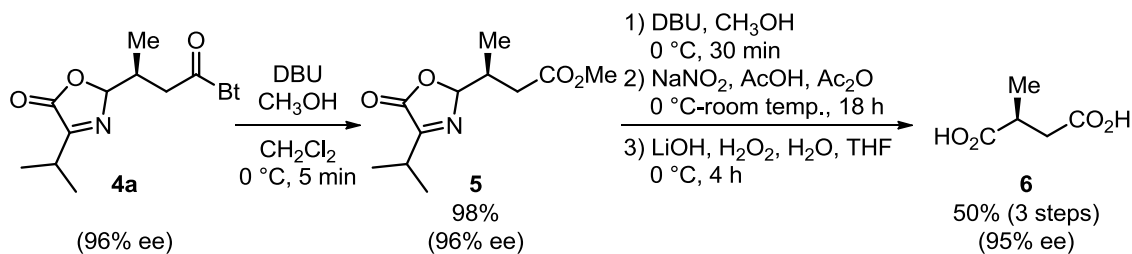


| entry | R (3) | time (h) | yield (%) | ee (%) | prod |
|-------|---|----------|-----------|--------|-------------|
| 1 | 4-MeO-C ₆ H ₄ (3b) | 24 | 98 | 97 | 4b |
| 2 | 4-Br-C ₆ H ₄ (3c) | 21 | 98 | 98 | 4c |
| 3 | 2-Me-C ₆ H ₄ (3d) | 8 | 90 | 93 | 4d |
| 4 | 3-Br-C ₆ H ₄ (3e) | 4 | 96 | 95 | 4e |
| 5 | 1-Naph (3f) | 12 | 91 | 95 | 4f |
| 6 | 2-Furyl (3g) | 22 | 91 | 96 | 4g |
| 7 | Me (3h) | 2 | 97 | 96 | 4h * |
| 8 | Me(CH ₂) ₄ (3i) | 1 | 96 | 95 | 4i |
| 9 | Ph(CH ₂) ₂ (3j) | 2 | 92 | 96 | 4j |
| 10 | Cyclohexyl (3k) | 4 | 93 | 98 | 4k |

The reactions were performed with 0.22 mmol of **2** and 0.2 mmol of **3** under the influence of **1b**·(3,5-Cl₂-C₆H₃O)₃H₂ (1 mol%) in 0.2 mL of toluene at -40 °C under argon atmosphere. The isolated yields are reported. All diastereomeric ratios (dr) and enantiomeric excesses (ee) were determined by ¹H NMR (500 MHz) analysis of crude aliquots and chiral stationary phase HPLC, respectively. *Absolute configuration of the product **4h** was determined, after conversion to the known compound **6** (Fig. 2), by comparison of the optical rotation with the literature value.

The acylbenzotriazole and azlactone moieties of product **4** can be selectively converted to various useful functional groups, thus highlighting the synthetic potential of the present highly stereoselective conjugate addition protocol. For example, **4h** (96% ee) was successfully

derivatized into optically active methylsuccinic acid (**6**) in four steps without loss of the enantiomeric excess (Scheme 1).



Scheme 1. Conversion of **4h** to optically active methylsuccinic acid **6**. DBU = 1,8-diazabicyclo[5.4.0]undec-7-ene, Ac = acetyl, THF = tetrahydrofuran.

3. Conclusion

The author believe these results encourage further research efforts to determine the minimal chiral or achiral structural bias necessary to induce spontaneous yet discrete associations between simple organic molecules through weak noncovalent interactions. The resultant catalytically active and selective structures may greatly expand the possibilities for designing functional supramolecular catalysts.

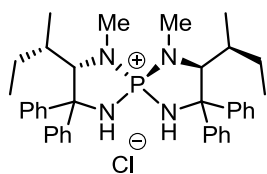
4. Experimental Section.

General Information: Infrared spectra were recorded on a JASCO FT/IR-300E spectrometer. ^1H NMR spectra were recorded on a Varian INOVA-500 (500 MHz) or INOVA-700 (700 MHz) spectrometer. Chemical shifts are reported in ppm from the solvent resonance (CD_3OD ; 3.31 ppm) or tetramethylsilane (0.0 ppm) resonance as the internal standard (CDCl_3). Data are reported as follows: chemical shift, integration, multiplicity (s = singlet, d = doublet, t = triplet, q = quartet, quin = quintet, sex = sextet, sept = septet, oct = octet, m = multiplet, and br = broad) and coupling constants (Hz). ^{13}C NMR spectra were recorded on a Varian INOVA-500 (126 MHz) or INOVA-700 (175 MHz) spectrometer with complete proton decoupling. Chemical shifts are reported in ppm from the solvent resonance as the internal standard (CDCl_3 ; 77.16 ppm, CD_3OD ; 49.0 ppm). ^{31}P NMR spectra were recorded on a Varian Mercury-300BB (121 MHz) spectrometer with complete proton decoupling. Chemical shifts are reported in ppm from H_3PO_4 (0.0 ppm) resonance as the external standard. Optical rotations were measured on a JASCO DIP-1000 polarimeter. The high resolution mass spectra were measured on an BRUKER DALTONICS microTOF focus-KR spectrometer. Analytical thin layer chromatography (TLC) was performed on Merck precoated TLC plates (silica gel 60 GF₂₅₄, 0.25 mm). Flash column chromatography was performed on silica gel 60 (spherical, 40-50 μm ; Kanto Chemical Co., Inc.). Enantiomeric excesses were determined by HPLC analysis using chiral columns (ϕ 4.6 mm x 250 mm, DAICEL CHIRALCEL OD-H (ODH), CHIRALPAK IA (IA) or CHIRALPAK IC (IC)) with hexane (H), isopropyl alcohol (IPA), and ethanol (EtOH) as eluent.

Toluene and tetrahydrofuran (THF) were supplied from Kanto Chemical Co., Inc. as “Dehydrated solvent system”. Tetraaminophosphonium salts **1a**·Cl and **1b**·Cl,^{14,18,19} azlactone **2**,¹² and α,β -unsaturated *N*-acylbenzotriazoles **3a-k**¹³ were prepared by following the literature procedures. Other simple chemicals were purchased and used as such.

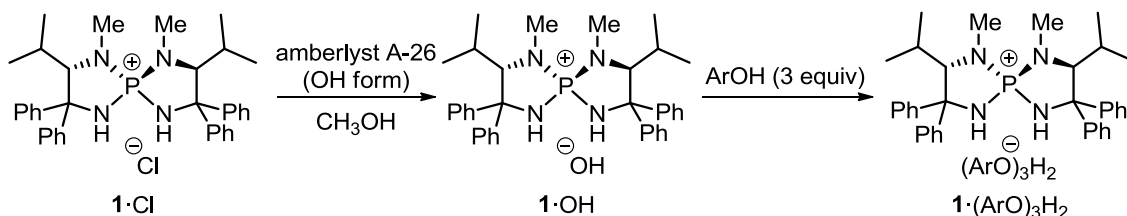
Experimental Section:

Characterization of Tetraaminophosphonium Salts 1:



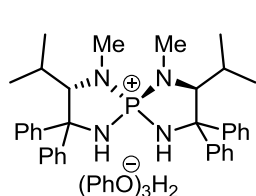
1b·Cl: ^1H NMR (500 MHz, CDCl_3) δ 7.70 (2H, d, $J = 16.5$ Hz), 7.68 (4H, br), 7.59 (4H, dd, $J = 7.5, 1.0$ Hz), 7.39 (4H, t, $J = 7.5$ Hz), 7.32 (4H, brt, $J = 7.5$ Hz), 7.28 (2H, t, $J = 7.5$ Hz), 7.20 (2H, t, $J = 7.5$ Hz), 3.79 (2H, dd, $J_{\text{P-H}} = 21.0$ Hz, $J_{\text{H-H}} = 5.0$ Hz), 1.95-1.85 (2H, m), 1.85-1.77 (2H, m), 1.80 (6H, d, $J_{\text{P-H}} = 10.0$ Hz), 0.94-0.82 (2H, m), 0.84 (6H, t, $J = 7.0$ Hz), 0.56 (6H, d, $J = 7.0$ Hz); ^{13}C NMR (175 MHz, CDCl_3) δ 148.0, 139.5 (d, $J_{\text{P-C}} = 11.4$ Hz), 128.7, 128.6, 128.0, 127.7, 127.6, 127.0, 73.4 (d, $J_{\text{P-C}} = 12.6$

Hz), 70.9 (d, $J_{P-C} = 9.3$ Hz), 36.1, 32.2 (d, $J_{P-C} = 6.0$ Hz), 25.2, 18.9, 12.1; ^{31}P NMR (121 MHz, CDCl_3) δ 37.7; IR (KBr): 3059, 2967, 2874, 1495, 1446, 1358, 1334, 1191, 1035, 751 cm^{-1} ; HRMS (ESI-TOF) Calcd for $\text{C}_{38}\text{H}_{48}\text{N}_4\text{P}^+$ ($[\text{M}-\text{Cl}]^+$) 591.3611. Found 591.3608; $[\alpha]_{\text{D}}^{24} -268.8$ ($c = 0.95$, CHCl_3).

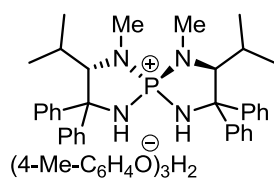


Counter Anion Exchange Procedure to Prepare Chiral Tetraaminophosphonium Phenoxide

1·(ArO)₃H₂²⁰: Chiral tetraaminophosphonium chloride **1·Cl** was transformed into the corresponding phosphonium hydroxide **1·OH** by passing a methanolic solution of **1·Cl** through an ion-exchange resin (amberlyst A-26, OH⁻ form). The resulting **1·OH** was then treated with phenol (3.0 equiv) in methanol at room temperature. The resulting mixture was co-evaporated with benzene three times, and subsequent crystallization of the residue from hexane and diethyl ether afforded white solids, which were collected by filtration and dried under reduced pressure to give the title compound.

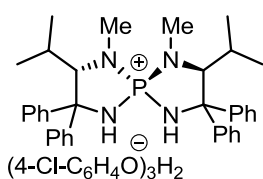


1a·(PhO)₃H₂: ^1H NMR (700 MHz, CD_3OD) δ 7.62 (4H, d, $J = 7.0$ Hz), 7.45 (4H, t, $J = 7.0$ Hz), 7.34 (2H, t, $J = 7.7$ Hz), 7.33 (4H, br), 7.32 (4H, t, $J = 7.7$ Hz), 7.28 (2H, t, $J = 7.7$ Hz), 7.09 (6H, t, $J = 7.0$ Hz), 6.71 (6H, d, $J = 7.0$ Hz), 6.66 (3H, t, $J = 7.0$ Hz), 4.00 (2H, dd, $J_{P-H} = 19.6$ Hz, $J_{H-H} = 6.3$ Hz), 1.89 (6H, d, $J_{P-H} = 9.8$ Hz), 1.87 (2H, oct, $J = 6.3$ Hz), 0.95 (6H, d, $J = 6.3$ Hz), 0.49 (6H, d, $J = 6.3$ Hz), N-H and O-H protons were not found due to deuteration; ^{13}C NMR (175 MHz, CD_3OD) δ 161.6, 148.9, 141.6 (d, $J_{P-C} = 12.8$ Hz), 130.2, 130.0, 129.2, 129.0, 128.9, 128.7, 127.9, 118.6, 117.4, 72.5 (d, $J_{P-C} = 10.7$ Hz), 71.6 (d, $J_{P-C} = 10.7$ Hz), 32.8 (d, $J_{P-C} = 6.1$ Hz), 30.9, 22.7, 19.8; ^{31}P NMR (121 MHz, CD_3OD) δ 36.4.



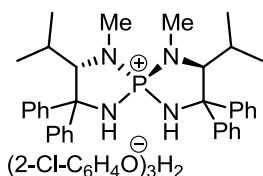
1a·(4-Me-C₆H₄O)₃H₂: ^1H NMR (700 MHz, CD_3OD) δ 7.62 (4H, d, $J = 7.7$ Hz), 7.45 (4H, t, $J = 7.7$ Hz), 7.35 (2H, t, $J = 7.7$ Hz), 7.33 (4H, br), 7.32 (4H, t, $J = 7.7$ Hz), 7.28 (2H, t, $J = 7.7$ Hz), 6.90 (6H, d, $J = 8.4$ Hz), 6.61 (6H, d, $J = 8.4$ Hz), 4.01 (2H, dd, $J_{P-H} = 19.6$ Hz, $J_{H-H} = 6.3$ Hz), 2.19 (9H, s), 1.89 (6H, d, $J_{P-H} = 9.8$ Hz), 1.87 (2H, oct, $J = 6.3$ Hz), 0.95 (6H, d, $J = 6.3$ Hz), 0.49 (6H, d, $J = 6.3$ Hz), N-H and O-H protons were not found due to deuteration; ^{13}C NMR (175 MHz, CD_3OD) δ 159.0, 148.9, 141.7 (d, $J_{P-C} = 13.3$ Hz), 130.6, 130.0, 129.2, 129.0, 128.9, 128.7, 127.9, 127.6, 117.1, 72.5 (d, $J_{P-C} = 10.6$ Hz), 71.7 (d, $J_{P-C} = 10.0$ Hz), 32.8 (d, $J_{P-C} = 6.1$ Hz), 30.9, 22.7, 20.5, 19.8; ^{31}P

NMR (121 MHz, CD₃OD) δ 36.4.



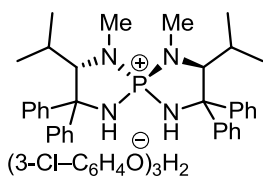
1a·(4-Cl-C₆H₄O)₃H₂: ¹H NMR (700 MHz, CD₃OD) δ 7.62 (4H, d, *J* = 7.7 Hz), 7.44 (4H, t, *J* = 7.7 Hz), 7.34 (2H, t, *J* = 7.7 Hz), 7.33 (4H, br), 7.32 (4H, t, *J* = 7.7 Hz), 7.28 (2H, t, *J* = 7.7 Hz), 7.07 (6H, d, *J* = 8.4 Hz), 6.68 (6H, d, *J* = 8.4 Hz), 4.00 (2H, dd, *J*_{P-H} = 19.6 Hz, *J*_{H-H} = 6.3 Hz), 1.89 (6H, d, *J*_{P-H} = 9.8 Hz), 1.86 (2H, oct, *J* = 6.3 Hz), 0.95 (6H, d, *J* = 6.3 Hz), 0.49 (6H, d, *J* = 6.3

Hz), N-H and O-H protons were not found due to deuteration; ¹³C NMR (175 MHz, CD₃OD) δ 160.0, 148.9, 141.6 (d, *J*_{P-C} = 12.6 Hz), 130.0, 129.2, 129.0, 128.9, 128.7, 127.9, 123.4, 118.6, 72.5 (d, *J*_{P-C} = 11.4 Hz), 71.6 (d, *J*_{P-C} = 10.0 Hz), 32.8 (d, *J*_{P-C} = 6.1 Hz), 30.9, 22.7, 19.8, one carbon was not found probably due to overlapping; ³¹P NMR (121 MHz, CD₃OD) δ 36.4.



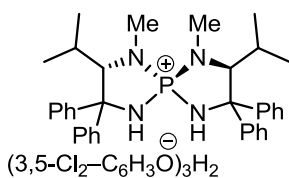
1a·(2-Cl-C₆H₄O)₃H₂: ¹H NMR (700 MHz, CD₃OD) δ 7.62 (4H, d, *J* = 7.7 Hz), 7.45 (4H, t, *J* = 7.7 Hz), 7.34 (2H, t, *J* = 7.7 Hz), 7.33 (4H, br), 7.32 (4H, t, *J* = 7.7 Hz), 7.28 (2H, t, *J* = 7.7 Hz), 7.17 (3H, dd, *J* = 7.7, 1.4 Hz), 6.98 (3H, td, *J* = 7.7, 1.4 Hz), 6.80 (3H, dd, *J* = 7.7, 1.4 Hz), 6.54 (3H, td, *J* = 7.7, 1.4 Hz), 4.00 (2H, dd, *J*_{P-H} = 19.6 Hz, *J*_{H-H} = 6.3 Hz), 1.89 (6H, d, *J*_{P-H} = 10.5 Hz),

1.87 (2H, oct, *J* = 6.3 Hz), 0.95 (6H, d, *J* = 6.3 Hz), 0.49 (6H, d, *J* = 6.3 Hz), N-H and O-H protons were not found due to deuteration; ¹³C NMR (175 MHz, CD₃OD) δ 159.1, 148.9, 141.6 (d, *J*_{P-C} = 12.8 Hz), 130.5, 130.0, 129.2, 129.0, 128.9, 128.7, 128.6, 127.9, 123.1, 119.4, 118.1, 72.5 (d, *J*_{P-C} = 10.7 Hz), 71.7 (d, *J*_{P-C} = 10.0 Hz), 32.8 (d, *J*_{P-C} = 6.0 Hz), 30.9, 22.7, 19.8; ³¹P NMR (121 MHz, CD₃OD) δ 36.4.



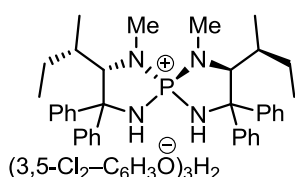
1a·(3-Cl-C₆H₄O)₃H₂: ¹H NMR (500 MHz, CD₃OD) δ 7.62 (4H, d, *J* = 7.5 Hz), 7.45 (4H, t, *J* = 7.5 Hz), 7.35 (2H, t, *J* = 7.5 Hz), 7.34 (4H, br), 7.32 (4H, t, *J* = 7.5 Hz), 7.30-7.26 (2H, m), 7.05 (3H, t, *J* = 8.0 Hz), 6.71 (3H, t, *J* = 2.0 Hz), 6.65 (3H, d, *J* = 8.0 Hz), 6.62 (3H, d, *J* = 8.0 Hz), 4.01 (2H, dd, *J*_{P-H} =

20.0 Hz, *J*_{H-H} = 6.5 Hz), 1.89 (6H, d, *J*_{P-H} = 10.0 Hz), 1.87 (2H, oct, *J* = 6.5 Hz), 0.95 (6H, d, *J* = 6.5 Hz), 0.49 (6H, d, *J* = 6.5 Hz), N-H and O-H protons were not found due to deuteration; ¹³C NMR (175 MHz, CD₃OD) δ 163.1, 148.9, 141.6 (d, *J*_{P-C} = 13.4 Hz), 135.5, 131.1, 130.0, 129.2, 129.0, 128.9, 128.7, 127.9, 118.4, 117.7, 116.1, 72.5 (d, *J*_{P-C} = 10.7 Hz), 71.6 (d, *J*_{P-C} = 10.2 Hz), 32.8 (d, *J*_{P-C} = 6.1 Hz), 30.9, 22.7, 19.8; ³¹P NMR (121 MHz, CD₃OD) δ 36.4.



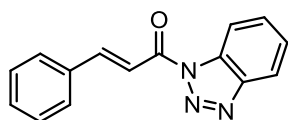
1a·(3,5-Cl₂-C₆H₃O)₃H₂: ¹H NMR (500 MHz, CD₃OD) δ 7.62 (4H, d, *J* = 7.5 Hz), 7.45 (4H, t, *J* = 7.5 Hz), 7.35 (2H, t, *J* = 7.5 Hz), 7.34 (4H, br), 7.32 (4H, t, *J* = 7.5 Hz), 7.30-7.26 (2H, m), 6.68 (3H, t, *J* = 2.0 Hz), 6.64 (6H, d, *J* = 2.0 Hz), 4.01 (2H, dd, *J*_{P-H} = 20.0 Hz, *J*_{H-H} = 6.5 Hz), 1.89 (6H, d,

$J_{P-H} = 10.0$ Hz), 1.87 (2H, oct, $J = 6.5$ Hz), 0.95 (6H, d, $J = 6.5$ Hz), 0.49 (6H, d, $J = 6.5$ Hz), N-H and O-H protons were not found due to deuteration; ^{13}C NMR (175 MHz, CD_3OD) δ 164.0, 148.9, 141.6 (d, $J_{P-C} = 12.8$ Hz), 136.1, 130.0, 129.2, 129.0, 128.9, 128.7, 127.9, 118.1, 116.5, 72.5 (d, $J_{P-C} = 10.7$ Hz), 71.7 (d, $J_{P-C} = 10.0$ Hz), 32.8 (d, $J_{P-C} = 6.0$ Hz), 30.9, 22.7, 19.8; ^{31}P NMR (121 MHz, CD_3OD) δ 36.4; IR (KBr): 2964, 1578, 1446, 1423, 1370, 1269, 1019, 936, 797, 753 cm^{-1} .

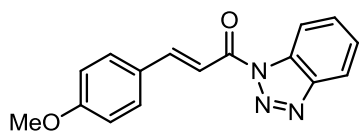


1b·(3,5-Cl₂-C₆H₃O)₃H₂: ^1H NMR (500 MHz, CD_3OD) δ 7.61 (4H, d, $J = 7.5$ Hz), 7.45 (4H, t, $J = 7.5$ Hz), 7.35 (2H, t, $J = 7.5$ Hz), 7.34 (4H, br), 7.33 (4H, t, $J = 7.5$ Hz), 7.31-7.26 (2H, m), 6.68 (3H, t, $J = 2.0$ Hz), 6.64 (6H, d, $J = 2.0$ Hz), 4.09 (2H, dd, $J_{P-H} = 19.0$ Hz, $J_{H-H} = 4.0$ Hz), 1.89 (6H, d, $J_{P-H} = 10.0$ Hz), 1.78 (2H, dqd, $J = 13.0, 7.0, 2.5$ Hz), 1.42 (2H, qtd, $J = 7.0, 4.0, 2.5$ Hz), 0.93 (2H, dqd, $J = 13.0, 7.0, 4.0$ Hz), 0.76 (6H, t, $J = 7.0$ Hz), 0.62 (6H, d, $J = 7.0$ Hz), N-H and O-H protons were not found due to deuteration; ^{13}C NMR (175 MHz, CD_3OD) δ 163.9, 148.9, 141.7 (d, $J_{P-C} = 12.6$ Hz), 136.0, 130.0, 129.1, 129.0, 128.8, 128.7, 127.9, 118.1, 116.5, 72.8 (d, $J_{P-C} = 10.7$ Hz), 71.5 (d, $J_{P-C} = 10.7$ Hz), 37.7, 32.6 (d, $J_{P-C} = 6.0$ Hz), 26.0, 18.8, 12.2; ^{31}P NMR (121 MHz, CD_3OD) δ 36.8; IR (KBr): 2971, 1581, 1424, 1374, 1210, 1034, 936, 827, 796, 752 cm^{-1} .

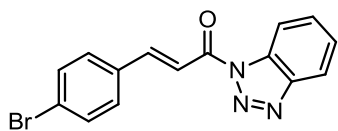
Characterization of α,β -Unsaturated *N*-Acylbenzotriazoles **3**:



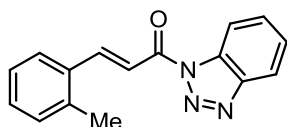
3a¹³: ^1H NMR (500 MHz, CDCl_3) δ 8.43 (1H, d, $J = 7.5$ Hz), 8.17 (1H, d, $J = 16.0$ Hz), 8.16 (1H, d, $J = 7.5$ Hz), 8.14 (1H, d, $J = 16.0$ Hz), 7.78-7.76 (2H, m), 7.70 (1H, t, $J = 7.5$ Hz), 7.54 (1H, t, $J = 7.5$ Hz), 7.51-7.46 (3H, m).



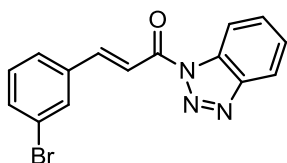
3b²¹: ^1H NMR (500 MHz, CDCl_3) δ 8.43 (1H, dt, $J = 8.0, 1.0$ Hz), 8.15 (1H, dt, $J = 8.0, 1.0$ Hz), 8.12 (1H, d, $J = 15.0$ Hz), 8.00 (1H, d, $J = 15.0$ Hz), 7.73 (2H, d, $J = 9.0$ Hz), 7.68 (1H, ddd, $J = 8.0, 7.0, 1.0$ Hz), 7.53 (1H, ddd, $J = 8.0, 7.0, 1.0$ Hz), 6.99 (2H, d, $J = 9.0$ Hz), 3.89 (3H, s).



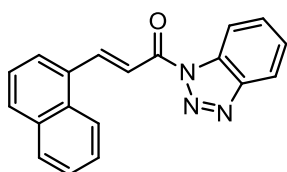
3c: ^1H NMR (700 MHz, CDCl_3) δ 8.40 (1H, dt, $J = 8.4, 1.4$ Hz), 8.15 (1H, dt, $J = 8.4, 1.4$ Hz), 8.11 (1H, d, $J = 15.4$ Hz), 8.06 (1H, d, $J = 15.4$ Hz), 7.68 (1H, ddd, $J = 8.4, 7.0, 1.4$ Hz), 7.63-7.58 (4H, m), 7.53 (1H, ddd, $J = 8.4, 7.0, 1.4$ Hz); ^{13}C NMR (175 MHz, CDCl_3) δ 163.8, 147.4, 146.5, 133.1, 132.6, 131.5, 130.5, 130.4, 126.5, 126.1, 120.4, 116.8, 114.9; IR (KBr): 1699, 1618, 1486, 1450, 1405, 1389, 1072, 995, 790, 753 cm^{-1} ; HRMS (ESI-TOF) Calcd for $\text{C}_{15}\text{H}_{11}\text{BrN}_3\text{ONa}^+$ ($[\text{M}+\text{Na}]^+$) 349.9899, 351.9880. Found 349.9898, 351.9894.



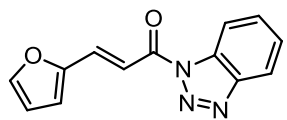
3d²¹: ¹H NMR (500 MHz, CDCl₃) δ 8.48 (1H, d, *J* = 15.5 Hz), 8.42 (1H, d, *J* = 8.0 Hz), 8.16 (1H, d, *J* = 8.0 Hz), 8.07 (1H, d, *J* = 15.5 Hz), 7.86 (1H, d, *J* = 7.5 Hz), 7.69 (1H, t, *J* = 8.0 Hz), 7.54 (1H, d, *J* = 8.0 Hz), 7.37 (1H, t, *J* = 7.5 Hz), 7.31 (1H, t, *J* = 7.5 Hz), 7.28 (1H, d, *J* = 7.5 Hz), 2.56 (3H, s).



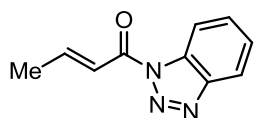
3e: ¹H NMR (500 MHz, CDCl₃) δ 8.41 (1H, d, *J* = 8.0 Hz), 8.17 (1H, d, *J* = 8.0 Hz), 8.13 (1H, d, *J* = 16.0 Hz), 8.06 (1H, d, *J* = 16.0 Hz), 7.90 (1H, t, *J* = 1.0 Hz), 7.70 (1H, t, *J* = 8.0 Hz), 7.67 (1H, dd, *J* = 8.0, 1.0 Hz), 7.60 (1H, dd, *J* = 8.0, 1.0 Hz), 7.55 (1H, t, *J* = 8.0 Hz), 7.35 (1H, t, *J* = 8.0 Hz); ¹³C NMR (175 MHz, CDCl₃) δ 163.6, 146.9, 146.5, 136.3, 134.3, 131.7, 131.5, 130.7, 130.6, 127.6, 126.5, 123.4, 120.4, 117.6, 114.9; IR (KBr): 1704, 1628, 1452, 1372, 1175, 1074, 998, 984, 758 cm⁻¹; HRMS (ESI-TOF) Calcd for C₁₅H₁₁BrN₃O⁺ ([M+H]⁺) 328.0080, 330.0061. Found 328.0066, 330.0003.



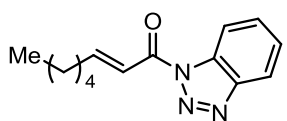
3f: ¹H NMR (500 MHz, CDCl₃) δ 9.04 (1H, d, *J* = 15.5 Hz), 8.46 (1H, dt, *J* = 8.0, 1.0 Hz), 8.34 (1H, d, *J* = 8.0 Hz), 8.25 (1H, d, *J* = 15.5 Hz), 8.17 (1H, dt, *J* = 8.0, 1.0 Hz), 8.09 (1H, d, *J* = 8.0 Hz), 8.00 (1H, d, *J* = 8.0 Hz), 7.93 (1H, d, *J* = 8.0 Hz), 7.71 (1H, ddd, *J* = 8.0, 7.0, 1.0 Hz), 7.65 (1H, ddd, *J* = 8.0, 7.0, 1.0 Hz), 7.58₂ (1H, t, *J* = 8.0 Hz), 7.57₉ (1H, ddd, *J* = 8.0, 7.0, 1.0 Hz), 7.55 (1H, ddd, *J* = 8.0, 7.0, 1.0 Hz); ¹³C NMR (175 MHz, CDCl₃) δ 164.0, 146.5, 145.5, 133.9, 132.0, 131.8, 131.6, 131.3, 130.5, 129.1, 127.5, 126.6, 126.4, 126.2, 125.7, 123.3, 120.3, 118.3, 115.0; IR (KBr): 1700, 1605, 1572, 1449, 1376, 1352, 1169, 982, 768, 746 cm⁻¹; HRMS (ESI-TOF) Calcd for C₁₉H₁₄N₃O⁺ ([M+H]⁺) 300.1131. Found 300.1132.



3g²²: ¹H NMR (500 MHz, CDCl₃) δ 8.41 (1H, dd, *J* = 8.0, 1.0 Hz), 8.15 (1H, dd, *J* = 8.0, 1.0 Hz), 7.98 (1H, d, *J* = 16.0 Hz), 7.88 (1H, d, *J* = 16.0 Hz), 7.68 (1H, t, *J* = 8.0 Hz), 7.62 (1H, d, *J* = 2.0 Hz), 7.53 (1H, t, *J* = 8.0 Hz), 6.87 (1H, d, *J* = 3.5 Hz), 6.57 (1H, dd, *J* = 3.5, 2.0 Hz).

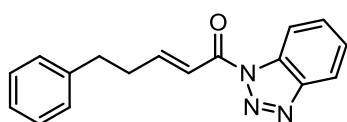


3h¹³: ¹H NMR (500 MHz, CDCl₃) δ 8.36 (1H, d, *J* = 8.0 Hz), 8.13 (1H, d, *J* = 8.0 Hz), 7.66 (1H, ddd, *J* = 8.0, 7.0, 1.0 Hz), 7.57-7.46 (3H, m), 2.13 (3H, d, *J* = 5.5 Hz).

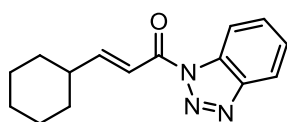


3i: ¹H NMR (500 MHz, CDCl₃) δ 8.37 (1H, dt, *J* = 8.0, 1.0 Hz), 8.14 (1H, dt, *J* = 8.0, 1.0 Hz), 7.66 (1H, ddd, *J* = 8.0, 7.0, 1.0 Hz), 7.53 (1H, d, *J* = 15.0 Hz), 7.52 (1H, ddd, *J* = 8.0, 7.0, 1.0 Hz), 2.44 (2H, dtd, *J* = 7.5, 5.0, 2.5 Hz),

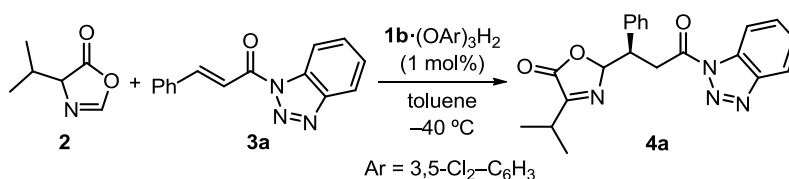
1.61 (2H, quin-t, $J = 7.5, 2.5$ Hz), 1.42-1.32 (4H, m), 0.93 (3H, t, $J = 7.5$ Hz); ^{13}C NMR (126 MHz, CDCl_3) δ 163.9, 155.2, 146.4, 131.6, 130.3, 126.3, 120.3, 119.9, 114.9, 33.2, 31.5, 27.7, 22.6, 14.1; IR (KBr): 2956, 2929, 1716, 1637, 1485, 1450, 1377, 1286, 988, 751 cm^{-1} ; HRMS (ESI-TOF) Calcd for $\text{C}_{14}\text{H}_{18}\text{N}_3\text{O}^+$ ($[\text{M}+\text{H}]^+$) 244.1444. Found 244.1446.



3j: ^1H NMR (500 MHz, CDCl_3) δ 8.35 (1H, dd, $J = 8.0, 1.0$ Hz), 8.13 (1H, dd, $J = 8.0, 1.0$ Hz), 7.66 (1H, td, $J = 8.0, 1.0$ Hz), 7.56 (1H, d, $J = 16.0$ Hz), 7.52 (1H, td, $J = 8.0, 1.0$ Hz), 7.51 (1H, dt, $J = 16.0, 5.0$ Hz), 7.32 (2H, t, $J = 7.5$ Hz), 7.24 (2H, d, $J = 7.5$ Hz), 7.23 (1H, t, $J = 7.5$ Hz), 2.93 (2H, t, $J = 8.0$ Hz), 2.77 (2H, td, $J = 8.0, 5.0$ Hz); ^{13}C NMR (175 MHz, CDCl_3) δ 163.6, 153.4, 146.3, 140.5, 131.5, 130.3, 128.7, 128.4, 126.4, 126.2, 120.5, 120.2, 114.8, 34.7, 34.3; IR (KBr): 3029, 2904, 1711, 1632, 1450, 1380, 1077, 995, 957, 819, 754, 716 cm^{-1} ; HRMS (ESI-TOF) Calcd for $\text{C}_{17}\text{H}_{16}\text{N}_3\text{O}^+$ ($[\text{M}+\text{H}]^+$) 278.1288. Found 278.1295.

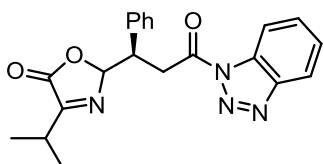


3k: ^1H NMR (500 MHz, CDCl_3) δ 8.36 (1H, dt, $J = 8.5, 1.0$ Hz), 8.13 (1H, dt, $J = 8.5, 1.0$ Hz), 7.66 (1H, ddd, $J = 8.5, 7.0, 1.0$ Hz), 7.51 (1H, ddd, $J = 8.5, 7.0, 1.0$ Hz), 7.47 (1H, dd, $J = 19.0, 3.5$ Hz), 7.44 (1H, d, $J = 19.0$ Hz), 2.39 (1H, tq, $J = 12.5, 3.5$ Hz), 1.92 (2H, brd, $J = 12.5$ Hz), 1.83 (2H, dq, $J = 12.5, 3.5$ Hz), 1.73 (1H, dq, $J = 12.5, 3.5, 1.5$ Hz), 1.37 (2H, qt, $J = 12.5, 3.5$ Hz), 1.32 (2H, q, $J = 12.5$ Hz), 1.27 (2H, qt, $J = 12.5, 3.5$ Hz); ^{13}C NMR (175 MHz, CDCl_3) δ 164.2, 159.7, 146.4, 131.6, 130.3, 126.2, 120.2, 117.7, 114.9, 41.4, 31.7, 26.0, 25.8; IR (KBr): 2926, 2852, 1715, 1634, 1449, 1378, 987, 959, 826, 750 cm^{-1} ; HRMS (ESI-TOF) Calcd for $\text{C}_{15}\text{H}_{18}\text{N}_3\text{O}^+$ ($[\text{M}+\text{H}]^+$) 256.1444. Found 256.1443.

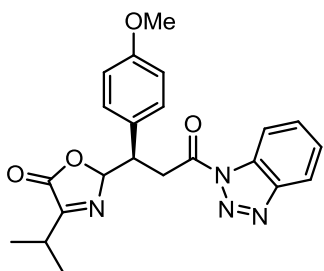


Representative Procedure for Chiral Tetraaminophosphonium Phenoxide $1\cdot(\text{ArO})_3\text{H}_2$ -Catalyzed Asymmetric Conjugate Addition of Azlactone **2:** α,β -Unsaturated *N*-acylbenzotriazole **3a** (49.9 mg, 0.2 mmol) and **1b**·(3,5- Cl_2 - $\text{C}_6\text{H}_3\text{O}$) $_3\text{H}_2$ (0.01 equiv, 2.16 mg, 2.0 μmol) were placed in a dried test tube and dissolved into toluene (0.2 mL) under Ar atmosphere. Azlactone **2a** (28.0 mg, 0.22 mmol) was then introduced dropwise slowly at -40 $^\circ\text{C}$ and the stirring was continued for 4 hours. A solution of trifluoroacetic acid in toluene (0.5 M, 20 μL) was added to the reaction mixture. The mixture was poured into ice-cooled 1 *N* HCl aqueous solution and the aqueous phase was extracted with ethyl acetate (EA). The combined organic phase was washed with brine, dried over Na_2SO_4 , and filtered. All

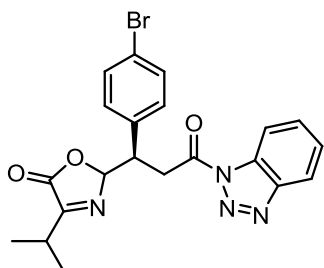
volatiles were removed by evaporation and the diastereomeric ratio was determined by ^1H NMR analysis of the crude aliquot. Purification of the residue by column chromatography on silica gel (H/EtOH = 5:1 as eluent) afforded **4a** in 95% yield (71.5 mg, 0.19 mmol), whose enantiomeric excess was determined to be 95% ee by HPLC analysis. **4a**: IC, H/EtOH = 10:1, flow rate = 0.5 mL/min, λ = 210 nm, 24.5 min (minor diastereomer), 27.5 min (major; major diastereomer), 30.5 min (minor; major diastereomer), 38.0



min (minor diastereomer); ^1H NMR (700 MHz, CDCl_3) δ 8.23 (1H, dt, J = 8.4, 0.7 Hz), 8.12 (1H, dt, J = 8.4, 0.7 Hz), 7.64 (1H, ddd, J = 8.4, 7.0, 0.7 Hz), 7.51 (1H, ddd, J = 8.4, 7.0, 0.7 Hz), 7.30-7.26 (2H, m), 7.26-7.22 (3H, m), 6.28 (1H, dd, J = 4.2, 2.1 Hz), 4.24 (1H, td, J = 7.0, 4.2 Hz), 4.18 (1H, dd, J = 17.5, 7.0 Hz), 4.09 (1H, dd, J = 17.5, 7.0 Hz), 2.79 (1H, sept-d, J = 7.0, 2.1 Hz), 1.18 (3H, d, J = 7.0 Hz), 1.04 (3H, d, J = 7.0 Hz); ^{13}C NMR (175 MHz, CDCl_3) δ 170.2, 169.9, 164.5, 146.3, 134.5, 131.1, 130.8, 129.7, 128.4, 128.2, 126.5, 120.4, 114.5, 44.1, 99.7, 36.1, 28.1, 18.9, one carbon was not found probably due to overlapping; IR (liq. film): 2973, 1781, 1737, 1451, 1390, 1167, 1064, 995, 965, 752 cm^{-1} ; HRMS (ESI-TOF) Calcd for $\text{C}_{21}\text{H}_{20}\text{N}_4\text{O}_3\text{Na}$ ($[\text{M}+\text{Na}]^+$) 399.1428. Found 399.1429.

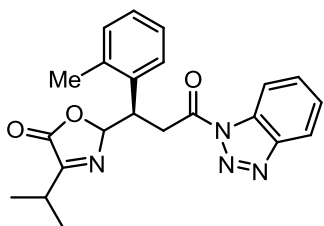


4b: IC, H/EtOH = 10:1, flow rate = 0.5 mL/min, λ = 210 nm, 33.6 min (minor diastereomer), 39.5 min (minor; major diastereomer), 41.8 min (major; major diastereomer), 53.9 min (minor diastereomer); ^1H NMR (700 MHz, CDCl_3) δ 8.24 (1H, dt, J = 8.4, 0.7 Hz), 8.13 (1H, dt, J = 8.4, 0.7 Hz), 7.65 (1H, ddd, J = 8.4, 7.7, 0.7 Hz), 7.51 (1H, ddd, J = 8.4, 7.7, 0.7 Hz), 7.15 (2H, d, J = 8.4 Hz), 6.80 (2H, d, J = 8.4 Hz), 6.26 (1H, dd, J = 4.2, 2.1 Hz), 4.19 (1H, td, J = 7.7, 4.2 Hz), 4.16 (1H, dd, J = 17.5, 7.7 Hz), 4.04 (1H, dd, J = 17.5, 7.7 Hz), 3.75 (3H, s), 2.81 (1H, sept-d, J = 7.7, 2.1 Hz), 1.19 (3H, d, J = 7.7 Hz), 1.08 (3H, d, J = 7.7 Hz); ^{13}C NMR (126 MHz, CDCl_3) δ 170.2, 169.8, 164.6, 159.3, 146.3, 131.1, 130.8₁, 130.7₆, 126.5, 126.2, 120.4, 114.5, 113.8, 99.8, 55.3, 43.4, 36.3, 28.1, 19.0, one carbon was not found probably due to overlapping; IR (liq. film): 2972, 1779, 1738, 1515, 1451, 1389, 1254, 1065, 996, 966, 753 cm^{-1} ; HRMS (ESI-TOF) Calcd for $\text{C}_{22}\text{H}_{22}\text{N}_4\text{O}_4\text{Na}$ ($[\text{M}+\text{Na}]^+$) 429.1533. Found 429.1535.

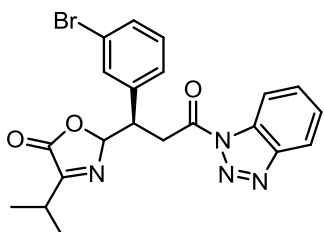


4c: IA, H/EtOH = 2:1, flow rate = 0.5 mL/min, λ = 210 nm, 26.4 min (major; major diastereomer), 33.9 min (minor diastereomer), 45.4 min (minor diastereomer), 68.9 min (minor; major diastereomer); ^1H NMR (500 MHz, CDCl_3) δ 8.22 (1H, dt, J = 8.0, 1.0 Hz), 8.13 (1H, dt, J = 8.0, 1.0 Hz), 7.66 (1H, ddd, J = 8.0, 7.0, 1.0 Hz), 7.53 (1H, ddd, J = 8.0, 7.0, 1.0 Hz), 7.42 (2H, dt, J = 8.5, 2.5 Hz), 7.14 (2H, dt, J = 8.5, 2.5 Hz), 6.25 (1H, dd, J = 4.0, 2.0 Hz), 4.20 (1H, ddd, J = 7.5, 6.0, 4.0 Hz), 4.16 (1H, dd, J = 17.0, 7.5 Hz), 4.05

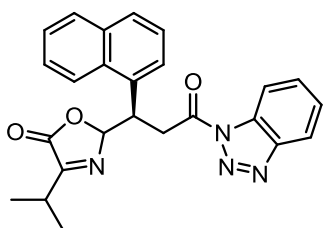
(1H, dd, $J = 17.0, 6.0$ Hz), 2.83 (1H, sept-d, $J = 7.0, 2.0$ Hz), 1.20 (3H, d, $J = 7.0$ Hz), 1.08 (3H, d, $J = 7.0$ Hz); ^{13}C NMR (175 MHz, CDCl_3) δ 170.2, 169.9, 164.3, 146.4, 133.6, 131.6, 131.3, 131.1, 130.9, 126.6, 122.4, 120.5, 114.4, 99.4, 43.7, 36.0, 28.2, 19.0₁, 19.0₀; IR (liq. film): 2973, 1782, 1738, 1487, 1450, 1389, 1167, 1065, 968, 753 cm^{-1} ; HRMS (ESI-TOF) Calcd for $\text{C}_{21}\text{H}_{19}\text{N}_4\text{O}_3\text{BrNa}$ ($[\text{M}+\text{Na}]^+$) 477.0533, 479.0515. Found 477.0537, 479.0527.



4d: IA, H/IPA/EtOH = 36:1:3, flow rate = 0.5 mL/min, $\lambda = 210$ nm, 26.3 min (major; major diastereomer), 32.3 min (minor diastereomer), 34.6 min (minor diastereomer), 38.4 min (minor; major diastereomer); ^1H NMR (500 MHz, CDCl_3) δ 8.22 (1H, dd, $J = 8.0, 1.0$ Hz), 8.12 (1H, dd, $J = 8.0, 1.0$ Hz), 7.64 (1H, ddd, $J = 8.0, 7.0, 1.0$ Hz), 7.51 (1H, ddd, $J = 8.0, 7.0, 1.0$ Hz), 7.18-7.08 (4H, m), 6.25 (1H, dd, $J = 5.0, 2.0$ Hz), 4.52 (1H, ddd, $J = 8.0, 7.0, 5.0$ Hz), 4.20 (1H, dd, $J = 18.0, 8.0$ Hz), 4.06 (1H, dd, $J = 18.0, 7.0$ Hz), 2.85 (1H, sept-d, $J = 7.0, 2.0$ Hz), 1.22 (3H, d, $J = 7.0$ Hz), 1.13 (3H, d, $J = 7.0$ Hz); ^{13}C NMR (126 MHz, CDCl_3) δ 170.2, 169.7, 164.4, 146.2, 138.1, 133.3, 131.0, 130.9, 130.7, 128.3, 127.8, 126.4, 125.6, 120.3, 114.4, 100.4, 39.1, 36.9, 28.2, 20.2, 19.0₂, 19.0₀; IR (liq. film): 2972, 1780, 1738, 1450, 1390, 1064, 968, 911, 752, 730 cm^{-1} ; HRMS (ESI-TOF) Calcd for $\text{C}_{22}\text{H}_{22}\text{N}_4\text{O}_3\text{Na}$ ($[\text{M}+\text{Na}]^+$) 413.1584. Found 413.1584.

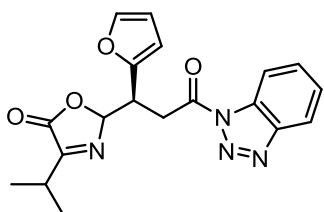


4e: IC, H/EtOH = 10:1, flow rate = 0.5 mL/min, $\lambda = 210$ nm, 24.5 min (minor diastereomer), 27.5 min (major; major diastereomer), 31.0 min (minor; major diastereomer), 36.5 min (minor diastereomer); ^1H NMR (500 MHz, CDCl_3) δ 8.24 (1H, dt, $J = 8.5, 1.0$ Hz), 8.14 (1H, dt, $J = 8.5, 1.0$ Hz), 7.67 (1H, ddd, $J = 8.5, 7.0, 1.0$ Hz), 7.53 (1H, ddd, $J = 8.5, 7.0, 1.0$ Hz), 7.39 (1H, dt, $J = 8.0, 1.5$ Hz), 7.37 (1H, t, $J = 1.5$ Hz), 7.21 (1H, dt, $J = 8.0, 1.5$ Hz), 7.17 (1H, t, $J = 8.0$ Hz), 6.27 (1H, dd, $J = 4.5, 2.0$ Hz), 4.21 (1H, td, $J = 7.0, 4.0$ Hz), 4.14 (1H, dd, $J = 18.0, 7.0$ Hz), 4.10 (1H, dd, $J = 18.0, 7.0$ Hz), 2.84 (1H, sept-d, $J = 7.0, 2.0$ Hz), 1.22 (3H, d, $J = 7.0$ Hz), 1.10 (3H, d, $J = 7.0$ Hz); ^{13}C NMR (175 MHz, CDCl_3) δ 170.2, 169.8, 164.3, 146.3, 136.9, 132.4, 131.3, 131.0, 130.8, 130.0, 128.8, 126.6, 122.4, 120.4, 114.4, 99.2, 43.7, 36.1, 28.2, 19.0, 18.9; IR (liq. film): 2973, 1781, 1737, 1450, 1391, 1065, 998, 965, 733, 708 cm^{-1} ; HRMS (ESI-TOF) Calcd for $\text{C}_{21}\text{H}_{19}\text{N}_4\text{O}_3\text{BrNa}$ ($[\text{M}+\text{Na}]^+$) 477.0533, 479.0515. Found 477.0530, 479.0503.

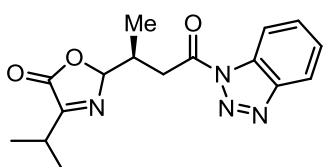


4f: IC, H/IPA = 3:1, flow rate = 0.5 mL/min, $\lambda = 210$ nm, 24.4 min (minor diastereomer), 30.1 min (major; major diastereomer), 33.5 min (minor; major diastereomer), 43.1 min (minor diastereomer); ^1H NMR (500 MHz, CDCl_3) δ 8.29 (1H, d, $J = 8.0$ Hz), 8.18 (1H, d, $J = 8.0$ Hz), 8.12 (1H, dt, $J = 8.0, 1.0$ Hz), 7.85 (1H, dt, $J = 8.0, 1.0$ Hz), 7.77 (1H, d,

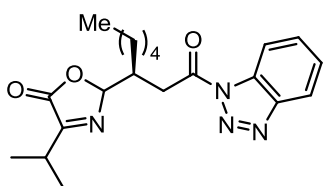
$J = 8.0$ Hz), 7.61 (2H, t, $J = 8.0$ Hz), 7.51 (1H, t, $J = 8.0$ Hz), 7.50 (1H, t, $J = 8.0$ Hz), 7.47 (1H, d, $J = 8.0$ Hz), 7.41 (1H, t, $J = 8.0$ Hz), 6.38 (1H, dd, $J = 4.5, 2.0$ Hz), 5.22 (1H, brs), 4.23 (1H, dd, $J = 17.5, 7.5$ Hz), 4.13 (1H, dd, $J = 17.5, 6.5$ Hz), 2.84 (1H, sept-d, $J = 7.0, 2.0$ Hz), 1.20 (3H, d, $J = 7.0$ Hz), 1.08 (3H, d, $J = 7.0$ Hz); ^{13}C NMR (126 MHz, CDCl_3) δ 170.1, 169.7, 164.3, 146.2, 134.0, 132.2, 131.9, 131.0, 130.7, 129.1, 128.8, 126.8, 126.5, 126.3, 126.0, 124.8, 123.1, 120.3, 114.4, 100.3, 38.0, 36.3, 28.2, 19.0, one carbon was not found probably due to overlapping; IR (liq. film): 2973, 1781, 1738, 1450, 1391, 1055, 969, 910, 782, 733 cm^{-1} ; HRMS (ESI-TOF) Calcd for $\text{C}_{25}\text{H}_{22}\text{N}_4\text{O}_3\text{Na}$ ($[\text{M}+\text{Na}]^+$) 449.1584. Found 449.1583.



4g: IC, H/EtOH = 10:1, flow rate = 0.5 mL/min, $\lambda = 210$ nm, 30.8 min (minor diastereomer), 33.2 min (major; major diastereomer), 38.5 min (minor; major diastereomer), 47.7 min (minor diastereomer); ^1H NMR (500 MHz, CDCl_3) δ 8.27 (1H, dt, $J = 8.0, 1.0$ Hz), 8.15 (1H, dt, $J = 8.0, 1.0$ Hz), 7.68 (1H, ddd, $J = 8.0, 7.0, 1.0$ Hz), 7.54 (1H, ddd, $J = 8.0, 7.0, 1.0$ Hz), 7.31 (1H, dd, $J = 2.0, 1.0$ Hz), 6.29 (2H, dd, $J = 4.0, 2.0$ Hz), 6.23 (1H, d, $J = 4.0$ Hz), 4.34 (1H, td, $J = 7.0, 4.0$ Hz), 4.20 (1H, dd, $J = 18.0, 7.0$ Hz), 4.03 (1H, dd, $J = 18.0, 7.0$ Hz), 2.87 (1H, sept-d, $J = 7.0, 2.0$ Hz), 1.21 (3H, d, $J = 7.0$ Hz), 1.10 (3H, d, $J = 7.0$ Hz); ^{13}C NMR (175 MHz, CDCl_3) δ 169.9, 169.8, 164.5, 148.8, 146.3, 142.6, 131.1, 130.8, 126.6, 120.4, 114.5, 110.6, 109.5, 98.7, 38.5, 34.6, 28.2, 19.1, 18.9; IR (liq. film): 2973, 1782, 1738, 1451, 1393, 1167, 1063, 1000, 966, 736 cm^{-1} ; HRMS (ESI-TOF) Calcd for $\text{C}_{19}\text{H}_{18}\text{N}_4\text{O}_4\text{Na}$ ($[\text{M}+\text{Na}]^+$) 389.1220. Found 389.1211.

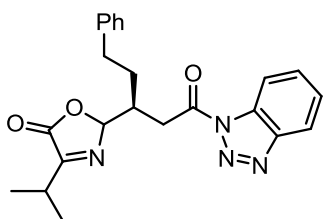


4h: IC, H/EtOH = 10:1, flow rate = 0.5 mL/min, $\lambda = 210$ nm, 25.1 min (minor diastereomer), 28.3 min (minor; major diastereomer), 34.4 min (major; major diastereomer), 36.9 min (minor diastereomer); ^1H NMR (500 MHz, CDCl_3) δ 8.30 (1H, dt, $J = 8.0, 1.0$ Hz), 8.14 (1H, dt, $J = 8.0, 1.0$ Hz), 7.69 (1H, ddd, $J = 8.0, 7.0, 1.0$ Hz), 7.54 (1H, ddd, $J = 8.0, 7.0, 1.0$ Hz), 6.03 (1H, dd, $J = 5.0, 2.0$ Hz), 3.66 (1H, dd, $J = 17.0, 6.0$ Hz), 3.50 (1H, dd, $J = 17.0, 7.5$ Hz), 3.00 (1H, sept-d, $J = 6.5, 2.0$ Hz), 2.93 (1H, quin-dd, $J = 7.0, 6.0, 5.0$ Hz), 1.28 (3H, d, $J = 6.5$ Hz), 1.26 (3H, d, $J = 7.0$ Hz), 1.12 (3H, d, $J = 6.5$ Hz); ^{13}C NMR (126 MHz, CDCl_3) δ 170.7, 169.5, 164.9, 146.3, 131.1, 130.8, 126.5, 120.4, 114.5, 101.4, 37.4, 33.7, 28.3, 19.4, 19.1, 14.0; IR (liq. film): 2973, 1781, 1739, 1485, 1451, 1392, 1059, 984, 937, 752 cm^{-1} ; HRMS (ESI-TOF) Calcd for $\text{C}_{16}\text{H}_{18}\text{N}_4\text{O}_3\text{Na}$ ($[\text{M}+\text{Na}]^+$) 337.1271. Found 337.1271.

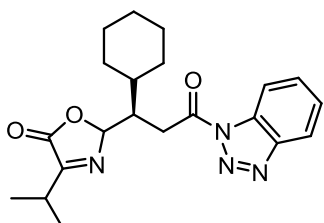


4i: IC, H/EtOH = 10:1, flow rate = 0.5 mL/min, $\lambda = 210$ nm, 14.4 min (minor diastereomer), 16.7 min (minor; major diastereomer), 19.9 min (major; major diastereomer), 20.8 min (minor diastereomer); ^1H NMR (500 MHz, CDCl_3) δ 8.29 (1H, d, $J = 8.0$ Hz), 8.14 (1H, d, $J = 8.0$ Hz),

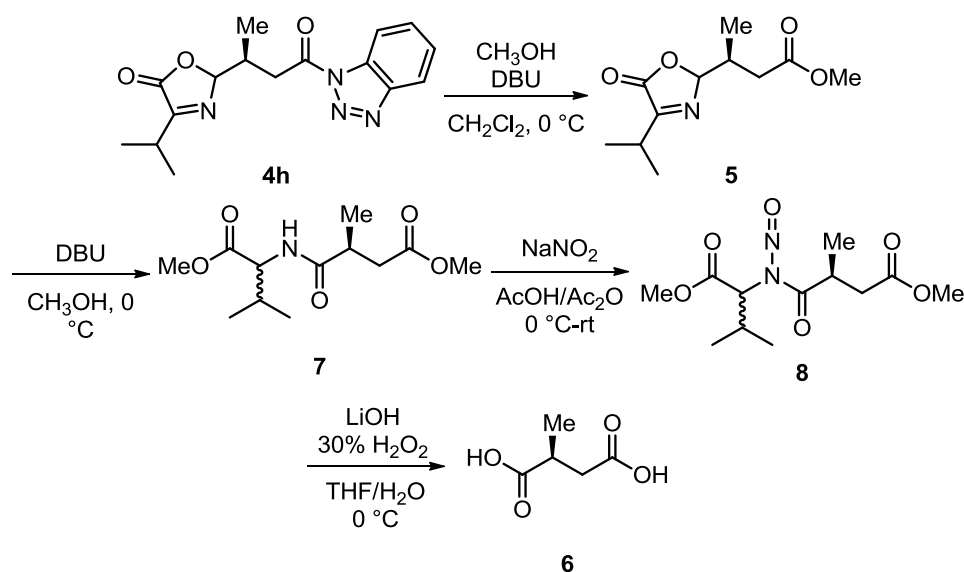
7.68 (1H, ddd, $J = 8.0, 7.0, 1.0$ Hz), 7.53 (1H, ddd, $J = 8.0, 7.0, 1.0$ Hz), 6.09 (1H, dd, $J = 5.0, 2.0$ Hz), 3.50 (1H, dd, $J = 17.5, 7.0$ Hz), 3.46 (1H, dd, $J = 17.5, 7.0$ Hz), 2.95 (1H, sept-d, $J = 7.0, 2.0$ Hz), 2.86 (1H, quin-d, $J = 7.0, 5.0$ Hz), 1.60 (1H, ddd, $J = 10.0, 7.0, 5.0$ Hz), 1.53-1.40 (3H, m), 1.38-1.26 (4H, m), 1.24 (3H, d, $J = 7.0$ Hz), 1.19 (3H, d, $J = 7.0$ Hz), 0.88 (3H, t, $J = 7.0$ Hz); ^{13}C NMR (126 MHz, CDCl_3) δ 170.9, 169.2, 164.9, 146.3, 131.1, 130.7, 126.4, 120.4, 114.5, 100.6, 38.3, 34.8, 31.7, 29.1, 28.3, 26.6, 22.5, 19.1₄, 19.0₈, 14.1; IR (liq. film): 2931, 1781, 1737, 1450, 1389, 1168, 1057, 975, 771, 752 cm^{-1} ; HRMS (ESI-TOF) Calcd for $\text{C}_{20}\text{H}_{26}\text{N}_4\text{O}_3\text{Na}$ ($[\text{M}+\text{Na}]^+$) 393.1897. Found 393.1889.



4j: IC, H/EtOH = 10:1, flow rate = 0.5 mL/min, $\lambda = 210$ nm, 21.0 min (minor diastereomer), 24.7 min (minor; major diastereomer), 29.6 min (minor diastereomer), 31.6 min (major; major diastereomer); ^1H NMR (500 MHz, CDCl_3) δ 8.29 (1H, d, $J = 8.0$ Hz), 8.14 (1H, d, $J = 8.0$ Hz), 7.68 (1H, t, $J = 8.0$ Hz), 7.53 (1H, t, $J = 8.0$ Hz), 7.27 (2H, t, $J = 7.0$ Hz), 7.19 (2H, d, $J = 7.0$ Hz), 7.17 (1H, t, $J = 7.0$ Hz), 6.11 (1H, dd, $J = 5.0, 2.0$ Hz), 3.56 (1H, dd, $J = 17.5, 7.0$ Hz), 3.51 (1H, dd, $J = 17.5, 6.0$ Hz), 2.99 (1H, sept-d, $J = 7.0, 2.0$ Hz), 2.89 (1H, brsex, $J = 6.5$ Hz), 2.84 (1H, ddd, $J = 18.0, 14.0, 6.5$ Hz), 2.80 (1H, ddd, $J = 18.0, 14.0, 6.5$ Hz), 1.97 (1H, ddt, $J = 14.0, 9.5, 6.5$ Hz), 1.81 (1H, ddt, $J = 14.0, 9.5, 6.5$ Hz), 1.24 (3H, d, $J = 7.0$ Hz), 1.18 (3H, d, $J = 7.0$ Hz); ^{13}C NMR (175 MHz, CDCl_3) δ 170.7, 169.4, 164.8, 146.3, 140.9, 131.1, 130.7, 128.6, 128.4, 126.4, 126.3, 120.4, 114.5, 100.6, 38.1, 34.8, 33.3, 30.8, 28.3, 19.1₁, 19.0₉; IR (liq. film): 2972, 2932, 1780, 1737, 1485, 1451, 1389, 1060, 974, 910, 733 cm^{-1} ; HRMS (ESI-TOF) Calcd for $\text{C}_{23}\text{H}_{24}\text{N}_4\text{O}_3\text{Na}$ ($[\text{M}+\text{Na}]^+$) 427.1741. Found 427.1744.



4k: IA, H/EtOH = 10:1, flow rate = 0.5 mL/min, $\lambda = 210$ nm, 21.5 min (minor diastereomer), 25.9 min (minor diastereomer), 29.8 min (major; major diastereomer), 33.5 min (minor; major diastereomer); ^1H NMR (500 MHz, CDCl_3) δ 8.28 (1H, dt, $J = 8.5, 1.0$ Hz), 8.14 (1H, dt, $J = 8.5, 1.0$ Hz), 7.67 (1H, ddd, $J = 8.5, 7.0, 1.0$ Hz), 7.53 (1H, ddd, $J = 8.5, 7.0, 1.0$ Hz), 6.09 (1H, dd, $J = 5.0, 2.0$ Hz), 3.41 (1H, dd, $J = 17.0, 5.0$ Hz), 3.32 (1H, dd, $J = 17.0, 7.5$ Hz), 2.89 (1H, sept-d, $J = 7.0, 2.0$ Hz), 2.83 (1H, dq, $J = 7.5, 5.0$ Hz), 1.93-1.66 (6H, m), 1.36-1.14 (5H, m), 1.22 (3H, d, $J = 7.0$ Hz), 1.11 (3H, d, $J = 7.0$ Hz); ^{13}C NMR (126 MHz, CDCl_3) δ 171.3, 169.0, 165.0, 146.4, 131.2, 130.7, 126.4, 120.4, 114.5, 100.1, 43.6, 38.8, 31.9, 30.9, 30.4, 28.3, 26.6, 26.5, 26.4, 19.1, 18.9; IR (liq. film): 2928, 2853, 1780, 1738, 1450, 1389, 1062, 964, 751, 733 cm^{-1} ; HRMS (ESI-TOF) Calcd for $\text{C}_{21}\text{H}_{26}\text{N}_4\text{O}_3\text{Na}$ ($[\text{M}+\text{Na}]^+$) 405.1897. Found 405.1898.



Derivatization of 4h to Methylsuccinic Acid 6:

Methanolysis of 4h: To a solution of **4h** (157.2 mg, 0.5 mmol, 96% ee) in dichloromethane (5 mL) was added methanol (40.5 μL , 1.0 mmol) and 1,8-diazabicyclo[5.4.0]undec-7-ene (DBU) (74.8 μL , 0.5 mmol) dropwise at $0\text{ }^\circ\text{C}$. The reaction mixture was stirred for 5 min and diluted with 1 *N* HCl aqueous solution to quench the reaction. The resulting aqueous phase was extracted with EA three times. The combined organic extracts were dried over Na_2SO_4 and filtered. After concentration, the residue was purified by column chromatography on silica gel (H/EA = 5:1 as eluent) to give **5** in 98% yield and its diastereomeric ratio was >20:1. The enantiomeric purity of **5** was determined to be 96% ee by chiral stationary phase HPLC analysis. **5**: IC, H/EtOH = 20:1, flow rate = 0.5 mL/min, $\lambda = 210\text{ nm}$, 24.5 min (minor diastereomer), 28.4 min (major; major diastereomer), 29.4 min (minor diastereomer), 30.9 min (minor; major diastereomer); $^1\text{H NMR}$ (500 MHz, CDCl_3) δ 5.85 (1H, dd, $J = 5.0, 2.0\text{ Hz}$), 3.70 (3H, s), 2.99 (1H, sept-d, $J = 7.0, 2.0\text{ Hz}$), 2.59-2.51 (1H, m), 2.52 (1H, dd, $J = 15.5, 6.0\text{ Hz}$), 2.30 (1H, dd, $J = 15.5, 7.5\text{ Hz}$), 1.29 (3H, d, $J = 7.0\text{ Hz}$), 1.28 (3H, d, $J = 7.0\text{ Hz}$), 0.98 (3H, d, $J = 7.0\text{ Hz}$).

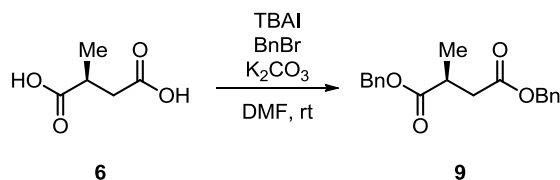
Isomerization and Methanolysis of 5: A solution of **5** (111.4 mg, 0.49 mmol) and DBU (73.3 μL , 0.49 mmol) in methanol (10 mL) was stirred at $0\text{ }^\circ\text{C}$ for 30 min. 1 *N* HCl aqueous solution was then added to the mixture to quench the reaction. The mixture was extracted with EA three times and organic phases were washed with brine. The combined organic extracts were dried over Na_2SO_4 and filtered. After evaporation, the residue was purified by column chromatography on silica gel (H/EA = 2:1 as eluent) to furnish **7** as a mixture of diastereomers in 87% yield. **7**: $^1\text{H NMR}$ (500 MHz, CDCl_3) δ 6.25 (0.5H, d, $J = 8.5\text{ Hz}$), 6.18 (0.5H, d, $J = 8.5\text{ Hz}$), 4.57 (0.5H, dd, $J = 8.5, 5.0\text{ Hz}$), 4.54 (0.5H, dd, $J = 8.5, 5.0\text{ Hz}$),

3.74₃ (1.5H, s), 3.73₅ (1.5H, s), 3.68 (1.5H, s), 3.67 (1.5H, s), 2.86-2.72 (2H, m), 2.42-2.35 (1H, m), 2.17₀ (0.5H, sept-d, $J = 7.0, 5.0$ Hz), 2.16₆ (0.5H, sept-d, $J = 7.0, 5.0$ Hz), 1.23 (1.5H, d, $J = 7.0$ Hz), 1.20 (1.5H, d, $J = 7.0$ Hz), 0.94 (1.5H, d, $J = 7.0$ Hz), 0.93 (1.5H, d, $J = 7.0$ Hz), 0.91 (3H, d, $J = 7.0$ Hz).

N-Nitrosation of 7²³: To a solution of **7** (77.8 mg, 0.3 mmol) in glacial acetic acid (1 mL) and acetic anhydride (2 mL) was added NaNO₂ (207.0 mg, 3.0 mmol) at 0 °C. The reaction mixture was allowed to warm to room temperature and stirred for 18 hours. The resulting solution was poured onto ice and the aqueous phase was extracted with diethyl ether twice. The organic phase was washed with water, saturated NaHCO₃ aqueous solution, and brine. The combined organic extracts were dried over Na₂SO₄, filtered, and concentrated. Purification of the residue by column chromatography on silica gel (H/EA = 10:1 as eluent) afforded **8** as a mixture of diastereomers in 77 % yield. **8**: ¹H NMR (500 MHz, CDCl₃) δ 4.94 (0.5H, d, $J = 9.0$ Hz), 4.86 (0.5H, d, $J = 9.0$ Hz), 4.32-4.23 (1H, m), 3.67₂ (1.5H, s), 3.66₆ (1.5H, s), 3.62 (1.5H, s), 3.61 (1.5H, s), 3.08 (1H, dd, $J = 17.0, 10.0$ Hz), 2.57 (1H, dd, $J = 17.5, 5.0$ Hz), 2.49 (1H, d-sept, $J = 9.0, 7.0$ Hz), 1.35 (1.5H, d, $J = 7.0$ Hz), 1.33 (1.5H, d, $J = 7.0$ Hz), 1.11 (3H, d, $J = 7.0$ Hz), 0.61 (1.5H, d, $J = 7.0$ Hz), 0.59 (1.5H, d, $J = 7.0$ Hz).

Hydrolysis of 8²³: A solution of **8** (66.3 mg, 0.23 mmol) in THF (23 mL) was treated with 30% H₂O₂ solution (1.3 mL) and a 1.0 M aqueous solution of LiOH (2.3 mL, 2.3 mmol) at 0 °C for 4 hours. Then, a saturated aqueous solution of NaHSO₃ was added to the resulting solution until peroxides were completely reduced. After concentration, the residual aqueous phase was washed with diethyl ether, acidified with *conc.* HCl and extracted with EA twice. The organic extracts were dried over Na₂SO₄ and evaporated under reduced pressure to give (*S*)-**6** in 75 % yield. (*S*)-**6**: ¹H NMR (500 MHz, CD₃OD) δ 2.83 (1H, dqd, $J = 8.0, 7.0, 6.0$), 2.66 (1H, dd, $J = 17.0, 8.0$ Hz), 2.39 (2H, dd, $J = 17.0, 6.0$ Hz), 1.21 (3H, d, $J = 7.0$ Hz); [α]_D²⁷ -14.4 ($c = 1.18$, EtOH) [lit.²⁴ [α]_D^{24.2} -15.0 ($c = 1.89$, EtOH) for *S* isomer, 99% ee].

Conservation of Enantiomeric Purity: The enantiomeric purity of **6** was determined by HPLC analysis after esterification.



Esterification of 6: To a solution of **6** (21.0 mg, 0.16 mmol), tetrabutylammonium iodide (TBAI) (5.9 mg, 0.01 mmol) and K₂CO₃ (132.7 mg, 0.96 mmol) in *N,N*-dimethylformamide (DMF) (2 mL) was added benzyl bromide (57.1 μ L, 0.48 mmol) dropwise at room temperature. The reaction mixture was

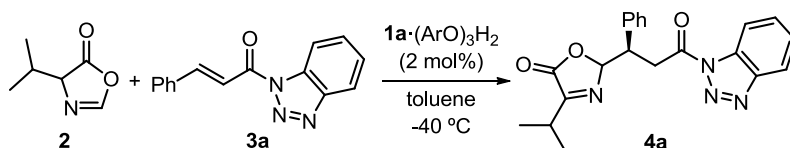
vigorously stirred for 8 hours and diluted with H₂O. The resulting aqueous solution was extracted with diethyl ether three times. The combined organic extracts were dried over Na₂SO₄ and filtered. Evaporation of solvents and purification of the residue by column chromatography on silica gel (H/EA = 10:1 as eluent) gave **9** in 83% yield. The enantiomeric purity of **9** was determined to be 95% ee by chiral stationary phase HPLC analysis. **9**: ODH, H/IPA = 10:1, flow rate = 0.5 mL/min, λ = 210 nm, 16.1 min (*R*), 21.1 min (*S*); ¹H NMR (700 MHz, CDCl₃) δ 7.36-7.33 (4H, m), 7.33-7.30 (6H, m), 5.12 (1H, d, *J* = 12.6 Hz), 5.10 (1H, d, *J* = 11.9 Hz), 5.08 (1H, d, *J* = 12.6 Hz), 5.07 (1H, d, *J* = 11.9 Hz), 3.00 (1H, sex, *J* = 7.0 Hz), 2.81 (1H, dd, *J* = 16.1, 7.0 Hz), 2.48 (1H, dd, *J* = 16.1, 7.0 Hz), 1.24 (3H, d, *J* = 7.0 Hz).

Additional Experimental Data and Discussion:

Effect of Phenol Structure on the Selectivity: α,β -Unsaturated *N*-acylbenzotriazole **3a** (24.9 mg, 0.10 mmol) and **1a**·(ArO)₃H₂ (0.02 equiv, 2.0 μ mol) were placed in a dried test tube and dissolved into toluene (1.0 mL) under Ar atmosphere. Azlactone **2** (14.0 mg, 0.11 mmol) was then introduced dropwise slowly at -40 °C and the stirring was continued for indicated hours. A solution of trifluoroacetic acid in toluene (0.5 M, 20 μ L) was added to the mixture at -40 °C to quench the reaction. The resulting mixture was poured into ice-cooled 1 *N* HCl aqueous solution and the aqueous phase was extracted with EA. The combined organic phase was washed with brine, dried over Na₂SO₄, and filtered. After removing all volatiles by evaporation, purification of the residue by column chromatography on silica gel (H/EA = 5:1 as eluent) afforded **4a**, whose enantiomeric excess was determined by HPLC analysis.

The results with a series of catalysts that possess different phenols are listed in Table S1. Although it seems to be difficult to see any tendency of correlation between the phenol structure and enantioselectivity, the use of 3,5-Cl₂-C₆H₃OH leads to the highest selectivity so far.

Table S1. Optimization of Phenol Structure



| entry | catalyst | time (h) | yield (%) | ee (%) |
|-------|---|----------|-----------|--------|
| 1 | 1a ·(PhO) ₃ H ₂ | 9 | 98 | 67 |
| 2 | 1a ·(4-CF ₃ -C ₆ H ₄ O) ₃ H ₂ | 12 | 91 | 74 |
| 3 | 1a ·(4-F-C ₆ H ₄ O) ₃ H ₂ | 8 | 99 | 71 |
| 4 | 1a ·(4-Cl-C ₆ H ₄ O) ₃ H ₂ | 10 | 94 | 77 |
| 5 | 1a ·(4-Br-C ₆ H ₄ O) ₃ H ₂ | 15 | 95 | 75 |
| 6 | 1a ·(4-Me-C ₆ H ₄ O) ₃ H ₂ | 8 | 95 | 65 |
| 7 | 1a ·(4-MeO-C ₆ H ₄ O) ₃ H ₂ | 36 | 54 | 76 |
| 8 | 1a ·(2-naphthoxide) ₃ H ₂ | 12 | 93 | 45 |
| 9 | 1a ·(2-Cl-C ₆ H ₄ O) ₃ H ₂ | 18 | 95 | 65 |
| 10 | 1a ·(2-Me-C ₆ H ₄ O) ₃ H ₂ | 6 | 90 | 67 |
| 11 | 1a ·(2-Ph-C ₆ H ₄ O) ₃ H ₂ | 10 | 96 | 43 |
| 12 | 1a ·(3-Cl-C ₆ H ₄ O) ₃ H ₂ | 8 | 97 | 75 |
| 13 | 1a ·(3,5-Cl ₂ -C ₆ H ₃ O) ₃ H ₂ | 24 | 99 | 85 |
| 14 | 1a ·(3,5-Me ₂ -C ₆ H ₃ O) ₃ H ₂ | 13 | 90 | 58 |
| 15 | 1a ·(2,4-Me ₂ -C ₆ H ₃ O) ₃ H ₂ | 12 | 97 | 68 |
| 16 | 1a ·(2,6-Me ₂ -C ₆ H ₃ O) ₃ H ₂ | 12 | 99 | 37 |
| 17 | 1b ·(PhO) ₃ H ₂ | 12 | 99 | 85 |
| 18 | 1b ·(4-Cl-C ₆ H ₄ O) ₃ H ₂ | 18 | 95 | 91 |

Selectivity Dependence on Phenol Concentration: To a solution of **1a**·Cl (8.24 mg, 13.75 μ mol) in toluene (2.4 mL) was introduced a 1.0 M THF solution of KO^tBu (12.5 μ L, 12.5 μ mol) at -78 °C and the mixture was stirred there for 30 min. After addition of a solution of phenol (PhOH or 4-Cl-C₆H₄OH) in 0.1 mL of toluene at -40 °C, the resulting catalyst solution was aged for 30 min. Then, *N*-acylbenzotriazole **3a** (62.3 mg, 0.25 mmol) and azlactone **2** (35.0 mg, 0.275 mmol) were added sequentially, and stirring was continued at -40 °C. The reaction was quenched by the addition of a solution of trifluoroacetic acid (0.5 M, 150 μ L) at -40 °C and the whole mixture was poured into ice-cooled 1 *N* HCl aqueous solution. After extractive workup with EA and evaporation of solvents, the crude residue was purified by silica gel column chromatography (H/EA = 5:1 as eluent) to give the adduct **4a**, whose enantiomeric excess was determined by HPLC analysis.

The enantioselectivity of the reaction was plotted against the concentration of phenol under the influence of **1a** as a cationic component of the catalyst (Fig. S1). The form of each plotting clearly showed the strong dependence of the selectivity on the phenol concentration. In consideration of this observation and the effect of the catalyst concentration described in the manuscript, there would be an equilibrium in the assembly of an enolate ion pair such as shown in Fig. S2. The lower enantioselectivity observed under lower phenol concentration might stem from the intervention of the enolate assembly of either **A** or **B**. Higher concentration of phenol should push this equilibrium to right and increased population of the assembly **C** would lead to the higher selectivity [30 mol% of phenol (30 mM of phenol concentration) corresponds to that of the optimized reaction conditions, which is 0.2 mmol scale with 1 mol% of **1a**·(PhO)₃H₂ in 0.2 mL of toluene].

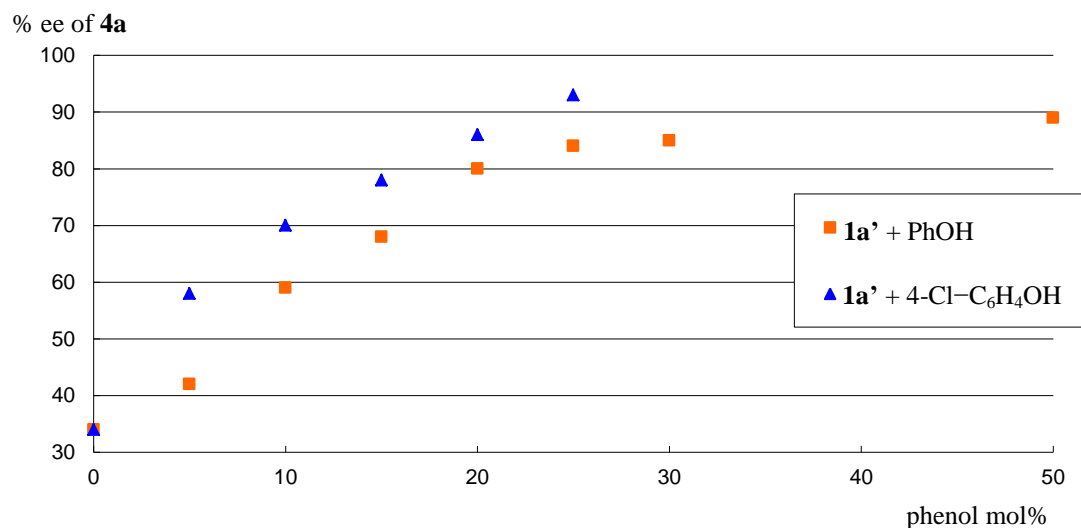
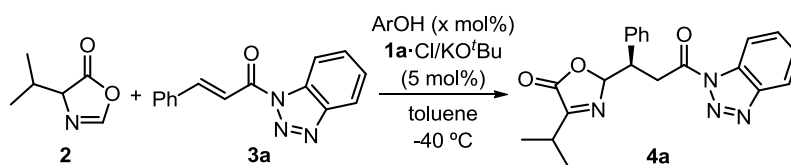


Fig. S1. Selectivity Dependence on Phenol Concentration

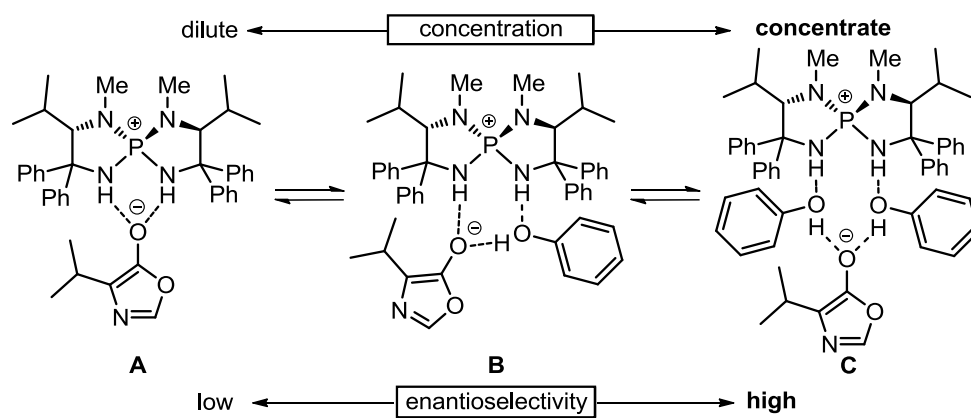


Fig. S2.

Crystallographic Structure Determination:

Recrystallization of $1a \cdot (\text{PhO})_3\text{H}_2$ (CCDC 741902): Tetraaminophosphonium phenoxide $1a \cdot (\text{PhO})_3\text{H}_2$ was recrystallized from hexane/diethyl ether solvent system at room temperature.

The single crystal thus obtained was mounted on CryoLoop. Data of X-ray diffraction were collected at 153 K on a Bruker SMART APEX CCD diffractometer with graphite-monochromated Mo K α radiation ($\lambda = 0.71073 \text{ \AA}$). An absorption correction was made using SADABS. The structure was solved by direct methods and Fourier syntheses, and refined by full-matrix least squares on F^2 by using SHELXTL.²⁵ All non-hydrogen atoms were refined with anisotropic displacement parameters. Hydrogen atoms bonded to nitrogen and oxygen atoms were located from a difference synthesis and their coordinates and isotropic thermal parameters refined. The other hydrogen atoms were placed in calculated positions. The crystallographic data were summarized in Table S2, S3 and ORTEP diagram was shown in Fig. S3.

Table S2. Crystal Data and Structure Refinement for $1a \cdot (\text{PhO})_3\text{H}_2$.

| | | |
|--|--|-----------------------|
| Empirical formula | C54 H61 N4 O3 P | |
| Formula weight | 845.04 | |
| Temperature | 153(2) K | |
| Wavelength | 0.71073 \AA | |
| Crystal system | Orthorhombic | |
| Space group | P2(1)2(1)2(1) | |
| Unit cell dimensions | $a = 10.5801(5) \text{ \AA}$ | $\alpha = 90^\circ$. |
| | $b = 21.0028(10) \text{ \AA}$ | $\beta = 90^\circ$. |
| | $c = 21.1066(11) \text{ \AA}$ | $\gamma = 90^\circ$. |
| Volume | 4690.1(4) \AA^3 | |
| Z | 4 | |
| Density (calculated) | 1.197 Mg/m^3 | |
| Absorption coefficient | 0.106 mm^{-1} | |
| F(000) | 1808 | |
| Crystal size | 0.60 x 0.20 x 0.10 mm^3 | |
| Theta range for data collection | 1.37 to 28.30 $^\circ$. | |
| Index ranges | $-11 \leq h \leq 14$, $-28 \leq k \leq 22$, $-27 \leq l \leq 28$ | |
| Reflections collected | 35732 | |
| Independent reflections | 11630 [R(int) = 0.0576] | |
| Completeness to theta = 28.30 $^\circ$ | 99.9 % | |
| Absorption correction | Empirical | |

| | |
|--------------------------------------|--|
| Max. and min. transmission | 0.9895 and 0.9390 |
| Refinement method | Full-matrix least-squares on F^2 |
| Data / restraints / parameters | 11630 / 0 / 581 |
| Goodness-of-fit on F^2 | 1.039 |
| Final R indices [$I > 2\sigma(I)$] | $R_1 = 0.0559$, $wR_2 = 0.1171$ |
| R indices (all data) | $R_1 = 0.0838$, $wR_2 = 0.1328$ |
| Absolute structure parameter | 0.13(8) |
| Largest diff. peak and hole | 0.358 and $-0.224 \text{ e.}\text{\AA}^{-3}$ |

Table S3. Hydrogen Bonds for **1a**·(PhO)₃H₂ [\AA and $^\circ$].

| D-H...A | d(D-H) | d(H...A) | d(D...A) | $\angle(\text{DHA})$ |
|---------------------|---------|----------|----------|----------------------|
| O(1)-H(58)...O(3)#1 | 0.95(4) | 1.60(4) | 2.539(3) | 168(4) |
| O(2)-H(57)...O(3)#2 | 0.94(4) | 1.58(4) | 2.506(3) | 167(3) |
| N(4)-H(56)...O(1)#3 | 0.89(3) | 2.00(3) | 2.881(3) | 172(2) |
| N(2)-H(55)...O(2)#4 | 0.89(3) | 1.97(3) | 2.838(3) | 163(2) |

Symmetry transformations used to generate equivalent atoms: #1 $x, y-1, z$; #2 $x, y-1, z+1$; #3 $x-1, y, z$; #4 $x-1, y, z-1$.

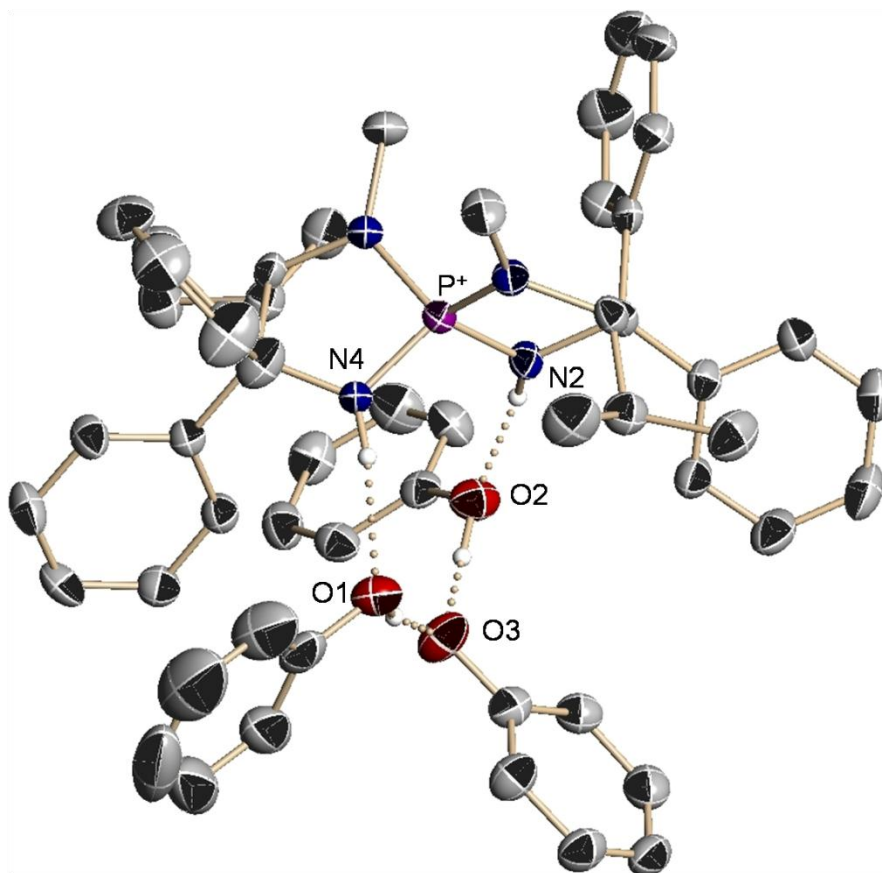


Fig. S3. Molecular Structure of Tetraaminophosphonium Phenoxide **1a**·(PhO)₃H₂. All calculated hydrogen atoms are omitted for clarity. Purple = phosphorus, blue = nitrogen, red = oxygen, black = carbon.

References and Notes

- (1) Supramolecular Catalysis; van Leeuwen, P. W. N. M., Ed.; Wiley-VCH, Weinheim, 2008. and references therein.
- (2) Breit, B. *Pure Appl. Chem.* **2008**, *80*, 855.
- (3) Park, J.; Lang, K.; Abboud, K. A.; Hong, S. *J. Am. Chem. Soc.* **2008**, *130*, 16484.
- (4) Breuil, P.-A. R.; Patureau, F. W.; Reek, J. N. H. *Angew. Chem., Int. Ed.* **2009**, *48*, 2162.
- (5) Clarke, M. L.; Fuentes, J. A. *Angew. Chem., Int. Ed.* **2007**, *46*, 930.
- (6) Uraguchi, D.; Ueki, Y.; Ooi, T. *J. Am. Chem. Soc.* **2008**, *130*, 14088. and references therein.
- (7) Materials and Methods are available as Experimental Section.
- (8) Tozawa, T.; Nagao, H.; Yamane, Y.; Mukaiyama, T. *Chem. Asian J.* **2007**, *2*, 123.
- (9) Saenger, W. *Nature* **1979**, *279*, 343.
- (10) Mautner, M. *Chem. Rev.* **2005**, *105*, 213.
- (11) Yamamoto, H.; Futatsugi, K. *Angew. Chem., Int. Ed.* **2005**, *44*, 1924.
- (12) Barco, A.; Benetti, S.; De Risi, C.; Pollini, G. P.; Spalluto, G.; Zanirato, V. *Tetrahedron* **1996**, *52*, 4719.
- (13) Katritzky, A. R.; Zang, Y.; Singh, S. K. *Synthesis* **2003**, 2795.
- (14) Uraguchi, D.; Sakaki, S.; Ooi, T. *J. Am. Chem. Soc.* **2007**, *129*, 12393.
- (15) For the results with other representative phenols, see Experimental Section.
- (16) For further experimental supports for the molecular assembly, see Experimental Section.
- (17) Structural parameters for **1a**·(PhO)₃H₂ are available free of charge from the Cambridge Crystallographic Data Centre under reference number CCDC 741902.
- (18) Uraguchi, D.; Sakaki, S.; Ueki, Y.; Ito, T.; Ooi, T. *Heterocycles* **2008**, *76*, 1081.
- (19) Uraguchi, D.; Ueki, Y.; Ooi, T. *J. Am. Chem. Soc.* **2008**, *130*, 14088.
- (20) T. Tozawa, H. Nagao, Y. Yamane, T. Mukaiyama, *Chem. Asian J.* **2**, 123 (2007).
- (21) C. Pardin, J. N. Pelletier, W. D. Lubell, J. W. Keillor, *J. Org. Chem.* **73**, 5766 (2008).
- (22) A. R. Katritzky, M. Wang, S. Zhang, *ARKIVOC* **9**, 19 (2001).
- (23) D. A. Evans, P. H. Carter, C. J. Dinsmore, J. C. Barrow, J. L. Katz, D. W. Kung, *Tetrahedron Lett.* **38**, 4535 (1997).
- (24) E. J. Eisenbraun, S. M. McElvain, *J. Am. Chem. Soc.* **77**, 3383 (1955).
- (25) G. M. Sheldrick, SHELXTL 5.1, Bruker AXS Inc., Madison, Wisconsin, 1997.

1. Introduction.

The chemistry at the interface between homogeneous catalysis and supramolecular chemistry, namely supramolecular catalysis, has attracted sustained attention over the last decade.¹ Depart from the early endeavor to create preorganized molecular receptors as an artificial enzyme, the current approach toward understanding and mimicking enzymatic catalysis has focused on the design of systems capable of spontaneously generating well-defined, functional supramolecular architectures by self-assembly. The inner spaces of these assemblies served as an isolated reaction vessel that could confine the substrates, thus delivering otherwise unattainable reactivity and selectivity.²

In parallel, new possibilities of supramolecular catalysis have been demonstrated via the marriage of multicomponent assemblies with homogeneous transition metal catalyses and organic molecular catalyses since the seminal studies of Breit, von Leeuwen and Reek in 2003.³ Within the latter context, the author recently reported that chiral *P*-spiro triaminoiminophosphorane **1** and three equivalents of aryloxides (ArOH) spontaneously assembled into the highly organized molecular structure **1**·[ArOH]₃ through the formation of an ion-pair-assisted hydrogen-bonding network (Figure 1).^{4,5} Further, the resultant **1**·[ArOH]₃, particularly the one with a 3,5-dichlorophenol (3,5-Cl₂-C₆H₃OH, **2**) component, exerted efficient cooperative catalysis in the stereoselective conjugate addition of an acyl anion equivalent. Although the discrete three-dimensional structure of **1**·[PhOH]₃ in solid state was determined by single-crystal X-ray diffraction analysis, the actual behavior of this type of supramolecular catalyst in solution remains as an important issue to be uncovered.

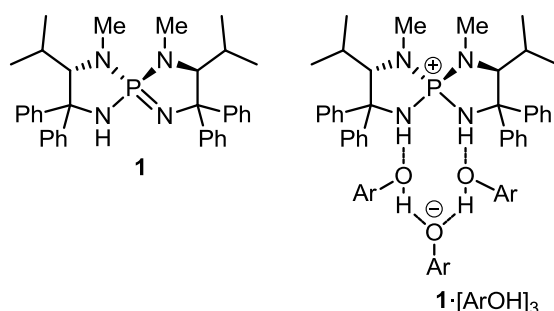


Figure 1. Chiral *P*-spiro tetraaminophosphonium aryloxide assembly **1**·[ArOH]₃.

This situation prompted us to conduct a series of spectroscopic analyses of a solution of **1** and **2** in an organic solvent, which revealed not only the effectiveness of the low temperature ³¹P NMR measurement for tracing the solution structure but also unexpected, yet intriguing, phenomenon regarding the mode of the molecular associations. Herein, the author disclose the stepwise and exclusive generation of three types of molecular assemblies, **1**·[**2**]_n (n = 1-3), in

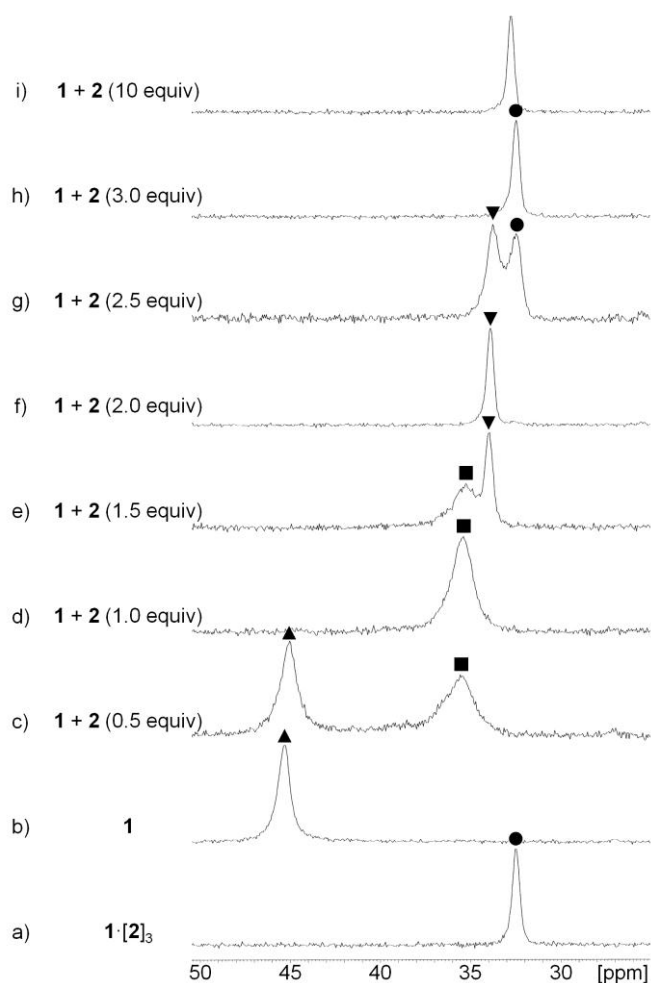
solution by simply adjusting the stoichiometry of **2**. Each structure was unequivocally verified in the solid state by X-ray crystallographic analysis. This finding, that the mode of the spontaneous assembly of **1** and **2** can be precisely controlled in solution, suggests the possibility of selective use of $\mathbf{1}\cdot[\text{ArOH}]_n$ ($n = 1-3$) as a requisite catalyst for target organic transformation and could also provide an expedient means to gain insights into the structural integrity of the reactive intermediate.

2. Result and Discussion.

2.1. ^{31}P NMR Analysis of In Situ Generated Molecular Assemblies of Triaminoiminophosphorane **1** and 3,5- $\text{Cl}_2\text{-C}_6\text{H}_3\text{OH}$ (**2**) at -98°C in Toluene.

Initially, ^{31}P NMR analysis of isolated $\mathbf{1}\cdot[\mathbf{2}]_3$ (Figure 2c) was performed in toluene (10.0 mM) at -98°C , and a sharp singlet was observed at 32.4 ppm (Chart 1a, ●). In order to assess the validity of assigning this signal to $\mathbf{1}\cdot[\mathbf{2}]_3$ even in solution, the stoichiometry in generating the same signal in situ from iminophosphorane **1** and **2** was probed by varying the amount of **2** to **1**; this led to some rather surprising yet interesting observations. For a toluene solution of **1** (Chart 1b, ▲) treated with a half equivalent of **2**, two separate signals were detected at 45.0 and 35.5 ppm, respectively (Chart 1c). The new signal that appeared in the upper field (■) was essentially different from that observed in the case of $\mathbf{1}\cdot[\mathbf{2}]_3$. Since this signal grew as a single peak at 35.4 ppm upon introducing one equivalent of **2** (Chart 1d), it could be assigned to $\mathbf{1}\cdot[\mathbf{2}]_1$, i.e., the simplest ion pair of aminophosphonium cation $\mathbf{1}\cdot\text{H}$ with aryloxide (Figure 2a). Further, treatment of **1** with one and a half equivalents of **2** resulted in the appearance of a new upfield resonance with a decrease in the resonance corresponding to $\mathbf{1}\cdot[\mathbf{2}]_1$ (Chart 1e), and it became an only detectable peak at 33.9 ppm when the amount of **2** was increased to two equivalents (Chart 1f, ▼). This signal was still different from the one observed in the case of $\mathbf{1}\cdot[\mathbf{2}]_3$, and it could correspond to another molecular assembly such as $\mathbf{1}\cdot[\mathbf{2}]_2$ (▼) (Figure 2b). Indeed, a similar tendency was observed when two and a half equivalents of **2** were added (Chart 1g), and the spectrum measured after the treatment of **1** with three equivalents of **2** showed a sharp singlet at 32.4 ppm (Chart 1h, ●), which was identical to the chemical shift observed for isolated $\mathbf{1}\cdot[\mathbf{2}]_3$. Consequently, there seems to exist a stepwise equilibrium between **1** and $\mathbf{1}\cdot[\mathbf{2}]_3$ depending on the stoichiometry of **2**, and each assembly could be predominantly organized under the influence of a requisite least equivalent (1-3 equiv) of **2**. It should be noted that the presence of large excess of **2** did not significantly affect the mode of assembly (Chart 1i), and thus $\mathbf{1}\cdot[\mathbf{2}]_3$ would be a terminal assembly.

Chart 1. ^{31}P NMR Spectra of in situ Generated Molecular Assemblies of Triaminoiminophosphorane **1** and 3,5- $\text{Cl}_2\text{-C}_6\text{H}_3\text{OH}$ (**2**) at -98°C in Toluene.



2.2 The X-ray diffraction analyses of each molecular assembly of $\mathbf{1}\cdot[\mathbf{2}]_1$, $\mathbf{1}\cdot[\mathbf{2}]_2$ and $\mathbf{1}\cdot[\mathbf{2}]_3$

On the basis of these observations, the author attempted to obtain further compelling evidence to prove the intervention of each plausible mode of assembly. Fortunately, the author found that each molecular assembly was sufficiently stable to be crystallized from a solution of **1** and **2** in an appropriate molar ratio. The X-ray diffraction analyses of these single crystals nicely visualized three dimensional structures of $\mathbf{1}\cdot[\mathbf{2}]_1$, $\mathbf{1}\cdot[\mathbf{2}]_2$ and $\mathbf{1}\cdot[\mathbf{2}]_3$, respectively (ORTEP diagrams in Figure 2).⁶ Moreover, the ^{31}P NMR analyses of toluene solutions prepared from each single crystal at -98°C provided a signal at exactly the same chemical shift as that of the in situ generated one. These results unambiguously confirm the contribution of the stepwise equilibrium and suggest that k_1 is substantially greater than k_2 for all the steps. Thus, it would be possible to precisely control the mode of the spontaneous assemblies of chiral

tetraaminophosphonium aryloxide-arylhydroxide(s) in solution by adjusting the stoichiometry of each component voluntarily.

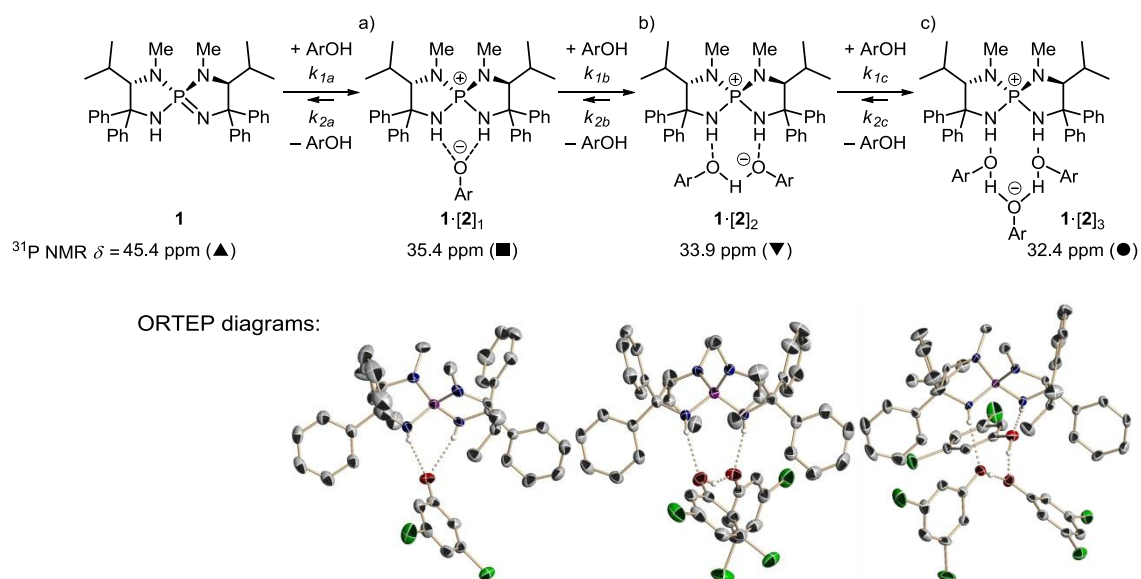
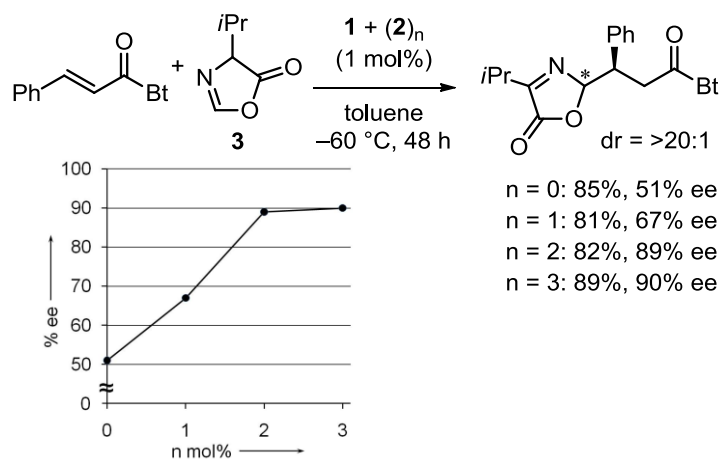


Figure 2. Equilibrium between molecular assemblies $1 \cdot [2]_n$ ($n = 1-3$) ($\text{Ar} = 3,5\text{-Cl}_2\text{-C}_6\text{H}_3$) and ORTEP diagrams of each assembly. Calculated hydrogens are omitted for clarity. P = purple, N = blue, O = red, Cl = light green, C = gray.

2.3. The mechanistic elucidation of their catalyses for the asymmetric conjugate addition with three types of chiral supramolecular catalysts.

Having been able to selectively utilize $1 \cdot [\text{ArOH}]_n$ ($n = 1-3$) as a catalyst, the author evaluated the synthetic relevance of this possibility in the conjugate addition of 2-unsubstituted azlactone **3** to cinnamoyl benzotriazole (Scheme 1).⁴



Scheme 1. Asymmetric conjugate addition of **3** to cinnamoyl acylbenzotriazole (Bt = benzotriazol-1-yl) catalyzed by in situ generated chiral *P*-spiro tetraaminophosphonium aryloxide assembly $1 \cdot [2]_n$ ($n = 0-3$).

The reactions were carried out at $-60\text{ }^{\circ}\text{C}$ in toluene with catalysts prepared by the treatment of **1** (1 mol%) with **2** (n mol%, $n = 0-3$), respectively. As the author assumed, the enantioselectivity was significantly enhanced as the number of **2** incorporated in the catalyst assembly was increased and reached 90% ee when $\mathbf{1}\cdot[\mathbf{2}]_3$ was employed. Notably, however, the selectivity was almost saturated under these conditions after 2 mol% of **2** ($n = 2$) was used for the catalyst preparation,⁷ in sharp contrast to the nearly proportional increase from 51% ee with **1** ($n = 0$) to 89% ee with $\mathbf{1}\cdot[\mathbf{2}]_2$ ($n = 2$). This observation provides an important clue to the nature of the assembly of the reactive intermediate (Figure 3).⁸

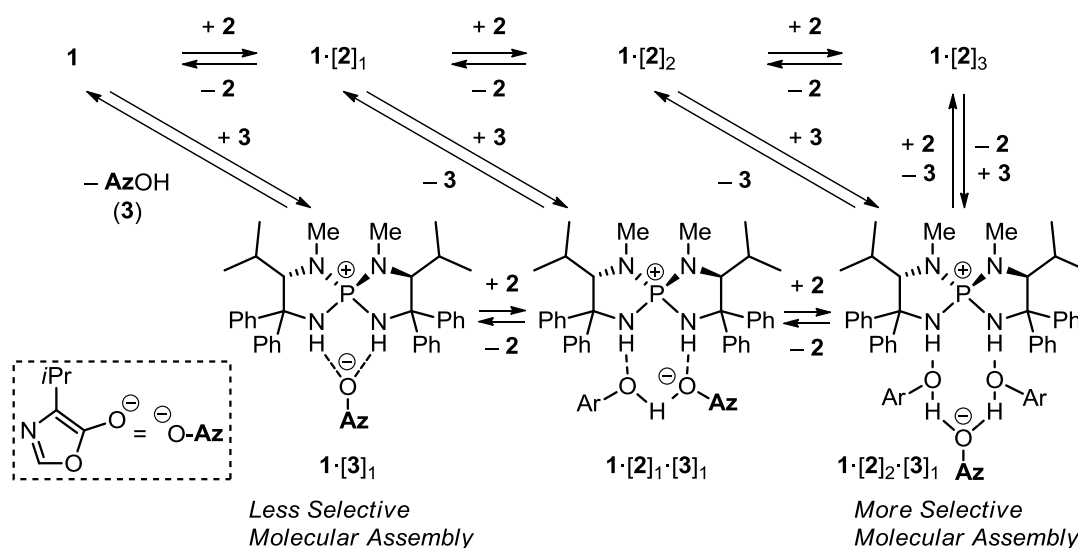


Figure 3. Plausible molecular assemblies of **1**, **2**, and azlactone **3** in solution (Ar = 3,5-Cl₂-C₆H₃).

In the reactions the author attempted with $\mathbf{1}\cdot[\mathbf{2}]_n$ ($n = 0-2$), initial deprotonation of **3** by $\mathbf{1}\cdot[\mathbf{2}]_n$ would give a reactive intermediate incorporating an enolate of **3** (O-Az^-) in the form of $\mathbf{1}\cdot[\mathbf{2}]_n\cdot[\mathbf{3}]_1$, each of which was responsible for the stereochemical control in its addition to cinnamoyl benzotriazole. Judging from the fact that $\mathbf{1}\cdot[\mathbf{2}]_3$ is a terminal assembly even in the presence of excess **2**, the reaction under the influence of $\mathbf{1}\cdot[\mathbf{2}]_3$ would involve the generation of $\mathbf{1}\cdot[\mathbf{2}]_2\cdot[\mathbf{3}]_1$ through the formal replacement of **2** by **3** in the deprotonation event. Thus, both $\mathbf{1}\cdot[\mathbf{2}]_2$ and $\mathbf{1}\cdot[\mathbf{2}]_3$, upon reacting with **3**, would afford the same molecular assembly, $\mathbf{1}\cdot[\mathbf{2}]_2\cdot[\mathbf{3}]_1$, accounting for the observed similar enantioselectivity.

3. Conclusion.

In conclusion, the author have successfully revealed that chiral *P*-spiro iminophosphorane **1** and 3,5-Cl₂-C₆H₃OH (**2**) assemble into three types of discrete molecular associations, $\mathbf{1}\cdot[\mathbf{2}]_1$,

1·**2**]₂, and **1**·**2**]₃, in a stepwise manner, depending on the stoichiometry of **2** by using low temperature ³¹P NMR technique and X-ray crystallographic analysis. This enables a facile and selective generation of a requisite mode of assembly in solution, which could not only amplify the structural diversity of this type of chiral supramolecular catalysts but also constitute a basis for the mechanistic elucidation of their catalyses as demonstrated in the asymmetric conjugate addition of 2-unsubstituted azlactone **3** to cinnamoyl benzotriazol. The present study offers a new, yet fruitful, opportunity for the design and application of supramolecularly assembled, chiral organic molecular catalysts.

4. Experimental Section.

General Information: ^1H NMR spectra were recorded on a JEOL JNM-ECS400 (400 MHz) or a Varian INOVA-700 (700 MHz). Chemical shifts are reported in ppm from the tetramethylsilane (0.0 ppm) resonance as the internal standard. Data are reported as follows: chemical shift, integration, multiplicity (s = singlet, d = doublet, t = triplet, q = quartet, sept = septet, m = multiplet, br = broad), and coupling constants (Hz). ^{31}P NMR spectra were recorded on a JEOL JNM-ECS400 (162 MHz) spectrometer with complete proton decoupling. Chemical shifts are reported in ppm from H_3PO_4 (0.0 ppm) resonance as the external standard. Analytical thin layer chromatography (TLC) was performed on Merck precoated TLC plates (silica gel 60 GF₂₅₄, 0.25 mm). Flash column chromatography was performed on PSQ60AB (spherical, av. 55 μm ; Fuji Silysia Chemical LTD.). Enantiomeric excesses were determined by HPLC analysis using DAICEL CHIRALPAK IC (IC) (ϕ 4.6 mm x 250 mm) with hexane and ethanol as eluent.

Toluene was supplied from Kanto Chemical Co., Inc. as “Dehydrated solvent system”. Tetraaminophosphonium chloride **1**·HCl and its iminophosphorane **1** were prepared by following the literature procedure.^{4,9} Other simple chemicals were purchased and used as such.

Low Temperature ^{31}P NMR Study:

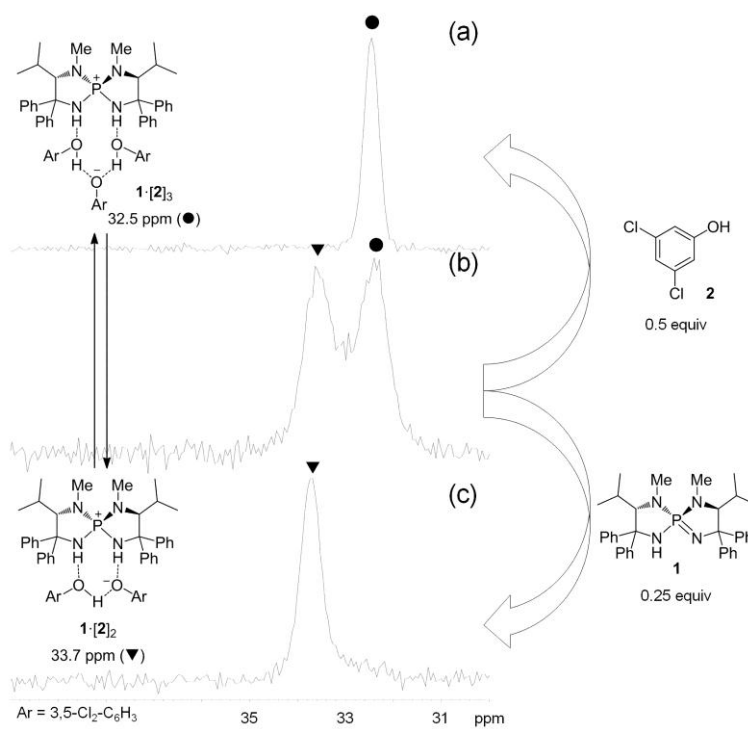
Representative Procedure for the Preparation of a NMR Sample: To a 0.025 M solution of triaminoiminophosphorane **1** in toluene (0.20 mL) in a ϕ 5 mm NMR tube was added a 0.050 M or 0.25 M solution of 3,5-Cl₂-C₆H₃OH (**2**) in toluene in varying molar ratios (**1/2** = 1:0 to 1:10) under Ar. After the adjustment of whole volume to 0.50 mL by the addition of toluene (10.0 mM based on the amount of **1**), the samples thus prepared were analyzed by ^{31}P NMR at $-98\text{ }^\circ\text{C}$.

Confirmation of Equilibrium at Low Temperature:

Existence of equilibrium between representative molecular assemblies **1**·**[2]**₂ and **1**·**[2]**₃ at low temperature was confirmed by means of titration method at $-98\text{ }^\circ\text{C}$. Experimental procedure and collected ^{31}P NMR charts are shown below.

**Procedure for the NMR Study
by Means of Titration**

Method: Two NMR samples of $1 \cdot [2]_{2.5}$ were prepared following the above procedure except for their concentrations (8.7 or 11.1 mM based on the amount of **1**) and their total volume (0.46 or 0.45 mL). The nearly identical ^{31}P NMR spectra were collected for these samples at $-98\text{ }^\circ\text{C}$ (one of them is shown as Chart S1b). To each NMR tube was



carefully added a solution of **1** (0.025 M, 0.040 mL) or **2** (0.050 M, 0.050 mL) in toluene at $-98\text{ }^\circ\text{C}$, respectively, and the resulting samples were analyzed by ^{31}P NMR at the same temperature (Chart S1c and S1a).

Crystallographic Structure Determination: The single crystal, which was obtained by the procedure exemplified below, was mounted on CryoLoop. Data of X-ray diffraction were collected at 153 K on a Bruker SMART APEX CCD diffractometer with graphite-monochromated Mo K α radiation ($\lambda = 0.71073$ Å). An absorption correction was made using SADABS. The structure was solved by direct methods and Fourier syntheses, and refined by full-matrix least squares on F^2 by using SHELXTL.¹⁰ All non-hydrogen atoms were refined with anisotropic displacement parameters. Hydrogen atoms bonded to nitrogen and oxygen atoms were located from a difference synthesis and their coordinates and isotropic thermal parameters refined. The other hydrogen atoms were placed in calculated positions and isotropic thermal parameters refined.

Recrystallization of 1·[2]₁: Recrystallization from a solution of **1** and **2** (1:1 molar ratio) in a hexane/diethyl ether solvent system at room temperature afforded single crystals of a equimolar mixture of tetraaminophosphonium aryloxide 1·[2]₁ and its water complex 1·[2]₁·H₂O. The crystallographic data were summarized in Table S1 and ORTEP diagrams were shown in Fig. S1.

Recrystallization of 1·[2]₂: Recrystallization from a solution of **1** and **2** (1:2 molar ratio) in a hexane/diethyl ether solvent system at room temperature afforded single crystals of a equimolar mixture of tetraaminophosphonium aryloxide-arylhydroxide 1·[2]₂ and its water complex 1·[2]₂·H₂O. The crystallographic data were summarized in Table S2 and ORTEP diagrams were shown in Fig. S2.

Recrystallization of 1·[2]₃: Recrystallization from a solution of **1** and **2** (1:3 molar ratio) in a hexane/diethyl ether solvent system at room temperature afforded single crystals of tetraaminophosphonium aryloxide-arylhydroxides 1·[2]₃. The crystallographic data were summarized in Table S3 and ORTEP diagram was shown in Fig. S3.

Table S1a. Crystal data and structure refinement for **1**·[**2**]₁. (CCDC 801437)

| | | |
|-----------------------------------|--|-----------------|
| Empirical formula | C ₁₆₈ H ₁₈₅ Cl ₈ N ₁₆ O ₆ P ₄ (1 : 2 :H ₂ O = 4:4:2) | |
| Formula weight | 2931.80 | |
| Temperature | 153(2) K | |
| Wavelength | 0.71073 Å | |
| Crystal system | Monoclinic | |
| Space group | P2(1) | |
| Unit cell dimensions | a = 17.1713(11) Å | α = 90°. |
| | b = 21.8824(14) Å | β = 90.833(2)°. |
| | c = 21.0555(14) Å | γ = 90°. |
| Volume | 7910.8(9) Å ³ | |
| Z | 2 | |
| Density (calculated) | 1.231 Mg/m ³ | |
| Absorption coefficient | 0.243 mm ⁻¹ | |
| F(000) | 3098 | |
| Crystal size | 0.30 x 0.30 x 0.20 mm ³ | |
| Theta range for data collection | 0.97 to 28.31°. | |
| Index ranges | -22 ≤ h ≤ 19, -28 ≤ k ≤ 29, -28 ≤ l ≤ 24 | |
| Reflections collected | 59882 | |
| Independent reflections | 35411 [R(int) = 0.0506] | |
| Completeness to theta = 28.31° | 99.6 % | |
| Absorption correction | Empirical | |
| Max. and min. transmission | 0.9530 and 0.9306 | |
| Refinement method | Full-matrix least-squares on F ² | |
| Data / restraints / parameters | 35411 / 1 / 1898 | |
| Goodness-of-fit on F ² | 1.135 | |
| Final R indices [I > 2σ(I)] | R ₁ = 0.0884, wR ₂ = 0.1706 | |
| R indices (all data) | R ₁ = 0.1195, wR ₂ = 0.1861 | |
| Absolute structure parameter | -0.04(5) | |
| Largest diff. peak and hole | 0.658 and -0.347 e.Å ⁻³ | |

Table S1b. Hydrogen bonds for **1**·[**2**]₁ [Å and °].

| D-H...A | d(D-H) | d(H...A) | d(D...A) | <(DHA) |
|----------------------------------|----------|----------|-----------|---------|
| O(1)-H(198)...O(5) ^{#1} | 0.75(11) | 1.98(11) | 2.713(10) | 166(12) |
| N(14)-H(196)...O(6) | 0.65(7) | 2.12(7) | 2.750(6) | 162(9) |
| O(1)-H(194)...O(3) | 0.63(5) | 2.16(6) | 2.763(8) | 163(7) |
| O(2)-H(193)...O(6) | 0.89(4) | 1.84(5) | 2.726(5) | 169(4) |
| N(2)-H(192)...O(1) | 0.88(4) | 1.97(4) | 2.842(7) | 173(4) |
| N(16)-H(190)...O(6) | 0.70(4) | 2.25(4) | 2.934(5) | 164(5) |
| N(6)-H(189)...O(2) | 0.85(5) | 1.93(5) | 2.746(5) | 159(5) |
| N(4)-H(191)...O(5) ^{#1} | 0.77(5) | 1.98(6) | 2.742(6) | 170(6) |
| N(9)-H(187)...O(3) ^{#2} | 0.86(6) | 1.86(6) | 2.704(5) | 165(6) |
| O(2)-H(195)...O(4) ^{#1} | 0.81(7) | 1.96(8) | 2.764(5) | 171(7) |
| N(8)-H(188)...O(4) ^{#1} | 0.75(5) | 2.03(5) | 2.757(5) | 161(5) |

Symmetry transformations used to generate equivalent atoms: ^{#1} x,y-1,z; ^{#2} x,y,z+1.

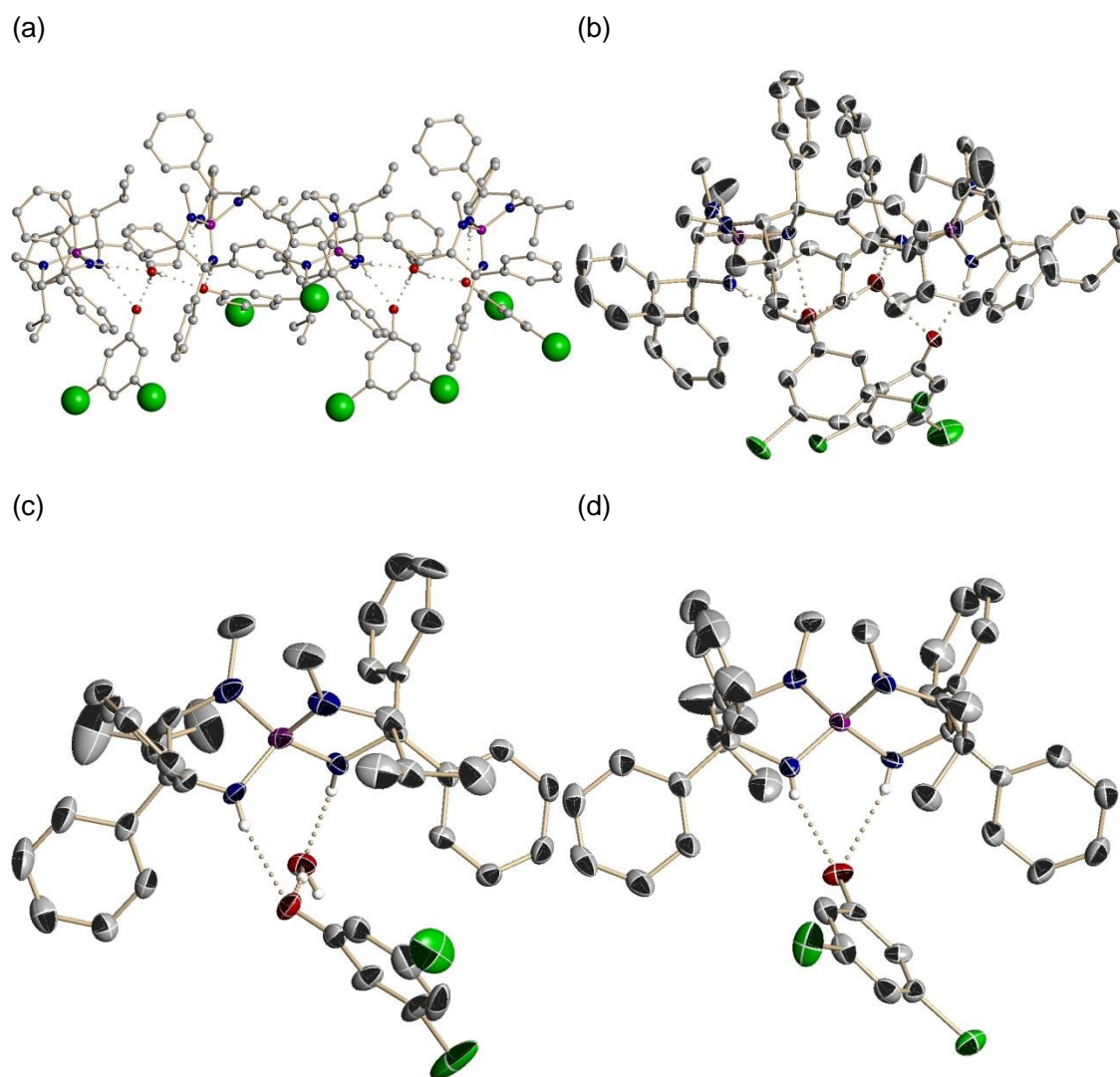


Fig. S1. Molecular structures of tetraaminophosphonium aryloxide $1 \cdot [2]_1$. (a) Ball and Stick picture of a calculation unit. (b) ORTEP drawing of hydrogen-bonding network between $1 \cdot [2]_1$ and $1 \cdot [2]_1 \cdot H_2O$. (c) ORTEP diagram of a section of $1 \cdot [2]_1 \cdot H_2O$. (d) ORTEP diagram of a section of $1 \cdot [2]_1$. All calculated hydrogen atoms are omitted for clarity. Purple = phosphorus, blue = nitrogen, red = oxygen, green = chlorine, gray = carbon.

Table S2a. Crystal data and structure refinement for **1**·[**2**]₂. (CCDC 801438)

| | | |
|-----------------------------------|--|----------|
| Empirical formula | C ₉₆ H ₁₀₄ Cl ₈ N ₈ O ₅ P ₂ (1 : 2 :H ₂ O = 2:4:1) | |
| Formula weight | 1795.41 | |
| Temperature | 153(2) K | |
| Wavelength | 0.71073 Å | |
| Crystal system | Orthorhombic | |
| Space group | P2(1)2(1)2(1) | |
| Unit cell dimensions | a = 14.443(2) Å | α = 90°. |
| | b = 14.992(2) Å | β = 90°. |
| | c = 42.826(6) Å | γ = 90°. |
| Volume | 9273(2) Å ³ | |
| Z | 4 | |
| Density (calculated) | 1.286 Mg/m ³ | |
| Absorption coefficient | 0.334 mm ⁻¹ | |
| F(000) | 3768 | |
| Crystal size | 0.30 x 0.20 x 0.20 mm ³ | |
| Theta range for data collection | 0.95 to 28.34°. | |
| Index ranges | -11 ≤ h ≤ 19, -19 ≤ k ≤ 19, -57 ≤ l ≤ 53 | |
| Reflections collected | 69607 | |
| Independent reflections | 22977 [R(int) = 0.0816] | |
| Completeness to theta = 28.34° | 99.3 % | |
| Absorption correction | Empirical | |
| Max. and min. transmission | 0.9363 and 0.9066 | |
| Refinement method | Full-matrix least-squares on F ² | |
| Data / restraints / parameters | 22977 / 0 / 1116 | |
| Goodness-of-fit on F ² | 1.012 | |
| Final R indices [I > 2σ(I)] | R ₁ = 0.0615, wR ₂ = 0.1145 | |
| R indices (all data) | R ₁ = 0.1183, wR ₂ = 0.1321 | |
| Absolute structure parameter | -0.02(4) | |
| Largest diff. peak and hole | 0.682 and -0.641 e.Å ⁻³ | |

Table S2b. Hydrogen bonds for **1**·[**2**]₂ [Å and °].

| D-H...A | d(D-H) | d(H...A) | d(D...A) | <(DHA) |
|-----------------------------------|---------|----------|----------|--------|
| N(2)-H(97)...O(5) | 0.79(4) | 2.22(4) | 2.998(4) | 167(4) |
| N(4)-H(98)...O(3) | 0.80(4) | 2.11(4) | 2.887(4) | 167(4) |
| N(6)-H(99)...O(1) | 0.76(3) | 2.19(4) | 2.915(4) | 160(4) |
| N(8)-H(100)...O(2) | 0.80(3) | 2.01(4) | 2.766(4) | 158(3) |
| O(5)-H(101)...Cl(3) ^{#1} | 0.83(5) | 2.81(5) | 3.378(3) | 127(4) |
| O(5)-H(102)...O(4) | 1.05(4) | 1.64(4) | 2.677(4) | 169(4) |
| O(3)-H(104)...O(4) | 0.86(4) | 1.59(4) | 2.445(4) | 176(4) |
| O(1)-H(103)...O(2) | 1.05(5) | 1.44(5) | 2.432(3) | 154(4) |

Symmetry transformations used to generate equivalent atoms: ^{#1} -x+1/2,-y+1,z+1/2

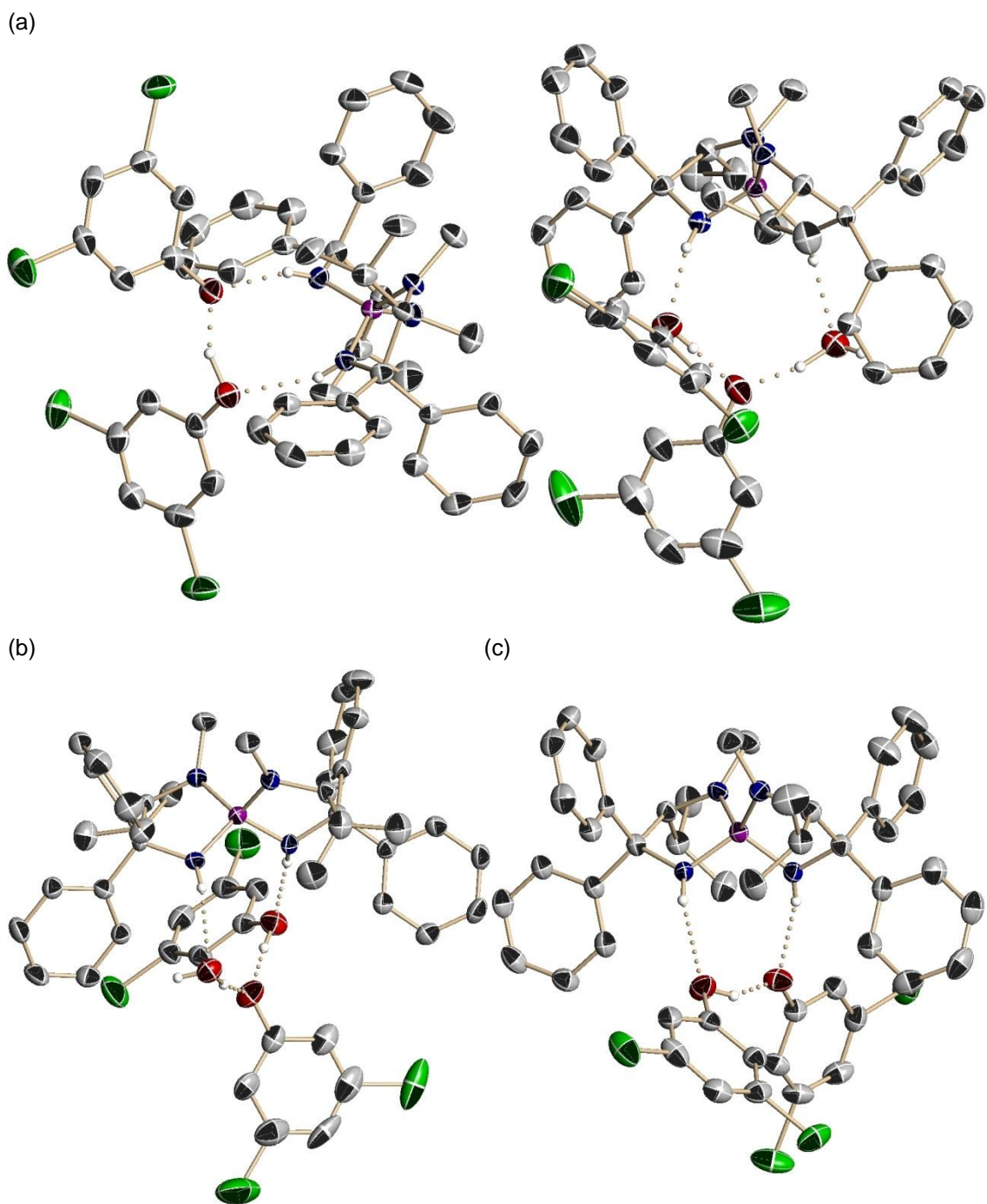


Fig. S2. Molecular structures of tetraaminophosphonium aryloxide $1 \cdot [2]_2$. (a) ORTEP drawing of a calculation unit. (b) ORTEP diagram of a section of $1 \cdot [2]_2 \cdot H_2O$. (c) ORTEP diagram of a section of $1 \cdot [2]_2$. Purple = phosphorus, blue = nitrogen, red = oxygen, green = chlorine, gray = carbon.

Table S3a. Crystal data and structure refinement for **1**·[**2**]₃. (CCDC 801439)

| | | |
|-----------------------------------|--|----------|
| Empirical formula | C ₅₄ H ₅₅ Cl ₆ N ₄ O ₃ P ₁ | |
| Formula weight | 1051.69 | |
| Temperature | 153(2) K | |
| Wavelength | 0.71073 Å | |
| Crystal system | Orthorhombic | |
| Space group | P2(1)2(1)2(1) | |
| Unit cell dimensions | a = 10.8227(6) Å | α = 90°. |
| | b = 18.5069(10) Å | β = 90°. |
| | c = 26.3320(14) Å | γ = 90°. |
| Volume | 5274.2(5) Å ³ | |
| Z | 4 | |
| Density (calculated) | 1.324 Mg/m ³ | |
| Absorption coefficient | 0.403 mm ⁻¹ | |
| F(000) | 2192 | |
| Crystal size | 0.50 x 0.40 x 0.30 mm ³ | |
| Theta range for data collection | 1.90 to 28.31°. | |
| Index ranges | -14 ≤ h ≤ 14, -24 ≤ k ≤ 24, -35 ≤ l ≤ 22 | |
| Reflections collected | 39902 | |
| Independent reflections | 13034 [R(int) = 0.0636] | |
| Completeness to theta = 28.31° | 99.8 % | |
| Absorption correction | Empirical | |
| Max. and min. transmission | 0.8887 and 0.8240 | |
| Refinement method | Full-matrix least-squares on F ² | |
| Data / restraints / parameters | 13034 / 0 / 635 | |
| Goodness-of-fit on F ² | 1.177 | |
| Final R indices [I > 2σ(I)] | R ₁ = 0.0745, wR ₂ = 0.1317 | |
| R indices (all data) | R ₁ = 0.0947, wR ₂ = 0.1389 | |
| Absolute structure parameter | 0.01(5) | |
| Largest diff. peak and hole | 0.516 and -0.311 e.Å ⁻³ | |

Table S3b. Hydrogen bonds for **1**·[**2**]₃ [Å and °].

| D-H...A | d(D-H) | d(H...A) | d(D...A) | <(DHA) |
|-------------------|---------|----------|----------|--------|
| N(4)-H(58)...O(2) | 0.85(4) | 2.11(4) | 2.943(4) | 167(3) |
| N(2)-H(57)...O(1) | 0.78(4) | 2.28(4) | 3.023(4) | 160(4) |
| O(1)-H(56)...O(3) | 0.86(4) | 1.68(5) | 3.023(4) | 175(4) |
| O(2)-H(55)...O(3) | 0.94(5) | 1.53(5) | 2.466(4) | 171(5) |

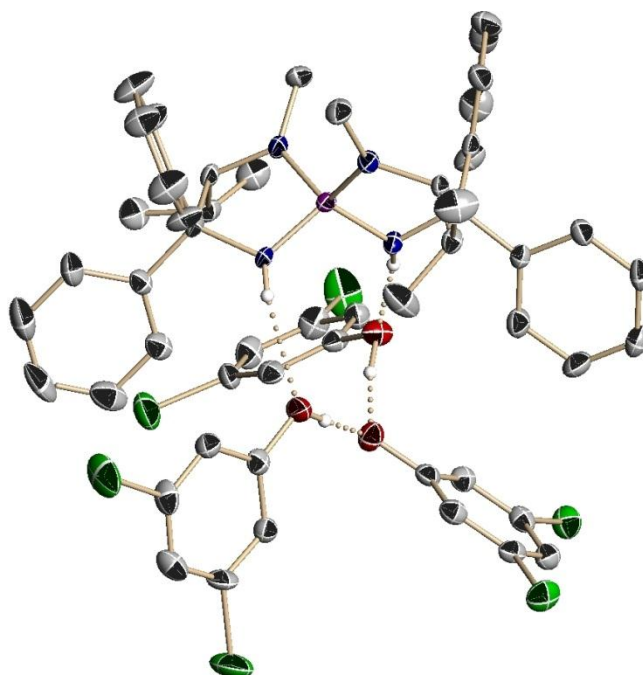
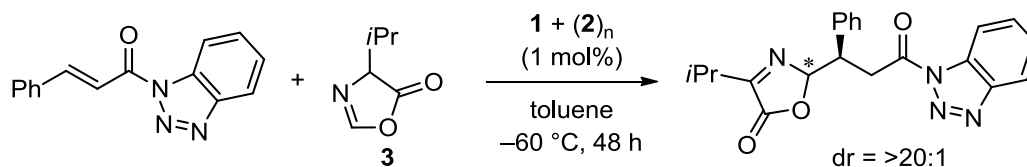


Fig. S3. ORTEP diagram of tetraaminophosphonium aryloxide **1**·[**2**]₃. All calculated hydrogen atoms are omitted for clarity. Purple = phosphorus, blue = nitrogen, red = oxygen, green = chlorine, gray = carbon.

Evaluation of Selectivity Dependence on the Ratio of Triaminoiminophosphorane **1 to 3,5-Cl₂-C₆H₃OH (**2**):**



General Procedure: Cinnamoyl benzotriazole (49.9 mg, 0.20 mmol) was placed in a dried test tube under Ar. Then, a 0.020 M solution of **1** in toluene (0.10 mL, 0.002 mmol) and a 0.10 M solution of **2** in toluene were added to the tube sequentially in varying molar ratios (**1/2** = 1:0 to 1:3). Whole volume of the solution was adjusted to 0.20 mL by the addition of toluene (10.0 mM based on the amount of **1**) and the mixture was cooled to $-60\text{ }^\circ\text{C}$. Azlactone **3** (28.0 mg, 0.22 mmol) was introduced dropwise slowly and the resulting slurry was stirred for 48 h. The reaction was quenched by the addition of a solution of trifluoroacetic acid in toluene (0.5 M, 20 μL) at $-60\text{ }^\circ\text{C}$ and the whole mixture was poured into ice-cooled 1 N HCl aqueous solution. The aqueous phase was extracted with ethyl acetate twice and the organic phases were washed with brine. The combined organic extracts were dried over Na₂SO₄ and filtered. All volatiles were removed by evaporation and the diastereomeric ratio was determined by ¹H NMR (400 MHz) analysis of the crude aliquot. The crude residue was purified by column chromatography on silica gel (hexane/ethyl acetate = 5:1 as eluent) to give the product, whose enantiomeric excess was determined by HPLC analysis.⁴ ¹H NMR (700 MHz, CDCl₃) δ 8.23 (1H, dt, $J = 8.4, 0.7$ Hz), 8.12 (1H, dt, $J = 8.4, 0.7$ Hz), 7.64 (1H, ddd, $J = 8.4, 7.0, 0.7$ Hz), 7.51 (1H, ddd, $J = 8.4, 7.0, 0.7$ Hz), 7.30-7.26 (2H, m), 7.26-7.22 (3H, m), 6.28 (1H, dd, $J = 4.2, 2.1$ Hz), 4.24 (1H, td, $J = 7.0, 4.2$ Hz), 4.18 (1H, dd, $J = 17.5, 7.0$ Hz), 4.09 (1H, dd, $J = 17.5, 7.0$ Hz), 2.79 (1H, sept-d, $J = 7.0, 2.1$ Hz), 1.18 (3H, d, $J = 7.0$ Hz), 1.04 (3H, d, $J = 7.0$ Hz).

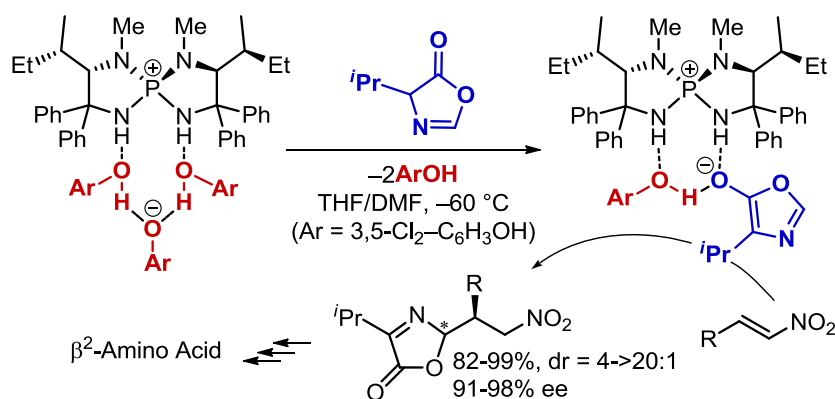
References and Notes

- (1) Supramolecular Catalysis; van Leeuwen, P. W. N. M., Ed.; Wiley-VCH, Weinheim, 2008. and references therein.
- (2) Yoshizawa, M.; Klosterman, J. K.; Fujita, M. *Angew. Chem., Int. Ed.* **2009**, *48*, 3418.
- (3) (a) Breit, B.; Seiche, W. *J. Am. Chem. Soc.* **2003**, *125*, 6608. (b) Slagt, V. F.; van Leeuwen, P. W. N. M.; Reek, J. N. H. *Chem. Comm.* **2003**, 2474. For review, see: Meeuwissen, J.; Reek, J. N. H. *Nat. Chem.* **2010**, *2*, 615.
- (4) Uraguchi, D.; Ueki, Y.; Ooi, T. *Science* **2009**, *326*, 120.
- (5) Rix, D.; Lacour, J. *Angew. Chem., Int. Ed.* **2010**, *49*, 1918.
- (6) See Experimental Section for details of X-ray analysis, particularly in view of the presence of another H₂O-bridged structure in the unit cells of **1**·[**2**]₁ and **1**·[**2**]₂, respectively. CCDC 801437 (**1**·[**2**]₁), CCDC 801438 (**1**·[**2**]₂), CCDC 801439 (**1**·[**2**]₃) contain the supplementary crystallographic data for this paper. These data can be obtained free of charge from The Cambridge Crystallographic Data Centre via www.ccdc.cam.ac.uk/data_request/cif.
- (7) When the reaction was conducted at higher temperature (−40 °C), use of **1**·[**2**]₃ was crucial for attaining a highest level of enantioselectivity^[4] probably because an excess amount of **2** would be necessary for shifting the equilibrium to the terminal assembly in order to ensure the intervention of **1**·[**2**]₂·[**3**]₁.
- (8) Attempts to detect the equilibrium between the enolate assemblies by the low temperature ³¹P NMR analysis were unsuccessful primarily due to the higher pK_a of **3** than that of **2**.
- (9) (a) Uraguchi, D.; Sakaki, S.; Ooi, T. *J. Am. Chem. Soc.* **2007**, *129*, 12392. (b) Uraguchi, D.; Sakaki, S.; Ueki, Y.; Ito, T.; Ooi, T. *Heterocycles* **2008**, *76*, 1081. (c) Uraguchi, D.; Ueki, Y.; Ooi, T. *J. Am. Chem. Soc.* **2008**, *130*, 14088.
- (10) G. M. Sheldrick, SHELXTL 5.1, Bruker AXS Inc., Madison, Wisconsin, 1997.

Chapter 5

Catalytic Asymmetric Conjugate Addition of Acyl Anion Equivalent to Nitroolefins

Abstract:

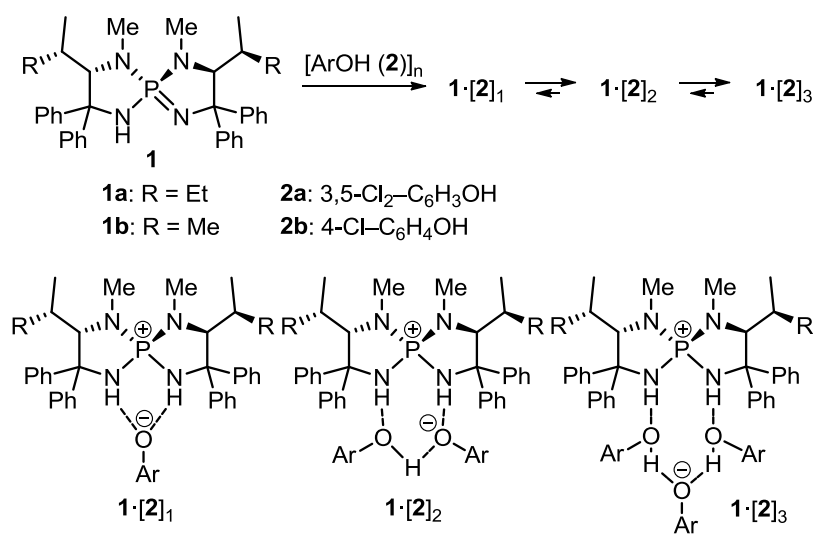


Highly enantioselective conjugate addition of 2-unsubstituted azlactone **3** to various nitroolefins **4** is accomplished by the selective utilization of supramolecularly assembled, chiral tetraaminophosphonium aryloxy-aryloxy $\mathbf{1a} \cdot [\mathbf{2a}]_2$ as a requisite catalyst. The key for this achievement is the polarity dependence of the molecular associations of type $\mathbf{1} \cdot [\mathbf{2}]_n$ and the crucial role of the proximal aryloxy **2** as a proton donor. The present method offers an attractive route to various optically active amino carbonyl compounds including β^2 -amino acids.

1. Introduction.

The design and synthetic application of self-assembled multicomponent catalysts has been emerging as a new field between supramolecular chemistry and homogeneous catalysis.¹ The strength and potential of this approach stem from the facile and rapid accessibility to a multitude of combinations of a relatively small number of simple catalyst components.² Such inherent modularity of the catalysts greatly facilitates the identification of the most reactive and selective system for the target organic transformation.

The author recently introduced a novel supramolecular catalyst of type $1\cdot[2]_3$ assembled from chiral *P*-spiro triaminoiminophosphorane **1** and three equivalents of arylhydroxides **2** via an ion-pair-assisted hydrogen-bonding network.^{3,4} This chiral onium salt exhibited a remarkable catalytic performance in achieving highly stereoselective conjugate addition of an acyl anion equivalent to α,β -unsaturated ester surrogates, and the structures of both chiral cation and arylhydroxide moieties had a significant influence on the enantioselectivity.^{3a} Furthermore, elucidation of the solution structure of $1\cdot[2]_3$ revealed that not only $1\cdot[2]_3$ but also the related modes of assembly, $1\cdot[2]_1$ and $1\cdot[2]_2$, could be exclusively generated in situ by simply treating **1** with **2** in an appropriate stoichiometry (Scheme 1).^{3b}



Scheme 1.

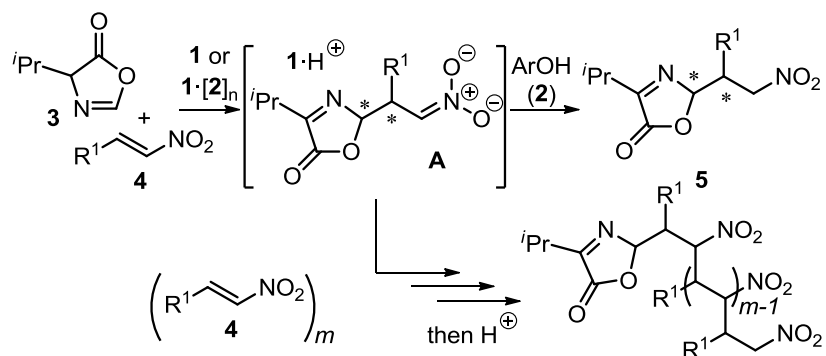
In the course of our continuous research efforts toward further eliciting the potential of our unique catalyst system, the author were intrigued by the possibility of selectively utilizing a requisite molecular assembly for developing synthetically valuable bond-forming processes. As an initial yet crucial step, the author describe herein the highly enantioselective conjugate addition⁵ of 2-unsubstituted azlactone **3** to nitroolefins **4**^{6,7} catalyzed efficiently by one to two molecular assembly $1a\cdot[2a]_2$. The success of this transformation relies heavily on the

discovery of a polarity-dependent mode for the catalyst assembly, which enables the selective molecular association of type $1 \cdot [2]_2$ even in the presence of exceeding stoichiometry of **2** as a crucial proton donor for product derivatization.

2. Result and Discussion.

2.1.

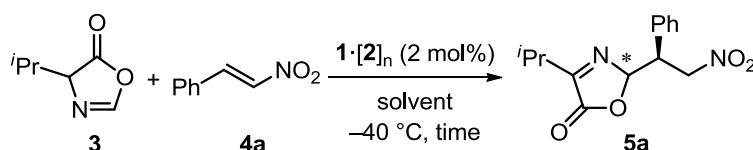
The catalytic asymmetric conjugate addition to nitroolefins has been extensively studied because of the inherent attractiveness of this Michael acceptor, and various Michael donors have been accommodated through the development of different types of catalyst system.⁶ Nevertheless, azlactones have scarcely been used as an acyl anion equivalent in combination with nitroolefins despite the potential utility of the corresponding conjugate adducts as a precursor of optically active β -amino carbonyl compounds.⁷ Taking into consideration this methodological deficiency as well, the author first attempted the reaction of **3** with β -nitrostyrene (**4a**) under the influence of $1a \cdot [2a]_3$ (2 mol%), which was prepared from L-isoleucine-derived iminophosphorane **1a** and three equivalents of 3,5-dichlorophenol (3,5-Cl₂-C₆H₃OH, **2a**), in toluene at -40 °C.^{3a} After 8 h, **4a** was completely consumed and the corresponding conjugate adduct **5a** was obtained in 90% isolated yield (Table 1, entry 1). However, its diastereomeric ratio was 1:1.3, and the enantiomeric excess of major diastereomer was 13% ee, albeit with good enantioselectivity of minor diastereomer (82% ee). Changing the chiral cationic component to L-valine-derived one **1b**·H at this point led to a decrease in the stereoselectivity, as expected (entry 2). Although the replacement of the phenolic component in turn by the less acidic 4-chlorophenol (4-Cl-C₆H₄OH, **2b**)^{8,9} resulted in a slight increase in the enantioselectivity, an unexpected loss of chemical yield was observed (entry 3). This was probably due to the intervention of the oligomerization pathway induced by the addition of the intermediary generated nitronate **A** to **4a** (Scheme 2).



Scheme 2.

Indeed, a gradual but substantial decrease in the yield of **5a** was also observed as the amount of **2a** incorporated in the catalyst assembly was reduced, while, more importantly, the enantioselectivity gradually improved (entries 4 and 5). These results indicated that the phenolic components of the catalysts behaved as effective proton donors¹⁰ to nitronate **A** and that the self-assembled **1a**·[**2a**]_n with a lesser amount of **2a** functioned as a more selective catalyst despite the fact that a certain amount of arylhydroxide possessing appropriate p*K*_a was crucial for the clean formation of **5a** by minimizing the possibility of oligomerization.¹¹ Interestingly, this dilemma was overcome by carrying out the reaction in a relatively polar solvent such as THF. Bond formation occurred smoothly in 3 h with reasonable selectivity profile, thus affording **5a** with a diastereomeric ratio of 5.9:1 and 90% enantiomeric excess for the major diastereomer (entry 6). The observed reactivity enhancement prompted us to lower the reaction temperature, which yielded a significant improvement in the stereoselectivity (entry 7). Finally, the author found that further tuning of the solvent polarity by the addition of *N,N*-dimethylformamide (DMF) (5% v/v) enabled the production of almost stereochemically pure **5a** in 90% yield (entry 8).

Table 1. Optimization of the reaction conditions.^a



| entry | catalyst | solvent | time (h) | yield ^b (%) | dr ^c | ee ^d (%) |
|----------------|--|----------------------|----------|------------------------|-----------------|---------------------|
| 1 | 1a ·[2a] ₃ | toluene | 8 | 90 | 1:1.3 | 82, 13 |
| 2 | 1b ·[2a] ₃ | toluene | 12 | 96 | 1:1.5 | 72, rac |
| 3 | 1a ·[2b] ₃ ^e | toluene | 12 | <62 | 1:1.1 | 89, 19 |
| 4 | 1a ·[2a] ₂ ^e | toluene | 4 | <77 | 1:1.3 | 89, 10 |
| 5 | 1a ·[2a] ₁ ^e | toluene | 4 | <61 | 1:1 | 93, 10 |
| 6 | 1a ·[2a] ₃ | THF | 3 | 99 | 5.9:1 | 90, rac |
| 7 ^f | 1a ·[2a] ₃ | THF | 12 | 96 | 13:1 | 94, rac |
| 8 ^g | 1a ·[2a] ₃ | THF/DMF ^h | 12 | 90 | >20:1 | 96, 31 |

^a Unless otherwise noted, reactions were performed on 0.1 mmol scale with 1.1 equiv of **3** in solvent (0.2 mL) at -40 °C. ^b Isolated yield. ^c Diastereomeric ratio was determined by 400 MHz ¹H NMR analysis of crude aliquot. ^d Enantiomeric excess was analyzed by chiral HPLC. Absolute configuration was determined to be *S*, see ESI.† ^e Catalyst was prepared in situ via self-assembly. ^f Reaction was conducted at -60 °C. ^g 5% v/v of DMF in THF was used as a solvent.

2.2. ³¹P NMR Analysis of In Situ Generated Molecular Assemblies of Triaminoiminophosphorane **1** and 3,5-Cl₂-C₆H₃OH (**2**) at -98 °C in THF.

In order to gain insight into the actual catalyst structure in THF, low temperature ^{31}P NMR analyses of THF solution of iminophosphorane **1b** and 3,5- $\text{Cl}_2\text{-C}_6\text{H}_3\text{OH}$ (**2a**) were performed at $-98\text{ }^\circ\text{C}$ (Figure 1). The addition of half equivalent of **2a** to a solution of **1b** (■: 44.4 ppm) gave two separate signals at 44.4 ppm (■) and 37.7 ppm (●) and the new upfield signal could be assigned to amino phosphonium aryloxide **1b**·**[2a]**₁ (Figure 1b). In fact, only a single sharp signal was detected at 37.6 ppm (●) in the case of an equimolar mixture of **1b** and **2a** (Figure 1c). When one and quarter equivalents of **2a** were added, a peak corresponding to aminophosphonium aryloxide-arylhydroxide **1b**·**[2a]**₂ appeared at 36.5 ppm (▼) (Figure 1d). This peak grew and became a single detectable signal as the amount of **2a** was increased to one and half, and then to two equivalents (Figure 1e and 1f). In marked contrast to the phenomena observed in toluene,^{3b} the four-component molecular assembly of type **1b**·**[2a]**₃ was not detected in this analysis even in the presence of large excess of **2a** (Figure 1g and 1h).

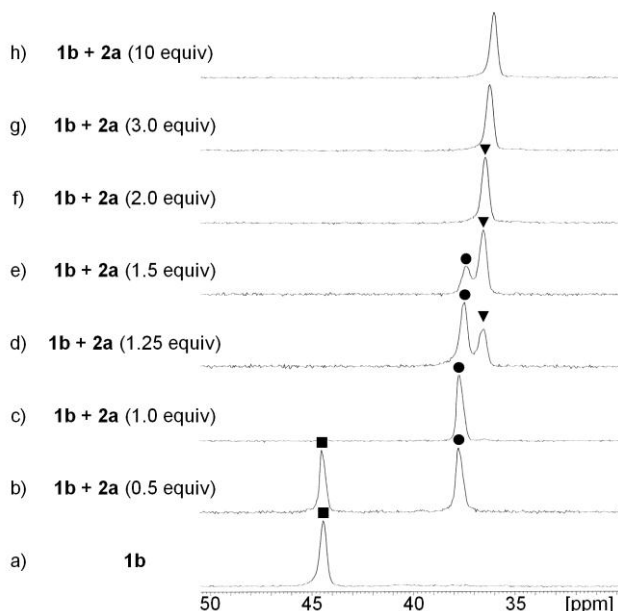
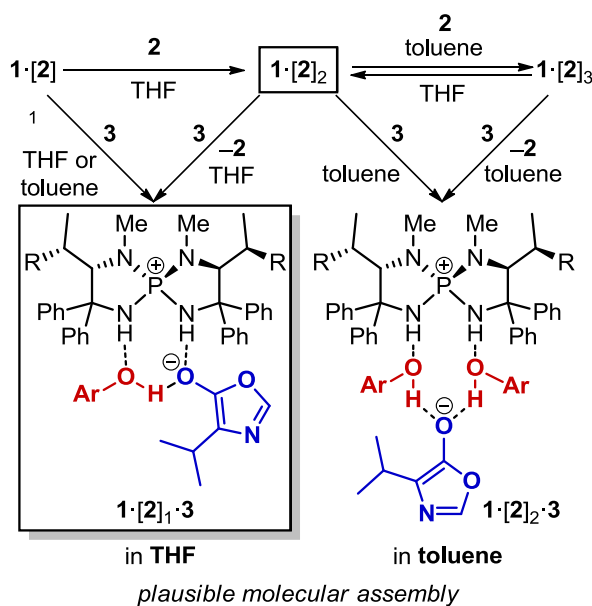


Figure 1. ^{31}P NMR charts of aminophosphonium aryloxides **1b**·**[2a]**_n in THF at $-98\text{ }^\circ\text{C}$. ■: **1b**; ●: **1b**·**[2a]**₁; ▼: **1b**·**[2a]**₂.

As a result, the preferable mode of ion-pair-assisted molecular assembly appeared to be **1**·**[2]**₂ in THF,¹² and it most likely acted as the actual catalyst for the present stereoselective conjugate addition under optimized conditions. Thus, upon the addition of **3** to a solution of **1**·**[2]**₃ in THF, **1**·**[2]**₁·**3** could be formed preferentially as a reactive intermediate rather than **1**·**[2]**₂·**3** even in the presence of **2** in a sufficient amount for efficient product derivatization (Scheme 3).

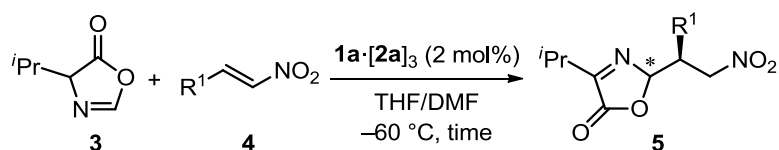


Scheme 3. Plausible molecular assembly from **1**, **2**, and **3** in THF and toluene.

2.3. Substrate Scope and Derivatization of **5a** to Amino Carbonyl Compounds and Amino Alcohol.

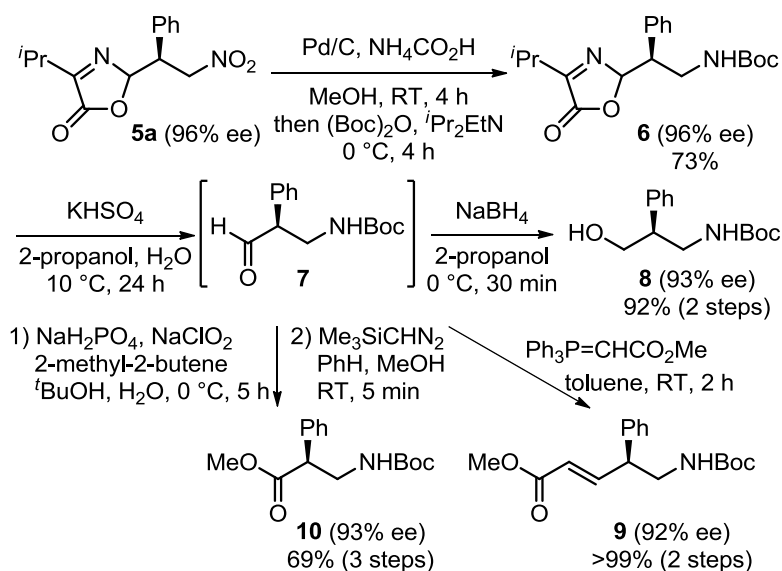
In the case of a reaction in toluene, however, the generation of molecular assembly $1 \cdot [2]_2 \cdot 3$ would be more favorable than $1 \cdot [2]_1 \cdot 3$, and the resultant $1 \cdot [2]_2 \cdot 3$ would cause lower selectivity. It is noteworthy that this hypothesis agrees well with the enantioselectivity improvements attained in the reactions with $1\mathbf{a} \cdot [2\mathbf{a}]_2$ and $1\mathbf{a} \cdot [2\mathbf{a}]_1$ (Table 1, entries 4 and 5), and the origin of the beneficial solvent effect would be the prevention of the formation of less selective $1 \cdot [2]_2 \cdot 3$.

With this information in hand, the author conducted further experiments to determine the scope of the nitroolefin component in this asymmetric conjugate addition protocol. As listed in Table 2, a wide variety of aromatic β -substituents with different electronic and steric properties were tolerated and excellent levels of stereocontrol were uniformly realized (entries 1-5). Moreover, the present system is compatible with fused- and heteroaromatic functional groups, as exemplified by the reaction with *N*-protected indole derivative **4i** (entries 6-8). Further, aliphatic nitroolefins appeared to be good candidates, although a notable decrease in diastereoselectivity seemed inevitable (entry 9).

Table 2 Substrate scope.^a

| entry | R ¹ | 4 | time [h] | yield ^b [%] | dr ^c | ee ^d [%] | 5 |
|----------------|---|-----------|----------|------------------------|-----------------|---------------------|-----------|
| 1 | <i>p</i> -MeO-C ₆ H ₄ | 4b | 24 | 93 | >20:1 | 96 | 5b |
| 2 | <i>p</i> -Br-C ₆ H ₄ | 4c | 18 | 91 | >20:1 | 98 | 5c |
| 3 | <i>m</i> -Br-C ₆ H ₄ | 4d | 20 | 99 | >20:1 | 97 | 5d |
| 4 | <i>p</i> -Me-C ₆ H ₄ | 4e | 10 | 89 | >20:1 | 97 | 5e |
| 5 | <i>o</i> -Me-C ₆ H ₄ | 4f | 12 | 90 | >20:1 | 96 | 5f |
| 6 | 2-naphthyl | 4g | 12 | 99 | >20:1 | 96 | 5g |
| 7 | 2-furyl | 4h | 12 | 92 | >20:1 | 91 | 5h |
| 8 ^e | <i>N</i> -Me-3-indolyl | 4i | 36 | 86 | >20:1 | 98 | 5i |
| 9 | cyclohexyl | 4j | 24 | 82 | 4:1 | 94 | 5j |

^a Unless otherwise noted, reactions were performed on 0.1 mmol scale with 1.1 equiv of **3** in THF/5% DMF (0.2 mL). ^b Isolated yield. ^c Diastereomeric ratio was determined by 400 MHz ¹H NMR analysis of crude aliquot. ^d Enantiomeric excess was analyzed by chiral HPLC. Absolute configurations were assigned by analogy to **5a**. ^e 0.5 mL of THF/5% DMF was used because of low solubility of **4i**.

**Scheme 4.** Derivatization of **5a** to amino carbonyl compounds and amino alcohol.

The product **5** was readily converted into β -amino aldehyde such as **7**, which could serve as a versatile precursor of synthetically useful chiral building blocks owing to the reactivity of aldehyde carbonyl. For example, after hydrogenation of the nitro moiety of **5a** with palladium on charcoal and ammonium formate followed by Boc-protection of the resulting primary amino group, *2H*-oxazolone protection was removed under mildly acidic conditions, giving **7** in an almost pure form. Simple reduction of **7** furnished 1,3-amino alcohol **8** and quantitative derivatization into the corresponding 4-amino α,β -unsaturated ester **9** was also feasible by Wittig reaction, although slight decrease in enantiomeric excess was observed in both cases. Furthermore, Pinnick oxidation of **7** and subsequent treatment with trimethylsilyldiazomethane afforded protected β^2 -homophenylglycine **10**,¹³ which belongs to one of the most challenging classes of β^2 -amino acids to be synthesized in a catalytic enantioselective manner (Scheme 4).¹⁴

3. Conclusion.

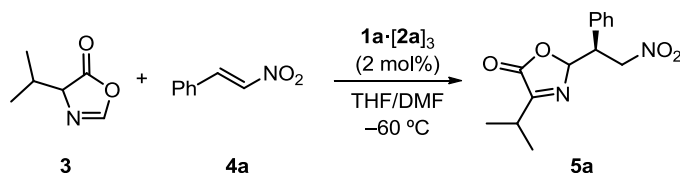
In conclusion, the author have successfully achieved the highly enantioselective conjugate addition of 2-unsubstituted azlactone to a range of nitroolefins for the first time by selectively utilizing a requisite mode of assembly of chiral tetraaminophosphonium aryloxide-arylhydroxide as a catalyst, thus providing a reliable tool for stereoselective construction of various amino carbonyl architectures including β^2 -amino acid derivatives. The key findings in this achievement are the polarity dependence of the molecular associations between chiral triaminoiminophosphorane and arylhydroxides in organic solvent as well as the crucial role of the proximal arylhydroxide as an effective proton donor. The author believes that the present study represents an important stride toward new direction of the development and applications of asymmetric supramolecular catalysis.

4. Experimental Section.

General Information: Infrared spectra were recorded on a JASCO FT/IR-300E and Shimadzu IRAffinity-1 spectrometer. ^1H NMR spectra were recorded on a JEOL JNM-ECS400 (400 MHz). Chemical shifts are reported in ppm from the tetramethylsilane (0.0 ppm) resonance as the internal standard. Data are reported as follows: chemical shift, integration, multiplicity (s = singlet, d = doublet, t = triplet, q = quartet, sept = septet, m = multiplet, br = broad), and coupling constants (Hz). ^{13}C NMR spectra were recorded on a JEOL JNM-ECS400 (101 MHz) spectrometer with complete proton decoupling. Chemical shifts are reported in ppm from the solvent resonance as the internal standard (CDCl_3 ; 77.16 ppm). ^{31}P NMR spectra were recorded on a JEOL JNM-ECS400 (162 MHz) spectrometer with complete proton decoupling. Chemical shifts are reported in ppm from H_3PO_4 (0.0 ppm) resonance as the external standard. Optical rotations were measured on a JASCO DIP-1000 and HORIBA SEPA-500 polarimeter. The high resolution mass spectra were conducted on JEOL JMS-700 (MStation) and Thermo Fisher Scientific Exactive. Analytical thin layer chromatography (TLC) was performed on Merck precoated TLC plates (silica gel 60 GF₂₅₄, 0.25 mm). Flash column chromatography was performed on silica gel 60 (spherical, 40-50 μm ; Kanto Chemical Co., Inc.) and PSQ60AB (spherical, av. 55 μm ; Fuji Silysia Chemical Ltd.). Enantiomeric excesses were determined by HPLC analysis using chiral columns (ϕ 4.6 mm x 250 mm, DAICEL CHIRALPAK AD-H (ADH), CHIRALCEL OD-H (ODH), CHIRALPAK AS-H (ASH), CHIRALPAK IA (IA), or CHIRALPAK IC (IC)) with hexane (H), 2-propanol (IPA), and ethanol (EtOH) as eluent.

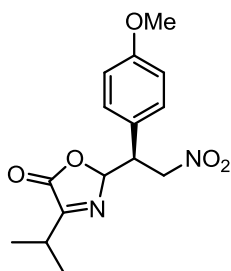
Toluene, tetrahydrofuran (THF), and dichloromethane (CH_2Cl_2) were supplied from Kanto Chemical Co., Inc. as “Dehydrated solvent system”. Tetraaminophosphonium salts **1**,^{3a,10,15} azlactone **3**,¹⁶ and nitroolefins **4**¹⁷ were prepared by following the literature procedure. Other simple chemicals were purchased and used as such.

Experimental Section:

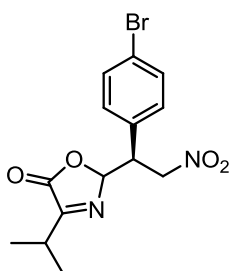


Representative Procedure for Asymmetric Conjugate Addition of Azlactone 3 to Nitroolefin 4 Catalyzed by Chiral Tetraaminophosphonium Aryloxide 1a·[2a]₃: Nitroolefin **4a** (14.9 mg, 0.10 mmol) and **1a·[2a]₃** (2.16 mg, 2.0 μmol) were placed in a dried test tube and dissolved into THF (0.19

mL) and *N,N*-dimethylformamide (DMF) (0.10 mL) under Ar atmosphere. Azlactone **3** (14.0 mg, 0.11 mmol) was introduced dropwise to the solution at $-60\text{ }^{\circ}\text{C}$ and the reaction mixture was stirred for 12 h under the conditions. A solution of trifluoroacetic acid in toluene (0.50 M, 20.0 μL) was added to the reaction mixture and whole mixture was poured into an ice-cooled 1 *N* hydrochloric acid. The aqueous phase was extracted with ethyl acetate (EA) twice and the organic phases were washed with brine. The combined organic extracts were dried over Na_2SO_4 and filtered. All volatiles were removed by evaporation and the diastereomeric ratio of **5a** thus obtained was determined to be $>20:1$ by ^1H NMR (400 MHz) analysis of the crude residue. Purification of the residue by column chromatography on silica gel (H/EA = 5:1 as eluent) afforded a diastereomeric mixture of **5a** in 90% yield (24.9 mg, 0.09 mmol) and the enantiomeric excess of the major diastereomer was determined to be 96% by chiral stationary phase HPLC analysis. **5a**: HPLC ODH, H/EtOH = 4:1, flow rate = 0.5 mL/min, $\lambda = 210\text{ nm}$, 20.3 min (minor isomer of major diastereomer), 22.0 min (minor diastereomer), 26.7 min (major isomer of major diastereomer), 32.6 min (minor diastereomer); ^1H NMR (400 MHz, CDCl_3) major diastereomer δ 7.33-7.29 (3H, m), 7.14-7.08 (2H, m), 6.15 (1H, dd, $J = 4.1, 2.0\text{ Hz}$), 5.03 (1H, dd, $J = 13.7, 7.6\text{ Hz}$), 4.87 (1H, dd, $J = 13.7, 7.6\text{ Hz}$), 4.25 (1H, td, $J = 7.6, 4.1\text{ Hz}$), 2.81 (1H, sept-d, $J = 7.1, 2.0\text{ Hz}$), 1.19 (3H, d, $J = 7.1\text{ Hz}$), 1.07 (3H, d, $J = 7.1\text{ Hz}$); ^{13}C NMR (101 MHz, CDCl_3) major diastereomer δ 170.3, 164.1, 131.3, 129.4, 129.0, 128.8, 97.6, 74.8, 46.6, 28.3, 18.9, 18.8; IR (liq. film): 2974, 1784, 1557, 1456, 1379, 1337, 1124, 1049, 997, 757 cm^{-1} ; HRMS (FAB) Calcd for $\text{C}_{14}\text{H}_{17}\text{N}_2\text{O}_4$ ($[\text{M}+\text{H}]^+$) 277.1189. Found 277.1192.

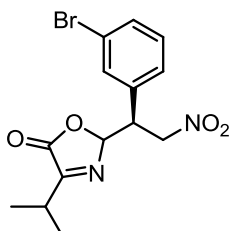


5b: HPLC ODH, H/IPA = 3:1, flow rate = 1.0 mL/min, $\lambda = 210\text{ nm}$, 17.7 min (minor diastereomer), 21.3 min (minor isomer of major diastereomer), 25.0 min (major isomer of major diastereomer), 37.3 min (minor diastereomer); ^1H NMR (400 MHz, CDCl_3) major diastereomer δ 7.02 (2H, d, $J = 8.7\text{ Hz}$), 6.82 (2H, d, $J = 8.7\text{ Hz}$), 6.12 (1H, dd, $J = 4.1, 1.4\text{ Hz}$), 4.99 (1H, dd, $J = 13.8, 7.6\text{ Hz}$), 4.82 (1H, dd, $J = 13.8, 7.6\text{ Hz}$), 4.20 (1H, td, $J = 7.6, 4.1\text{ Hz}$), 3.77 (3H, s), 2.82 (1H, sept-d, $J = 6.9, 1.4\text{ Hz}$), 1.20 (3H, d, $J = 6.9\text{ Hz}$), 1.10 (3H, d, $J = 6.9\text{ Hz}$); ^{13}C NMR (101 MHz, CDCl_3) major diastereomer δ 170.2, 164.1, 159.9, 130.6, 123.0, 114.1, 97.7, 75.0, 55.4, 46.0, 28.2, 18.9₃, 18.8₅; IR (liq. film): 2973, 1783, 1556, 1515, 1464, 1378, 1255, 1182, 1049, 1032, 992 cm^{-1} ; HRMS (FAB) Calcd for $\text{C}_{15}\text{H}_{19}\text{N}_2\text{O}_5$ ($[\text{M}+\text{H}]^+$) 307.1294. Found 307.1291.

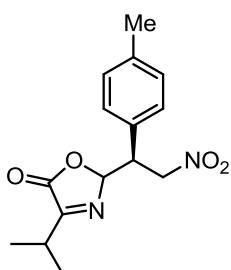


5c: HPLC IC, H/EtOH = 10:1, flow rate = 0.5 mL/min, $\lambda = 210\text{ nm}$, 20.8 min (minor diastereomer), 24.6 min (minor isomer of major diastereomer), 26.0 min (major isomer of major diastereomer), 33.1 min (minor diastereomer); ^1H NMR (400 MHz, CDCl_3) major diastereomer δ 7.45 (2H, d, $J = 8.2\text{ Hz}$), 7.01 (2H, d, $J = 8.2\text{ Hz}$), 6.11 (1H, dd, $J = 4.1, 1.8\text{ Hz}$), 4.98 (1H, dd, $J = 13.7, 7.5\text{ Hz}$), 4.83 (1H, dd, $J = 13.7, 7.5\text{ Hz}$), 4.21 (1H, td, $J = 7.5, 4.1\text{ Hz}$), 2.84 (1H, sept-d, $J = 6.9,$

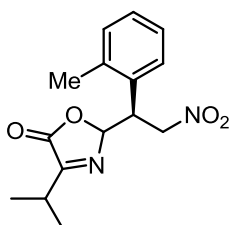
1.8 Hz), 1.20 (3H, d, $J = 6.9$ Hz), 1.11 (3H, d, $J = 6.9$ Hz); ^{13}C NMR (101 MHz, CDCl_3) major diastereomer δ 170.6, 163.9, 132.0, 131.0, 130.5, 123.2, 97.3, 74.5, 46.1, 28.3, 18.9₂, 18.9₀; IR (liq. film): 2973, 1784, 1638, 1557, 1491, 1377, 1123, 1070, 1049, 1011 cm^{-1} ; HRMS (FAB) Calcd for $\text{C}_{14}\text{H}_{16}\text{BrN}_2\text{O}_4$ ($[\text{M}+\text{H}]^+$) 355.0294. Found 355.0310.



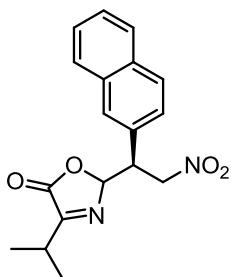
5d: HPLC IA, H/EtOH = 10:1, flow rate = 1.0 mL/min, $\lambda = 210$ nm, 17.0 min (minor diastereomer), 18.8 min (minor isomer of major diastereomer), 20.1 min (major isomer of major diastereomer), 25.8 min (minor diastereomer); ^1H NMR (400 MHz, CDCl_3) major diastereomer δ 7.45 (1H, d, $J = 8.2$ Hz), 7.22 (1H, s), 7.20 (1H, t, $J = 8.2$ Hz), 7.10 (1H, d, $J = 8.2$ Hz), 6.13 (1H, dd, $J = 4.1, 2.1$ Hz), 5.00 (1H, dd, $J = 14.2, 7.6$ Hz), 4.83 (1H, dd, $J = 14.2, 7.6$ Hz), 4.23 (1H, td, $J = 7.6, 4.1$ Hz), 2.86 (1H, sept-d, $J = 6.9, 2.1$ Hz), 1.22 (3H, d, $J = 6.9$ Hz), 1.12 (3H, d, $J = 6.9$ Hz); ^{13}C NMR (101 MHz, CDCl_3) major diastereomer δ 170.7, 163.9, 133.6, 132.2, 132.1, 130.4, 128.6, 122.7, 97.2, 74.5, 46.2, 28.3, 19.0, one carbon was not found probably due to overlapping; IR (liq. film): 2973, 1785, 1639, 1558, 1476, 1431, 1377, 1049, 997 cm^{-1} ; HRMS (FAB) Calcd for $\text{C}_{14}\text{H}_{16}\text{BrN}_2\text{O}_4$ ($[\text{M}+\text{H}]^+$) 355.0293. Found 355.0307.



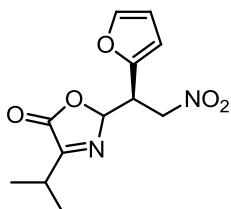
5e: HPLC IC, H/IPA/EtOH = 18:1:1, flow rate = 0.5 mL/min, $\lambda = 210$ nm, 20.8 min (minor diastereomer), 25.2 min (minor isomer of major diastereomer), 27.0 min (major isomer of major diastereomer), 40.8 min (minor diastereomer); ^1H NMR (400 MHz, CDCl_3) major diastereomer δ 7.11 (2H, d, $J = 8.2$ Hz), 6.99 (2H, d, $J = 8.2$ Hz), 6.13 (1H, dd, $J = 4.1, 1.8$ Hz), 4.99 (1H, dd, $J = 14.0, 7.5$ Hz), 4.83 (1H, dd, $J = 14.0, 7.5$ Hz), 4.20 (1H, td, $J = 7.5, 4.1$ Hz), 2.82 (1H, sept-d, $J = 6.8, 1.8$ Hz), 2.30 (3H, s), 1.19 (3H, d, $J = 6.8$ Hz), 1.09 (3H, d, $J = 6.8$ Hz); ^{13}C NMR (101 MHz, CDCl_3) major diastereomer δ 170.2, 164.1, 138.8, 129.4, 129.3, 128.3, 97.8, 75.0, 46.3, 28.2, 21.2, 18.9, 18.8; IR (liq. film): 2972, 1783, 1645, 1556, 1516, 1377, 1122, 1049, 991 cm^{-1} ; HRMS (FAB) Calcd for $\text{C}_{15}\text{H}_{19}\text{N}_2\text{O}_4$ ($[\text{M}+\text{H}]^+$) 291.1345. Found 291.1345.



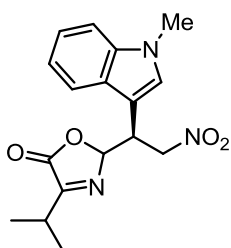
5f: HPLC IA, H/EtOH = 10:1, flow rate = 0.5 mL/min, $\lambda = 210$ nm, 17.8 min (major isomer of major diastereomer), 19.4 min (minor diastereomer), 21.3 min (minor isomer of major diastereomer), 22.5 min (minor diastereomer); ^1H NMR (400 MHz, CDCl_3) major diastereomer δ 7.21-7.16 (2H, m), 7.16-7.09 (1H, m), 6.93 (1H, d, $J = 7.3$ Hz), 6.13 (1H, dd, $J = 4.8, 1.8$ Hz), 5.02 (1H, dd, $J = 14.2, 7.3$ Hz), 4.83 (1H, dd, $J = 14.2, 7.3$ Hz), 4.56 (1H, td, $J = 7.3, 4.8$ Hz), 2.85 (1H, sept-d, $J = 6.8, 1.8$ Hz), 2.42 (3H, s), 1.22 (3H, d, $J = 7.1$ Hz), 1.14 (3H, d, $J = 7.1$ Hz); ^{13}C NMR (101 MHz, CDCl_3) major diastereomer δ 170.2, 164.0, 138.3, 131.4, 130.1, 128.7, 127.8, 125.9, 98.2, 75.3, 41.8, 28.3, 20.0, 19.0, 18.9; IR (liq. film): 2974, 1784, 1644, 1556, 1465, 1377, 1067, 1048, 991, 967 cm^{-1} ; HRMS (FAB) Calcd for $\text{C}_{15}\text{H}_{19}\text{N}_2\text{O}_4$ ($[\text{M}+\text{H}]^+$) 291.1345. Found 291.1359.



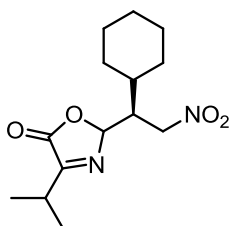
5g: HPLC IA, H/EtOH = 5.5:1, flow rate = 1.0 mL/min, λ = 254 nm, 13.9 min (minor isomer of major diastereomer), 16.2 min (minor diastereomer), 25.6 min (minor diastereomer), 32.6 min (major isomer of major diastereomer); ^1H NMR (400 MHz, CDCl_3) major diastereomer δ 7.82-7.76 (3H, m), 7.58 (1H, d, J = 1.4 Hz), 7.53-7.47 (2H, m), 7.23 (1H, dd, J = 8.7, 1.8 Hz), 6.23 (1H, dd, J = 4.3, 1.8 Hz), 5.10 (1H, dd, J = 13.7, 7.6 Hz), 4.96 (1H, dd, J = 13.7, 7.6 Hz), 4.42 (1H, td, J = 7.6, 4.3 Hz), 2.78 (1H, sept-d, J = 7.1, 1.8 Hz), 1.18 (3H, d, J = 7.1 Hz), 1.02 (3H, d, J = 7.1 Hz); ^{13}C NMR (101 MHz, CDCl_3) major diastereomer δ 170.3, 164.0, 133.2, 132.9, 128.9₄, 128.8₆, 128.6, 128.0, 127.8, 126.9, 126.8, 126.7, 97.9, 74.9, 46.8, 28.2, 18.9, 18.8; IR (liq. film): 2973, 1783, 1642, 1556, 1434, 1377, 1050, 989, 817, 748 cm^{-1} ; HRMS (FAB) Calcd for $\text{C}_{18}\text{H}_{19}\text{N}_2\text{O}_4$ ($[\text{M}+\text{H}]^+$) 327.1345. Found 327.1341.



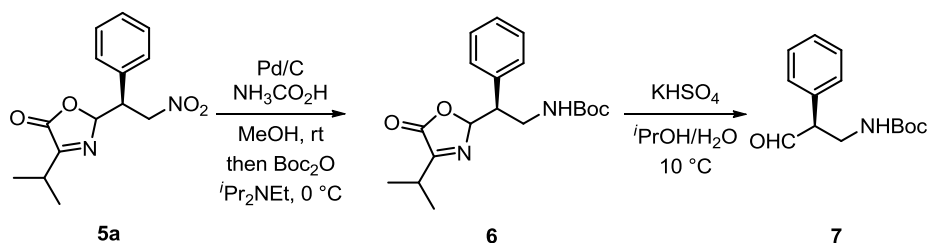
5h: HPLC IA, H/IPA = 10:1, flow rate = 1.0 mL/min, λ = 210 nm, 14.5 min (minor isomer of major diastereomer), 17.3 min (minor diastereomer), 18.8 min (minor diastereomer), 31.8 min (major isomer of major diastereomer); ^1H NMR (400 MHz, CDCl_3) major diastereomer δ 7.34 (1H, d, J = 1.6 Hz), 6.32 (1H, dd, J = 3.4, 1.6 Hz), 6.23 (1H, d, J = 3.4 Hz), 6.14 (1H, dd, J = 4.6, 1.6 Hz), 4.95 (1H, dd, J = 14.2, 7.6 Hz), 4.90 (1H, dd, J = 14.2, 7.6 Hz), 4.37 (1H, td, J = 7.6, 4.6 Hz), 2.88 (1H, sept-d, J = 7.3, 1.6 Hz), 1.22 (3H, d, J = 7.3 Hz), 1.12 (3H, d, J = 7.3 Hz); ^{13}C NMR (101 MHz, CDCl_3) major diastereomer δ 170.1, 164.1, 145.5, 143.3, 110.8, 110.6, 96.7, 73.0, 41.1, 28.3, 18.9, 18.8; IR (liq. film): 2974, 1784, 1643, 1558, 1376, 1148, 1051, 994, 916, 742 cm^{-1} ; HRMS (FAB) Calcd for $\text{C}_{12}\text{H}_{15}\text{N}_2\text{O}_5$ ($[\text{M}+\text{H}]^+$) 267.0981. Found 267.0975.



5i: HPLC ADH, H/IPA = 10:1, flow rate = 1.0 mL/min, λ = 210 nm, 16.9 min (minor isomer of major diastereomer), 18.7 min (minor diastereomer), 20.1 min (minor diastereomer), 21.9 min (major isomer of major diastereomer); ^1H NMR (400 MHz, CDCl_3) major diastereomer δ 7.58 (1H, d, J = 8.0 Hz), 7.28 (1H, d, J = 8.0 Hz), 7.24 (1H, t, J = 8.0 Hz), 7.15 (1H, t, J = 8.0 Hz), 6.94 (1H, s), 6.24 (1H, dd, J = 3.9, 1.8 Hz), 5.02 (1H, dd, J = 13.7, 8.2 Hz), 4.81 (1H, dd, J = 13.7, 6.4 Hz), 4.59 (1H, ddd, J = 8.2, 6.4, 3.9 Hz), 2.79 (1H, sept-d, J = 7.1, 1.8 Hz), 1.16 (3H, d, J = 7.1 Hz), 0.96 (3H, d, J = 7.1 Hz); ^{13}C NMR (101 MHz, CDCl_3) major diastereomer δ 169.8, 164.4, 137.0, 128.8, 126.9, 122.5, 120.1, 119.6, 109.8, 104.9, 98.5, 75.0, 39.4, 33.1, 28.3, 18.7, 18.5; IR (liq. film): 2972, 1781, 1642, 1555, 1473, 1428, 1377, 1335, 1055, 996, 741 cm^{-1} ; HRMS (FAB) Calcd for $\text{C}_{17}\text{H}_{20}\text{N}_3\text{O}_4$ ($[\text{M}+\text{H}]^+$) 330.1453. Found 330.1469.



5j: HPLC ASH, H/EtOH = 19:1, flow rate = 0.5 mL/min, λ = 210 nm, 17.0 min (minor diastereomer), 17.8 min (major isomer of major diastereomer), 19.0 min (minor isomer of major diastereomer), 19.9 min (minor diastereomer); ^1H NMR (400 MHz, CDCl_3) major diastereomer δ 6.01 (1H, dd, J = 4.4, 2.0 Hz), 4.33 (1H, dd, J = 13.5, 4.4 Hz), 4.20 (1H, dd, J = 13.5, 8.5 Hz), 2.97 (1H, sept-d, J = 6.7, 2.0 Hz), 2.86 (1H, dq, J = 8.5, 4.4 Hz), 1.87-1.58 (6H, m), 1.34-1.02 (5H, m), 1.28 (6H, d, J = 6.7 Hz); ^{13}C NMR (101 MHz, CDCl_3) major diastereomer δ 169.4, 164.8, 98.5, 72.2, 45.8, 37.7, 30.6, 30.4, 28.5, 26.4, 26.3, 26.1, 19.0, 18.8; IR (KBr): 2930, 2852, 1782, 1651, 1555, 1447, 1385, 1062, 960, 909 cm^{-1} ; HRMS (FAB) Calcd for $\text{C}_{14}\text{H}_{23}\text{N}_2\text{O}_4$ ($[\text{M}+\text{H}]^+$) 283.1658. Found 283.1663.

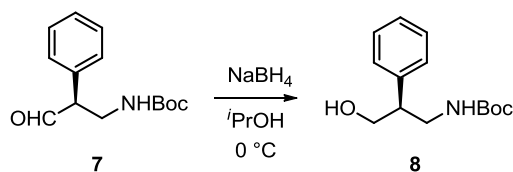


Derivatization of 5a to *N*-Boc-3-Amino-2-phenylpropanal 7:

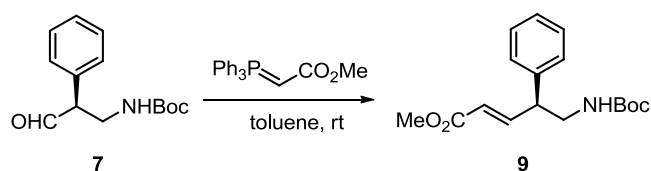
Reduction of Nitro Group of 5a and Boc-Protection of Amino Moiety: To a solution of **5a** (138.1 mg, 0.50 mmol) in MeOH (10 mL) were added ammonium formate (157.6 mg, 2.50 mmol) and 10% Pd/C (100 mg) under Ar atmosphere. The reaction mixture was stirred for 4 h at room temperature and the solution was then filtered through a plug of Celite by the aid of MeOH (10 mL). $i\text{Pr}_2\text{NEt}$ (0.17 mL, 1.0 mmol) and Boc_2O (0.69 mL, 3.0 mmol) were added to the filtrate at 0 °C and the mixture was stirred for 4 h under Ar atmosphere. After addition of water, the mixture was extracted with EA twice and the organic phases were washed with brine. The combined organic extracts were dried over Na_2SO_4 and filtered. After concentration, the residue was purified by column chromatography on silica gel (H/EA = 5:1 as eluent) to furnish **6** as a mixture of diastereomers in 73% yield. **6**: ^1H NMR (400 MHz, CDCl_3) major diastereomer δ 7.31-7.22 (3H, m), 7.10 (2H, d, $J = 7.3$ Hz), 6.12 (1H, dd, $J = 3.2, 1.8$ Hz), 4.66 (1H, br), 3.92-3.80 (1H, m), 3.66-3.52 (2H, m), 2.79 (1H, sept, $J = 6.9$ Hz), 1.42 (9H, s), 1.17 (3H, d, $J = 6.9$ Hz), 1.04 (3H, d, $J = 6.9$ Hz); ^{13}C NMR (101 MHz, CDCl_3) major diastereomer δ 160.3, 164.6, 155.9, 133.9, 129.8, 128.4, 128.1, 99.3, 79.9, 49.1, 40.9, 28.5, 28.1, 18.9, one carbon was not found probably due to overlapping; IR (liq. film): 3354, 2974, 1778, 1699, 1516, 1366, 1252, 1167, 1049, 978, 702 cm^{-1} ; HRMS (ESI) Calcd for $\text{C}_{19}\text{H}_{26}\text{N}_2\text{O}_4\text{Na}$ ($[\text{M}+\text{Na}]^+$) 369.1785. Found 369.1782.

Cleavage of Oxazolone Ring of 6 to Give 7: A solution of **6** (17.3 mg, 0.05 mmol) in IPA (2.5 mL) was treated with a solution of KHSO_4 (34.0 mg, 0.25 mmol) in water (2.5 mL) at 10 °C until complete conversion was indicated by TLC analysis. The reaction mixture was diluted with water and then extracted with diethyl ether twice. The organic layers were washed with a saturated aqueous solution of NaHCO_3 . The combined organic extracts were dried over Na_2SO_4 , filtered, and concentrated under reduced pressure. Almost pure aldehyde **7** thus obtained was used for next steps without further purification. The NMR data of **7** agreed with literature data.¹⁸ **7**: ^1H NMR (400 MHz, CDCl_3) δ 9.74 (1H, s), 7.40 (2H, t, $J = 7.3$ Hz), 7.34 (1H, t, $J = 7.3$ Hz), 7.19 (2H, d, $J = 7.3$ Hz), 4.88 (1H, br), 3.90 (1H, dd, $J = 7.3, 6.0$ Hz), 3.66 (1H, ddd, $J = 14.4, 8.4, 6.0$ Hz), 3.49 (1H, ddd, $J = 14.4, 8.4, 7.3$ Hz), 1.42 (9H, s).

Various Derivatizations of *N*-Boc-3-Amino-2-phenylpropanal **7**:

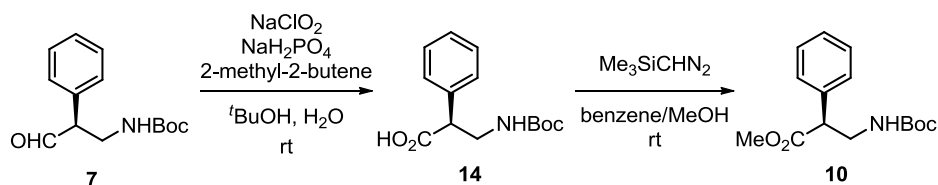


Reduction of 7: The crude aldehyde **7** (ca. 0.05 mmol) was dissolved in IPA (5.0 mL) and the solution was cooled to 0 °C. NaBH₄ (2.84 mg, 0.075 mmol) was added portionwise and the reaction mixture was stirred for 30 min. The resulting solution was diluted with brine and the aqueous phase was extracted with diethyl ether twice. The combined organic extracts were dried over Na₂SO₄, filtered, and concentrated. Purification of the residue by column chromatography on silica gel (H/EA = 3:1 as eluent) afforded **8** in 92% yield (2 steps). The conservation of enantiomeric purity of **8** was determined by chiral stationary phase HPLC analysis (93% ee). The absolute configuration of **8** was determined to be *S* by comparison of its optical rotation with literature value.¹⁹ **8**^{4,5}: HPLC IC, H/EtOH = 10:1, flow rate = 0.5 mL/min, λ = 210 nm, 17.3 min (*R*), 19.2 min (*S*); ¹H NMR (400 MHz, CDCl₃) δ 7.32 (2H, t, *J* = 7.3 Hz), 7.24 (1H, t, *J* = 7.3 Hz), 7.22 (2H, d, *J* = 7.3 Hz), 4.68 (1H, br), 3.79 (2H, brt, *J* = 6.4 Hz), 3.49 (1H, dd, *J* = 15.6, 8.0 Hz), 3.44 (1H, dd, *J* = 15.6, 7.2 Hz), 3.08 (1H, brt, *J* = 6.4 Hz), 2.91 (1H, ddt, *J* = 8.0, 7.2, 6.4 Hz), 1.44 (9H, s); [α]_D²⁰ +12.6 (*c* = 0.5, CH₂Cl₂) [lit.¹⁹ [α]_D²⁰ +17 (*c* = 1.0, CH₂Cl₂) for *S* isomer, 98% ee].



Wittig Reaction of 7: A solution of the crude aldehyde **7** (ca. 0.05 mmol) and methyl 2-(triphenylphosphoranylidene)acetate (25.1 mg, 0.075 mmol) in toluene (2.0 mL) was stirred for 2 h at room temperature under Ar atmosphere. All volatiles were removed by evaporation and the *E/Z* ratio of **9** thus obtained was determined to be >20:1 by ¹H NMR (400 MHz) analysis of the crude residue. The residue was purified by silica gel column chromatography (H/EA = 5:1 as eluent) to afford **9** in quantitative yield (2 steps). The conservation of enantiomeric purity of **9** was determined by chiral stationary phase HPLC analysis (92% ee). **9**: HPLC ASH, H/IPA = 10:1, flow rate = 1.0 mL/min, λ = 210 nm, 8.3 min (*S*), 10.0 min (*R*); ¹H NMR (400 MHz, CDCl₃) δ 7.34 (2H, t, *J* = 7.8 Hz), 7.27 (1H, t, *J* = 7.8 Hz), 7.20 (1H, d, *J* = 7.8 Hz), 7.09 (1H, dd, *J* = 16.0, 7.8 Hz), 5.86 (1H, d, *J* = 16.0 Hz), 4.53 (1H, br), 3.72 (3H, s), 3.69 (1H, ddd, *J* = 7.8, 7.3, 6.9 Hz), 3.54 (1H, ddd, *J* = 13.3, 7.3, 6.9 Hz), 3.42 (3H, dt, *J* =

13.3, 6.9 Hz), 1.48 (9H, s); ^{13}C NMR (101 MHz, CDCl_3) δ 166.8, 155.9, 148.6, 139.5, 129.1, 128.1, 127.6, 122.4, 79.7, 51.8, 48.6, 44.8, 28.5; IR (liq. film): 3366, 2976, 1713, 1516, 1454, 1366, 1269, 1250, 1169, 980, 700 cm^{-1} ; HRMS (ESI) Calcd for $\text{C}_{17}\text{H}_{23}\text{NO}_4\text{Na}$ ($[\text{M}+\text{Na}]^+$) 328.1519. Found 328.1519; $[\alpha]_{\text{D}}^{20} +2.8$ ($c = 0.60$, CHCl_3).

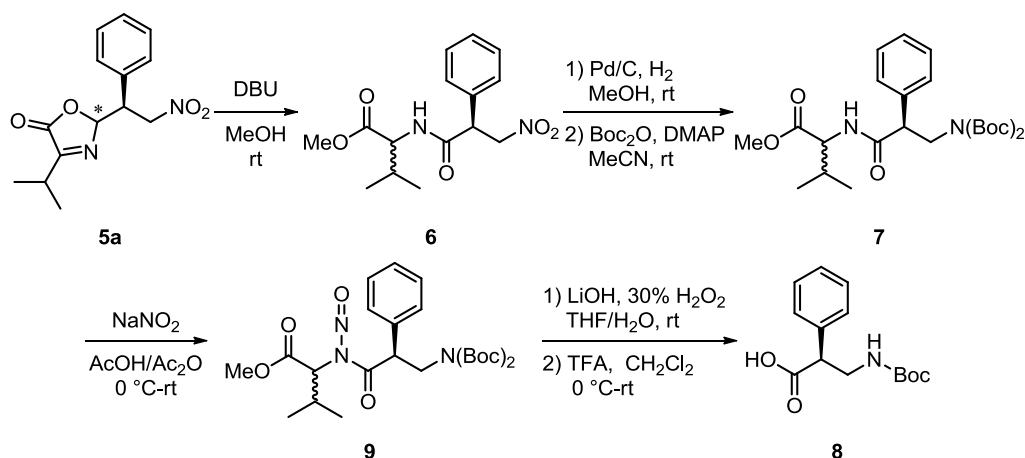


Pinnick Oxidation of 7 and Following Esterification of 14²⁰: The crude aldehyde **7** was dissolved in *tert*-butyl alcohol (1.3 mL) and 2-methyl-2-butene (0.3 mL). A solution of sodium chlorite (25.0 mg, 0.28 mmol) and sodium dihydrogenphosphate (25.0 mg, 0.21 mmol) in water (0.5 mL) was added to the reaction mixture dropwise at 0 °C. The resulting solution was stirred for 5 h at 0 °C and diluted with water. After washing with diethyl ether, the aqueous layer was acidified with a 2.0 M aqueous solution of KHSO_4 and extracted with EA twice. The combined organic extracts were dried over Na_2SO_4 , filtered, and concentrated. The residual crude mixture was dissolved in benzene (0.70 mL) and MeOH (0.30 mL). A 2.0 M solution of $\text{Me}_3\text{SiCHN}_2$ in diethyl ether (37.5 μL , 0.075 mmol) was added to the solution dropwise at room temperature and the reaction mixture was stirred for 5 min. After removing volatiles, purification of the residue by column chromatography (H/EA = 10:1 as eluent) gave **10** in 69% yield (3 steps). The conservation of enantiomeric purity of **10** was determined by chiral stationary phase HPLC analysis (93% ee). See following section (page S7) for determination of absolute configuration of **14**. **10**: HPLC ADH, H/IPA = 19:1, flow rate = 1.0 mL/min, $\lambda = 210$ nm, 8.9 min (*R*), 9.9 min (*S*); ^1H NMR (400 MHz, CDCl_3) δ 7.37-7.24 (5H, m), 4.87 (1H, br), 3.89 (1H, dd, $J = 6.9, 5.7$ Hz), 3.96 (3H, s), 3.60 (1H, ddd, $J = 13.7, 8.5, 5.7$ Hz), 3.51 (1H, dt, $J = 13.7, 6.9$ Hz), 1.43 (9H, s); ^{13}C NMR (101 MHz, CDCl_3) δ 173.5, 155.9, 136.5, 129.0, 128.1, 127.8, 79.6, 52.3, 51.8, 43.6, 28.5; IR (liq. film): 3384, 2977, 1713, 1505, 1366, 1279, 1251, 1169, 951, 739 cm^{-1} ; HRMS (FAB) Calcd for $\text{C}_{15}\text{H}_{22}\text{NO}_4$ ($[\text{M}+\text{H}]^+$) 280.1549. Found 280.1553; $[\alpha]_{\text{D}}^{19} -60.2$ ($c = 0.55$, CHCl_3).

Low Temperature ^{31}P NMR Study:

Representative Procedure for the Preparation of a NMR Sample: To a 0.025 M solution of **1b** in THF (0.20 mL) in a ϕ 5 mm NMR tube was added a 0.05 M or 0.25 M solution of 3,5- Cl_2 - $\text{C}_6\text{H}_3\text{OH}$ (**2a**) in THF in varying molar ratios (**1b/2a** = 1:0 to 1:10) under Ar atmosphere. After the adjustment of whole volume to 0.50 mL by the addition of THF (10 mM based on the amount of **1b**), the sample was then applied to ^{31}P NMR analysis at -98 °C.

Derivatization of **5a** to *N*-Boc- β^2 -homophenylglycine **14** without Loss of Enantiomeric Purity:



Isomerization and Methanolysis of **5a:** A solution of **5a** (138.1 mg, 0.50 mmol) and 1,8-diazabicyclo[5.4.0]undec-7-ene (DBU) (74.8 μ L, 0.50 mmol) in MeOH (100 mL) was stirred for 30 min at room temperature. To the mixture was then added 1 *N* hydrochloric acid to quench the reaction. The aqueous phase was extracted with EA three times and the organic phases were washed with brine. The combined organic extracts were dried over Na₂SO₄ and filtered. After concentration, the residue was purified by column chromatography on silica gel (H/EA = 5:1 as eluent) to furnish **11** as a mixture of diastereomers in 92% yield. **11**: ¹H NMR (400 MHz, CDCl₃) a mixture of two diastereomers δ 7.43-7.35 (3H, m), 7.35-7.29 (2H, m), 6.02 (0.5H, d, *J* = 8.8 Hz), 5.94 (0.5H, d, *J* = 8.8 Hz), 5.22 (0.5H, dd, *J* = 14.6, 8.8 Hz), 5.19 (0.5H, dd, *J* = 14.6, 8.8 Hz), 4.58 (0.5H, dd, *J* = 14.6, 6.4 Hz), 4.55 (0.5H, dd, *J* = 8.8, 5.6 Hz), 4.54 (0.5H, dd, *J* = 14.6, 6.4 Hz), 4.51 (0.5H, dd, *J* = 8.8, 6.4 Hz), 4.37 (0.5H, dd, *J* = 8.8, 6.4 Hz), 4.35 (0.5H, dd, *J* = 8.8, 5.6 Hz), 4.39-4.33 (1H, m), 3.74 (1.5H, s), 3.66 (1.5H, s), 2.16 (0.5H, sept-d, *J* = 6.8, 5.6 Hz), 2.05 (0.5H, sept-d, *J* = 6.8, 5.6 Hz), 0.93 (1.5H, d, *J* = 6.8 Hz), 0.87 (1.5H, d, *J* = 6.8 Hz), 0.73 (1.5H, d, *J* = 6.8 Hz), 0.66 (1.5H, d, *J* = 6.8 Hz); ¹³C NMR (101 MHz, CDCl₃) a mixture of two diastereomers δ 172.2, 172.0, 169.6₂, 169.6₀, 134.7, 134.0, 129.6₄, 129.6₀, 128.9, 128.1₉, 128.1₂, 76.3, 76.1, 57.6, 57.2, 52.5, 52.3, 50.1, 31.5, 31.4, 18.9₃, 18.8₆, 17.8, 17.5, two carbons were not found probably due to overlapping; IR (KBr): 3333, 2965, 1740, 1656, 1554, 1375, 1268, 1209 cm⁻¹; HRMS (FAB) Calcd for C₁₅H₂₁N₂O₅ ([M+H]⁺) 309.1451. Found 309.1465.

Reduction of Nitro Group of **11 and Boc-Protection of Amino Moiety:** A diastereomeric mixture of **11** (92.5 mg, 0.30 mmol) was dissolved in MeOH (3.0 mL) and the mixture was cooled to 0 °C under Ar atmosphere. 10% Pd/C (0.30 g) was added to the solution and the atmosphere was replaced with H₂ (balloon). After being stirred for 12 h at room temperature, Pd/C was removed by filtration and the filtrate was concentrated under reduced pressure. The residue and *N,N*-dimethylaminopyridine (DMAP)

(3.67 mg, 0.030 mmol) were dissolved in MeCN (0.30 mL) and (Boc)₂O (207.0 μL, 0.90 mmol) was added to the solution at room temperature. After 4 h of stirring, additional (Boc)₂O (138.0 μL, 0.60 mmol) was introduced and the reaction mixture was further stirred for 24 h. The resulting mixture was concentrated and the crude residue was purified by column chromatography on silica gel (H/EA = 10:1 as eluent) to give **12** as a mixture of diastereomers in 88% yield. **12**: ¹H NMR (400 MHz, CDCl₃) a mixture of two diastereomers δ 7.34-7.25 (5H, m), 6.02 (0.5H, d, *J* = 8.7 Hz), 5.92 (0.5H, d, *J* = 8.7 Hz), 4.55 (0.5H, dd, *J* = 8.7, 4.9 Hz), 4.51 (0.5H, dd, *J* = 8.7, 4.9 Hz), 4.20 (0.5H, dd, *J* = 14.2, 9.1 Hz), 4.17 (0.5H, dd, *J* = 14.2, 6.9 Hz), 4.12 (0.5H, dd, *J* = 14.2, 5.9 Hz), 4.10 (0.5H, dd, *J* = 14.2, 8.5 Hz), 4.00 (0.5H, dd, *J* = 8.5, 6.9 Hz), 3.96 (0.5H, dd, *J* = 9.1, 5.9 Hz), 3.72 (1.5H, s), 3.65 (1.5H, s), 2.13 (0.5H, sept-d, *J* = 6.9, 4.9 Hz), 2.04 (0.5H, sept-d, *J* = 6.9, 4.9 Hz), 1.40 (9H, s), 1.38 (9H, s), 0.91 (1.5H, d, *J* = 6.9 Hz), 0.86 (1.5H, d, *J* = 6.9 Hz), 0.77 (1.5H, d, *J* = 6.9 Hz), 0.70 (1.5H, d, *J* = 6.9 Hz); ¹³C NMR (101 MHz, CDCl₃) a mixture of two diastereomers δ 172.3, 172.1, 171.6, 171.5, 152.6, 152.5, 137.3, 136.8, 128.9, 128.8, 127.8, 127.7, 82.3₈, 82.3₅, 57.2, 56.9, 52.2, 52.0₉, 52.0₅, 49.0, 48.5, 31.5, 31.3, 27.9₇, 27.9₆, 19.0, 18.9, 17.9, 17.7, three carbons were not found probably due to overlapping; IR (liq. film): 3363, 2978, 1783, 1731, 1681, 1531, 1370, 1257, 1149, 1105, 755 cm⁻¹; HRMS (FAB) Calcd for C₂₅H₃₉N₂O₇ ([M+H]⁺) 479.2757. Found 479.2746.

N-Nitrosation of 12²¹: To a solution of **12** (126.8 mg, 0.265 mmol) in glacial acetic acid (0.44 mL) and acetic anhydride (0.88 mL) was added NaNO₂ (182.9 mg, 2.65 mmol) at 0 °C. The reaction mixture was allowed to warm to room temperature and stirred for 9 h. The resulting solution was poured onto ice and the aqueous phase was extracted with diethyl ether twice. The organic phases were washed with a saturated aqueous solution of NaHCO₃ and brine. The combined organic extracts were dried over Na₂SO₄, filtered, and concentrated. Purification of the residue by column chromatography on silica gel (H/EA = 20:1 as eluent) afforded a mixture of diastereomers of **13** in 94% yield. **13**: ¹H NMR (400 MHz, CDCl₃) a mixture of two diastereomers δ 7.32-7.22 (5H, m), 5.50 (0.5H, dd, *J* = 8.2, 6.9 Hz), 5.49 (0.5H, dd, *J* = 8.2, 6.9 Hz), 4.82 (0.5H, d, *J* = 9.2 Hz), 4.80 (0.5H, d, *J* = 9.2 Hz), 4.36 (0.5H, dd, *J* = 14.2, 6.9 Hz), 4.35 (0.5H, dd, *J* = 14.2, 6.9 Hz), 4.27 (0.5H, dd, *J* = 14.2, 8.2 Hz), 4.26 (0.5H, dd, *J* = 14.2, 8.2 Hz), 3.48 (1.5H, s), 3.46 (1.5H, s), 2.42 (0.5H, dsept, *J* = 9.2, 6.9 Hz), 2.40 (0.5H, dsept, *J* = 9.2, 6.9 Hz), 1.42 (9H, s), 1.41 (9H, s), 1.05₃ (1.5H, d, *J* = 6.9 Hz), 1.04₇ (1.5H, d, *J* = 6.9 Hz), 0.36 (1.5H, d, *J* = 6.9 Hz), 0.35 (1.5H, d, *J* = 6.9 Hz); ¹³C NMR (101 MHz, CDCl₃) a mixture of two diastereomers δ 175.6, 167.7₁, 167.6₇, 152.3₈, 152.3₇, 135.1, 128.9, 128.8, 128.1₀, 128.0₆, 82.6, 56.8, 56.6, 52.2, 52.1, 49.8, 49.7, 48.4, 48.3, 28.0, 27.5, 26.9, 21.6, 21.5, 18.5, 18.4, six carbons were not found probably due to overlapping; IR (liq. film): 2978, 1753, 1523, 1368, 1345, 1280, 1219, 1145, 1120, 852 cm⁻¹; HRMS (FAB) Calcd for C₂₅H₃₈N₃O₈ ([M+H]⁺) 508.2659. Found 508.2674.

Hydrolysis of 13²²: A solution of **13** (71.1 mg, 0.14 mmol) in THF (15.0 mL) was treated with a 30%

aqueous solution of H₂O₂ (0.50 mL) and a 1.0 M aqueous solution of LiOH (0.75 mL, 0.75 mmol) for 4 h at room temperature. Then, to a resulting solution was added a saturated aqueous solution of Na₂SO₃ until peroxides were completely reduced. After concentration, the residual aqueous phase was washed with diethyl ether and acidified with a 2.0 M aqueous solution of KHSO₄. The aqueous phase was extracted with EA twice and the combined organic extracts were dried over Na₂SO₄. All volatiles were removed under reduced pressure and the resulting residue was dissolved into CH₂Cl₂ (7.5 mL), to which a solution of trifluoroacetic acid in CH₂Cl₂ (0.10 M, 1.5 mL) was added at 0 °C. After being stirred for 4 h at room temperature, the resulting mixture was concentrated. The residue thus obtained was purified by column chromatography on silica gel (H/EA = 1/1) to give **14** in 72% yield. The absolute configuration of **14** was determined to be *S* by comparison of its optical rotation with literature value.⁸

14: ¹H NMR (400 MHz, CDCl₃) δ 7.38-7.26 (5H, m), 6.95 (0.5H, brs, cis-trans isomerism NH), 4.95 (0.5H, brs, cis-trans isomerism NH), 3.93 (1H, br), 3.80 (1H, br), 3.69-3.44 (2H, m), 1.48 (4.5H, brs, cis-trans isomerism Boc), 1.43 (4.5H, brs, cis-trans isomerism Boc); [α]_D²⁹ -84.4 (*c* = 1.11, CHCl₃) [lit.²² [α]_D²⁰ -86.0 (*c* = 1.25, CHCl₃) for *S* isomer, 99% ee].

Confirmation of Enantiomeric Purity Conservation: The enantiomeric purity of **14** obtained from this protocol was also determined by HPLC analysis after conversion to its methyl ester **10**.



Esterification of 14: To a solution of **14** (26.5 mg, 0.10 mmol) in benzene (0.70 mL) and MeOH (0.30 mL) was added a 2.0 M solution of Me₃SiCHN₂ in diethyl ether (50.0 μL, 0.10 mmol) dropwise at room temperature. The reaction mixture was stirred for 5 min. After removing volatiles, purification of the residue by column chromatography (H/EA = 10:1 as eluent) gave **10** in 87% yield. The conservation of enantiomeric purity of **10** was confirmed by chiral stationary phase HPLC analysis as describe above (95% ee). [α]_D¹⁹ -62.6 (*c* = 0.5, CHCl₃).

Notes and references

- (1) Supramolecular Catalysis; van Leeuwen, P. W. N. M., Ed.; Wiley-VCH, Weinheim, 2008. and references therein.
- (2) Meeuwissen, J.; Reek, J. N. H. *Nat. Chem.* **2010**, *2*, 615.
- (3) (a) Uraguchi, D.; Ueki, Y.; Ooi, T. *Science* **2009**, *326*, 120. (b) Uraguchi, D.; Ueki, Y.; Ooi, T. *Angew. Chem., Int. Ed.* **2011**, *50*, 3681.
- (4) Rix, D.; Lacour, J. *Angew. Chem., Int. Ed.* **2010**, *49*, 1918.
- (5) For reviews on organocatalytic asymmetric conjugate additions, see: (a) Tsogoeva, S. B. *Eur. J. Org. Chem.* **2007**, 1701. (b) Almaşi, D.; Alonso D. A.; Nájera, C. *Tetrahedron: Asymmetry* **2007**, *18*, 299. (c) Vicario, J. L.; Badía D.; Carrillo, L. *Synthesis* **2007**, 2065.
- (6) For review on the asymmetric conjugate addition to nitroolefins, see: Berner, O. M.; Tedeschi, L.; Enders, D. *Eur. J. Org. Chem.* **2002**, 1877.
- (7) Only one example of the stereoselective conjugate addition of 2,4-disubstituted azlactones to nitroalkenes at 2-position was reported. See: Alemán, J.; Milelli, A.; Cabrera, S.; Reyes E.; Jørgensen, K. A. *Chem. Eur. J.* **2008**, *14*, 10958.
- (8) Calculated pK_a values in water were reported; 3,5-Cl₂-C₆H₃OH: 7.77; 4-Cl-C₆H₄OH: 9.36. Schüürmann, G. *J. Chem. Phys.* **1998**, *109*, 9523.
- (9) When the reaction was performed with **1a**·[PhOH]₃ in toluene at -40 °C, significant loss of the chemical yield and enantioselectivity was observed and **5a** was isolated in less than 20% yield with a diastereomeric ratio of 1:1.4 (57% ee/34% ee, respectively). This result clearly indicates the importance of suitable pK_a (9.82 for PhOH, see ref 8) and the structure of phenolic components.
- (10) Uraguchi, D.; Ueki, Y.; Ooi, T. *J. Am. Chem. Soc.* **2008**, *130*, 14088.
- (11) Use of triaminoiminophosphorane **1a** itself as a catalyst under otherwise identical conditions led to the predominant formation of the oligomerization product, and only a trace amount of **5a** (<10%) was isolated with low stereoselectivity (dr = 1:2.4, 72% ee/69% ee, respectively). The observed decrease in stereoselectivity supports the crucial role of phenolic component in the stereocontrolling event.
- (12) The origin of this phenomena is unclear at present. One possible explanation would be that ion-pairing of the sterically rather demanding chiral cation **1**-H and aryloxide ion could be more stabilized by incorporating arylhydroxide **2** between the two ions to put them in an appropriate spatial distance. In a polar solvent such as THF, **1**-H and the aryloxide ion would be spaced reasonably apart from each other compared to the case in toluene because of the effective solvation of the cation, which might make it feasible to gain similar level of stabilization with incorporation of a lesser amount of **2**.

- (13) Although the enantiomeric excess of **10** was slightly decreased through the deprotection-oxidation sequence as shown in Scheme 3, we also established another route to access **10** from **5a** without detectable racemization. See ESI for details of the procedure.
- (14) (a) Seebach, D.; Beck, A. K.; Capone, S.; Deniau, G.; Grošelj, U.; Zass, E. *Synthesis* **2009**, 1; (b) Weiner, B.; Szymański, W.; Janssen, D. B.; Minnaard A. J.; Feringa, B. L. *Chem. Soc. Rev.* **2010**, 39, 1656.
- (15) (a) Uraguchi, D.; Sakaki, S.; Ooi, T. *J. Am. Chem. Soc.* **2007**, 129, 12392. (b) Uraguchi, D.; Sakaki, S.; Ueki, Y.; Ito, T.; Ooi, T. *Heterocycles* **2008**, 76, 1081.
- (16) Barco, A.; Benetti, S.; De Risi, C.; Pollini, G. P.; Spalluto, G.; Zanirato, V. *Tetrahedron* **1996**, 52, 4719.
- (17) (a) Andrew, R. G.; Raphael, R. A. *Tetrahedron* **1987**, 43, 4803. (b) Palais, L.; Alexakis, A. *Chem. Eur. J.* **2009**, 15, 10473.
- (18) Clive, D. L. J.; Huang, X. *J. Org. Chem.* **2004**, 69, 1872.
- (19) Calmès, M.; Escalé, F.; Martinez, J. *Synthesis* **2001**, 1302.
- (20) Hashimoto, N.; Aoyama, T.; Shioiri, T. *Chem. Pharm. Bull.* **1981**, 29, 1475.
- (21) Evans, D. A.; Carter, P. H.; Dinsmore, C. J.; Barrow, J. C.; Katz, J. L.; Kung, D. W. *Tetrahedron Lett.* **1997**, 38, 4535.
- (22) Ponsinet, R.; Chassaing, G.; Lavielle, S. *Tetrahedron: Asymmetry* **1998**, 9, 865.

List of Publications

Original Papers

- 1) Synthesis of Chiral Tetraaminophosphonium Chlorides from *N*-BOC α -Amino Acid Esters
D. Uraguchi, S. Sakaki, Y. Ueki, T. Ito, T. Ooi, *Heterocycles* **2008**, *76*, 1081-1085.
- 2) Chiral Tetraaminophosphonium Carboxylate-Catalyzed Direct Mannich-Type Reaction
D. Uraguchi, Y. Ueki, T. Ooi, *J. Am. Chem. Soc.* **2008**, *130*, 14088-14089.
- 3) Chiral Organic Ion Pair Catalysts Assembled Through a Hydrogen-Bonding Network
D. Uraguchi, Y. Ueki, T. Ooi, *Science* **2009**, *326*, 120-123.
- 4) Development of Ion-Pair Cooperative Asymmetric Catalyses of Chiral Phosphonium Salts Possessing an Organic Anion
Y. Ueki, D. Uraguchi, T. Ooi, *Catalysts and Catalysis*, **2010**, *52*, 509-514.
- 5) Controlled Assembly of Chiral Tetraaminophosphonium Aryloxide-Arylhydroxide(s) in Solution
D. Uraguchi, Y. Ueki, T. Ooi, *Angew. Chem. Int. Ed.* **2011**, *50*, 3681-3683.
- 6) Formation of Quaternary Carbon Centers by Highly Regioselective Hydroformylation with Catalytic Amount of a Reversibly Bound Directing Group
Y. Ueki, H. Ito, I. Usui, B. Breit, *Chem. Eur. J.* **2011**, *17*, 8555-8558.
- 7) Catalytic Asymmetric Conjugate Addition of Acyl Anion Equivalent to Nitroolefins
D. Uraguchi, Y. Ueki, T. Ooi, *Chem. Sci.* DOI: 10.1039/c1sc00678A.
- 8) Highly Enantioselective Conjugate Addition of Azlactones to Electron-Deficient Triple Bonds Followed by Stereoselective Protonation under *P*-spiro Chiral Iminophosphorane Catalysis
D. Uraguchi, Y. Ueki, A. Sugiyama, T. Ooi, submitted for publication.

Acknowledgement

The studies in this thesis have been carried out under the direction of Professor Takashi Ooi at Nagoya University during March 2006 – March 2012. The studies are concerned with Development of Ion-Pair Cooperative Asymmetric Catalyses of Chiral Tetraaminophosphonium Salts Possessing Organic Anions. I would like to express my sincere gratitude to my supervisor, Professor Takashi Ooi for providing me this precious study opportunity as a Ph.D student in his laboratory.

I especially would like to express my deepest appreciation to my supervisor, Dr. Daisuke Uraguchi for his elaborated guidance, considerable encouragement and invaluable discussion that make my research of great achievement and my study life unforgettable.

I wish to express his appreciations to Dr. Kohsuke Ohmatsu for his constant discussions, encouragement, and technical assistance.

I would like to express my special thanks to Professor Hisao Nishiyama and Professor Kenichiro Itami for their helpful suggestions and discussion on my dissertation committee. It is my great honor to have had my thesis reviewed by two of the foremost experts in the area of synthetic organic chemistry.

The author wishes to express great appreciations to; Professor Bernhard Breit for accepting him as a visiting student at University of Freiburg and supporting fruitful life there, Dr. Ippei Usui, Dr. Kazuhiko Mitsui and all other member of Breit group for their kind assistance and hospitality during his stay at Freiburg, and Assistant Professor Jun-ichi Ito, Assistant Professor Satoru Hiroto, and Dr. Shigeru Yamaguchi for his technical support of X-ray crystal structure analysis,

The author would like to thank Mr. Kyohei Koshimoto for his kind encouragement and discussions, and the author thanks all other members of Ooi group their kind considerations.

I gratefully appreciate the financial support of the Japan Society for the promotion of Science (JSPS) for the Fellowship for Junior Scientist that made it possible to complete my thesis.

Finally, the author expresses his deep appreciation to his family, Mr. Koki Ueki, Mrs. Yoshimi Ueki, and Mr. Koichi Ueki for their constant assistance and encouragement.

Yusuke Ueki

Department of Applied Chemistry
Graduate School of Engineering
Nagoya University
March 2012